

ROLE OF MAHOGANY IN MELANOCORTIN SIGNALING

by

Daniela M. Dinulescu

A DISSERTATION

Presented to the Department of Cell and Developmental Biology

and the Oregon Health Sciences University

School of Medicine

in partial fulfillment of

the requirements for the degree of


Doctor of Philosophy


April 2000


School of Medicine
Oregon Health Sciences University

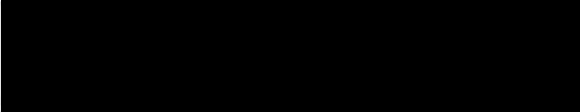
CERTIFICATION OF APPROVAL

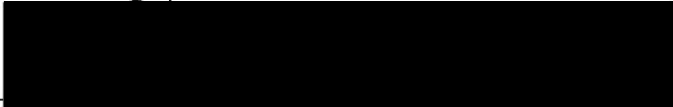
This is to certify that the Ph.D. thesis of
Daniela M. Dinulescu
has been approved


Professor in charge of thesis


Member


Member


Member


Member



Associate Dean for Graduate Studies

TABLE OF CONTENTS

TABLE OF CONTENTS	i
LIST OF FIGURES	vi
LIST OF ABBREVIATIONS	xi
ACKNOWLEDGEMENTS	xiv
ABSTRACT	xvi
 CHAPTER ONE. INTRODUCTION	 1
1. EXTENSION AND AGOUTI-A BRIEF HISTORY	2
2. PRO-OPIOMELANOCORTIN (POMC).....	6
2.1. <i>POMC Processing</i>	6
2.2. <i>Melanocortin Functions</i>	16
3. MELANOCORTIN RECEPTORS, A FAMILY OF Gs-PROTEIN COUPLED RECEPTORS (GPCRs)	21
3.1. <i>Structural and Functional Characteristics of Melanocortin Receptors</i>	23
3.2. <i>MCL-R</i>	27
3.3. <i>MC4-R</i>	34
4. AGOUTI-THE FIRST EXAMPLE OF A NATURALLY-OCCURRING ANTAGONIST OF GPCRs	36
4.1. <i>Discovery of Agouti</i>	36
4.2. <i>Regulation of Murine Agouti Gene Expression</i>	38
4.3. <i>Structural Characteristics of Murine Agouti</i>	44

4.4.	<i>Functional Characterization of Murine Agouti</i>	46
4.4.1.	<i>In Vitro Effects of Agouti</i>	46
4.4.2.	<i>In Vivo Effects of Agouti: the Lethal Yellow Syndrome</i>	47
5.	AGOUTI RELATED PROTEIN (AGRP).....	52
5.1.	<i>Discovery of AGRP</i>	52
5.2.	<i>Parallelism between Agouti and AGRP</i>	53
5.3.	<i>Regulation of AGRP Expression by Leptin and Nutritional Status</i>	60
5.4.	<i>Fine-tuning the Mechanism of Agouti and AGRP Action</i>	62
6.	CONTRASTING AGOUTI AND LEPTIN DEFICIENT OBESITY	
	MODELS	66
6.1.	<i>Leptin and Leptin Receptors</i>	66
6.2.	<i>Comparison Between A^Y and ob (db) Obesity Models</i>	69
7.	OF MICE AND MEN	72
7.1.	<i>Role of Leptin in Human Obesity</i>	72
7.2.	<i>Role of Pro-opiomelanocortin (POMC) in Human Obesity</i>	75
7.3.	<i>First Cases of Altered MC4-R Signaling Identified in Human Population</i>	79
8.	MAHOGANY AND MAHOGANOID: SPECIFIC ACTIVATORS OF	
	AGOUTI AND AGRP	83
8.1.	<i>Discovery of Mahogany and Mahoganoid</i>	83
8.2.	<i>Distribution and Structural Characteristics of Mahogany</i>	84
8.3.	<i>Physiological Characterization of Mahogany</i>	89
8.4.	<i>Insights into the Molecular Mechanism of Mahogany Action</i>	92

9.	SPECIFIC AIMS AND OUTLINE OF THE THESIS.....	95
----	--	----

CHAPTER TWO. GENETIC INTERACTION BETWEEN CANINE

<i>EXTENSION AND AGOUTI</i>	97
-----------------------------------	----

ABSTRACT	98
----------------	----

INTRODUCTION	99
--------------------	----

MATERIALS AND METHODS	100
-----------------------------	-----

RESULTS	102
---------------	-----

DISCUSSION	105
------------------	-----

CHAPTER THREE. <i>MAHOGANY (mg)</i> STIMULATES FEEDING AND INCREASES BASAL METABOLIC RATE INDEPENDENT OF ITS SUPPRESSION OF AGOUTI.....	113
---	-----

ABSTRACT	114
----------------	-----

INTRODUCTION	115
--------------------	-----

MATERIALS AND METHODS	118
-----------------------------	-----

RESULTS	121
---------------	-----

DISCUSSION	125
------------------	-----

CHAPTER FOUR. EFFECTS OF THE CENTRAL MELANOCORTIN SYSTEM ON INSULIN RELEASE AND INSULIN SENSITIVITY	135
---	-----

ABSTRACT	136
INTRODUCTION	137
MATERIALS AND METHODS	138
RESULTS	141
DISCUSSION	145

CHAPTER FIVE. INCREASED INSULIN SECRETION AND GLUCOSE CLEARANCE RATE IN MICE LACKING

MAHOGANY	151
ABSTRACT	152
INTRODUCTION	153
MATERIALS AND METHODS	154
RESULTS AND DISCUSSION.....	156

CHAPTER SIX. A ROLE FOR MAHOGANY IN AXONAL GUIDANCE.....

GUIDANCE.....	165
ABSTRACT	166
INTRODUCTION	167
MATERIALS AND METHODS	168
RESULTS	171
DISCUSSION	176

SUMMARY AND CONCLUSIONS.....	185
-------------------------------------	-----

REFERENCES.....	188
------------------------	------------

LIST OF FIGURES

CHAPTER ONE

FIGURE 1. POMC PROCESSING IN THE ANTERIOR AND INTERMEDIATE PITUITARY	15
FIGURE 2. AMINO ACID SEQUENCE ALIGNMENT OF HUMAN MELANOCORTIN PEPTIDES	19
FIGURE 3. PROTEIN SEQUENCE ALIGNMENT OF MAMMALIAN MELANOCORTIN 1 RECEPTORS (MC1-Rs)	31
FIGURE 4. NATURALLY-OCCURRING MUTATIONS IN MAMMALIAN MC1-Rs	32
FIGURE 5. REGULATION OF MURINE <i>AGOUTI</i> GENE EXPRESSION	42
FIGURE 6. REVERSION OF <i>a</i> TO <i>a'</i> OR <i>A^W</i> ALLELE TAKES PLACE THROUGH A MECHANISM OF HOMOLOGOUS RECOMBINATION.....	43
FIGURE 7. AMINO ACID SEQUENCE ALIGNMENT OF MAMMALIAN AGOUTI PROTEINS	45
FIGURE 8. AMINO ACID SEQUENCE ALIGNMENT OF MURINE AGOUTI AND AGOUTI-RELATED PROTEIN (AGRP).....	57
FIGURE 9. DISULFIDE ARRANGEMENT OF MURINE AGOUTI, AGRP, AND CONOTOXIN GVIA (CONUS GLORIMARIS)	58
FIGURE 10. POMC AND AGRP DISTRIBUTION PATTERNS IN THE CENTRAL NERVOUS SYSTEM (CNS)	59
FIGURE 11. COMPARISON BETWEEN THE <i>LETHAL YELLOW</i> (<i>A^Y</i>) AND LEPTIN-DEFICIENT (<i>ob</i>) OBESITY MODELS.....	71

FIGURE 12. STRUCTURAL FEATURES OF MAHOGANY/ATTRACTIN	88
FIGURE 13. ABSENCE OF MAHOGANY DOES NOT SUPPRESS THE PHENOTYPE OF THE MC4-R KNOCKOUT (MC4-R KO) MOUSE	91
FIGURE 14. POTENTIAL MODELS OF MAHOGANY-AGOUTI/AGRP INTERACTION	94

TABLE 1. CENTRAL AND PERIPHERAL EFFECTS OF MELANOCORTIN PEPTIDES	20
TABLE 2. MELANOCORTIN RECEPTOR DISTRIBUTION, BIOLOGICAL FUNCTION, AND PHARMACOLOGY	26
TABLE 3. PHARMACOLOGY OF NATURALLY-OCCURRING MC1-R VARIANTS	33
TABLE 4. NATURAL MC4-R VARIANTS ASSOCIATED WITH HUMAN OBESITY	82

CHAPTER TWO

FIGURE 1. GENOMIC STRUCTURE AND AMINO ACID SEQUENCE OF THE CANINE AGOUTI	107
FIGURE 2. EXPRESSION PATTERN OF THE <i>A^s</i> <i>AGOUTI</i> ALLELE	108
FIGURE 3. AMINO ACID SEQUENCE OF THE CANINE MC1-R	109
FIGURE 4. THE CANINE <i>e</i> ALLELE ENCODES A NON-FUNCTIONAL MC1-R	110

FIGURE 5. NO DIFFERENCE IN mRNA LEVELS BETWEEN FULL-LENGTH (<i>E</i>) AND TRUNCATED MC1R-R306ter (<i>e</i>)	111
FIGURE 6. MC1R-R306ter IS NON-FUNCTIONAL BECAUSE OF DECREASED PROTEIN STABILITY AND LOSS OF CELL SURFACE EXPRESSION	112

CHAPTER THREE

FIGURE 1. <i>mg</i> SUPPRESSES THE A^Y -INDUCED OBESITY SYNDROME BUT HAS NO EFFECT ON <i>ob</i> -INDUCED WEIGHT GAIN.....	128
FIGURE 2. <i>mg</i> SUPPRESSES THE A^Y -INDUCED INCREASE IN LINEAR GROWTH	129
FIGURE 3. <i>mg</i> SUPPRESSES THE ENDOCRINE EFFECTS OF THE A^Y OBESITY SYNDROME	130
FIGURE 4. <i>mg</i> AND <i>md</i> INDEPENDENTLY INDUCE HYPERPHAGIA	131
FIGURE 5. <i>mg</i> INCREASES BOTH MOTOR ACTIVITY AND BASAL METABOLIC RATE.....	132
TABLE 1. <i>mg</i> SUPPRESSES THE A^Y -INDUCED INCREASE IN ADIPOSITY	133
FIGURE 6. HYPOTHALAMIC NPY EXPRESSION IS NOT AFFECTED BY MAHOGANY	134

CHAPTER FOUR

FIGURE 1. EFFECT OF MELANOCORTIN AGONIST ADMINISTRATION ON SERUM INSULIN IN THE HYPERINSULINEMIC <i>ob/ob</i> MOUSE.....	146
---	-----

FIGURE 2. ROLE OF THE SYMPATHETIC NERVOUS SYSTEM IN THE REDUCTION OF SERUM INSULIN BY MTII ADMINISTRATION.....	147
FIGURE 3. EFFECT OF MTII ON INSULIN RELEASE AND GLUCOSE TOLERANCE IN THE LEAN C57BL/6J MOUSE.....	148
FIGURE 4. DECREASED PERIPHERAL INSULIN SENSITIVITY IN THE YOUNG MC4-R KNOCKOUT (MC4-R KO) MOUSE.....	149
FIGURE 5. NO SIGNIFICANT CHANGE IN THE GLUCOSE TOLERANCE OF YOUNG MC4-R KO AND CONTROL ANIMALS	150

CHAPTER FIVE

FIGURE 1. GLUCOSE CLEARANCE RATE IS INCREASED IN <i>mg/mg</i> ANIMALS	159
FIGURE 2. ABSENCE OF MAHOGANY PROTECTS <i>ob/ob</i> MICE FROM DEVELOPING NON-INSULIN DEPENDENT DIABETES (NIDDM)	160
FIGURE 3. EFFECT OF MAHOGANY ON PERIPHERAL INSULIN SENSITIVITY	161
FIGURE 4. INCREASED INSULIN RELEASE IN RESPONSE TO A GLUCOSE CHALLENGE IN <i>mg/mg</i> MICE	162
FIGURE 5. MAHOGANY HAS NO EFFECTS ON GLUCOSE HOMEOSTASIS IN THE ABSENCE OF A FUNCTIONAL MC4-R	163
FIGURE 6. SPECIFIC MAHOGANY EXPRESSION IN THE PANCREAS	164

CHAPTER SIX

FIGURE 1. NORMAL RESPONSE OF <i>mg/mg</i> ANIMALS TO CENTRALLY-ADMINISTERED AGRP	179
FIGURE 2. <i>mg</i> DOES NOT SUPPRESS THE OBESITY OF AGRP TRANSGENIC ANIMALS	180
FIGURE 3. REDUCED SENSITIVITY OF <i>mg/mg</i> ANIMALS TO CENTRALLY-ADMINISTERED MTH	181
FIGURE 4. AGRP SYNTHESIS IS NOT LIKELY TO BE AFFECTED BY MAHOGANY	182
FIGURE 5. MAHOGANY CONTROLS AGRP AXON GUIDANCE IN THE PVH	183

LIST OF ABBREVIATIONS

ACTH	Adrenocorticotrophic Hormone
AGRP	Agouti-related Protein
α -MSH	α Melanocyte-stimulating Hormone
<i>Atrn</i>	<i>Attractin</i> Gene
<i>A^y</i>	<i>Lethal Yellow</i> Mouse Model
BAT	Brown Adipose Tissue
β -gal	β Galactosidase
BMR	Basal Metabolic Rate
cAMP	Cyclic 3 , 5 -Adenosine Monophosphate
CLIP	Corticotropin-like Intermediate Lobe Peptide
CNS	Central Nervous System
CPE	Carboxypeptidase E
CRE	cAMP Responsive Element
C-terminal	Carboxy-terminal Domain
<i>db/db</i>	Leptin Receptor-deficient Mouse Model
EC	Extracellular Loop
ER	Endoplasmic Reticulum
EC ₅₀	Effective Concentration Producing a Half Maximal Response
GPCR	G-Protein Coupled Receptor
HEK 293	Human Embryonic Kidney 293 Cells
HPA-axis	Hypothalamic-Pituitary-Adrenal Axis

HPLC	High Performance Liquid Chromatography
IC	Intracellular Loop
I.c.v.	Intracerebroventricular
I.p.	Intraperitoneal
IC ₅₀	Inhibitory Concentration Giving Half Maximal Binding
LPH	Lipotropic Hormone
<i>mg</i>	Hypomorphic Mutation at the <i>mahogany</i> Locus
<i>md</i>	Hypomorphic Mutation at the <i>mahoganoid</i> Locus
MCn-R	The Nth Melanocortin Receptor
MC4-R KO	MC4-R Knockout Mouse
MTII	Melanotan II
NDP- α -MSH	[Nle ⁴ , D-Phe ⁷]- α -MSH
NPY	Neuropeptide Y
N-terminal	Amino-terminal Domain
NTS	Nucleus Tractus Solitarius
<i>OB</i>	<i>Leptin</i> Gene
<i>ob/ob</i>	Leptin-deficient Mouse Model
PBS	Phosphate-buffered Saline
PC	Prohormone Convertase
PCR	Polymerase Chain Reaction
POMC	Pro-opiomelanocortin
PVH	Paraventricular Nucleus of the Hypothalamus
RIA	Radioimmunoassay

TM	Transmembrane Domain
SEM	Standard Error of the Mean
SNS	Sympathetic Nervous System

ACKNOWLEDGEMENTS

I would like to thank my advisor, Dr. Roger Cone, for his continuous support and encouragement during the four and a half years of my thesis research. I am extremely grateful to him for giving me the chance to work in his laboratory and sharing with me the depth of his knowledge.

My appreciation also goes to my thesis committee for their advice and encouragement. I am indebted to them all for helping me shape the beginning of my scientific career.

I thank all members of the Cone laboratory for their kindness and stimulating discussions. I especially thank Dr. Wei Fan and Jeanie Zhou for their technical assistance with the physiology experiments. My appreciation goes to Ruth Thomas for her participation in the glucose and energy homeostasis studies. I also thank Ruth for her support, friendship, and many exciting discussions.

Finally, I would like to thank my family, friends, and my loving husband.

To my parents, Dr. Dorel and Despina Dinulescu

To Matthew and Alyssa

In memory of my father-in-law

ABSTRACT

The central melanocortin system has recently been demonstrated to play a key role in the regulation of energy homeostasis in both humans and rodents. This process is mediated by MC4-R, a melanocortin receptor with a wide distribution in the central nervous system (CNS), including the hypothalamus. Melanocortin receptors, such as MC4-R, are unique in that they are regulated by an endogenous antagonist, agouti-related protein (AGRP), which blocks the action of melanocortin agonists (i.e. α -MSH or other POMC-derived melanotropins) at these receptors. Recent studies have established that central melanocortinergetic neurons exert a tonic inhibition on feeding behavior and metabolism. This tonic inhibition is relaxed as a result of AGRP antagonism at MC4-R and downregulation of agonist expression, resulting in the stimulation of caloric intake and energy storage.

The hypomorphic *mahogany* (*mg*) mutation was initially characterized as a suppressor of the yellow pigmentation induced by ectopic agouti (A^Y) expression. Since A^Y expression in the brain leads to the development of a severe murine obesity syndrome, it became of great interest to determine whether the phenotype is reversed in the absence of mahogany. The first physiological characterization of mahogany was also accomplished in the process. It was thus determined that mahogany has multiple physiological effects in the presence or absence of the A^Y gene. Our analysis indicated that the *mg* mutation not only suppressed agouti-induced yellow pigmentation but also the A^Y obesity syndrome, suggesting that it blocked agouti action at both MC1 and MC4-

Rs. In addition, we determined that mahogany had independent effects on feeding behavior and metabolism in the normal, lean mouse that did not express agouti in the brain. Homozygous *mg* was thus shown to induce an increase in energy expenditure as well as caloric intake; both metabolic rate and motor activity were increased in *mg/mg* mice, presumably via activation of the sympathetic nervous system (SNS). Since endogenous AGRP mimics the function of agouti overexpression (A^Y) in normal animals, these findings strongly argue that the absence of mahogany suppresses AGRP binding to MC4-R as well.

This conclusion prompted us to investigate the molecular mechanism that enables mahogany to alter AGRP signaling. Mahogany was recently proposed to function as a co-receptor for agouti binding to MC1-R in melanocytes. This model, however, does not adequately describe the interaction between mahogany and AGRP in the brain. We found that not only did *mg/mg* animals have a normal response to exogenous AGRP administration, but they could also adequately sense constitutive levels of endogenous AGRP. It was thus determined that the absence of mahogany did not suppress the obesity of AGRP transgenic mice, suggesting that the effect of AGRP overexpression was similar in *mg/mg* and control animals. Taken together, these results indicate that if AGRP is able to access the MC4-R, via diffusion as in the case of exogenous administration or overproduction as in AGRP transgenic animals, the absence of mahogany does not preclude it from binding to the receptor and being physiologically active. This led us to pursue the hypothesis that endogenous AGRP is not properly accessing the MC4-R in *mg/mg* animals. Immunoelectron microscopy studies of AGRP fiber distribution and

their interaction with α -MSH projections confirmed the presence of major developmental defects in *mg/mg* animals. These defects reflect an inadequate AGRP signal at MC4-R target sites and may have an etiological role in the lean phenotype of the *mg/mg* mouse.

CHAPTER ONE

INTRODUCTION

1. EXTENSION AND AGOUTI-A BRIEF HISTORY

Extension and *agouti* were first described several decades ago (Silvers, 1961; Silvers and Russel, 1955) as the genetic loci that control the relative amount and distribution of eumelanin (brown/black) and pheomelanin (red/yellow) pigments, respectively, in mammalian fur. Phenotypically, the two genetic systems have opposite effects. The mammalian coat color is thus the consequence of their competition to achieve different pigmentary effects. Normal *extension* alleles promote the spread of a solid dark color throughout the fur. *Agouti* alleles, on the other hand, restrict the dark pigmentation, substituting it with a light coat color. The agouti-banded pattern is easily distinguishable in individual hairs; wild-type mouse hair is black at the root and tip, with a yellow stripe in between. Differences in agouti pigmentation are also visible throughout the coat, with dorsal regions of the body darker than ventral areas. Mutations at both *agouti* and *extension* loci affect this pattern. For instance, dominant (gain of function) mutations at the *extension* locus, such as *sombre*, result in a dark black phenotype. By contrast, dominant (gain of function) mutations at the *agouti* locus, such as the *lethal yellow* (A^Y), produce a yellow coat color. Recessive (loss of function) mutations at the *extension* locus also result in a yellow color (dusty yellow), although not identical with the A^Y phenotype (bright yellow coat color). Likewise, recessive (loss of function) mutations at the *agouti* locus produce a black coat color, although, again, not identical with the *sombre* phenotype (pheomelanin is still visible in a/a mice around the pinnae, mammae, and perineum areas whereas animals carrying the *sombre* mutation have a solid black coat color).

Chimera and grafting experiments indicated early on that the *agouti* gene product did not operate within the melanocyte, the pigment-producing cell, but rather from the surrounding follicular microenvironment (Jackson, 1993). Analysis of the phenotypes produced by the various *agouti* alleles (i.e. dominant alleles produce a yellow coat color, loss-of-function mutations result in black pigmentation, and wild-type alleles give an intermediate phenotype, a banded pattern) suggested, many years ago, that pheomelanin synthesis was the default pathway. Experiments carried out by Takeuchi *et al.* (Takeuchi et al., 1989) provided further clues into the nature of the *agouti-extension* interaction. It was thus demonstrated that α -melanocyte-stimulating hormone (α -MSH) and cholera toxin, as well as forskolin, induced eumelanin synthesis in explants from lethal yellow mice (*A^y/a*) but did not stimulate eumelanogenesis in the hair follicles of recessive yellow (*e/e*) animals (Takeuchi et al., 1989). These results suggested that the gene product of the *agouti* locus, which probably functioned in follicle cells, interacted with α -MSH at the α -MSH-R and that the *extension* locus controlled the activity of adenylyl cyclase in melanocytes (Takeuchi et al., 1989; Jackson, 1993). It was thus proposed that *extension* encoded a receptor for α -MSH; *agouti*, on the other hand, was predicted to encode an antagonist that blocked α -MSH signaling, possibly by preventing its binding to the receptor (Takeuchi et al., 1989; Jackson, 1993). This model was confirmed in the early 90 s when the two genes were cloned; *extension* was found to encode the MSH-R (melanocortin 1 receptor, MC1-R), whereas *agouti* turned out to be a high affinity antagonist for the same receptor (Bultman et al., 1992; Lu et al., 1994; Miller et al., 1993; Mountjoy et al., 1992).

Molecular analysis of the *agouti* and *extension* genes has allowed a better understanding of the complex process of mammalian pigmentation. The two genetic systems and the nature of their interaction have proved to be highly conserved in mammals; it is not entirely clear, however, if this is true in humans as well. Several *extension* alleles have been associated with specific human complexions and hair colors, but the cause and effect relationship between the two has yet to be proven. Furthermore, *agouti* does not appear to play any role in human pigmentation and its exact biological function in humans remains thus far unknown.

Mountjoy and collaborators reported in 1992 that the *extension* locus encodes a member of the melanocortin receptors (MC1-R), a family of Gs-coupled receptors, of which five isoforms are presently known (Cone et al., 1993; Mountjoy et al., 1992). MC1 and MC2-R are the classical melanocyte-stimulating hormone receptor (MSH-R) and adrenocorticotrophic receptor (ACTH-R), respectively, whereas MC3, 4, and 5-R are novel receptors with a multitude of physiological effects. Melanocortins such as α -MSH and ACTH are the natural ligands for this family of receptors: α -MSH for MC1, 3, 4, and 5-R, and ACTH for MC2-R, respectively. They are secreted mainly by the pituitary gland and by several other tissues, albeit in reduced quantities, following cleavage from a common precursor, the pro-opiomelanocortin (POMC). The activity of melanocortin receptors is unique in that it is regulated by endogenous antagonists, such as *agouti*, and the recently discovered *agouti* homologue, *agouti*-related protein (AGRP). A detailed description of the melanocortin system, including ligands (melanocortins, POMC),

endogenous antagonists (agouti, AGRP), and melanocortin receptors, is presented in the next chapters.

2. PRO-OPIOMELANOCORTIN (POMC)

2.1. POMC Processing

Melanocortins are a family of peptide hormones derived from pro-opiomelanocortin (POMC), a prohormone that is synthesized mainly in the anterior and intermediate pituitary of vertebrates. Other sites of POMC expression include the hypothalamus and medulla (i.e. arcuate nucleus, nucleus tractus solitarius), as well as numerous peripheral tissues, such as the skin, skeletal muscle, pancreas, gastrointestinal tract, thyroid, and placenta (Smith and Funder, 1988). In both anterior and intermediate pituitary POMC is post-translationally cleaved to yield three fragments: the amino-terminus (N-terminus), the adrenocorticotrophic hormone (ACTH), and β -lipotropin (β -LPH). These polypeptidic fragments are further processed in the intermediate lobe to yield five additional hormones: α and γ -melanocyte stimulating hormone (α/γ -MSH), corticotropin-like intermediate lobe peptide (CLIP), γ -LPH, and β -endorphin (β -END) (Figure 1).

The production of multiple peptides from a common precursor (POMC) is the result of a series of post-translational events that include exo- and endopeptidase cleavage, acetylation, α -amidation, and phosphorylation. The extent of these modifications varies widely, being tissue and species-specific. The amino acid sequence of the precursor, POMC, is however, highly homologous among various species. It consists of an N-terminal fragment (16 K peptide or pro- γ -MSH), ACTH, and β -LPH at the C-terminus. ACTH generates α -MSH and CLIP upon further cleavage, whereas β -

LPH is sequentially processed to γ -LPH and different forms of β -endorphin (β -EP): β -EP₁₋₃₁, β -EP₁₋₂₇, β -EP₁₋₂₆, β -EP₁₋₁₇ (γ -EP), and β -EP₁₋₁₆ (α -EP) (Figure 1). All peptides within the POMC precursor, with the exception of α and γ -EP, are flanked by pairs of dibasic residues such as Lys/Arg, Arg/Lys, Arg/Arg, and Lys/Lys; this results in POMC being preferentially cleaved at dibasic residues.

The post-translational process of POMC maturation starts in the endoplasmic reticulum (ER) with the cleavage of the N-terminal signal peptide by a signal peptidase, followed by the protein release into the ER lumen. Since the POMC precursor is intended for transport to the Golgi apparatus, it must be first glycosylated in the ER lumen. A preformed oligosaccharide core, consisting of 14 glucose, mannose, and N-acetyl-glucosamine residues, is attached to the protein via an N-linked (asparagine-linked) glycosylation event. The process of N-glycosylation is catalyzed by oligosaccharyl transferases and occurs at the asparagine (Asn) residue of the Asn-X-Ser triplet that borders the γ -MSH sequence; the CLIP peptide is, also, N-glycosylated to some extent (Eipper and Mains, 1980). The trimming of the oligosaccharide core is catalyzed by glucosidases and mannosidases, it starts within the ER and continues after transfer to the Golgi apparatus. The oligosaccharide chains are further processed in the Golgi by glycosyl transferases, which add N-acetylglucosamine, galactose, and N-acetylneuraminic acid residues to the mannose residues of the core. A second process of glycosylation, this time O-linked, takes place in the Golgi apparatus. It consists in the addition of N-acetylgalactosamine residues to the hydroxyl (OH) groups of serine (Ser), threonine

(Thr), or hydroxylysine (Lys-OH) residues, and is catalyzed by O-glycosyltransferases (Seidah and Chretien, 1981).

There is now significant evidence of additional postranslational events (phosphorylation and sulfation) that take place in the Golgi apparatus. For instance, ACTH is phosphorylated at Ser³¹ within the anterior pituitary (Bennett et al., 1983). The sugar residues of the larger POMC fragments may also be sulfated within the intermediate pituitary (Bourbonnais and Crine, 1985; Hoshina et al., 1982). The functional significance of these modifications remains thus far unknown.

Following maturation, the POMC precursor is transferred to secretory vesicles where it undergoes further processing; as a result of this process, a variety of peptides with a large spectrum of biological activities are generated. Posttranslational events that occur in the secretory granule pathway include: proteolytic (endo- and exopeptidase) cleavage, acetylation, and α -amidation. The current model of POMC processing in the anterior and intermediate pituitary has been developed based on studies performed in AtT-20 cells (anterior pituitary corticotrope tumor cell line) and Rin m5F insulinoma cells, as well as high performance liquid chromatography (HPLC) analysis of pituitary extracts from various species.

Endopeptidase Cleavage

POMC processing occurs preferentially at dibasic residues and is catalyzed by prohormone convertases: PC1/PC3 and PC2. Both enzymes are endopeptidases with

trypsin-like activities that are evolutionarily conserved within vertebrates. They are expressed primarily in neuroendocrine tissues but their distribution varies depending on the tissue. For example, PC1/3 is highly expressed in the anterior pituitary where PC2 can be found at only low levels. By contrast, in the intermediate lobe both enzymes are highly expressed, with PC2 being more abundant. The pattern of POMC processing as well as the enzymes utilized in the process differ between the two pituitary lobes, suggesting a highly specialized process. Studies in AtT-20 (anterior pituitary corticotrope tumor cell line) and Rin m5F insulinoma cells, which closely resemble the pattern of POMC cleavage in intermediate pituitary, demonstrate that PC1/3 and PC2 process POMC in a sequential fashion (Benjannet et al., 1991; Thomas et al., 1991; Thorne et al., 1991). PC1/3 is mainly responsible for POMC processing in the anterior lobe and uses only Lys/Arg dibasic residues as cleavage sites. By contrast, PC2 is the primary enzyme for POMC processing in the intermediate lobe and employs all combinations of dibasic (Lys, Arg) residues: Arg/Lys, Lys/Arg, Lys/Lys, and Arg/Arg; this suggests that PC2 has a broader spectrum of activity than PC1. Thus, PC1/3 cleaves POMC into ACTH and β -LPH, whereas POMC processing by PC2 yields β -EP, AJP, and α -MSH (Benjannet et al., 1991; Thomas et al., 1991).

Together PC1/3 and PC2 process POMC in a concerted manner; as a result of their action the prohormone is extensively cleaved in the intermediate pituitary, generating a variety of small peptides, including γ -MSHs, CLIP, α -MSH, β -MSH, and β -EP. The two enzymes are responsible, therefore, for producing all the main POMC-derived peptides, with the exception of α and γ -EP. γ -EP is generated as a result of a different

endopeptidase cleavage between two hydrophobic residues, leucine (Leu¹⁷) and phenylalanine (Phe¹⁸). Cathepsin D and renin have been assigned as potential enzymes for this process (Smith and Funder, 1988).

Exopeptidase Cleavage

Several exopeptidase activities have been described for POMC processing. First, POMC cleavage at dibasic residues is followed by the removal of the basic carboxy-terminal (C-terminal) residue by carboxypeptidase E (CPE) (Smith and Funder, 1988). A second carboxypeptidase activity is responsible for the generation of β -EP₁₋₂₆ from β -EP₁₋₂₇ (Smith and Funder, 1988). A third carboxypeptidase cleaves ACTH by removing the phenylalanine residue at position 39 and generates ACTH₁₋₃₈ and ACTH₁₈₋₃₈ (CLIP) (Smith and Funder, 1988).

α -Amidation

α -MSH and the acidic joining peptide (AJP), located in the POMC precursor between γ -MSH and ACTH, are the only end products α -amidated at the C-terminus (Eipper et al., 1986; Seidah et al., 1981). The amidation process is thought to protect the peptides from carboxypeptidase cleavage and may be critical for their function (Smith and Funder, 1988). The α -amidation process is catalyzed by peptidyl glycine α -amidating monooxygenase (Murthy et al., 1986), an enzyme that requires a glycine (Gly) residue at the C-terminus. It is not surprising, therefore, that the precursors of all α -amidated peptides derived from POMC have Gly residues preceding dibasic residues (Smith and Funder, 1988).

Acetylation

The acetylation of α -MSH (both mono- and di-) and β -EP occurs mainly in the neurointermediate lobe of the pituitary. α -MSH is both α -N-acetylated (monoacetylated) and α -N-O-diacetylated at the N and O positions of the N-terminal Ser residue; β -EP, on the other hand, is α -N-acetylated at the amino-terminal tyrosine (Tyr) residue. The same acetyltransferase is responsible for the acetylation of desacetyl α -MSH, α -MSH, and β -EP in the intermediate pituitary (Glembotski, 1982). Whether this holds true for other sites of POMC processing, such as the hypothalamus, is still controversial (Barnea and Cho, 1983; O'Donohue, 1983). The acetylation process is thought to play opposite roles in the activation of the two peptides. The N-acetylation increases the biological activity of α -MSH whereas the acetylated β -EP is virtually inactive (Guttmann, 1961; Smyth et al., 1979).

Central and Peripheral Sites of POMC Processing

It is now well established that POMC synthesis occurs at central sites (pituitary, central nervous system, CNS) and in a variety of peripheral tissues. The processing of the precursor is tissue-specific, suggesting a broad spectrum of biological activities for POMC-derived peptides.

Pituitary gland

The anterior and intermediate lobes of the pituitary gland are the predominant sites of POMC production. In the pituitary gland 3% of the anterior lobe cells and more than 90% of the intermediate lobe cells synthesize POMC (Gee and Roberts, 1983). POMC

processing occurs within both anterior and intermediate pituitary lobes; the end products that are generated as a result of this process vary, however, between the two compartments. The roles of the POMC-derived peptides produced in the anterior and intermediate pituitary differ, suggesting that the two lobes are functionally distinct. POMC processing in the anterior pituitary results in the production of four main fragments: the N-terminal 16 K fragment, ACTH, β -LPH, and β -EP (Eipper and Mains, 1981). β -EP₁₋₃₁ is the major β -EP species present in the anterior pituitary, with the other β -EP peptides (β -EP₁₋₂₇, β -EP₁₋₂₆, γ -EP, and α -EP) and N-acetylated forms (NacEP₁₋₃₁, NacEP₁₋₂₇, and NacEP₁₋₂₆) being less abundant (Burbach and Wiegant, 1984; Zakarian and Smyth, 1982). A small proportion of ACTH is further processed to α -MSH (mainly desacetyl) and CLIP (Smith et al., 1982). By contrast, the main fragments produced in the intermediate pituitary lobe are: the N-terminal fragment, γ -MSH, AJP, α -MSH, CLIP, γ -LPH, and β -EP (Bennett, 1984; Bohlen et al., 1981; Browne et al., 1981; Crine et al., 1978; Crine et al., 1979; Mains and Eipper, 1979). The majority of α -MSH in the intermediate lobe is diacetylated at the amino-terminal Ser residue. β -EP is present in the intermediate lobe as mainly NacEP₁₋₂₇ and NacEP₁₋₂₆; NacEP₁₋₃₁, Nac α -EP, and Nac γ -EP are also found in the intermediate pituitary but in smaller amounts (Al-Noaemi et al., 1982; Cheng et al., 1987; Smith and Funder, 1988). A combination of eight CLIP forms are found in the intermediate lobe that are generated following glycosylation at position 29 (Asn), phosphorylation at position 31 (ACTH), and cleavage of the C-terminal phenylalanine (Phe) residue (Bennett et al., 1982).

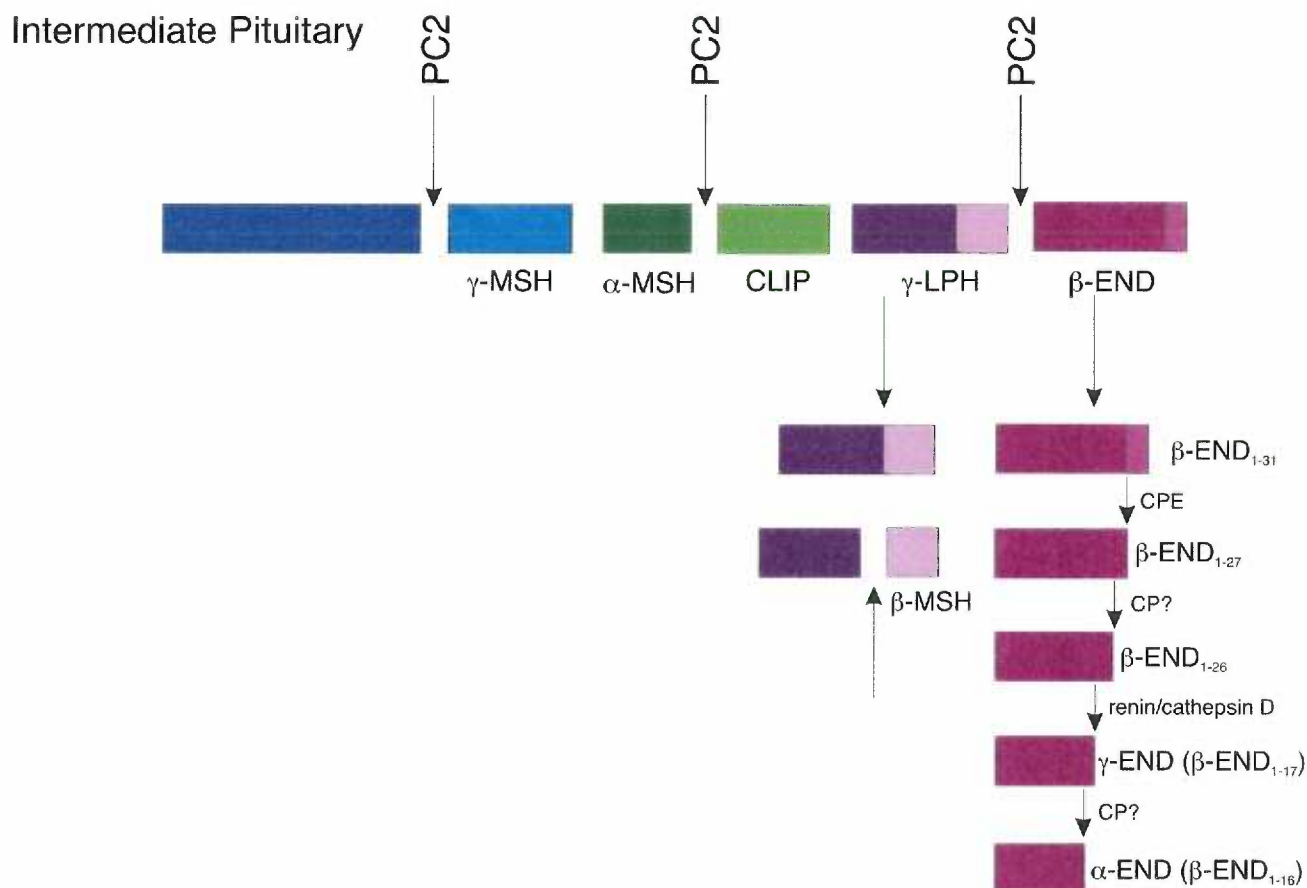
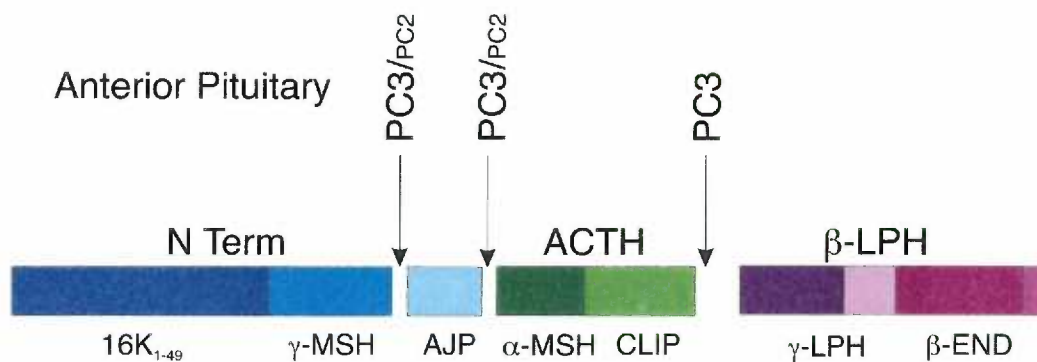
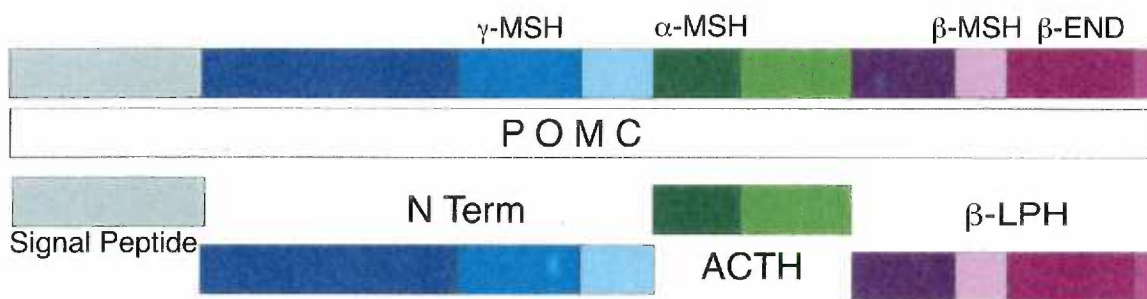
Central Nervous System (CNS)

POMC is found in brain in relatively low amounts compared to the pituitary gland. For instance, the total amount of POMC-derived peptides present in the hypothalamus represents only 0.1% of that produced in the pituitary (Smith and Funder, 1988). Immunohistochemical data indicate that the localization of neuronal cell bodies staining positively for α -MSH, ACTH, and β -EP is limited to the arcuate nucleus of the hypothalamus and the commissural part of the nucleus tractus solitarius (NTS) (Orwoll et al., 1979; Palkovits et al., 1987). By contrast, there is a vast network of α -MSH, ACTH, and β -EP-positive fibers that innervate numerous brain areas, including hypothalamic nuclei, median eminence, preoptic and septal areas, thalamus, and brainstem. POMC processing in the CNS resembles the cleavage pattern of the intermediate pituitary. Therefore, the main fragments generated upon POMC cleavage in the brain are: α -MSH, CLIP, γ -LPH, and β -EP. In the hypothalamus, the majority of α -MSH is not acetylated; outside the hypothalamus, however, mainly acetylated forms of α -MSH are found (Chretien et al., 1984). For instance, both mono- and diacetyl- α -MSH are present in nucleus accumbens, whereas des-acetyl α -MSH is found in amygdala (Chretien et al., 1984). The main form of β -EP in the hypothalamus is β -EP₁₋₃₁; in amygdala and midbrain, however, the shorter forms of β -EP predominate (Smith and Funder, 1988). In hippocampus, brain stem, and nucleus accumbens β -EP undergoes extensive acetylation and proteolytic cleavage, resulting in a variety of shorter, acetylated β -EP peptides (Smith and Funder, 1988).

Skin

POMC is synthesized in a variety of peripheral tissues, albeit in a much lower amount than that found in the pituitary. Peripheral tissues that produce POMC include the thyroid, pancreas, gastrointestinal tract, reproductive tract, immune system, skeletal muscle, and skin (Smith and Funder, 1988). The small amount of prohormone found in the peripheral tissues argues for an autocrine or paracrine, rather than endocrine, role for POMC-derived peptides (Smith and Funder, 1988). Recent *in vitro* studies, using cultured human and murine skin-derived cells, demonstrate that POMC protein and its derivatives, β -LPH and β -EP, are synthesized in cutaneous cells, such as keratinocytes. In addition, normal skin and hair follicles have been shown to stain positively for POMC-derived peptides, suggesting that POMC is synthesized and processed correctly *in vivo* as well (Wintzen and Gilchrest, 1996). POMC transcription and processing are reportedly upregulated following exposure to ultraviolet radiation (UVR), cytokines (interleukin-1- α or IL-1- α), and mitogenic agents (phorbol 12-tetradecanoate 13-acetate or TPA) (Wintzen and Gilchrest, 1996). Possible functions for POMC-derived peptides in the epidermis include melanogenesis, cell cycle regulation, cell differentiation, immunomodulation, and skin protection after sun exposure (Wintzen and Gilchrest, 1996).

Figure 1. POMC processing in the anterior and intermediate pituitary.



2.2. *Melanocortin Functions*

POMC-derived peptides have a large spectrum of physiological roles. The first biological activity described for the melanocortin peptides was the ability of amphibian pituitary extracts, containing α -MSH and ACTH, to enhance melanogenesis (Hogben and Winton, 1922). Consequently, the agonist activity of melanocortins has been determined based on their ability to induce pigment dispersion in frog and lizard skin bioassays.

Melanocortin peptides, such as ACTH, α , β , and γ -MSH, share a common His⁶-Phe⁷-Arg⁸-Trp⁹ (HFRW) pharmacophore that is indispensable for their function (Figure 2). This tetrapeptide core was deemed sufficient for the agonist activity of α -MSH and its analogues, as tested in frog and lizard skin bioassays (Castrucci et al., 1989; Hruby et al., 1987). A likely explanation for this phenomenon has recently been offered by computer modeling studies. Thus, receptor-ligand docking analysis suggests that the HFRW tetrapeptide binds directly to the melanocortin receptor and controls the agonist activity of the ligand.

A variety of α -MSH-analogues have been chemically synthesized based on the HFRW scaffold and tested *in vitro* for their agonist activity. The stereochemistry of the tetrapeptide core appears to be important, since replacing the L-Phe⁷ residue with its D-isomer results in a more potent agonist. The combination of D-Phe⁷, which increases the potency of the agonist, and norleucine (Nle) at position 4 (instead of Met) that increases the stability of the compound by preventing its oxidation, generates the [Nle⁴, D-Phe⁷]- α -

MSH or NDP- α -MSH compound. NDP- α -MSH turned out to be a super-potent, long-lasting agonist of the melanocortin receptors (Sawyer et al., 1980). Furthermore, cyclic α -MSH analogues proved to be even better agonists than the linear compounds. For instance, a cyclic compound, cyclo[Cys⁴, Cys¹⁰]- α -MSH, containing a disulfide bridge, which stabilizes a β -turn critical for α -MSH conformation, exhibits a superagonist activity (Sawyer et al., 1980). Likewise, the introduction of a lactam bridge (between positions 4 and 10) in the NDP- α -MSH structure resulted in a highly potent and very stable agonist, Ac-Nle⁴-cyclo[Asp⁵, D-Phe⁷, Lys¹⁰]- α -MSH (4-10)-NH₂, melanotan II or MTII (Al-Obeidi et al., 1989; Hruby et al., 1995). A similar design was used to generate a highly potent, selective antagonist, Shu 9119 (Al-Obeidi et al., 1989; Hruby et al., 1995). All three compounds: NDP- α -MSH, MTII, and Shu 9119 have proved to be essential tools in delineating the specific functions of the various melanocortin receptors.

Melanocortins have a multitude of physiological effects, including the stimulation of pigmentation, adrenal steroidogenesis, lipolysis, natriuresis, sexual activity, pheromone release, sebum secretion, grooming behavior, learning and memory, nerve regeneration, neurite outgrowth, and HPA axis activation (Table 1). In addition, antipyretic and anti-inflammatory effects have been reported for melanocortin peptides together with their ability to modulate heart rate and blood pressure (Table 1). In recent years, α -MSH and its analogues, such as MTII, have generated a lot of interest because of their dramatic effects on energy and glucose homeostasis. It is now well established that central administration of melanocortin peptides suppresses feeding behavior and increases metabolic rate (Cowley et al., 1999; Fan et al., 1997). Additional effects of melanocortins

have been reported on the suppression of insulin secretion via activation of the sympathetic nervous system (see chapter 4). The majority of the effects described in Table 1 have a central origin, since they can be reproduced by intracerebroventricular (i.c.v.) administration of melanocortin peptides. Exceptions include the stimulatory effects on lipolysis, sebum secretion, natriuresis, adrenal steroidogenesis, and pigmentation that originate in adipocytes, sebaceous and preputial glands, kidney, adrenal gland cortex, and melanocytes, respectively. Finally, the ability of melanocortin peptides to reduce inflammatory responses and stimulate nerve regeneration has a dual origin, both central and peripheral.

Figure 2. Amino acid sequence alignment of human melanocortin peptides.

The pharmacophore is highlighted in red. Conserved residues outside the pharmacophore sequence are colored in blue.

	1	2	3	4	5	6	7	8	9	10	11	12	13
ACTH	H-Ser- Tyr -Ser- Met - Glu - His - Phe - Arg - Trp -Gly-Lys-Pro-Val-Gly-Lys-Lys-Arg// -Phe ³⁹ -OH												
α -MSH	Ac-Ser- Tyr -Ser- Met -Glu- His - Phe - Arg - Trp -Gly-Lys-Pro-Val-NH ₂												
β -MSH	H-Asp-Glu-Gly-Pro- Tyr -Arg- Met -Glu- His - Phe - Arg - Trp -Gly-Ser-Pro-Pro-Lys-Asp-OH												
γ_1 -MSH	H-Lys- Tyr -Val- Met -Gly- His - Phe - Arg - Trp -Asp-Arg-Phe-NH ₂												
γ_2 -MSH	H-Lys- Tyr -Val- Met -Gly- His - Phe - Arg - Trp -Asp-Arg-Phe-Gly-OH												
γ_3 -MSH	H-Lys- Tyr -Val- Met -Gly- His - Phe - Arg - Trp -Asp-Arg-Phe-Gly-Arg-Arg-Asn-Ser-// -Gln ²⁷ -OH												

Table 1. Central and peripheral effects of melanocortin peptides.

Physiological Effect	Biological Activity	Melanocortin peptide	Reference
Melanogenesis	Stimulate	α -MSH	(Castrucci et al., 1989; Hruby et al., 1987; Thody et al., 1998)
Adrenal steroidogenesis	Stimulate	α -MSH, ACTH, ACTH ₁₋₂₄ , γ -MSH, β -MSH, pro- γ -MSH	(Pedersen, et al., 1980; Al-Dujaili et al., 1981)
Lipolysis	Stimulate	α -MSH, ACTH, ACTH ₁₋₁₀	(Richter et al., 1987)
Natriuresis	Stimulate	α -MSH, ACTH, ACTH ₄₋₁₀ , γ -MSH	(Gruber et al., 1989; Valentin et al., 1993; Lymangrover et al., 1985; Ni et al., 1998; Gruber et al., 1985)
Activity of the HPA axis	Stimulate	ACTH ₁₋₂₄	(Wiegant et al., 1979)
Immunomodulation (Anti-inflammatory)	Stimulate	α -MSH	(Lipton et al., 1997; Robertson et al., 1988)
Antipyresis (Thermoregulation)	Stimulate	α -MSH, ACTH ₁₋₂₄	(Glyn et al., 1981; Robertson et al., 1988; Huang et al., 1997; Holdeman et al., 1985; Huang et al., 1998)
Endotoxin-induced anorexia/hypoactivity	Stimulate	α -MSH	(Huang et al., 1999)
Feeding behavior	Inhibit	α -MSH, ACTH ₁₋₂₄	(Fan et al., 1997; Vergoni et al., 1990; Giraudo et al., 1998)
Cardiac effects			
Hypotension/Bradycardia	Stimulate	α -MSH, ACTH ₄₋₁₀ , γ -MSH	(Gruber et al., 1989; Li et al., 1996)
Pressor response/Tachycardia	Stimulate	γ -MSH, γ_2 -MSH, Lys- γ_2 -MSH, ACTH ₄₋₁₀	(Li et al., 1996; Versteeg et al., 1998)
Depressor response/Tachycardia	Stimulate	ACTH ₁₋₂₄	(Versteeg et al., 1998)

Sexual behavior (Pheromone release)	Stimulate	α -MSH, ACTH	(Bertolini et al., 1969; Thody et al., 1981; Thody et al., 1981)
Sebum secretion	Stimulate	α -MSH	(Thody et al., 1975)
Grooming behavior	Stimulate	α -MSH, ACTH ₁₋₂₄ , ACTH ₅₋₁₃ , ACTH ₄₋₁₃	(de Wied et al., 1982; de Wied et al., 1993; de Wied et al., 1999; Gispen et al., 1975; Kobobun et al., 1983; O'Donohue et al., 1981)
Learning and memory	Stimulate	α -MSH, ACTH ₄₋₁₀ , ACTH ₁₋₂₄ , ACTH ₄₋₇ , ACTH ₇₋₁₆	(de Wied et al., 1997; Beckwith et al., 1989; Kobobun et al., 1983)
Opiate-induced analgesia, dependence, and tolerance	Inhibit	α -MSH, ACTH	(Alvaro et al., 1997; Contreras et al., 1984; Sandman et al., 1981)
Nerve regeneration (Central/peripheral)	Stimulate	α -MSH, ACTH ₁₋₂₄ , ACTH ₄₋₁₀ , ACTH ₁₋₁₆	(Bijlsma et al., 1981; Strand et al., 1991; Wolterink et al., 1990; Wolterink et al., 1990)
Neurite outgrowth	Stimulate	α -MSH	(Adan et al., 1996)

3. MELANOCORTIN RECEPTORS, A FAMILY OF Gs-PROTEIN COUPLED RECEPTORS (GPCRs)

Once the importance of melanocortin peptides in the regulation of feeding behavior, inflammation, immunity, and behavior was revealed, it became critical to determine their site of action. The first indication came in the late 1980 s when receptor autoradiography experiments were performed. Iodinated [^{125}I] NDP- α -MSH was used as a tracer in these assays because of its potency and prolonged biological activity. The use of an iodinated ligand served a dual purpose in these studies: it allowed both the localization and characterization of the binding sites for melanotropins. Receptor distribution was thus studied *in vivo* by monitoring the tracer uptake in the CNS and peripheral organs (Tatro, 1990; Tatro and Reichlin, 1987). The results of those studies indicated that melanocortin receptors had a wide distribution, suggesting that they had effects on the functions of multiple organs (Tatro and Reichlin, 1987) (Table 2).

Tatro and collaborators were thus able to assemble a neuroanatomic map of specific α -MSH binding sites in the brain, which included various structures within the medial preoptic area, caudate putamen, olfactory tubercle, bed nucleus of the stria terminalis, ventral part of the lateral septal nucleus, hypothalamic periventricular and paraventricular nuclei, dorsal anterior amygdaloid area, substantia innominata and thalamic paraventricular nucleus, as well as the lower brainstem (Tatro, 1990; Tatro, 1993; Tatro and Entwistle, 1994a; Tatro and Entwistle, 1994b). A number of peripheral organs were also found to contain specific α -MSH binding sites; among them were the Harderian,

lacrimal, preputial, submandibular, thyroid and adrenal glands, pancreas, duodenum, bladder, spleen, skin, as well as brown and white adipose tissue (Tatro and Reichlin, 1987). Each brain structure showed a characteristic binding pattern, indicating the existence of multiple receptors that were distinguishable from each other based on their pharmacology. Thus, the pharmacological analysis of melanocortin binding sites in the CNS revealed the presence of two receptor subtypes with different radioligand affinities (Tatro and Entwistle, 1994a). The same was true for peripheral organs. For instance, α -MSH did not compete with iodinated ACTH for binding to adrenal tissue sites, suggesting the presence of a melanocortin receptor subtype that was selective for ACTH (Klemcke and Pond, 1991).

The ability of melanocortin peptides to stimulate adenylate cyclase activity in cultured cells and brain slices suggested that the melanocortin receptors were part of the G-protein-coupled (GPCR) family (Florijn et al., 1993; Mac Neil et al., 1981; Mackie et al., 1972). The melanocortin receptor family (MC-R) was thus cloned based on their homology with other members of the GPCR family (Mountjoy et al., 1992). Mountjoy and collaborators used a polymerase chain reaction (PCR) with degenerate primers approach to amplify DNA sequences from a melanoma line, previously shown to contain a high level of specific [125 I] NDP- α -MSH binding sites (Mountjoy et al., 1992). Using these sequences, they were soon able to obtain clones for the full length mouse and human MSH-R (MC1-R) as well as human ACTH receptor (MC2-R). This discovery was quickly followed by the identification of additional members of the melanocortin receptor family based on a similar technique. The newly discovered receptor subtypes included

the MC3, MC4, and MC5-R (Chhajlani et al., 1993; Gantz et al., 1993a; Gantz et al., 1993b; Gantz et al., 1994; Labbe et al., 1994; Mountjoy and Wild, 1998; Roselli-Reh fuss et al., 1993). There is now growing evidence suggesting the existence of a sixth melanocortin receptor that mediates central effects of γ -MSH, such as tachycardia and the pressor response.

The availability of the cloned MC-Rs offers a unique opportunity to confirm previous findings on melanocortin function and to assign physiological activities to specific receptor subtypes. In addition, the feasibility of molecular approaches for targeted inactivation of individual MCR subtypes in specific tissues should facilitate the discovery of new physiological functions for melanocortins and their receptors.

3.1. Structural and Functional Characteristics of Melanocortin Receptors

The five melanocortin receptors (Figure 4) are characterized by seven transmembrane (TM) domains, an extracellular N-terminal region, three extracellular (EC) loops, three intracellular (IC) loops, and a C-terminal domain. They are unique among the GPCRs by virtue of their short N- and C-termini, second extracellular (EC₂) and third intracellular loops (IC₃). All five receptor subtypes are associated with Gs and positively coupled to adenylyl cyclase, thus inducing intracellular cAMP synthesis upon activation. Melanocortin receptor subtypes share a significant degree of homology with each other. For instance, within a species, the amino acid identity of the different MC-R subtypes is

39-60%. The homology among various species for one receptor subtype is even higher. For example, the identity among all cloned MC1-Rs is 70%, and that of MC5-Rs is 80%. A large number of residues are conserved among all melanocortin receptor subtypes, suggesting that they are likely to bind the HFRW pharmacophore of the melanocortin peptides. In addition, a significant number of residues are conserved in each melanocortin receptor subtype from various species; these particular residues confer specificity to the ligand-receptor interaction.

Molecular and functional analysis of the five melanocortin receptors known to date indicates that they have a wide distribution within the body, specific pharmacology, and a multitude of biological activities (Table 2). *In situ* hybridization studies identify MC3 and MC4-R as the main receptor subtypes present in the brain. In the hypothalamus, MC4-R appears to be more prevalent than MC3-R, suggesting that it may be the main regulator of energy homeostasis. MC5-R is distributed in a variety of peripheral sites, although several reports indicate its presence in the brain as well. However, since the *MC5-R* mRNA levels reported are very low, the existence of this receptor subtype in the CNS remains uncertain.

All melanocortin receptors, with the exception of MC2-R, recognize a common group of ligands that includes various forms of MSH as well as ACTH; they do, however, exhibit ligand specificity. The adrenal MC2-R is the most selective melanocortin receptor subtype as it is activated only by ACTH. By contrast, MC3-R is the least selective subtype as it recognizes and binds all melanocortins, including γ -MSH. The recent

discovery of synthetic MC-R agonists and antagonists has helped elucidate specific *in vivo* functions of the melanocortin system. The lack of selective ligands for various MC-R subtypes is still a major setback in this effort. Nevertheless, ligand-receptor studies are instrumental in determining whether selective pharmacological targeting of the MC-Rs will ultimately have any therapeutic benefits.

The two receptor subtypes (i.e. MC1 and MC4-R), which are relevant to the mechanism of mahuang action, are discussed in more detail in the next section.

Table 2. Melanocortin receptor distribution, biological function, and pharmacology.

Receptor Subtype	Site of Action	Ligand	Biological Function
MC1-R	Melanocyte	α -MSH = β -MSH = ACTH > γ -MSH > ACTH ₄₋₁₀	Pigmentation
MC2-R	Adrenal cortex	ACTH	Steroidogenesis, lipolysis
MC3-R	CNS, stomach, duodenum, placenta, and pancreas	γ -MSH = γ -MSH = α -MSH = β -MSH = ACTH	Natriuresis
MC4-R	Adult CNS, spinal cord, fetal brain, spinal cord, autonomic nervous system, and adrenal medulla	α -MSH = β -MSH = ACTH > ACTH ₄₋₁₀ = γ -MSH > ACTH ₄₋₁₀	Energy and glucose homeostasis, anti-pyresis, anti-inflammation
MC5-R	Exocrine glands, skin, skeletal muscle, lung, adrenal gland, thymus, bone marrow, spleen, liver, thyroid, stomach, kidney, testis, ovary, and uterus	α -MS > β -MSH = ACTH > γ -MSH > ACTH ₄₋₁₀	Sebum secretion, porphyrin synthesis (Harderian gland), protein secretion (lacrimal gland), thermoregulation

3.2. MC1-R

The *extension* locus encodes the first member of the melanocortin receptor family, MC1-R. The identity of cloned MC1-Rs among various mammalian species is fairly high (70%, Figure 3). Originally designated as MSH-R, this melanocortin receptor subtype is expressed primarily in hair follicles and its main role is control of pigmentation (Mountjoy et al., 1992; Robbins et al., 1993). The rate limiting enzyme of eumelanin (black pigment) synthesis is the tyrosinase, which is regulated both transcriptionally and postrationally by cAMP. α -MSH and other POMC-derived melanotropic peptides bind to the Gs-coupled MC1-R and subsequently raise intracellular cAMP levels and activate the tyrosinase enzyme. α -MSH is the preferred ligand for MC1-R activation in most species; human MC1-R, however, binds α -MSH and ACTH equally well. The human receptor has, therefore, evolved to be super-sensitive to melanotropins (Mountjoy, 1994). This could be due to the fact that, unlike most mammals, adult humans lack the intermediate pituitary, the site of ACTH processing to α -MSH. As a result, circulating α -MSH is not detected in human serum.

Melanotropins, produced by the pituitary, are known to stimulate eumelanin synthesis in the skin; they are not necessary, however, for long term maintenance of eumelanogenesis. Hypophysectomized C57BL/6J mice, for instance, do not lose the ability of synthesizing eumelanin (Geschwind et al., 1972). Local production of POMC-derived melanocortin peptides has now been demonstrated to take place in hair follicles, especially in keratinocytes (Schauer et al., 1994). Thus, it may be possible that hair

follicle cells, rather than the pituitary, are the main sites of melanotropin synthesis and regulators of the pigmentation process.

MC1-R was the first GPCR to be identified as containing naturally-occurring mutations (Robbins et al., 1993). Functional variants of the MC1-R have now been found in many species, including rodents, dog, cattle, fox, sheep, guinea pig, panther, as well as humans (Figure 4). The pharmacology of MC1-R variants has been thoroughly investigated; these studies confirm, for the first time, the existence of GPCRs that are constitutively activated by naturally-occurring mutations (Table 3). In rodents, for instance, two dominant *extension* alleles, E^{so} and E^{so-3J} , have been described that encode constitutively active MC1-Rs; both receptors are 30-50% activated in the absence of any ligand and are associated phenotypically with an all-black coat color. The *sombre* mutation is the result of a Glu⁹² to Lys change in TM2 whereas the *sombre-3J* mutation is a Leu⁹⁸ to Pro change in the same region (Robbins et al., 1993). By contrast, the recessive yellow *e* allele encodes a non-functional, truncated receptor as a result of a frameshift mutation at position 183, located between TM4 and TM5, (Robbins et al., 1993). In bovines, genetic studies have identified a dominant E^D allele for black coat color and a recessive *e* mutation for red pigmentation. As in the mouse, a Leu⁹⁹ to Pro change (E^D) results in a constitutively active MC1-R, whereas a frameshift mutation caused by a deletion at position 104 is responsible for the *e* phenotype (Klungland et al., 1995). Furthermore, a dominant extension allele (E^A) has been described in Alaska Silver foxes with dark pigmentation, which is the result of a Cys¹²⁵ to Arg mutation and generates a constitutively activated MC1-R as well (Vage et al., 1997). Genetic analysis of the

extension locus in guinea pigs indicates that the tortoiseshell coat pattern is due to homozygosity of a recessive e^p allele, which is associated with a large deletion in the MC1-R (Cone, 2000). Finally, sequence analysis of the MC1-R cloned from a panther with a dominant black coat color revealed an Arg¹⁰⁶ to Leu change that may result in a constitutively active receptor; this prediction, however, has yet to be confirmed by *in vitro* pharmacology studies.

A large number of MC1-R mutations has been identified in humans (Table 3); they are usually changes in TM2 and are associated with red hair and fair skin (Box et al., 1997; Schioth et al., 1999). It is not entirely clear at this time whether these mutations are responsible for a loss of MC1-R function in humans. Several of them appear to be polymorphisms since the encoded MC1-Rs have a normal *in vitro* pharmacology (Table 3). Others proved to be less responsive to α -MSH, although they maintained fairly normal ligand affinity (Table 3) (Schioth et al., 1999). These particular receptors were unable to activate adenylyl cyclase in response to α -MSH stimulation as potently as the wild-type receptor (Schioth et al., 1999). None of the mutant receptors displayed a complete loss of ligand binding; the Arg¹⁴²His and Asp²⁹⁴His variants, however, showed a slight reduction in the affinity for α -MSH (Schioth et al., 1999). In addition, α -MSH was shown to have no effect in melanocyte cultures from red hair/fair skin individuals (Hunt et al., 1996), suggesting the existence of an MC1-R defective in either ligand binding or signal transduction. However, comparison of MC1-R genotypes in dizygotic twin pairs discordant for red hair color indicates that the *MC1-R* gene cannot be solely responsible for the red hair phenotype, since five of the thirteen pairs tested had both haplotypes

identical (Box et al., 1997). This result suggests the existence of additional modifier genes that contribute to the development of red hair and fair skin in humans. Mutations in MC1-R are therefore necessary, but not sufficient, for red hair production (Box et al., 1997).

Figure 3. Protein sequence alignment of mammalian melanocortin 1 receptors (MC1-Rs).

The alignment includes the amino acid sequences of mouse, human, bovine, panther, fox, and chicken MC1-Rs. Regions of high homology in the transmembrane (TM) and extracellular loops are featured in blue and red, respectively.

{-----TM-1-----}

MMC1R 1 MSTQEPQKSLVGSLS--NATSHLGLATNQSEPWCLYVSIPDGLFSLGLVSLVENVLVVI
HMC1R 1 MAVQGSQRRLLGSLNSTPTAI PQLGLAANQTGARCLEVSI SDGLFSLGLVSLVENALVVA
BMC1R 1 MPALGSQRRLLGSLNCTPPATLPFTLAPNRTGPQCLEVSSLDGLFSLGLVSLVENVLVVA
PMC1R 1 MSVQGP-RXLLGSXNSTSPAAPRLGLAANQTGPRCLEVSVPDGLFSLGLVSVVENVLVVA
FMC1R 1 MSGQGQRRLLGSPNATSPPTPHFKLAANQTGPRCLEVSI PDGLFSLGLVSVVENVLVVA
CMC1R 1 MSMLAPLR-LVREPWNASEGNQSNATAGAGGAWCQGLD-IPNELFLTGLVSLVENLLVVA

{-----TM-2-----}

MMC1R 60 AITKNRNLHSPMYFICCLALSDLMVSVSIVLETTIILLLEVGILVARVALVQQLDNLIDV
HMC1R 62 TIAKNRNLHSPMYCFICCLALSDLLVSGTNVLETAVILLLEAGALVARAVLQQLDNVIDV
BMC1R 62 AIAKNRNLHSPMYFICCLAVSDLLVSVSNVLETAVMLLLEAGVLATQAQAVVQQLDNVIDV
PMC1R 61 AIAKNRNLHSPMYFICCLAVSDLLVSVSSVLETAVMLLLEAGTLAGRAAVVQQLDDVIDV
FMC1R 62 AIAKNRNLHSPMYFICCLAVSDLLVSVTNVLETAVMLLVEAGALAAQAQAVVQQLDDI IDV
CMC1R 60 AILKNRNLHSPTYFICCLAVSDNLVSVSNLAKTLEFMLLMEHGVLVIRASIVRHMNDVIDM

---TM-3-----} {-----TM-4-----}

MMC1R 121 LICGSMVSSSLCFLGIIAIDRYISIFYALRYHSIVTLPARRAVVGIWMVSIVSSTLFITYY
HMC1R 123 ITCSSMLSSSLCFLGAIAVDRYISIFYALRYHSIVTLPAPRAVAAIIVASVVFSTLFIAYY
BMC1R 123 LICGSMVSSSLCFLGAIAVDRYISIFYALRYHSVVTLPRAWRIIAAIIVASILTSLLFITYY
PMC1R 122 LVCGAMVSSSLCFLGAIAVDRYISIFYALRYHSIVTLPRAWRAISAIIVASVLSSTLFIAYY
FMC1R 123 LICGSMVSSSLCFLGAIAVDRYLSIFYALRYHSIVTLPRAWRAISAIIVASVLSSTLFIAYY
CMC1R 121 LICSSVSSSLSFLGVIAVDRYITIFYALRYHSIMTLQRAVVTMASVWLASTVSSSTVLITYY

{-----TM-5-----}

MMC1R 182 KHTAVLLCLVTFFLAMLALMAILYAHMFTRACQHVQGIAQLHKRRRSIRQGFSLKGAATLT
HMC1R 184 DHVAVLLCLVVFFLAMLVLMVAVLYVHMLARACQHAQGIARLHKRQRPVHQGFGLKGAVTLT
BMC1R 184 NHKVIILCLVGLFTAMLALMAVLYVHMLARACQHARGIARLQKRQRPVHQGFGLKGAATLT
PMC1R 183 DHTAVLLCLVTFVAMLVLMVAVLYVHMLCSTCQHAXGTARLHKRQRPVHQGLGLKGAATLT
FMC1R 184 NHTAVLLCLVSEFFVAMLVLMVAVLYVHMLARARQHARGIARLRKRQHSVHQGFGLKGAATLT
CMC1R 182 RNNAILLCLIGFFLFMLVLMVLYIHMFFALACHHVRSSSQK-QPTIYRTSSSLKGAVTLT

----TM-6-----} {-----TM-7-----}

MMC1R 243 ILLGIFFLCWGPFFLHLLIIVLCQPQHPTCSCIFKNFNLFLLLIIVLSSTVDPLIYAFRSQEL
HMC1R 245 ILLGIFFLCWGPFFLHLTLIVLCPEHPTCGCIFKNFNLFLALIICNAIIDPLIYAFHSQEL
BMC1R 245 ILLGVFFLCWGPFFLHLSLIVLCQPQHPTCGCIFKNFNLFLALIICNAIVDPLIYAFRSQEL
PMC1R 244 MLLGIFFLCWGPFFLHLSLMVLCPRHPICGCVFKNFNLFLTLIICNSIVDPLIYAFRSQEL
FMC1R 245 ILLGIFFLCWGPFFLHLSLMVLCQPQHPICGCVFQNFNLFLTLIICNSIIDPFIYAFRSQEL
CMC1R 243 ILLGVFFICWGPFFFLILIVTCPTNPFCTCFPSYFNLFLILIICNSVVDPLIYAFRSQEL

MMC1R 304 RMTLKEVLLCSW
HMC1R 306 RRTLKEVLTCSW
BMC1R 306 RKTLQEVLLQCSW
FMC1R 306 RKTLQEVLLCSW
CMC1R 304 RRTLREVVLCSW

Figure 4. Naturally-occurring mutations in mammalian MC1-Rs.

- A.** Functional MC1-R variants are illustrated using the murine receptor as a model. Identical and conserved residues among all melanocortin receptors are featured in red and yellow, respectively. Blue residues indicate naturally-occurring mutations.
- B-E.** Mammalian extension and agouti phenotypes as illustrated in rodents (B), cattle (C), foxes (D), and sheep (E).

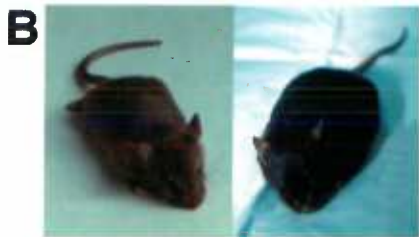
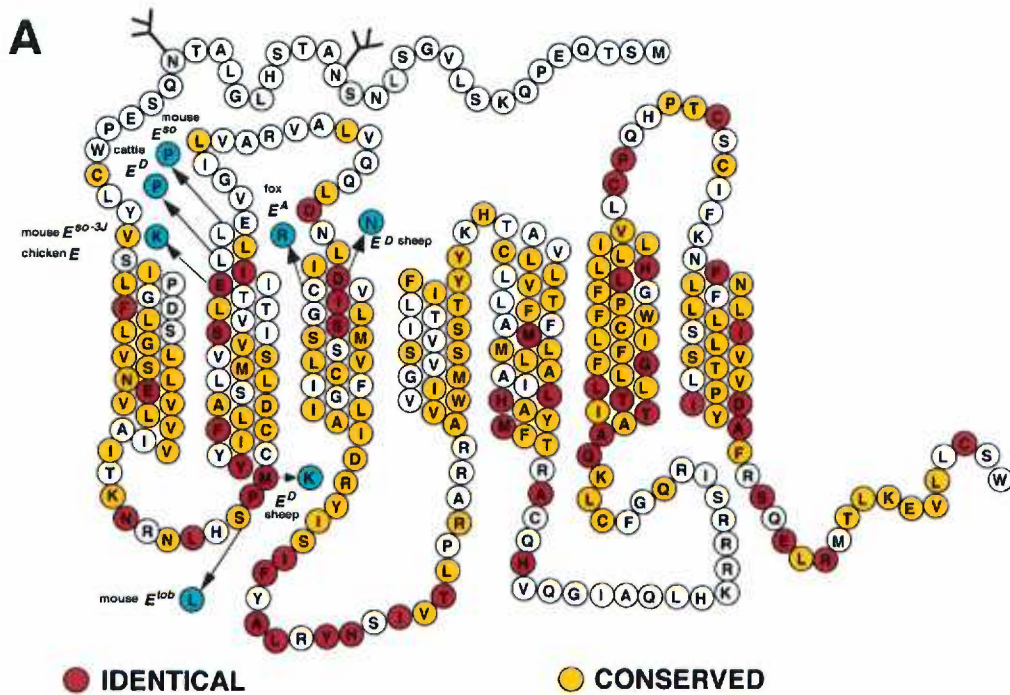


Table 3. Pharmacology of naturally-occurring MC1-R variants.

Species	Mutation	Type of Inheritance	Phenotype	Pharmacology	References
Mouse	E ^{so} (Leu ⁹⁸ to Pro)	Dominant	Black	Constitutively active	(Robbins et al., 1993)
Mouse	E ^{so-3J} (Glu ⁹² to Lys)	Dominant	Black	Constitutively active	(Robbins et al., 1993)
Mouse	E ^{tob} (Ser ⁶⁹ to Leu)	Dominant	Black	Slightly elevated basal activity, hyperactive receptor	(Robbins et al., 1993)
Mouse	e (Frameshift at His ¹⁸³)	Recessive	Yellow	Loss of function	(Robbins et al., 1993)
Bovine	E ^D (Leu ⁹⁹ to Pro)	Dominant	Black	Constitutively active (predicted)	(Klungland et al., 1995)
Bovine	e (Deletion at Gly ¹⁰⁴)	Recessive	Red	Loss of function (predicted)	(Klungland et al., 1995)
Sheep	E ^D (Met ⁷³ to Lys, Asp ¹²¹ to Asn)	Dominant	Black	Constitutively active	(Cone, 2000)
Pig	E ^{D1} (Val ⁹² to Met, Leu ⁹⁹ to Pro)	Dominant	Dark	Constitutively active (predicted)	(Cone, 2000)
Pig	E ^{D2/E^P} (Asp ¹²¹ to Asn)	Dominant	Dark	Decreased ligand affinity	(Cone, 2000)
Pig	e (Ala ¹⁶¹ to Val, Ala ²⁴⁰ to Thr)	Recessive	Red	Loss of function (predicted)	(Cone, 2000)
Horse	e (Ser ⁸³ to Phe)	Recessive	Light chestnut	Loss of function (predicted)	(Cone, 2000)

Fox	E^A (Cys ¹²⁵ to Arg)	Dominant	Dark	Constitutively active	(Vage et al., 1997)
Guinea pig	e^p (Gene deletion)	Recessive	Tortoiseshell pattern	Loss of function (predicted)	(Cone, 2000)
Panther	E^p? (Arg ¹⁰⁶ to Leu)	Dominant?	Black	Constitutively active (predicted)	(Cone, 2000)
Human	E (Asp ⁸⁴ to Glu, Val ⁹² to Met)	Polymorphism	Red hair/fair skin	Normal function	(Box et al., 1997; Schioth et al., 1999)
Human	? (Arg ¹⁵¹ to Cys, Arg ¹⁶⁰ to Trp, Val ¹⁶⁰ to Leu)	?	Red hair/fair skin	Normal ligand affinity, less activation by α -MSH	(Box et al., 1997; Schioth et al., 1999)
Human	? (Arg ¹⁴² to His, Asp ²⁹⁴ to His)	?	Red hair/fair skin	Decreased ligand affinity, less activation by α -MSH	(Box et al., 1997; Schioth et al., 1999)

3.3. MC4-R

The highly conserved MC4-R is found in all regions of the CNS, including the cortex, thalamus, hypothalamus, brainstem, as well as in the spinal cord (Cone, 2000; Mountjoy et al., 1994). MC4-R is more widely expressed in the brain than MC3-R; MC4-R is found, for instance, in both parvicellular and magnocellular divisions of the paraventricular hypothalamic nucleus (PVH), which has been implicated recently in the central control of energy homeostasis (Cowley et al., 1999). Targeted disruption of the murine MC4-R results in an obesity and diabetes phenotype that closely resembles the agouti-induced (A^Y) syndrome (Huszar et al., 1997). In addition, intra-PVH administration of an MC3/4-R agonist, MTII, reduces food intake and stimulates metabolic rate (Cowley et al., 1999). Interestingly, MC4-R has also been implicated in endotoxin-induced anorexia (Huang et al., 1999). These data provide evidence for the involvement of the melanocortin system, and MC4-R in particular, in the regulation of feeding behavior and energy expenditure. A number of MC4-R mutations have recently been demonstrated to co-segregate with a dominantly-inherited form of human obesity; this phenomenon and its implications are discussed in more detail later in the chapter.

Numerous functions have been assigned to MC4-R, aside from its regulation of energy homeostasis. For instance, MC4-R mediates the antipyretic role of central melanocortins during endotoxin-induced fever (Huang et al., 1997; Huang et al., 1998). Furthermore, endogenous melanocortins have now been implicated in the suppression of both acute and chronic inflammation (experimental arthritis) (Ceriani et al., 1994a; Ceriani

et al., 1994b). The anti-inflammatory effects of α -MSH are presumed to be centrally mediated, possibly via MC4-R in the septum (Glyn-Ballinger et al., 1983). In addition, MC4-R is at least partially responsible for the hypotensive and bradycardic effects elicited by the release of endogenous melanocortins (α -MSH) from arcuate neurons (Li et al., 1996). The pressor response and tachycardic effects elicited by central γ -MSH administration are, however, mediated by an as yet unidentified melanocortin receptor (Li et al., 1996). In addition, grooming behavior has now been demonstrated to be controlled by the melanocortin system, possibly via activation of the MC4-R (Adan et al., 1999). Finally, melanocortins have previously been shown to antagonize opiate-induced analgesia, dependence, and tolerance (Alvaro et al., 1997; Alvaro et al., 1996). Decreased melanocortin function, via downregulation of MC4-R expression in brain regions that mediate opiate addiction (i.e. striatum and periaqueductal gray) is presumed to account for this phenomenon (Alvaro et al., 1996).

4. AGOUTI-THE FIRST EXAMPLE OF A NATURALLY-OCCURRING ANTAGONIST OF GPCRs

4.1. *Discovery of Agouti*

The murine *agouti* gene was discovered in 1992 by positional cloning. The key to its cloning was finding a radiation-induced chromosomal inversion that mapped near the *agouti* locus on chromosome 2; this inversion created breakpoints in both *agouti* and a closely linked locus, designated as the *limb deformity* (*ld*) locus (Bultman et al., 1991; Jackson, 1993). As the *ld* gene was already cloned at the time, it became fairly easy to identify the *agouti* gene. It was thus discovered that the chromosomal inversion interrupted the third intron of an 18 kb gene, which appeared to encode a small 131 amino acid protein (Bultman et al., 1991; Jackson, 1993).

Agouti turned out to be a paracrine-signaling factor, secreted by dermal papillae cells, adjacent to melanocytes, which acted within the hair follicle microenvironment to block melanocortin action at MC1-R (Bultman et al., 1992; Lu et al., 1994). Binding of α -MSH to the receptor triggers an increase in cAMP levels, followed by tyrosinase activation and eumelanin production. In the presence of agouti the opposite is true: eumelanin synthesis is shut down and the default pathway, which has pheomelanin as the final product, is activated. There are now more than twenty dominant, recessive, and pseudoagouti alleles that have been identified in rodents, foxes, and cattle, with interesting functional variations from species to species. In rodents *agouti* is expressed only in skin

and testis. In humans, however, it has a wider pattern of distribution being expressed in adipose tissue, testis, ovary, heart and at lower levels in foreskin, kidney, and liver (Kwon et al., 1994; Wilson et al., 1995). Thus far, no evidence has linked agouti to human pigmentation; its biological function in humans remains to be investigated. Most of our present knowledge of agouti structure and function comes from experiments performed on rodents. A synopsis of these murine studies is presented in the next sections.

4.2. Regulation of Murine Agouti Gene Expression

Agouti gene expression is regulated in mice in a regional and temporal fashion to create a differential distribution of yellow and black pigment in individual hair shafts and throughout the body (Miller et al., 1993; Vrieling et al., 1994). Examples of murine *agouti* alleles written in their order of potency are the *lethal yellow* (A^Y), *white-bellied agouti* (A^w), wild-type (A), *black-and-tan* (a^t), and *non-agouti* (a) (Miller et al., 1993; Vrieling et al., 1994). The *agouti* phenotype, which is the true coloration of wild-type mice and characterizes animals with A and A^w alleles, consists of hairs with subapical yellow or tan bands on an otherwise black background. Little difference is seen between dorsal and ventral pigmentation in mice homozygous for the A allele. By contrast, the presence of A^w and a^t alleles creates regional differences in pigment distribution, with ventral surfaces lighter due to increased deposition of phaeomelanin (Miller et al., 1993; Vrieling et al., 1994).

A detailed genetic analysis of the different murine *agouti* alleles has led to the discovery of multiple *agouti* transcripts. Alternative processing of *agouti* mRNA is due to insertions in the intronic regions of A^w , a^t , and a alleles of retrovirus-like transposable VL30 elements (Bultman et al., 1994; Vrieling et al., 1994). The newly inserted sequences are of different sizes depending on allele type. The 11 kb insertion in the a allele includes a complete VL30 element (5.5 kb) and an additional genomic fragment of 4.5 kb, flanked by two 526 bp direct repeats. The 6 kb insertion in the a^t allele contains a VL30 element (5.5 kb) and a single 526 bp direct repeat. Finally, the 0.6 kb insertion in the A^w allele

consists of only one VL30 LTR. Interestingly, all inserts integrate at the same position and allow the *agouti* gene to retain its coding exons (Bultman et al., 1994; Vrieling et al., 1994). Therefore, the multiple *agouti* transcripts vary in their 5' non-coding sequences but they all encode the same protein. The first class of transcripts (transcript I) is expressed in the dorsal and ventral skins of A/A , A^w/A , and A^w/a animals (Bultman et al., 1994; Vrieling et al., 1994). Gene expression of transcript I is restricted to the mid-phase of the hair-growing cycle and is associated phenotypically with subapical-yellow banded hairs throughout the body. The second class of transcripts (II) is expressed in the ventral skins of A^w/A , A^w/a , and a^t/a^t animals, is not temporally restricted, and is responsible phenotypically for the lighter ventral pigmentation seen in A^w and a^t animals (Bultman et al., 1994; Vrieling et al., 1994). An interesting example of negative gene regulation is the recessive *non-agouti* (a) allele. Mice homozygous for the a allele have an all-dark phenotype with a few ventral phaeomelanin hairs scattered around the pinnae, mammae, and perineum (Silvers, 1979). The 11 kb insertion in the first intron of the a allele downregulates the production of either form of *agouti* transcripts (Bultman et al., 1994; Vrieling et al., 1994). Why is transcription differentially regulated, though, depending on insert size? Neither transcript (I or II) is synthesized for the a allele, form II only is allowed for a^t , whereas A^w retains both transcripts. The puzzle was easily solved once the molecular characterization of *agouti* was completed.

The genomic organization of the murine *agouti* gene is rather complex. It consists of three coding exons designated as 2, 3, and 4, as well as four non-coding exons: 1A, 1A', 1B, and 1C, located upstream (Bultman et al., 1994; Vrieling et al., 1994) (Figure 5). This

intricate pattern of gene regulation is achieved through the existence of alternatively spliced *agouti* transcripts that differ in their 5' untranslated exons and are controlled by two different sets of regulatory elements. Type I transcripts contain non-coding exons, 1B or 1C, and are regulated by temporal (hair-cycle-specific) elements (Vrieling et al., 1994) (Figure 5). Gene expression of transcript I is restricted to the mid-phase of the hair-growing cycle and is associated phenotypically with subapical-yellow banded hairs throughout the body (Vrieling et al., 1994). In contrast, type II transcripts contain non-coding exons, 1A and 1A', and are under the control of regional (ventral-specific) promoter elements (Vrieling et al., 1994) (Figure 5). The second class of transcripts is responsible phenotypically for the lighter ventral pigmentation seen in several *agouti* strains (i.e. *white-bellied agouti*) (Vrieling et al., 1994).

Insertion of a large 11 kb sequence in the intron between exon 1C and the first coding exon (i.e. exon 2) of the *a* allele results in down-regulation of transcription from either promoter. Integration of a smaller 6 kb insert (*a'* allele) allows ventral-specific expression only. Finally, insertion of an even smaller 0.6 kb fragment at the same position (*A^w* allele) does not seem to interfere with either regulatory elements, as a result *A^w/A* and *A^w/a* animals produce both transcripts (I and II). Based on the molecular analysis of the various *agouti* alleles, Bultman *et al.* suggest that *A^w* is in fact the true wild-type allele whereas *A* is a loss-of function mutation, which fails to produce type II transcripts (Bultman et al., 1994). This conclusion is in agreement with the phenotype displayed by the majority of wild-type *agouti* mice, which show a lighter ventral pigmentation (Silvers, 1979). The molecular characterization of the different *agouti* alleles

helps also to explain the high rate of spontaneous mutations that occur between a and a^t or a and A^w , respectively. Reversion of a to a^t or A^w is proposed to take place through a mechanism of homologous recombination that utilizes the 526 bp direct repeats (DTRs) or the long terminal repeats (LTRs) of the VL30 transposable elements, respectively, (Bultman et al., 1994) (Figure 6). The *agouti* locus is characterized, therefore, by great genetic complexity. The existence of multiple control elements that regulate alternatively spliced *agouti* transcripts makes possible an intricate pattern of gene regulation and accounts for the variability of *agouti* pigmentation.

Figure 5. Regulation of murine *agouti* gene expression.

Two sets of regulatory elements (hair-cycle and ventral-specific) control the alternative use of untranslated 5' *agouti* exons (1B-C and 1A-A').

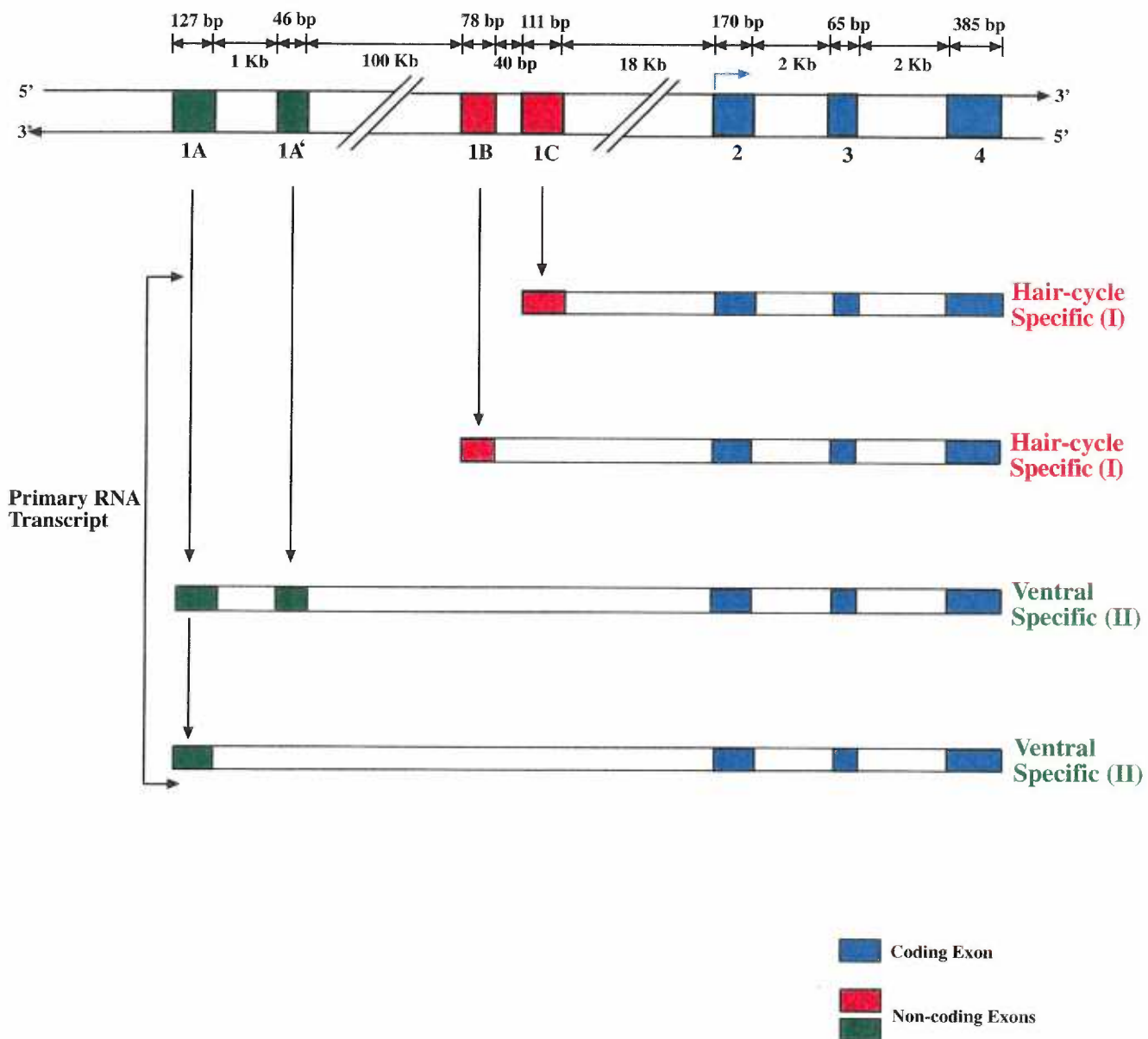
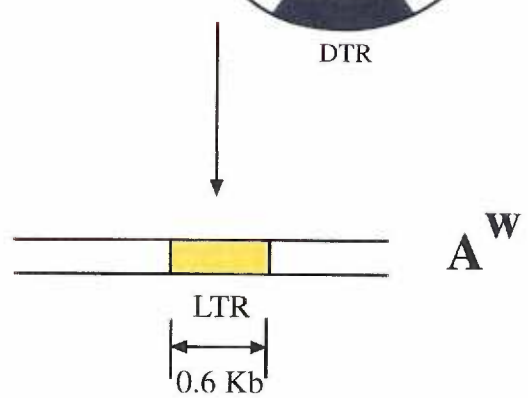
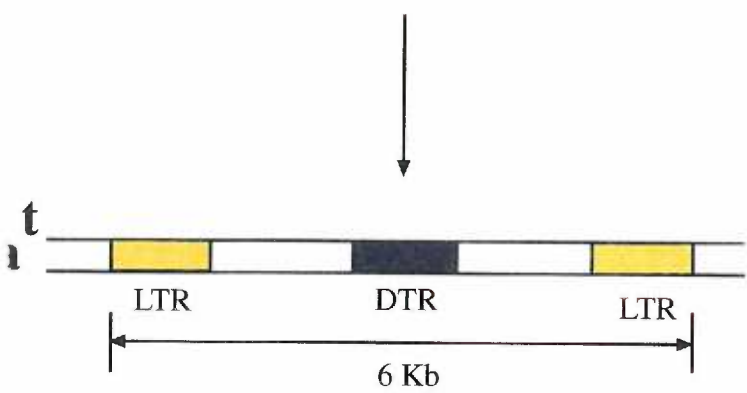
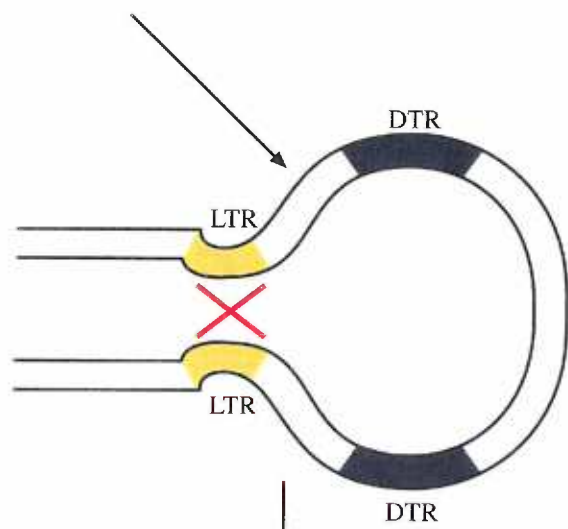
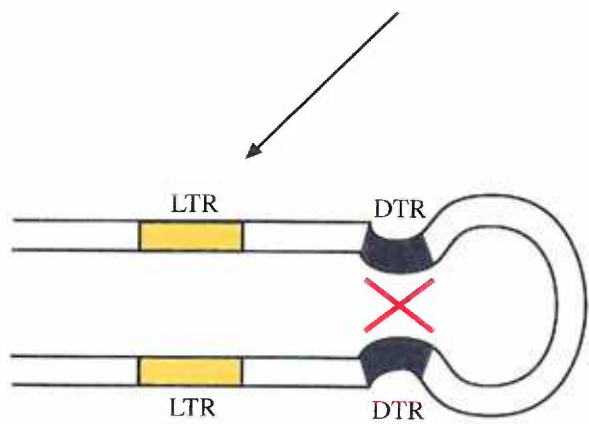
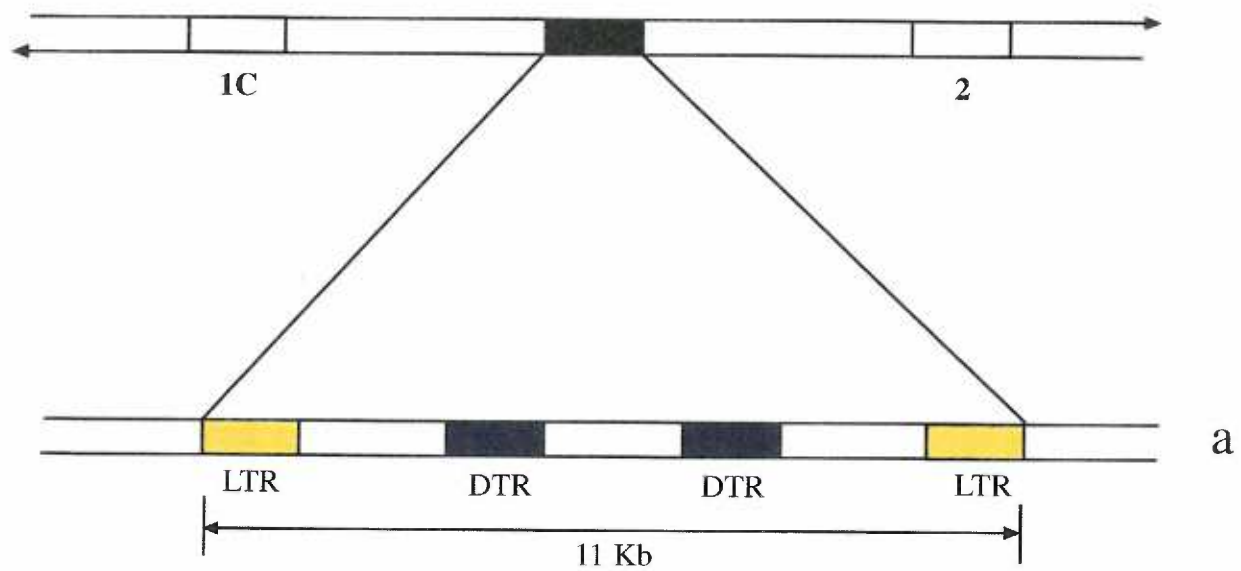


Figure 6. Reversion of a to a^t or A^w allele takes place through a mechanism of homologous recombination.

The ability of the a allele to mutate to a^t or A^w is the result of a homologous recombination process that utilizes either the 526 bp direct repeats (DTRs) or the long terminal repeats (LTRs) of the VL30 transposable elements, respectively.



4.3. *Structural Characteristics of Murine Agouti*

Despite its genetic complexity, the *agouti* locus encodes a small protein of only 131-amino acids that is fairly conserved among various species (Figure 7). Agouti displays the structural characteristics of a secreted protein having a hydrophobic signal sequence and lacking any transmembrane domains. The prominent structural features of the mature protein are an N-terminal signal peptide, a highly basic middle region, and a C-terminal domain rich in cysteine (Cys) and proline (Pro) residues (Bultman et al., 1994). Biochemical analysis of the agouti protein shows that it is highly glycosylated and very stable to thermal denaturation (Willard et al., 1995). The spacing pattern of the 10 Cys residues present in the C-terminus is reminiscent of cone snail (conotoxins) and spider toxins (plectoxins), suggesting a conserved three-dimensional motif. Based on this structural similarity it has been postulated that all Cys residues of the agouti protein are engaged in disulfide bonds (Willard et al., 1995).

Figure 7. Amino acid sequence alignment of mammalian agouti proteins.

The alignment includes amino acid sequences of the murine, human, and fox agouti proteins. The three coding exons of agouti are shown in blue, green, and red, respectively.

Exon 2

M-agouti	1MDVTRL LL LATLV S FLCFF T VHSHLALEETLGDDRSLRSN S SMNS
H-agouti	1MDVTRL LL LATLLV F LCFF T ANSHLPPEEKL R DDRSLRSN S SVNL
F-agouti	1MNIFR LL LATLLV S LCFLTAYSHLA-EEKPKDDRSLRSN S SVNL

Exon 3

M-agouti	45LDFSSVSIVALNKK S KKI S RKEAEK R KRSSK KK ASMKKVA--RP
H-agouti	45LDVPSVSIVALNKK S KQIGRKAEEK-KRSSK KE ASMKKVV--RP
F-agouti	45LDFPSVSIVALNKK S KKI S RKEAEK-KRSSK KK ASMKNKARPRP

Exon 4

M-agouti	87PPPS--PCVATRD S CKPPAPACCDPCASCQCRFFGSACTCRVLN
H-agouti	87RTPLSAPCVATRNSCKPPAPACCDPCASCQCRFFRSACSCRVL S
F-agouti	87PPPN-PCVATRNSCKSPAPACCDPCASCQCRFFRSACTCR----

M-agouti 129PNC

H-agouti 129LNC

F-agouti 129---

4.4. Functional Characterization of Murine Agouti

4.4.1. In Vitro Effects of Agouti

In vitro studies using recombinant mouse agouti protein proved that agouti was a potent melanocortin antagonist (nM range) at two different MC-R subtypes: 1 ($K_{I\text{ app}} = 2.6 \pm 0.8$ nM) and 4 ($K_{I\text{ app}} = 54 \pm 18$ nM), a relatively weak antagonist at MC3-R ($K_{I\text{ app}} = 190 \pm 74$ nM), and a very weak antagonist at MC5-R ($K_{I\text{ app}} = 12,000 \pm 340$ nM) (Kiefer et al., 1998; Lu et al., 1994; Willard et al., 1995). Thus, the ability of the antagonist to compete with α -MSH for binding to melanocortin receptors decreases as follows MC1-R > MC4-R >> MC3-R >>> MC5-R (Kiefer et al., 1998). Pharmacological studies of murine agouti conclude that its mechanism of action is a classical competitive antagonism of melanocortin receptors (Kiefer et al., 1998; Lu et al., 1994; Willard et al., 1995). In addition, a shorter version of agouti, residues 83 through 131, is shown to be as potent an antagonist as the full-length protein (Willard et al., 1995). The Cys-rich C-terminus is therefore deemed sufficient for effective antagonism of melanocortins action *in vitro* as well as *in vivo* (Perry et al., 1996; Willard et al., 1995). The basic domain, on the other hand, appears to play key roles in agouti biogenesis (i.e. protein folding, post-translational processing, sorting, and secretion) and/or in facilitating the interaction with the receptor (Miltenberger et al., 1999).

The mechanism of agouti action shows interesting variations across species. Functional analysis of recombinant agouti-signaling protein (ASIP), the human homologue

of murine *agouti*, indicates a similar pharmacological profile: ASIP is a potent antagonist at human MC1 ($K_{i\text{ app}} = 0.47 \pm 0.06$ nM) and MC4-R ($K_{i\text{ app}} = 0.14 \pm 0.02$ nM), and a relatively weak antagonist at MC3 ($K_{i\text{ app}} = 6.4 \pm 1.1$ nM) and MC5-R ($K_{i\text{ app}} = 1.16 \pm 0.17$ nM) (Yang et al., 1997). Competitive antagonism of ASIP is apparent, however, only towards MC1-R (Yang et al., 1997). By contrast, genetic analysis of fox *agouti* and *extension* variants suggests that *agouti* functions in this case as a negative antagonist (inverse agonist) of MC1-R, rather than as a classical competitive antagonist (Vage et al., 1997). In the mouse, *extension* is epistatic to *agouti*, meaning that constitutively active receptors encoded by dominant *extension* alleles cannot be blocked by *agouti* action. In the fox, however, the opposite is true: *agouti* is able to partially block eumelanin synthesis in the presence of a dominant *extension* allele (Vage et al., 1997).

4.4.2. *In Vivo Effects of Agouti: the Lethal Yellow Syndrome*

Once the *agouti* gene was cloned it became possible to address the molecular basis of A^Y , a dominant allele at the *agouti* locus, and its pleiotropic effects. In doing so scientists were able to reveal a much more complex picture of *agouti* functions than previously thought. It soon became clear that *agouti* and its homologues are part of a general signaling system that extends far beyond the hair follicle and the melanogenesis process. The *lethal yellow* (A^Y) mutation was identified at the turn of the century as the first murine obesity phenotype (Danforth, 1927). Animals heterozygous for the A^Y allele were not only characterized by a yellow coat color but also by late-onset obesity associated with hyperphagia, increased linear growth, and non-insulin dependent diabetes, as well as an

increased propensity for developing tumors [for review see (Yen et al., 1994)]. In addition, it was recognized early on that A^Y homozygosity is associated with embryonic lethality, a phenomenon that has puzzled scientists for many decades.

Genetic analysis shows that A^Y is in fact the result of a chromosomal rearrangement in which the promoter and the first non-coding exon of a closely linked gene, *Raly*, became spliced to exons of the wild-type *agouti* gene (Michaud et al., 1994; Miller et al., 1993). Therefore, similar to a^t and A^w alleles, A^Y maintains the 3' end of the normal gene and encodes the same gene product now under the regulatory control of the *Raly* promoter. Unlike a^t and A^w alleles, which arise through incorporation of novel DNA sequences, A^Y is the result of a large deletion in the *Raly* gene that leaves only the promoter and its first non-coding exon intact (Michaud et al., 1994; Miller et al., 1993). Further analysis of the *Raly* gene indicates that this housekeeping gene is ubiquitously expressed and encodes an RNA-binding protein essential for mRNA processing, which is required for normal development (Michaud et al., 1994; Miller et al., 1993). Once this information was revealed, the pieces of the puzzle started falling into place. First, homozygosity for the A^Y allele results in embryonic lethality due to the absence of the RNA-binding *Raly* protein, which is necessary for blastocyst formation (Michaud et al., 1994; Miller et al., 1993). Secondly, the *agouti* gene, now under the control of the relaxed *Raly* promoter and devoid of temporal and regional restrictions, becomes ectopically expressed. Overexpression of *agouti* in multiple tissues is therefore the cause of the A^Y phenotype. This conclusion is further supported by the ability of *agouti*, under the

control of a β -actin promoter, to recapitulate the A^Y phenotype in transgenic animals (Klebig et al., 1995).

The pharmacological characterization of agouti makes it now easy to understand why ectopic agouti expression *per se* is responsible for the A^Y phenotype. The primary cause of the A^Y syndrome is identified as disruption of melanocortin receptor signaling in both skin and brain. Chronic antagonism by agouti of MC1-R in the skin results in yellow fur, whereas agouti competition at the hypothalamic MC4-R produces obesity. This conclusion is supported by most of the experimental data available to date. The most compelling evidence is the recent finding that MC4-R KO have a phenotype similar to the A^Y syndrome (Huszar et al., 1997); in addition, central administration of MC4-R agonists and antagonists has been shown to stimulate and inhibit feeding behavior, respectively (Fan et al., 1997).

Several studies, however, have proposed an alternative mechanism for agouti action that does not involve melanocortin receptor antagonism [for review see (Zemel, 1998)]. On the basis of structural similarities between agouti and invertebrate neurotoxins, which are known to block calcium channels, it has been speculated that agouti might in fact regulate lipogenesis and insulin release via a calcium-mediated mechanism (Zemel, 1998). In support of this model, both murine and human agouti proteins were shown to cause dose-dependent increases in calcium influx in adipocytes and pancreatic β -cells (Zemel, 1998). Therefore, it may seem that agouti, like invertebrate toxins, is able to modulate intracellular calcium levels by directly regulating calcium

channels. However, there are striking differences not only in their mechanism of action but also in their potency and kinetics. Conotoxins, for example, are rapid and irreversible calcium channels inactivators (Olivera et al., 1991) whereas agouti is a slow-acting, transient activator (Zemel, 1998). Moreover, the increase in lipogenesis that is seen upon transfection of agouti protein in adipocytes can be elicited in the absence of agouti through activation of calcium channels (Zemel, 1998). This suggests that modulation of intracellular calcium levels may simply be secondary to agouti action. According to the calcium hypothesis, development of *agouti*-induced obesity is elicited by a combination of factors that include agouti expression in adipose tissue and hyperinsulinemia (Zemel, 1998). This conclusion is, however, inconsistent with the finding that the MC4-R KO phenotype is more profound than the A^Y syndrome, suggesting that disruption of MC4-R signaling is necessary and sufficient for triggering all aspects of *agouti*-induced obesity. Furthermore, a recent study (Ollmann et al., 1998) indicates that agouti binds directly to MC1-R and that a functional MC1-R is required for agouti signaling. In light of these new findings, direct regulation of calcium channels by agouti seems less likely. It is still possible, however, that agouti binding to MC1-R results in modulation of calcium metabolism through an indirect mechanism.

There is now significant evidence that agouti has additional action targets on the melanocyte aside from MC1-R. This is suggested by the difference in coat color between A^Y and e/e animals, two genetic models that are characterized by a disruption in MC1-R signaling. Agouti overexpression in skin results in a bright yellow pigmentation (A^Y) whereas inactivation of the MC1-R (e) gives rise to a dusty yellow coat color. In

addition, agouti was shown to reduce basal melanogenesis in B16 F1 murine melanoma cells in the absence of α -MSH (Hunt and Thody, 1995). Agouti was thus proposed to function as an inverse agonist (negative antagonist) of the MC1-R by binding to the receptor in the absence of ligand and inhibiting its basal signaling activity (Lefkowitz et al., 1993; Samama et al., 1994). This hypothesis was confirmed by *in vivo* studies of agouti. In the fox, unlike the mouse, *extension* is not epistatic to *agouti*, since areas of red pigment can still be seen in animals carrying one copy of a constitutively activated MC1-R. This phenomenon can be easily explained by the recently proposed allosteric ternary complex model. According to this model, GPCRs are in equilibrium between constrained, inactive (R) and relaxed, active (R*) conformations (Lefkowitz et al., 1993). The active receptor conformation, which couples to G-proteins, is promoted by either agonists or constitutively activating mutations in TM2/TM3 (Samama et al., 1994). Classical competitive antagonists (i.e. mouse agouti) bind equally well to either receptor and block receptor activation by inhibiting ligand binding. Inverse agonists (i.e. fox agouti) have properties opposite to those of agonists, in that they have a higher affinity for the constrained form of the receptor (R) and thus shift the equilibrium towards the inactive state (Samama et al., 1994).

5. AGOUTI RELATED PROTEIN (AGRP)

5.1. *Discovery of AGRP*

The discovery a decade ago of the murine *agouti* gene was intended to bring scientists a step closer to understanding the complexities of mammalian pigmentation. The first of the obesity genes was also uncovered in the process. What followed was an explosion of major discoveries with a dramatic impact on murine as well as human obesity and diabetes. Looking back it seems as if we have found a key for unlocking the neuroendocrine pathways that regulate energy and glucose homeostasis. Recently, a new gene, the *agouti related protein (AGRP)*, was discovered and found to share a striking similarity in structure and function with *agouti*, although the two gene products have different areas of distribution. Identification of a hypothalamic melanocortin receptor, MC4-R, together with AGRP as central components of feeding behavior and metabolism, has helped build a picture, albeit incomplete, of the neuronal pathways involved in energy homeostasis.

Two lines of evidence suggested the existence in the brain of an *agouti*-like protein that would block signaling at central melanocortin receptors, MC3/4-R. First, *in vitro* pharmacology studies found that *agouti* is a highly specific MC4-R antagonist even though *agouti* is not normally expressed in the brain (Blanchard et al., 1995; Lu et al., 1994; Willard et al., 1995). Secondly, central administration of synthetic MC3/4-R antagonists uncovered a functional role for melanocortin antagonists *in vivo*, namely

stimulation of feeding behavior (Fan et al., 1997). It came then as no surprise when a new gene, the *agouti related protein (AGRP)*, was isolated in 1997 based on its homology to agouti (Ollmann et al., 1997; Shutter et al., 1997). The pattern of Cys spacing from the C-terminal agouti region was used to screen a sequence tag database; two genes, murine and human, encoding a protein similar in size and structure to agouti, were thus identified (Ollmann et al., 1997; Shutter et al., 1997).

5.2. *Parallelism Between Agouti and AGRP*

Like agouti, AGRP contains three coding exons; however, depending on the site of expression (central versus peripheral) *AGRP* mRNA transcripts may or may not contain an upstream non-coding exon (Shutter et al., 1997). The genomic organization of the coding exons is similar between agouti and AGRP despite differences in intron/exon junctions (Shutter et al., 1997).

Both agouti and AGRP are 131-aminoacid-proteins with putative signal peptide sequences and Cys-rich C-terminal domains (Ollmann et al., 1997; Shutter et al., 1997) (Figure 8). Unlike agouti, AGRP lacks the central basic sequence and the Pro-rich C-terminal region (Ollmann et al., 1997; Shutter et al., 1997). The strongest homology between the two proteins is within the polyCys domain of the C-terminus. Interestingly, the pattern of Cys spacing that is shared by agouti and invertebrate toxins is also conserved in AGRP (Ollmann et al., 1997; Shutter et al., 1997) (Figure 9). Both agouti and AGRP contain 10 Cys residues, 9 of which are spatially conserved. Like agouti, all

10 of the AGRP Cys residues form disulfide bridges (Bures et al., 1998; Ollmann et al., 1997) that are essential for the protein's structural stability and biological function. Biochemical studies also indicate that AGRP is very stable to thermal denaturation (similar to agouti) as well as acid degradation (Rosenfeld et al., 1998). Furthermore, biophysical characterization of agouti and AGRP shows that both proteins have similar CD spectra, their secondary structure consisting of mainly random coils and β -sheets (Rosenfeld et al., 1998; Willard et al., 1995).

Both agouti and AGRP are competitive antagonists of α -MSH action at melanocortin receptors (Fong et al., 1997; Rossi et al., 1998; Yang et al., 1999b). Likewise, the C-terminus of AGRP, residues 83 through 131, retains the biological activity of the full-length protein *in vitro* (Yang et al., 1999b) as well as *in vivo* (Rossi et al., 1998). Agouti and AGRP differ, though, in their biochemical specificity towards individual receptor subtypes. In contrast to agouti, AGRP is equally potent in inhibiting signaling at central melanocortin receptors, MC3 and MC4-R (binding affinity of human AGRP close to 1 nM for both receptors), very little inhibition is detected at the MC5-R, and virtually no activity at MC1-R (Fong et al., 1997; Rossi et al., 1998; Yang et al., 1999b). Therefore, AGRP is as potent an antagonist at MC4-R as agouti, and a much stronger antagonist at MC3-R.

The tissue distribution of agouti and AGRP differ greatly. The expression of agouti is normally confined to hair follicles whereas AGRP is expressed primarily in the hypothalamus, adrenal medulla, and at low levels in testis, lung, and kidney (Ollmann et

al., 1997; Shutter et al., 1997). Unlike agouti, the localization pattern of human and murine AGRP is strikingly alike (Shutter et al., 1997), indicating similar roles for AGRP in both species. *In situ* hybridization studies show that brain expression of *AGRP* mRNA is confined to neuronal cell bodies localized in the arcuate nucleus of the hypothalamus (Figure 10) (Broberger et al., 1998; Haskell-Luevano et al., 1999; Shutter et al., 1997). These neurons are shown to project to many of the same hypothalamic nuclei to which the arcuate nucleus POMC neurons project (Broberger et al., 1998; Haskell-Luevano et al., 1999) (Figure 10). Furthermore, these nuclei are known to express the two central melanocortin receptors, MC3 and MC4-R (Cowley et al., 1999; Mountjoy et al., 1994; Roselli-Reh fuss et al., 1993).

The potency of AGRP action at MC3/4-R together with their similar distribution pattern suggest that AGRP and not agouti controls their function *in vivo*. Furthermore, the presence of AGRP-immunoreactive fibers in a subset of hypothalamic nuclei (i.e. arcuate, paraventricular, dorsomedial) strongly suggests a key role for AGRP and the melanocortin system in the regulation of energy homeostasis. This conclusion is supported by multiple findings. First, central administration of AGRP is shown to mimic the effect of synthetic MC3/4-R antagonists and stimulate feeding (Rossi et al., 1998). Furthermore, AGRP is able to specifically block the reduction in food intake elicited by α -MSH administration (Rossi et al., 1998). Secondly, overexpression of AGRP in transgenic animals results in an obesity phenotype strikingly similar to that of MC4-R KO or *A^y* mice (Graham et al., 1997; Ollmann et al., 1997). In conclusion, melanocortinergic neurons exert a tonic inhibition on feeding behavior and metabolism

while AGRP counteracts the effect. This tonic inhibition is relaxed as a result of AGRP antagonism at MC4-R and results in the stimulation of caloric intake and energy storage.

Figure 8. Amino acid sequence alignment of murine agouti and agouti-related protein (AGRP).

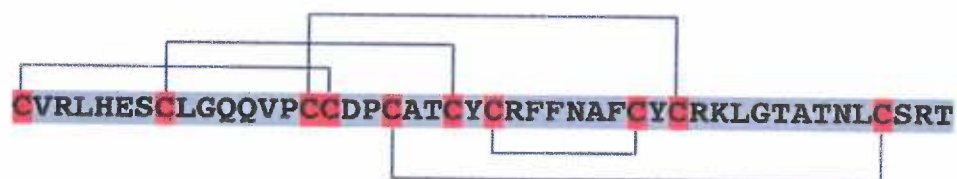
Identical amino acid residues are shown in red. Of particular interest for agouti/AGRP structure and function are the 10 Cys residues (marked by dots) and the conserved RFF triplet (white letters) in the C-terminal domains. The putative signal peptide sequences are colored in yellow and exon boundaries are indicated by arrows.

		Exon 2																				
m-AGRP		MLTAMLLSCVLLLALPPTLGVMGVAPLKGIIRPDQALFPEF																				
m-Agouti		MDVTRLILLATLVSLFCFFTVHSHLALEETLGDDRSLRSNSSMNSLDF																				
	↓	Exon 3										↓	Exon 4									
m-AGRP		PGLSLNG-LKKTADRAEEVLLQKAEALAEVLDPQNRESRSPRRCV																				
m-Agouti		SSVSIVALNKKSKKISRKEAEKKRRSSKKKASMKKVARPPPPSPCV																				
		↑										↑										
			
m-AGRP		RLHESCLGQQVPCCDFCATCYCRFFNAFCYCRKLGATNLCST																				
m-Agouti		ATRDSCKPPAPACCDPCASCQCRFFGSACTCRVLNPNC																				

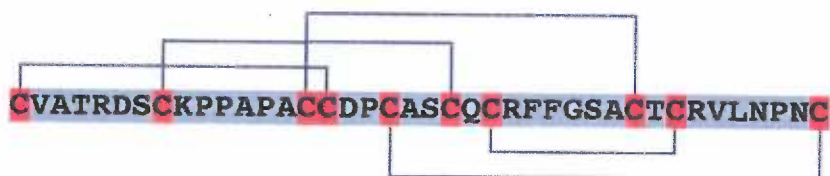
Figure 9. Disulfide arrangement of murine agouti, AGRP, and conotoxin GVIA (Conus glorimaris).

Cys residues are depicted in red. The Cys-spacing pattern and disulfide connectivity of both agouti and AGRP strongly resemble conotoxins.

m-AGRP



m-Agouti

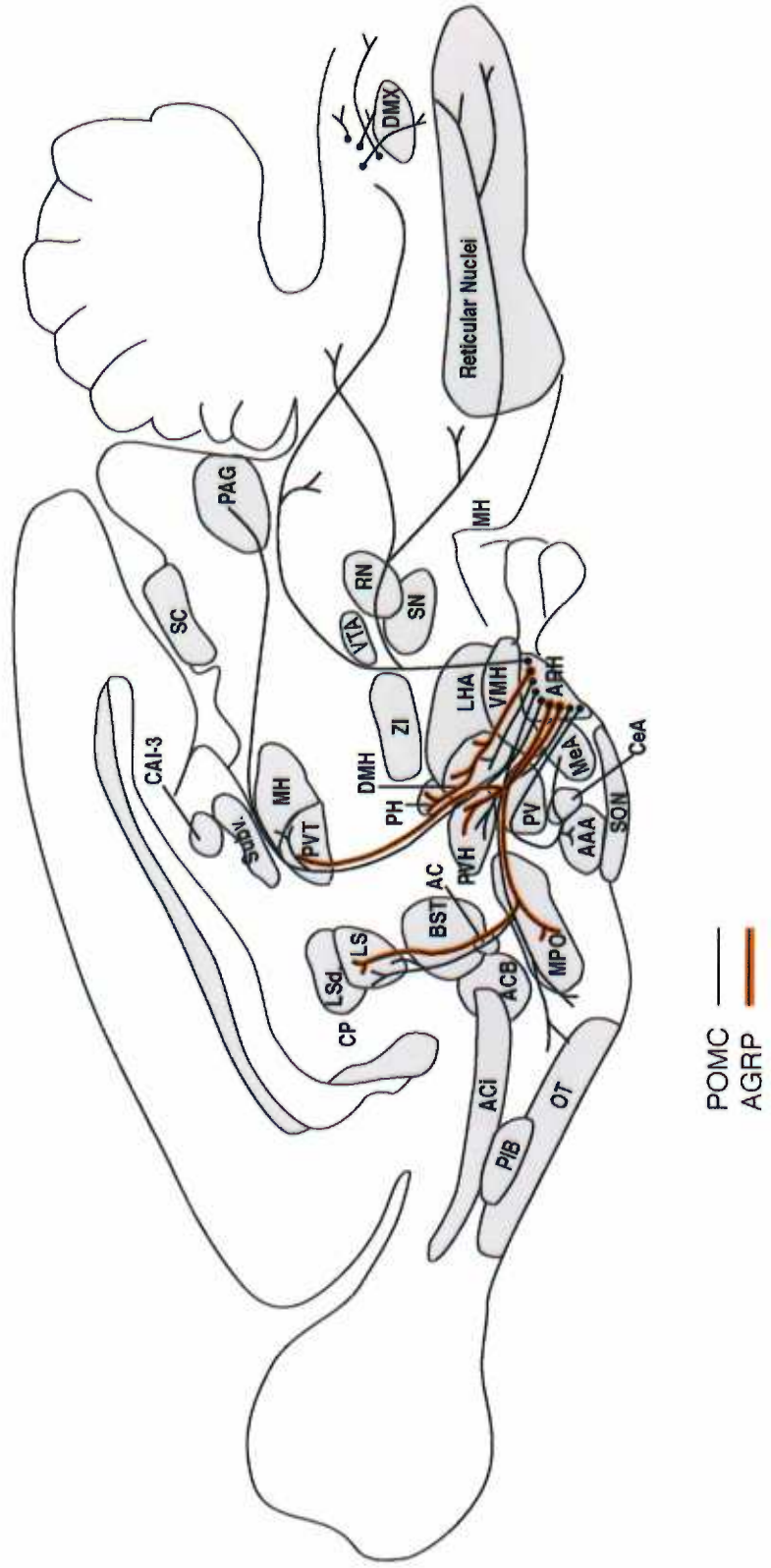


GVIA



Figure 10. POMC and AGRP distribution patterns in the central nervous system (CNS).

Sagittal section of the rodent brain schematically indicating the distribution of POMC-immunoreactive (black lines) and AGRP-immunoreactive (red lines) neuronal fibers. AGRP neurons originating in the arcuate nucleus are shown to project to many of the same CNS sites to which the arcuate nucleus POMC neurons project.



5.3. *Regulation of AGRP Expression by Leptin and Nutritional Status*

Unlike agouti, AGRP is modulated by leptin and nutritional status. Multiple lines of evidence indicate that leptin is in fact a negative regulator of *AGRP* expression. *AGRP* mRNA is upregulated in the absence of leptin (i.e. *ob/ob*) or when leptin levels are low (i.e. fasting) (Mizuno and Mobbs, 1999; Ollmann et al., 1997; Shutter et al., 1997). Central administration of leptin normalizes *AGRP* levels in leptin-deficient *ob/ob* mice but has no effect in leptin-resistant *db/db* animals (Ebihara et al., 1999). In addition, fasting further increases *AGRP* expression in *db/db* but not in *ob/ob* mice (Ebihara et al., 1999; Wilson et al., 1999b). Finally, AGRP levels are downregulated in certain obesity models characterized by chronic hyperleptinemia, such as A^Y , although they are not affected in others: *tubby* and *fat* (Ollmann et al., 1997; Wilson et al., 1999b). It is possible, however, that AGRP downregulation in A^Y animals is in fact the result of agouti overexpression. If ectopic agouti expression mimics the function of AGRP in the central control of energy homeostasis then presence of the first might downregulate the latter via a negative feedback mechanism. In conclusion, leptin action is signaled downstream by the melanocortin system via changes in the ratio between antagonist (AGRP) and agonist (α -MSH) concentration. AGRP is one of several orexigenic peptides that is tightly controlled by leptin levels. In the fed state elevated leptin levels suppress AGRP production and result in decreased food intake as well as increased metabolism. Conversely, during fasting, low leptin levels relax the tight regulatory control that leptin has upon AGRP production; as a result, AGRP becomes upregulated and

stimulates feeding behavior. Interestingly, a recent study proposes that AGRP may represent an important connection between feeding behavior and reproductive function, since AGRP was found to stimulate both systems (Stanley et al., 1999). This finding could potentially explain why a long-term caloric restriction is associated in most species with a decline in their reproduction.

Both AGRP and α -MSH levels are modulated by leptin and nutritional status. AGRP is considered, however, to be more dynamically regulated by metabolic state than POMC. It is AGRP expression that changes dramatically in leptin-deficient *ob/ob* and leptin-resistant *db/db* obesity models: *AGRP* mRNA is increased 5-10 fold (Ollmann et al., 1997; Shutter et al., 1997) compared to a 60-80% reduction in hypothalamic *POMC* level (Mizuno et al., 1998). Furthermore, *AGRP* message is upregulated in models of dietary obesity whereas α -MSH concentration is virtually unchanged in these animals (Harrold et al., 1999). A 24-48 h fasting period is associated with a much more robust increase in hypothalamic *AGRP* mRNA (Ebihara et al., 1999; Mizuno et al., 1999; Mizuno and Mobbs, 1999; Wilson et al., 1999a) than a reduction in *POMC* level (Mizuno and Mobbs, 1999). These data suggest therefore that homeostatic regulation of the melanocortin system is achieved through alterations in antagonist rather than agonist bioavailability.

It is possible that AGRP controls the activity of central melanocortin receptors in a manner similar to regulation of MC1-R signaling by agouti in the skin. Modulating the melanocortin system via changes in antagonist, rather than agonist, levels has certain

advantages. First, the homeostatic system can be more tightly regulated, as AGRP is more restricted in tissue distribution than α -MSH and has a less wide sphere of action. In addition, the functional specificity of AGRP makes it possible for the various melanocortin receptor subtypes to be selectively regulated. AGRP is therefore an attractive target for therapeutic intervention; the development of small molecule inhibitors, which would specifically suppress AGRP action, may lead to more efficient obesity treatments.

5.4. Fine-tuning the Mechanism of Agouti and AGRP Action

Both agouti and AGRP are known to block melanocortin receptor signaling but their mechanism of action is still under debate. The most accepted mechanism for agouti/AGRP action is a classical competitive antagonism of melanocortin receptors. However, several additional mechanisms have been proposed, including inverse agonism (Vage et al., 1997) and direct regulation of calcium channels (Zemel, 1998). Recent studies, however, were able to eliminate some of the controversies surrounding the exact biochemical mechanism of agouti/AGRP action. Ollmann and collaborators clearly demonstrate that MC1-R is indeed an agouti receptor and that presence of a functional MC1-R is absolutely necessary for agouti function *in vivo* (Ollmann et al., 1998). Furthermore, AGRP is shown to bind solely to melanocortin receptors in both conventional binding and photoemulsion assays (Yang et al., 1999b). The two studies indicate that agouti/AGRP and α -MSH bind to melanocortin receptors in a mutually exclusive fashion (Ollmann et al., 1998; Yang et al., 1999b). Finally, direct binding of

AGRP to the MC4-R has been recently demonstrated by protein cross-linking (Khong et al., 1999). It is not clear, however, if the agonist and antagonist compete for the same binding site on the receptor. At first glance, no amino acid sequence similarity between agouti/AGRP and α -MSH seems obvious. Careful comparison of agouti and AGRP C-terminal sequences reveals, however, the presence of a conserved RFF motif that resembles the α -MSH pharmacophore HFRW (Tota et al., 1999). A loop of 8 residues flanked by two Cys residues and including the RFF triplet (residues 110-117 in AGRP, 115-122 in agouti, respectively) is shown to be critical for both agouti and AGRP antagonism at melanocortin receptors (Tota et al., 1999). This octapeptide loop contains therefore most of the structural determinants for melanocortin receptor binding and antagonism. Furthermore, alanine (Ala) scanning mutagenesis of this octapeptide indicates that the RFF motif is the most critical in determining antagonist activity ($IC_{50} = 0.5 \pm 0.1$ nM for AGRP binding to MC4-R whereas IC_{50} for the three Ala mutants are: 67 ± 46 nM for R111A, 61 ± 35 nM for F112A, and 25 ± 13 nM for F113A, respectively) (Tota et al., 1999). The octapeptide loop of the antagonist is therefore proposed to mimic the conformation of α -MSH and interact with the receptor through a similar mechanism (Tota et al., 1999). This model would thus imply that the agonist and antagonist occupy the same binding site on the receptor. An alternative model suggests that the antagonist attaches itself to a different receptor site and blocks ligand binding through an allosteric mechanism. In support of this model it was determined that extracellular loops 2 and 3 of the MC4-R are critical sites for antagonist (AGRP) binding but had little effect on agonist (α -MSH) binding (Yang et al., 1999a). Future studies will concentrate on finding definitive proof in support of either mechanism.

Although agouti and AGRP have been shown to share structural and functional similarities, an intriguing difference in their mechanism of action has been recently reported (Ollmann and Barsh, 1999). This particular study tests the pharmacology of agouti and AGRP in *Xenopus melanophores*, an assay system considered by some accounts to be more sensitive than the 293 HEK or B16 cell lines. The C-terminus of agouti and all AGRP forms examined follow the competitive antagonist profiles that have been previously described. Full-length agouti, however, is characterized by a dual mechanism at the *Xenopus MC1-R*: competitive antagonism of ligand binding by the C-terminus and receptor down-regulation elicited by the N-terminal domain (Ollmann and Barsh, 1999). The reduction in melanocortin signaling is achieved either by receptor internalization or post-translational modification (Ollmann and Barsh, 1999). The results of this study are, however, in disagreement with previous reports, which showed identical pharmacological profiles for both full-length and C-terminal agouti (Willard et al., 1995). It is very likely that the conflicting results reflect in fact the properties of the different cell culture systems used: *Xenopus melanophores* (Ollmann and Barsh, 1999) and mammalian B16 melanoma cells (Willard et al., 1995). It may be that the pharmacological properties described for the N-terminal agouti domain are in fact specific only to the *Xenopus MC1-R*. Future studies employing endogenous cell types that express native melanocortin receptors should give us a better understanding of agouti pharmacology.

It is beyond dispute that clear differences exist between the structure and function of agouti and AGRP. Nevertheless, one cannot help but be amazed at the multitude of similarities displayed by the two proteins. It is uncertain whether agouti and AGRP are

the result of convergent or divergent evolution, and whether additional homologues remain to be discovered. The data available to date suggest remarkable functional similarities, in that both agouti and AGRP appear to function as regulators that antagonize relatively constitutive signaling pathways in the skin and brain, respectively. Further studies will help provide more insight into the intriguing biology of agouti and AGRP.

6. CONTRASTING AGOUTI AND LEPTIN DEFICIENT OBESITY MODELS

6.1. *Leptin and Leptin Receptors*

The concept of the adipostat is based on the existence of an adipose tissue-brain endocrine axis that regulates body weight (Kennedy, 1953). The mediator of this axis is leptin, an adipocyte-secreted circulating hormone that informs the CNS of the energy reserves available in the body (Zhang et al., 1994). Consequently, plasma leptin levels reflect the size of the adipose depot. Caloric restriction and weight loss are associated in both rodents and humans with decreased leptin levels. The brain senses the deviation from the preset weight and activates the orexigenic pathways in the hypothalamus. This results in the stimulation of caloric intake and a decrease in energy expenditure until the animals return to their previous weight. Conversely, in animals fed *ad libitum*, elevated leptin levels trigger the activation of anorexigenic signals in the brain and result in a reduced food intake and increased metabolism.

Animals that carry recessive mutations in the *obese (ob)* and *diabetes (db)* genes display severe obesity syndromes, which bear strong resemblance to each other. It has been proposed, therefore, that these genes encode the ligand and receptor, respectively, for a physiologic pathway that regulates energy intake and expenditure. In support of this proposal, *ob* mRNA was found to be highly expressed in the adipose tissue of *db/db* mice, suggesting that these mutant animals are resistant to the action of the *ob* gene

product (Maffei et al., 1995). Once the *ob* and *db* genes were cloned and fully characterized, it was revealed that they encode the leptin and leptin receptor, respectively (Chen et al., 1996; Tartaglia et al., 1995; Zhang et al., 1994).

The leptin receptor (OB-R) is a single-transmembrane receptor that shows sequence homology and functional similarity to members of the class I cytokine receptor family (Tartaglia et al., 1995). Two alternatively spliced isoforms of the OB-R have been described, they encode receptors that vary in the length of their cytoplasmic domain. The long form of the OB-R is highly expressed in the mouse hypothalamus (arcuate, ventromedial, dorsomedial, paraventricular, and ventral premammillary nuclei) and is coupled to multiple signal transducers in the STAT pathway, including STAT-3, STAT-5, and STAT-6 (Ghilardi et al., 1996; Hakansson et al., 1996; Huang et al., 1996; Mercer et al., 1996a; Tartaglia et al., 1995). The short OB-R form, on the other hand, is expressed at high levels in the mouse choroid plexus and leptomeninges and is unable to activate the STAT pathway (Ghilardi et al., 1996; Mercer et al., 1996a). The long cytoplasmic domain of the OB-R is deemed responsible; therefore, for intracellular signal transduction. It is presumed that leptin circulates from the adipose tissue to the choroid plexus, binds to the short form of the OB-R, crosses the blood-brain barrier, and subsequently reaches the hypothalamus where it binds to the long OB-R isoform. Several lines of evidence suggest that the failure to produce the long OB-R form is responsible for the generation of the *db/db* obesity syndrome. A G to T point mutation and a 106 nucleotide insertion were identified within the long OB-R isoform of *db/db* mice. The point mutation creates a novel donor splicing site that changes the 106 nucleotide

insertion into a new exon (Chen et al., 1996). The presence of this novel exon in the genomic sequence of the long OB-R results in a receptor with a truncated cytoplasmic domain; the mutant receptor is unable to transduce the leptin signal downstream to STAT proteins (Chen et al., 1996). By contrast, no differences in the levels of the short OB-R isoform levels were identified between *db/db* and control mice (Ghilardi et al., 1996).

Multiple lines of evidence indicate that both orexigenic and anorexigenic pathways in the arcuate nucleus are regulated by leptin. *In situ* hybridization studies, using probes specific for the long form of the OB-R and neuropeptide (NPY), showed extensive double labeling in the ventromedial subdivision of the arcuate nucleus (Baskin et al., 1999b; Hakansson et al., 1996; Mercer et al., 1996b). More recently, POMC-containing neurons in the arcuate nucleus were also found to co-express the long OB-R isoform (Cheung et al., 1997), suggesting that melanocortins may be key mediators of central leptin effects. Therefore, both anabolic NPY- and catabolic POMC-containing neurons are direct targets of leptin action. In support of this hypothesis, leptin administration to *ob/ob* mice was shown to increase the cellular levels of *POMC* mRNA in the arcuate nucleus (Schwartz et al., 1997; Thornton et al., 1997). By contrast, reduced leptin signaling in the brain, due to genetic defects (*ob*, *db*) or fasting, decreased *POMC* mRNA levels in the arcuate nucleus (Schwartz et al., 1997). Leptin signaling in the CNS is thus at least partially mediated by the hypothalamic melanocortin system. Furthermore, during fasting, both *OB-R* mRNA and leptin binding were found to be elevated in the arcuate nucleus, although leptin signaling was overall decreased (Baskin et al., 1999a). The increase in leptin receptor expression and function was seen primarily in NPY-containing neurons; this finding is

consistent with the activation of the orexigenic (NPY) pathways by leptin during a period of caloric restriction.

The wide distribution of leptin receptors in the hypothalamus together with the severity of the *ob* syndrome suggest that leptin mediates numerous pathways that control energy balance. A biologically active form of recombinant leptin was produced *in vitro* and used to assess the multiple *in vivo* roles of leptin. Leptin was thus demonstrated to inhibit food intake, reduce body fat stores, increase energy expenditure, and restore normal reproductive function when administered to *ob/ob* animals (Campfield et al., 1995; Chehab et al., 1996; Halaas et al., 1995; Pelleymounter et al., 1995). Leptin treatment had no effect in *db/db* animals, consistent with their leptin resistance (Campfield et al., 1995; Halaas et al., 1995). These studies indicate that leptin has multiple endocrine functions and may be an important therapeutic target for human obesity.

6.2. *Comparison between A^Y and ob (db) Obesity Models*

Several features differentiate the leptin obesity disorders (*ob*, *db*) from the agouti-induced or *A^Y* syndrome. First, defects in leptin signaling result in an early-onset morbid obesity syndrome that develops as early as 3 weeks of age; by contrast, the *A^Y* syndrome, caused by agouti overexpression, is characterized by a late-onset obesity, which does not become prevalent until 3-4 months of age. Secondly, the *A^Y* phenotype is less severe than either one of the leptin syndromes (Figure 11). For instance, *ob/ob* mice are characterized by increased body weight (60-80 g), hyperphagia (6-8 g food per day), reduced energy

expenditure (-30% of normal), hyperglycemia, hyperinsulinemia (40-50 ng/ml), high levels of corticosteroids, hypothyroidism, dyslipidaemia, and infertility due to hypogonadotropic hypogonadisms. A^Y animals, on the other hand, gain 40-50 g in body weight, consume 5-6 g of food per day, are less deficient in using their energy stores (-10% of normal), have normal corticosteroid and thyroid hormone levels, and no defects in reproductive function. In addition, the non-insulin dependent diabetes (NIDDM) syndrome that is associated with the A^Y obesity is less severe than the *ob* disorder. A^Y mice are characterized by a mild hyperglycemia (males only) and are less hyperinsulinemic than *ob* animals (3-5 ng/ml). The differences in the body lengths of *ob/ob* and A^Y animals are also of particular interest. The leptin deficiency and the high corticosteroid levels are responsible for the stunted growth of *ob/ob* animals. A^Y animals, on the other hand, are characterized by increased linear growth; the mechanism triggering this increase remains thus far unknown. All these features, suggest that the A^Y , rather than the *ob* syndrome, resembles much better the human obesity disorder.

Figure 11. Comparison between the *lethal yellow* (A^Y) and leptin-deficient (*ob*) obesity models.

Featured from left to right are the C57 BL/6J black (*a/a*), *lethal yellow* (A^Y/a), wild-type (A/a), and *obese* (*ob/ob*) mouse.



7. OF MICE AND MEN

7.1. *Role of Leptin in Human Obesity*

Epidemiological studies show that as much as 70% of body weight variation in humans is due to genetic factors. Several murine obesity genes have been cloned and characterized within the last decade. In rodents, altered leptin signaling, due either to absence of leptin (*ob/ob*) or leptin receptor (*db/db*), results in a morbid obesity syndrome that resembles the human disorder. The discovery of the *leptin* gene was received with a lot of enthusiasm by the scientific community. It was initially presumed that defective leptin signaling played a major role in the development of human obesity. Scientists hoped that the human disorder would be easily reversed by leptin treatment, as shown previously in rodents (Campfield et al., 1995; Halaas et al., 1995). To everybody's surprise, however, a low frequency of leptin and/or leptin-R mutations was found within the human population. Furthermore, the majority of obese individuals exhibit leptin resistance, which makes a potential leptin treatment extremely unlikely. Extensive genetic analysis of patients with juvenile obesity, anorexia, and bulimia nervosa has shown no association between these human disorders and mutations in the coding or upstream regions of the *leptin* gene (Considine et al., 1996; Echwald et al., 1997; Hinney et al., 1997; Hinney et al., 1998b; Maffei et al., 1996). Furthermore, numerous studies point to a lack of association between mutations in the *leptin-R* gene and human obesity (Gotoda et al., 1997a; Matsuoka et al., 1997; Rolland et al., 1998).

There are, however, several exceptions. Two children with early-onset obesity have been identified in a highly consanguineous pedigree of Pakistani origin (Montague et al., 1997). Both patients were shown to be homozygous for a frameshift mutation at codon 133 of the *leptin* gene (Montague et al., 1997). Because of this mutation, the normally secreted leptin protein is misfolded in the ER, accumulates intracellularly in an aggregate form, and is finally degraded by the proteasome (Rau et al., 1999). As a result, much like *ob/ob* mice, the subjects have undetectable plasma leptin levels despite their increased body fat (Montague et al., 1997). Remarkably, the two children with congenital leptin deficiency responded to leptin therapy. Peripherally administered leptin had a dramatic effect in these patients and improved their endocrine condition within a short amount of time (Farooqi et al., 1999).

A second group of leptin missense mutations associated with morbid obesity have been described in a highly consanguineous Turkish family (Ozata et al., 1999; Strobel et al., 1998). The affected individuals have multiple endocrine defects other than obesity, including hypogonadism, decreased sympathetic tone, and immune system dysfunction. Interestingly, leptin deficiency seems to be associated with an increased mortality rate during childhood, since 7 out of the 11 obese children in this family succumbed to infections very early in life (Ozata et al., 1999). Three other Turkish obese individuals were identified as having the same mutation in the *leptin* gene (Arg¹⁰⁵ to Trp) (Pankov, 1999). The leptin mutation at codon 105 suppresses the ability of leptin to be secreted, thus having a similar effect as the previously described mutation at codon 133 (Pankov, 1999; Rau et al., 1999). The same report describes homozygous mutations at the *db*

locus in a family of Kabilian origin (Pankov, 1999); these mutations result in truncated leptin receptors that lack both transmembrane and intracellular domains and are unable to couple to STAT proteins. Both groups of patients exhibit obesity, diabetes, reduced growth, and infertility. A similar mutation, described at the *db* locus, results in a truncated, nonfunctional leptin receptor (Clement et al., 1998). The clinical symptoms associated with this mutation include morbid obesity, hypogonadism, hypothyroidism, and reduced growth hormone secretion (Clement et al., 1998).

These examples provide the first evidence that leptin plays a role, albeit small, in the genetic inheritance of human obesity. It is now clear that *leptin* (*leptin-R*) gene defects segregating with human obesity are extremely rare (Considine et al., 1996; Echwald et al., 1997; Gotoda et al., 1997a; Hinney et al., 1997; Hinney et al., 1998b; Maffei et al., 1996; Matsuoka et al., 1997; Rolland et al., 1998). Homozygosity at the *ob* (*db*) locus is necessary for the development of obesity due to *leptin* (*leptin-R*) deficiency in both mice and humans. A low frequency of human *ob/+* (*db/+*) carriers may be responsible for the reduced number of obesity cases due to leptin deficiency, which have been found so far in the general population, and their predominant occurrence in highly consanguineous pedigrees.

7.2. Role of Proopiomelanocortin (POMC) in Human Obesity

Once it became clear that the frequency of leptin mutations associated with human obesity was extremely rare, additional targets, downstream of leptin signaling, were taken into consideration. Among them are components of the melanocortin system, such as MC4-R, POMC, and AGRP. The first indication of a connection between melanocortins and human obesity came in 1998 when the first two examples of POMC-deficiency in humans were uncovered (Krude et al., 1998). The pathophysiology of the human condition is strikingly similar to that of the POMC KO mouse (Yaswen et al., 1999). The two patients display early-onset obesity, hyperphagia, adrenal insufficiency, and red hair pigmentation (Krude et al., 1998). The molecular cause of the human disorder is a genetic defect within the POMC gene. Patient 1 was identified as a compound heterozygous for two mutations in exon 3 that blocked POMC processing to α -MSH and ACTH (Krude et al., 1998). The second patient was homozygous for a mutation in exon 2, which interfered with POMC translation (Krude et al., 1998). In both cases the production of α -MSH and ACTH is virtually compromised. The clinical symptoms of the two patients can be explained by the lack of ligands for the melanocortin receptors, MC1-R, MC2-R, and MC4-R. For instance, the lack of ACTH secretion results in adrenal insufficiency that is associated with hypocortisolism and hypoglycemia. Furthermore, the absence of α -MSH at both MC1-R and MC4-R results in pheomelanization (red hair pigmentation) and the development of a severe obesity syndrome.

Recently, the targeted disruption of the murine POMC gene was accomplished and produced a phenotype very similar to the human condition (Krude et al., 1998). Mice homozygous for the POMC null allele displayed severe obesity, adrenal insufficiency, and altered skin pigmentation (Yaswen et al., 1999). Interestingly, the POMC KO mouse was shown to respond to melanocortin agonists administered peripherally. As a consequence of the melanocortin treatment, the murine phenotype improved dramatically in a short amount of time. This intriguing result makes POMC and melanocortins excellent targets for the treatment of human obesity.

The important role that melanocortins play in the regulation of body weight is also suggested by the severe obesity phenotype displayed by both rodents and humans with impaired POMC processing (Jackson et al., 1997). A genetic defect in carboxypeptidase E (CPE), identified as the *fat* mutation, causes a severe obesity and diabetes syndrome in mice (Naggert et al., 1995). Likewise, mutations in prohormone convertase 1 (PC1) result in humans in an early-onset obesity associated with hyperglycemia, hypogonadotropic hypogonadism, and hypocortisolism (Jackson et al., 1997). The patient is identified as being a compound heterozygous for two mutations in PC1, one that prevents the processing of proPC1 and the second that introduces a stop codon within the catalytic domain (Jackson et al., 1997). PC1 acts proximally to carboxypeptidase E (CPE) in the processing pathways of several prohormones, including POMC and proinsulin. As a result, POMC and proinsulin levels are high whereas insulin concentrations are low, which triggers the development of obesity and diabetes in both mice and humans (Jackson et al., 1997; Naggert et al., 1995). In conclusion, genetic

defects in POMC synthesis and/or processing result in morbid obesity in both humans and rodents. This suggests that components of the melanocortin system may play a critical role in the etiology of human obesity.

A genome-wide scan for human obesity genes was carried out within the last years and culminated with the identification of two major susceptibility loci (Hager et al., 1998). The first locus, on chromosome 2, was found to be tightly linked to serum leptin levels and body fat stores in a large population of Mexican Americans affected by the disease (Hager et al., 1998). The linkage was later confirmed in African American and French populations as well (Rotimi et al., 1999). A second major locus associated with a high risk for obesity is located on chromosome 10 (Hager et al., 1998). This candidate region for human obesity was identified following a genome scan of affected siblings in a collection of French families.

Several candidate genes for human obesity, including POMC, have been identified within the quantitative trait locus (QTL) on chromosome 2 (Hager et al., 1998). A recent genetic study provides new evidence supporting the claim that POMC is indeed the leptin QTL previously identified in Mexican American families (Hixson et al., 1999). However, extensive genetic analysis in a large cohort of Caucasians with early-onset obesity has failed to reveal an association between mutations in the coding or promoter region of the *POMC* gene and juvenile obesity (Echwald et al., 1999; Hinney et al., 1998a). The same was true for patients suffering from anorexia nervosa (Hinney et al., 1998a). It is possible that the frequency of POMC mutations affecting eating disorders is

higher in certain ethnic groups, such as Mexican or African Americans, than in the general population. This hypothesis requires, however, further investigation.

Obese patients are at high risk factor for developing type 2 diabetes (NIDDM). The etiology of this disease is rather complex, with both genetic and environmental factors playing major roles. Recent studies conducted in a group of Mexican Americans indicate two major susceptibility loci for NIDDM on chromosomes 2 and 15, respectively (Cox et al., 1999; Hanis et al., 1996). No candidate genes have been thus far associated with a higher incidence of developing NIDDM. Identifying these genes remains, however, a high priority; it is hoped that genetic screening will help prevent the development of obesity as well as NIDDM.

7.3. First Cases of Altered MC4-R Signaling Identified in Human Population

Recently, two frameshift mutations in MC4-R (a deletion at codon 211 and an insertion at codon 245) were found to be associated with a dominantly-inherited form of human obesity (Vaisse et al., 1998; Yeo et al., 1998). As a consequence of these mutations, the MC4-R becomes truncated at either the fifth or sixth transmembrane domain and is therefore non-functional. The human subjects harboring these mutations are heterozygous at the *MC4-R* locus, suggesting that, similar to rodents, one copy of a defective MC4-R is sufficient for the development of morbid obesity (MC4-R haploinsufficiency). Extensive screenings of obese individuals resulted in the identification of additional MC4-R mutations, including a nonsense and several missense mutations (Table 4) (Gu et al., 1999; Hinney et al., 1999; Sina et al., 1999; Yeo et al., 1999). The nonsense mutation occurs at position 35 of the MC4-R and produces a truncated receptor that retains only the N-terminal extracellular domain (Hinney et al., 1999). This defect in MC4-R is presumed to result in a lack of receptor expression on the plasma membrane; the immature receptor is likely misfolded in the ER and degraded by the proteasome. MC4-Rs that harbor missense mutations are also presumed to be non-functional due to defects in synthesis, ligand binding, or coupling to signal transducers. However, only a few of these mutations have been pharmacologically tested. The Ile¹³⁷Thr MC4-R variant, for instance, which was identified in an extremely obese subject, displays reduced agonist affinity and functional activation when expressed in 293

HEK cells (Gu et al., 1999). The functional significance of the other missense mutations remains to be established.

These studies indicate that mutations in the coding region of the MC4-R are not uncommon and suggest that the melanocortin system plays an essential role in regulating weight homeostasis in humans. Hemizyosity of the *MC4-R* gene is considered today to be responsible for as much as 5% of the pediatric obesity cases (Vaisse et al., 1998; Yeo et al., 1998); this percentage is likely to increase in future years as more screening testing will be conducted. Not all allelic variants of the human MC4-R, however, are associated with morbid obesity. For example, Ile¹⁰³ Val, Thr¹¹²Met, and Ile²⁵¹Leu variants are polymorphisms since they have been detected with similar frequencies in both obese and lean human subjects (Gotoda et al., 1997b; Gu et al., 1999; Hinney et al., 1999). This prediction is supported by the observation that both Ile¹⁰³ Val and Thr¹¹²Met variants display normal *in vitro* pharmacology (Gu et al., 1999; Hinney et al., 1999).

An intriguing recent study (Cody et al., 1999) challenges previous conclusions (Hinney et al., 1999; Vaisse et al., 1998; Yeo et al., 1998) suggesting that dominantly-inherited obesity, which segregates with human MC4-R mutations, is due to haploinsufficiency of this gene (Cody et al., 1999). The authors have been investigating the phenotype of individuals that harbor large deletions of chromosome 18q (Cody et al., 1999). Since the *MC4-R* locus is mapped to 18q21.3, one third of the subjects included in the study were found to be hemizygous for this gene (Cody et al., 1999). If hemizyosity of the *MC4-R* gene is indeed associated with haploinsufficiency, then these

individuals would be expected to exhibit obesity. No differences were found, however, between them and individuals with deletions of 18q that did not include the MC4-R gene (Cody et al., 1999). The results of this study seem to indicate haplosufficiency rather than haploinsufficiency of the *MC4-R* gene. Furthermore, the authors attribute the obesity induced by human MC4-R mutations to a dominant negative effect (Cody et al., 1999). This implies that in human subjects, heterozygous for MC4-R mutations, the second receptor copy might be expressed at lower levels and be less functional than normal. The exact mechanism is, however, unclear at this time. The controversy is likely to generate more debate in the years to come.

Table 4. Natural MC4-R variants associated with human obesity.

Human Phenotype	MC4-R Mutation	Mode of Inheritance	MC4-R Pharmacology	Reference
Obese	Ser ³⁰ to Phe (missense)	Dominant?	Loss of function?	(Hinney et al., 1999)
Obese	Tyr ³⁵ to Stop (nonsense)	Dominant	Loss of function (predicted)	(Hinney et al., 1999)
Obese	Asp ³⁷ to Val (missense)	?	?	(Hinney et al., 1999)
Obese	Asn ⁶² to Ser (missense)	Dominant	Loss of function (predicted)	(Yeo et al., 1999)
Obese	Pro ⁷⁸ to Leu (missense)	Dominant	Loss of function (predicted)	(Hinney et al., 1999)
Obese/Lean	Val ¹⁰³ to Ile	Polymorphism	Normal function (confirmed)	(Gotoda et al., 1997b; Hinney et al., 1999)
Obese/Lean	Thr ¹¹² to Met	Polymorphism	Normal function (confirmed)	(Hinney et al., 1999; Gu et al., 1999)
Obese	Ile ¹³⁷ to Thr (missense)	Dominant	Loss of function (confirmed)	(Gu et al., 1999)
Obese	Arg ¹⁶⁵ to Trp (missense)	Dominant	Loss of function (predicted)	(Hinney et al., 1999)
Obese	Deletion (codon 211)	Dominant	Loss of function (predicted)	(Yeo et al., 1998; Hinney et al., 1999)
Obese/Lean	Ile ²⁵¹ to Leu	Polymorphism	Normal function (predicted)	(Hinney et al., 1999)
Obese	Gly ²⁵² to Ser (missense)	Dominant?	Loss of function?	(Hinney et al., 1999)

Obese	Insertion (codon 245)	Dominant	Loss of function (predicted)	(Vaisse et al., 1998)
Obese	Ile³¹⁷ to Thr (missense)	Dominant	Loss of function (predicted)	(Hinney et al., 1999)

8. MAHOGANY AND MAHOGANOID: SPECIFIC ACTIVATORS OF AGOUTI AND AGRP

8.1. *Discovery of Mahogany and Mahoganoid*

Two autosomal mutations, *mahogany* and *mahoganoid* were identified several decades ago as natural suppressors of A^Y -induced yellow pigmentation. Both mutations were thus capable of shifting melanogenesis from phaeomelanin to eumelanin synthesis (Lane and Green, 1960). Although they generate the same phenotype, the two genes are located on different chromosomes (2 and 16, respectively). This tends to suggest that *mahogany* and *mahoganoid* are part of the same pathway, although they might have different functions. Several mutations have been described at the *mahogany* locus; they include a loss-of-function mutation, mg^{3J} , that originated in the C3HeB/FeJ background, and two hypomorphic alleles, mg and mg^L , identified in the LDJ/Le and C3H/He backgrounds, respectively (Gunn et al., 1999; Miller et al., 1997; Nagle et al., 1999). Only one mutation (md) has been described at the *mahoganoid* locus and it was identified in the C3H/HeJ background (Miller et al., 1997). More recently, the mg mutation was recovered from its original LDJ/Le background and backcrossed into the C57BL/6J (Dinulescu et al., 1998). This allowed a much better analysis of the mg effects on the A^Y phenotype in a uniform genetic background.

8.2. *Distribution and Structural Characteristics of Mahogany*

The *mahogany* gene was identified by positional cloning last year, four decades after its discovery (Gunn et al., 1999; Nagle et al., 1999). As it turns out, the *mahogany* locus encodes a transmembrane form of attractin (Atrn), a human protein that was previously identified as an immunomodulatory molecule. Atrn is found on the cell surface of different cell types of the immune system. It is thought, however, that it accumulates rapidly on the plasma membrane of activated T cells, following their exposure to antigen (Duke-Cohan et al., 1998; Jackson, 1999). Atrn is then secreted in the serum where it mediates the spreading of monocytes, which can subsequently act as foci for T cells clustering (Duke-Cohan et al., 1998).

By contrast, the transmembrane form of Atrn, mahogany, is predominantly expressed in the brain, with lower levels in the adipose tissue, kidney, heart, spleen, liver, lung, skin, spinal cord, and skeletal muscle (Gunn et al., 1999; Nagle et al., 1999). Within the CNS, the *mahogany* gene has a wide but discrete distribution in specific populations of neurons (Lu et al., 1999). Interestingly, *mahogany* mRNA is present in neurons but not glial cells (Lu et al., 1999). Major sites of mahogany expression in the brain are the hippocampus, hypothalamus, and primary olfactory cortices (Lu et al., 1999). In the hypothalamus, mahogany is found in several nuclei, including arcuate, ventromedial, and paraventricular nuclei, that have been previously shown to be involved in energy homeostasis (Lu et al., 1999). Mahogany is also highly expressed in areas of the nervous system responsible for motor and balance control, including the cerebellum, inferior

olivary nucleus, and ventral horn of the spinal horn (Lu et al., 1999). Sensory areas, such as the nucleus of the solitary tract and parabrachial nucleus, contain a high density of *Atrn* mRNA as well (Lu et al., 1999). Finally, *mahogany* mRNA was detected in the thoracic and lumbar spinal cord, especially in the intermediolateral nucleus that controls cardiovascular activity and brown tissue thermogenesis (Lu et al., 1999).

Sequence (i.e. coding region and adjoining introns) comparison of normal and mutant *mahogany* mRNA transcripts allowed the identification of several defects. The mg^{3J} mutation, for instance, is a null allele at the *mahogany* locus, with no mRNA expression detected in mg^{3J}/mg^{3J} mice. Furthermore, a 5 bp deletion was found in the coding sequence of the mg^{3J} transcript, which introduces a stop codon at position 937 and results in a severely truncated protein (Nagle et al., 1999). Two hypomorphic alleles, *mg* and mg^L , have also been identified. Both of them are incorrectly spliced variants of *mahogany*, each containing a 5 kb insertion in adjacent introns of the normal gene. As a result, the two alleles are characterized by transcripts of abnormal sizes: 9.5 kb for the *mg* allele and 10 kb for mg^L , respectively; both of them, however, still maintain the normal 9 kb transcript, albeit at reduced levels (Gunn et al., 1999; Nagle et al., 1999). This aberrant pattern of RNA expression explains the hypomorphic nature of the two mutations (Gunn et al., 1999; Nagle et al., 1999). Of the three mutations, mg^{3J} is expected to have the strongest effect because of its total loss of mRNA expression. It has already been shown that mg^{3J} has a more dramatic effect on agouti pigmentation than the other mutations (Gunn et al., 1999).

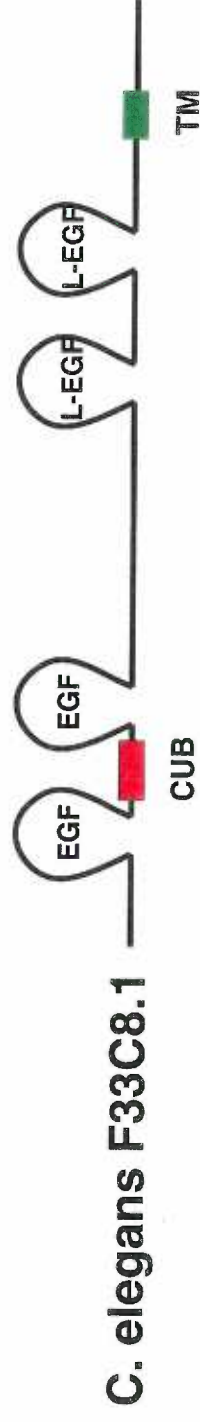
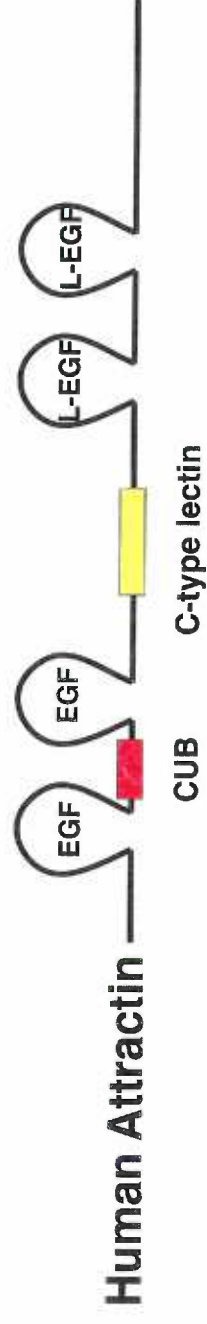
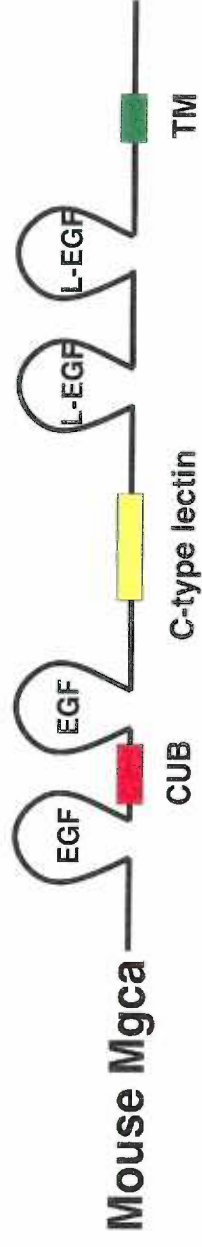
The murine *mahogany* gene is predicted to encode a 1,336 amino-acid protein, with a relative molecular mass of 150 kDa (Gunn et al., 1999; Nagle et al., 1999). The primary structure of mahogany shows homology with several domains of the *C. elegans* perlecan-like F33C8.1 protein, (Figure 12) (Gunn et al., 1999; Nagle et al., 1999), suggesting that it may be evolutionarily conserved. Mahogany is a single-transmembrane domain protein with a large extracellular region and a short cytoplasmic tail that shows no obvious signaling motifs, suggesting that its action may be entirely at the cell surface (Gunn et al., 1999; Nagle et al., 1999). The mahogany tail contains, however, a conserved eight amino-acid sequence that is present in human, mouse, and *C. elegans* proteins. Further investigations are required in order to establish whether this short amino acid sequence is in fact a signaling motif that has been conserved during evolution.

The structure of the extracellular domain reveals several distinct structural motifs, which might provide insight into the biological functions of mahogany (Figure 12) (Gunn et al., 1999; Nagle et al., 1999). The extracellular domain consists of three EGF domains (Nakayama et al., 1998), two laminin-like EGF repeats, a CUB domain (Bork and Beckmann, 1993), two plexin-like repeats (Maestrini et al., 1996), a C-type lectin motif (Drickamer, 1995; Weis and Drickamer, 1996), and seven Kelch repeats (Bork and Doolittle, 1994) (Figure 12). EGF and laminin-like EGF domains are characteristic of transmembrane proteins involved in cell adhesion and protein-protein interactions (i.e. ligand-receptor) (Nakayama et al., 1998). Mahogany is predicted to be highly glycosylated as it contains C-type lectin motifs, which are known to bind carbohydrate residues (Bork and Beckmann, 1993; Drickamer, 1995; Weis and Drickamer, 1996).

Lectins are thought to be important for cell surface sugar recognition. CUB domains, on the other hand, are considered signature motifs for developmentally-regulated proteins. They have been described so far in twenty-three functionally distinct proteins, most of them involved in development (i.e. dorso-ventral patterning, axonal pathfinding during embryogenesis) and cell migration and differentiation (Bork and Beckmann, 1993). Interestingly, CUB domains were identified in neuropilins, transmembrane proteins that mediate axonal guidance during neurodevelopment through a chemorepulsion mechanism. Furthermore, the CUB motifs were found to be critical for the specificity of the chemorepulsive response triggered by neuropilins. Another class of transmembrane proteins, plexins, were also shown to be involved in axonal pathfinding. The structural characteristics of the mahogany protein (CUB domains, plexin-like repeats) suggest that it may play an important role in the assembly and maintenance of neuronal connectivity during development. Thus, mahogany/attractin, in its either secreted and/or transmembrane form, could serve as a molecular cue for neurite pathfinding, outgrowth, and/or synapse formation.

Figure 12. Structural features of mahogany/attractin.

Alignment of the murine mahogany sequence with its homologues, human attractin and the *C. elegans* perlecan-like F33C8.1 protein. Featured are the large extracellular region, single transmembrane domain (TM), and short cytoplasmic tail. The high degree of homology between the extracellular region of mahogany and human attractin (93%) indicates that mahogany is in fact a transmembrane form of human attractin (Gunn et al., 1999). Prominent structural features of the extracellular sequence include several EGF repeats, a CUB domain, and a C-type lectin motif.



8.3. *Physiological Characterization of Mahogany*

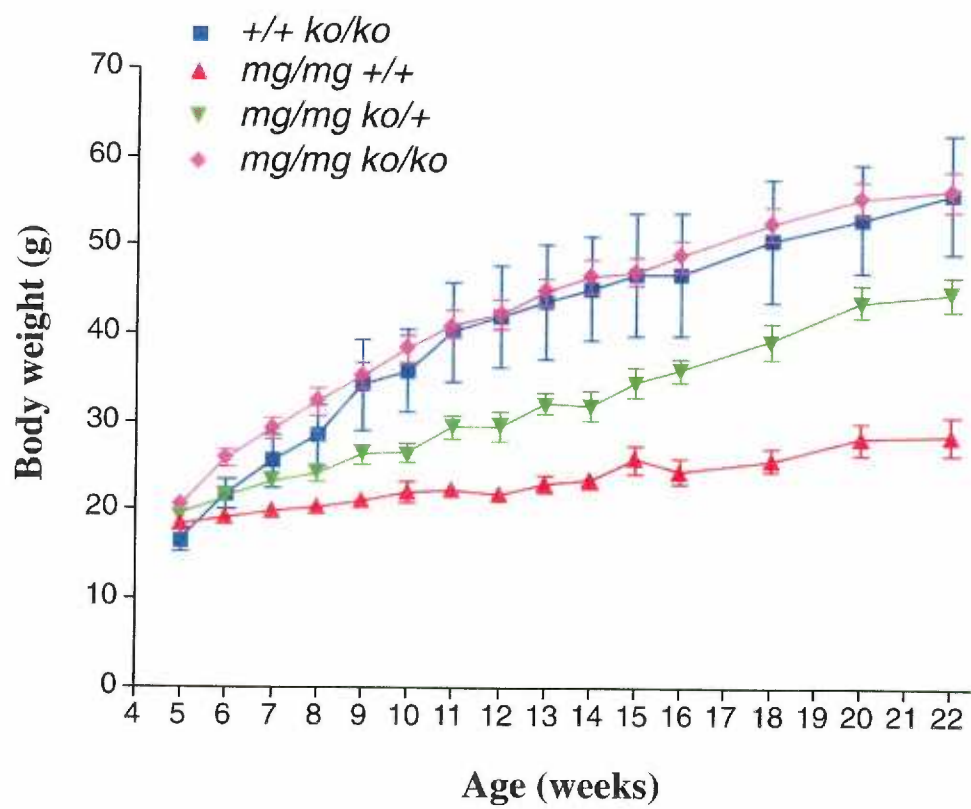
Major steps have been taken lately towards the molecular and functional characterization of the two *mg* and *md* mutations that result in suppression of agouti function. Genetic studies have positioned the *mg* mutation at the same level or upstream of the melanocortin receptors based on the fact that it cannot suppress the phenotype of either MC1-R or MC4-R KO [our results and others (Miller et al., 1997; Nagle et al., 1999)] (Figure 13). Detailed physiological analysis of animals carrying A^Y and *mg* mutations indicates that absence of mahogany suppresses not only phaeomelanin synthesis but also the *agouti*-induced obesity syndrome (Dinulescu et al., 1998). This topic is described in more detail in chapter three of the thesis. Recent evidence (Dinulescu et al., 1998; Miller et al., 1997) suggests that mahogany is involved in mediating the interaction between agouti and MC1/MC4-R. Furthermore, mahogany is shown to have physiological effects in the absence of A^Y (Dinulescu et al., 1998), which strongly argues for the role of mahogany in facilitating AGRP binding to MC4-R as well. However, a direct interaction between mahogany and AGRP has not yet been proven. It would be interesting to determine whether homozygous *mg* mutants are able to respond to exogenous and/or endogenous AGRP. Comparing the feeding patterns of *mg/mg* and control animals following central administration of AGRP, as well as examining the phenotype of the *mg/AGRP* transgenic cross would be instrumental in answering these questions.

Loss of mahogany suppresses agouti antagonism of the melanocortin receptor agonist, α -MSH. Thus, absence of mahogany is presumed to elicit increased signaling at

melanocortin receptors (MC1/4-R). Recent studies indicate that central administration of melanocortin agonists results in an increased energy expenditure (Cowley et al., 1999). A chronic increase in MC4-R signaling in *mg/mg* mice could thus explain the hypermetabolism of these animals (Dinulescu et al., 1998).

Figure 13. Absence of mahogany does not suppress the phenotype of the MC4-R knockout (MC4-R KO) mouse.

Weight analysis of MC4-R KO mice indicates no difference between animals homozygous at the *mahogany* locus and wild-type. Mahogany has thus no effect on energy homeostasis in the absence of the MC4-R, suggesting that it acts at or upstream of the melanocortin receptor.



8.4. *Insights into the Molecular Mechanism of Mahogany Action*

Several potential models have been proposed to illustrate the interaction between mahogany and the melanocortin system (Figure 14). A first model suggests that mahogany is in fact a low-affinity co-receptor of MC1/4-R, with the main function of increasing the concentration of antagonist (agouti/AGRP) in the immediate vicinity of melanocortin receptors (Figure 14) (Gunn et al., 1999; Miller et al., 1997; Nagle et al., 1999). Mahogany action would thus facilitate the antagonist-receptor interaction in two possible ways: 1) mahogany binds the antagonist and presents it to the receptor, or, 2) it removes the agonist from the immediate vicinity of the receptor, thereby allowing more access of the antagonist to the receptor.

There is significant doubt, however, as to whether the co-receptor model is a likely model of interaction for both agouti and AGRP. First, the N-terminus of the antagonist is proposed to interact with mahogany while the C-terminal domain is visualized as binding to the receptor (Gunn et al., 1999). Based on the absence of any structural similarities between agouti and AGRP it is difficult to imagine that this is indeed the case. In addition, the *mg* and *md* mutations appear to have the same phenotype. If mahogany is indeed a co-receptor, then what role does mahoganoid play? An alternative model of mahogany action focuses on the interaction of mahogany with the receptor rather than the agonist/antagonist. This model suggests that mahogany is involved in the process of receptor desensitization via post-translational modifications or cellular internalization (Figure 14) (Gunn et al., 1999; Miller et al., 1997).

I would like to propose a third model of mahogany action that takes into account the structural similarities between mahogany and membrane proteins involved in cell adhesion. This model suggests that mahogany plays a key role in mediating the proper formation of neuronal architecture and allowing the axonal delivery of antagonist-containing secretory vesicles to melanocortin receptors (Figure 14). Immunoelectron microscopy studies focused on comparing the distribution of AGRP/ α -MSH contacts on MC4-R-containing neurons in *mg* mutant and control animals may help test this model. The discovery of potential differences in the structural organization or in the overall distribution of α -MSH/AGRP termini at the MC4-R would constitute a big step forward in the molecular characterization of mahogany action.

Figure 14. Potential models of mahogany-agouti/AGRP interaction.

A. The co-receptor model.

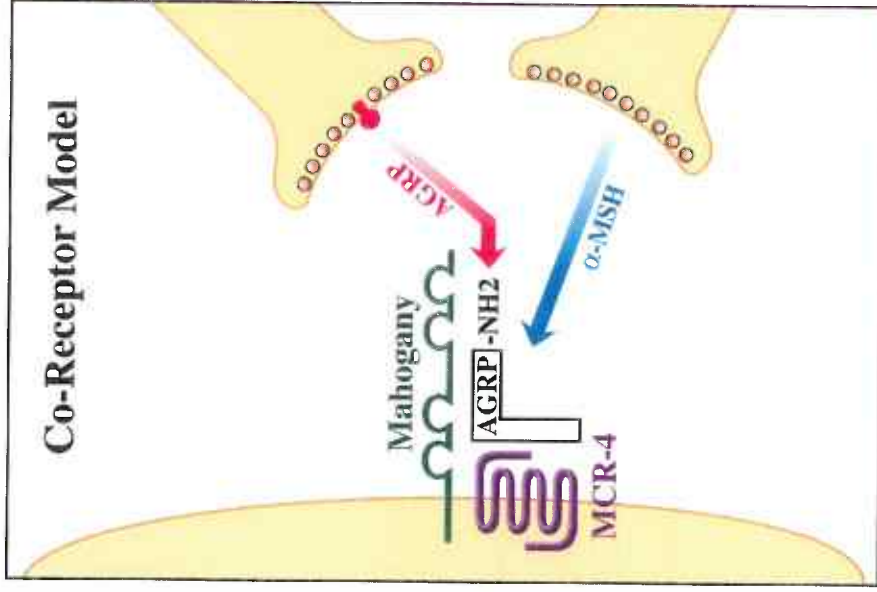
MC4-R and mahogany form a receptor complex. Mahogany increases the local concentration of agouti/AGRP by binding to the N-terminal portion of the antagonist and presenting it to the MC4-R.

B. The receptor desensitization model.

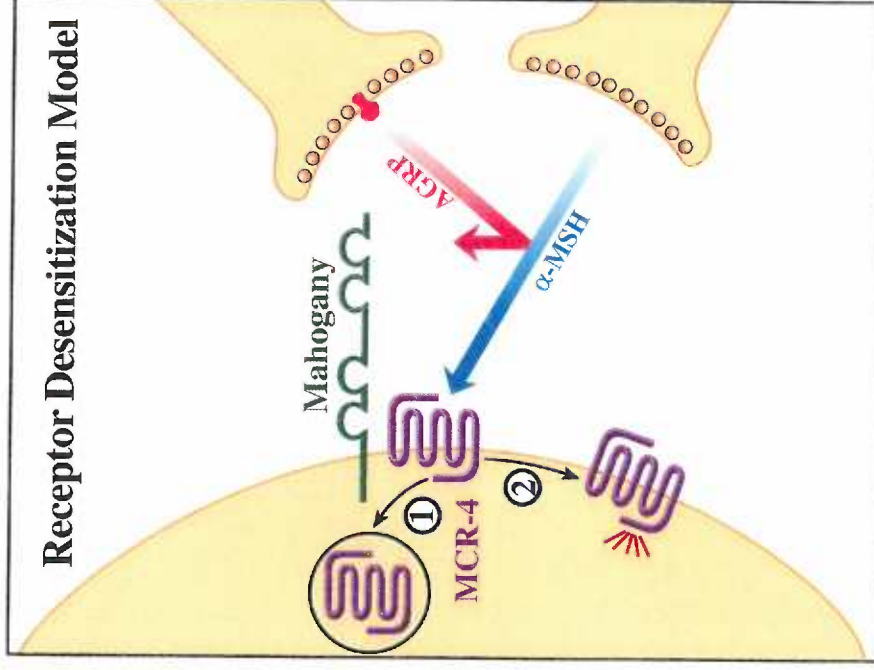
MC4-R downregulation is achieved as a result of mahogany action via two possible pathways: cellular internalization (1) and post-translational modification (2).

C. Cell adhesion model.

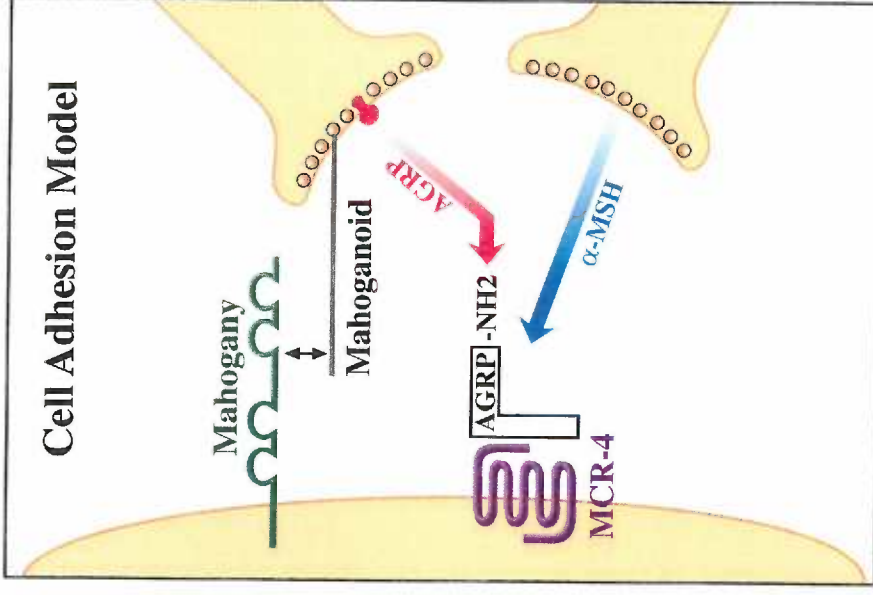
Mahogany is a cell adhesion molecule, which mediates the necessary cell-cell interactions that allow the axonal delivery of antagonist (agouti/AGRP)-containing secretory vesicles to MC4-R. Mahoganoid, which appears to have similar effects to mahogany, may be a target for mahogany action.



A.



B.



C.

9. SPECIFIC AIMS AND OUTLINE OF THE THESIS

The main focus of my thesis has been the characterization of the *mg* mutation, a specific agouti and AGRP suppressor. Three years ago, when this project was initiated, only limited data regarding mahogany was available. Thus, a report, dated 1960, indicated that the hypomorphic *mg* mutation was a natural suppressor of A^Y -induced yellow pigmentation. The sequence of the *mahogany* gene was published only a year ago, therefore, no information on the distribution or function of mahogany was available at the time. It became then critical to physiologically characterize the *mg/mg* animals, which lack normal mahogany expression. In addition, the effects of mahogany on energy and glucose homeostasis were investigated in two models of murine obesity: lethal-yellow (A^Y) and leptin-deficient (*ob*).

The goals of this research have been to determine:

- 1) Does absence of mahogany suppress the A^Y -induced obesity syndrome? The results of this investigation are presented in chapter three.
- 2) Does loss of mahogany have any effects on energy homeostasis, aside from A^Y suppression? Since agouti is not normally expressed in the brain and the role of ectopically expressed agouti is mimicked by endogenous AGRP, this finding would strongly argue for *mg* suppressing AGRP action as well. The results of this study are described in chapter three.
- 3) Does the melanocortin system and/or mahogany play any role in the regulation of glucose homeostasis? The absence of mahogany protein in *mg/mg* animals is presumed to

elicit increased signaling at both central and peripheral melanocortin receptors. The *mg/mg* mutant thus represents the first *in vivo* model of chronic melanocortin signaling. By contrast, i.c.v. administration of MTII, an MC3/4-R agonist, results in acute stimulation of central melanocortinergetic pathways. The existence of the two models (acute and chronic) of increased melanocortin signaling offered an unique opportunity to investigate whether the melanocortin system played any role in the regulation of insulin release and glucose metabolism. The effects of MTII administration on insulin release and insulin sensitivity are described in chapter four. The role of mahogany in the control of glucose homeostasis is outlined in chapter five.

4) Finally, what is the molecular mechanism of mahogany action in the brain? Our model of the interaction between mahogany and AGRP is presented in chapter six.

A second goal of my thesis was to decipher the relationship between canine agouti and MC1-R in order to determine whether it represents a novel type of interaction. Classical genetic studies suggested the existence of a dominant canine agouti that functions as an agonist, rather than antagonist, of the MC1-R. A second prediction of these studies (i.e. canine yellow coat color is due to a nonfunctional MC1-R) was also under investigation. The results of this study are outlined in chapter two.

CHAPTER TWO

GENETIC INTERACTION BETWEEN CANINE *EXTENSION AND AGOUTI*

Daniela M. Dinulescu^{1,2} and Roger D. Cone^{1,2}

¹Vollum Institute, ²Department of Cell and Developmental Biology, Oregon Health
Sciences University, Portland, OR 97201

ABSTRACT

Classic genetic studies (Little, 1957) have proposed that in dogs, unlike mice, black coat color is caused by a novel dominant *agouti* allele, A^s , which functions as an agonist of the melanocyte-stimulating hormone receptor (MSH-R). In addition, a recessive e allele at the *extension* locus was proposed to account for the canine yellow coat color (Little, 1957). A more recent genetic study (Carver, 1984), which uses statistics to analyze the inheritance of coat color in German Shepherd dogs, calls into question the existence of the putative A^s allele; it does, however, find statistical proof for the presence of the e allele. We have tried to resolve this controversy by analyzing the molecular structure and expression pattern of *agouti* in black-colored dogs. No evidence was found to support Little's proposal of the A^s allele. We thus conclude that the black coat color is likely caused by a recessive non-functional *agouti* allele much like in rodents. In addition, we provide evidence indicating that the canine e allele encodes a non-functional MC1-R, which is unable to either bind ligand or transduce the hormonal signal downstream to adenylyl cyclase. Our data suggest that the truncated MC1-R fails to reach the plasma membrane and is rapidly degraded intracellularly. Taken together, these results indicate that the relationship between *agouti* and *extension* loci in *Canis familiaris* closely resembles those described in other mammalian species.

INTRODUCTION

Agouti is a paracrine-signaling factor, secreted by dermal papillae cells, that acts within the hair follicle microenvironment to block melanocortin action at the MC1-R on melanocytes (Lu et al., 1994). Agouti has thus been demonstrated to be a specific competitive antagonist of MC1-R in all mammalian species studied so far. Classical genetic studies (Little, 1957) have proposed that in dogs the agouti series consists of dominant black, A^s , tan-sable a^y , gray-sable, a^w , and black-and-tan, a^l . With the exception of the dominant A^s allele, all the other canine *agouti* alleles are associated with conventional agouti phenotypes. Little's study, however, points out that dominant inheritance of black coat color in dogs co-segregates with the A^s allele. The A^s allele thus promotes, rather than restricts, the expansion of eumelanin throughout the coat, suggesting that it might function as a MC1-R agonist. This proposal has sparked a lot of controversies in the literature. A more recent genetic analysis has used statistics to check the accuracy of the data reported by classical breeders (Carver, 1984). Carver's study finds no evidence for the existence of A^s in several breeds under investigation (i.e. German shepherd). According to this study, the black coat color of German shepherd dogs is caused instead by a recessive *agouti* (a) allele, similar to other species.

Little also conducted studies of the canine *extension* (E) locus and found evidence for two alleles: E for normal *extension* of black pigment, and recessive e , which is associated with total loss of eumelanin (Little, 1957). The E allele is thus likely to encode a wild-type MC1-R whereas e is predicted to encode a non-functional receptor. The

genetics of the canine *extension* locus does not appear to differ greatly from those of other mammals. It is interesting, however, that, unlike other species (i.e. fox, mouse, bovine, sheep), there is no genetic evidence supporting the existence of a dominant *E* allele in dogs that co-segregates with black coat color. Furthermore, statistical analysis of the *E* series in German shepherd dogs found evidence only for the two *E* alleles proposed by Little (Carver, 1984).

The present report tries to clarify some of the existing confusion in the field. We have cloned the canine agouti and MC1-R genes and have analyzed the different alleles at the two loci, focusing mainly on the *A^s* and *e* alleles. This study describes the molecular and pharmacological characterization of the two *extension* alleles, as well as the structure and distribution of the *A^s* allele.

MATERIALS AND METHODS

Cloning of canine agouti. A canine genomic library was assembled using DNA from a black coat-colored dog and the Zap ExpressTM λ phage (Stratagene) as a vector. 100 ng of genomic DNA were ligated to 1 μ g of the BamHI digested Zap ExpressTM vector at 12°C overnight. The Zap ExpressTM Gigapack II Gold Cloning kit (Stratagene) was used to package the ligation products into the Rec A⁻ E. coli XL1-Blue MRF⁻ host strain. One million pfu of phages were screened at low stringency with two ³²P-labeled DNA fragments encompassing the murine agouti exons 2, 3, and exon 4, respectively. Positive clones were selected by two additional rounds of hybridization with the same probes.

The cloned inserts contained within the λ vector were isolated using a standard excision protocol (Stratagene). Three different clones were identified by restriction mapping, subsequently subcloned and sequenced. A homology search of the Genbank database using the cloned DNA fragments led to the identification of the complete canine agouti sequence.

PCR amplification and sequencing of canine MC1-R. The canine MC1-R was cloned by PCR amplification using degenerate primers based on the sequence of known MC1-Rs. DNA sequencing of MC1-Rs from a large family of Labrador Retrievers allowed the identification of a nonsense mutation (Arg³⁰⁶ to Stop) that co-segregates with yellow coat color.

Binding and adenylyl cyclase assays. MC1-Rs from black (*E*) and yellow (*e*) Labrador Retrievers were stably transfected into a human HEK 293 cell line following standard protocols (lipofectin transfection). Competition binding experiments were performed on HEK 293 stable cells expressing the wild-type (*E*) or truncated MC1-R (*e*). Cells were incubated for 1 h at 37°C with 1 nM ¹²⁵I-NDP- α -MSH and varying concentrations of cold NDP- α -MSH, washed with cold PBS, lysed, and counted in a γ -counter. Non-specific binding was determined by the number of counts remaining in the presence of 1 μ M cold NDP- α -MSH. Binding data was analyzed using Prism (Graphpad Software). Curves were fitted and IC₅₀ values determined by nonlinear regression (one site competition). Data indicate the mean and standard deviation of duplicate counts.

The ability of the two MC1-Rs (wild-type and MC1R-306ter) to couple to adenylyl cyclase and stimulate intracellular cAMP production was measured by using a β -gal assay. This is a rapid colorimetric assay using a β -gal (lacZ) gene fused to five copies of the cAMP response element (CRE) that detects intracellular CRE binding protein (CREB) activation caused by increased cAMP. 293 stable cells expressing canine MC1-Rs were transiently transfected with a pCRE- β -gal construct and stimulated with varying concentrations of cold NDP- α -MSH 48-72 h later. Following stimulation, cells were lysed and assayed for β -gal activity as previously described (Chen et al., 1995). Curves were fitted and EC₅₀ values determined by nonlinear regression using Prism (Graphpad Software). Data indicate the mean and standard deviation of triplicate counts.

Northern and Western analysis of MC1-R. Wild-type MC1-R and MC1R-R306ter, tagged at the N-terminus (Flag), were transiently transfected into HEK 293 cells. The transfection efficiency was determined by using a green fluorescent protein (GFP) construct. mRNA levels were examined by Northern analysis. Protein levels were determined by Western analysis on whole-cell or membrane extracts using the anti-Flag M2 antibody (Kodak and Sigma).

RESULTS

Our study was based on the assumption that the *A^s* allele, if real, must encode a protein with a novel mechanism of action. The goal of this analysis was to identify potential mutations in the *A^s* gene product that would convert it into an agonist of the MC1-R. We

have thus cloned and sequenced the complete coding region of the *agouti* gene from dogs with or without the proposed A^s allele. The genomic organization of the canine *agouti* gene proved to be rather complex, as it spanned over 12 kb; it was, however, equivalent to the *agouti* structures of other mammals. We have determined that, similar to other species, canine *agouti* consists of three exons and a putative first non-coding exon (Figure 1 A). Sequencing of the *agouti* gene uncovered a protein with a high degree of homology to mouse (85%) and fox (98%) *agouti* (Figure 1 B). The canine gene product has all the structural features characteristic of other *agouti* proteins, including an N-terminal signal peptide, a highly basic middle region, and a C-terminal domain rich in Cys and Pro residues (Figure 1 B). The high degree of homology between the canine and fox *agouti* proteins confirms that the two species are closely related.

In order to prove or disapprove the theory regarding the existence of the A^s allele we have amplified and sequenced the complete cDNA of all canine *agouti* alleles. No differences in the coding region or intron-exon junctions were detected between A^s and the other alleles of the *agouti* series. Furthermore, we have analyzed the tissue distribution of the A^s allele to determine whether it matched the localization pattern of dominant *agouti* alleles described in other species. Thus, in the mouse, wild-type *agouti* (A) is found only in skin and testis, with the recessive *agouti* (a) allele following a similar expression pattern but at much lower levels; by contrast, the dominant A^Y allele is characterized by constitutive, ectopic expression due to a promoter rearrangement. Northern analysis of various tissues from dogs carrying the A^s allele failed to detect *agouti* expression outside

the skin and testis (Figure 2). In addition, we detected reduced levels of agouti expression in these tissues, which is consistent with A^s being a recessive allele.

The second goal of our investigation was to establish whether the recessive *extension* allele (e) encodes in fact a non-functional MC1-R. We and others (Newton et al., 2000) have cloned and analyzed the complete sequence of the canine MC1-R (Figure 3). Again, the highest degree of homology was seen with the fox protein (98%). Interestingly, in fox, a constitutively activating C125R mutation in the MC1-R (E^d) was demonstrated to co-segregate with dark pigmentation. Our analysis of the canine *extension* locus has not identified this mutation in black-colored dogs, lending credence to Little and Carver's initial predictions that black coat color is not caused by a constitutively activated MC1-R.

We have characterized the *extension* locus in a large family of Labrador Retrievers and found a complete linkage between yellow coat color and homozygosity of the e allele. Sequence analysis of the MC1-R isolated from black Labrador dogs fails to reveal any constitutively activating mutations, suggesting that it is a wild-type receptor. By contrast, examination of the MC1-R sequence from yellow Labradors showed a nonsense mutation at Arg³⁰⁶ that caused premature termination of the aminoacid chain. As a result, the truncated receptor (MC1R-R306ter) lacked the C-terminal cytoplasmic domain, which might play an important role in receptor trafficking from ER to the plasma membrane. Once the sequence analysis was complete, we proceeded to investigate whether the receptor encoded by the recessive e allele was indeed non-functional. Both

receptors (wild-type and truncated) were stably expressed in the 293 HEK cell system for pharmacological analysis. The results of this study are illustrated in Figure 4. The IC_{50} (5.4×10^{-10}) and EC_{50} (5×10^{-9}) values determined for the black Labrador MC1-R were comparable to those reported for the wild-type mouse MC1-R, further suggesting that the canine *E* allele encodes a wild-type receptor. By contrast, the truncated MC1R-306ter can neither bind the NDP- α -MSH ligand (Figure 4 A) or increase intracellular cAMP production by coupling to adenylyl cyclase (Figure 4 B).

This prompted us to investigate the possible molecular causes for the loss of MC1-R function in *e/e* dogs. The main defect does not appear to be at the transcriptional level, since no differences were detected between the mRNA levels of full-length and truncated MC1-R (Figure 5). Our study rather points to evidence of decreased protein stability for MC1R-R306ter, as indicated by Western analysis of total cellular extracts transiently transfected with either full-length or truncated receptor (Figure 6). Furthermore, Western analysis of membrane preparations from the same cells revealed a total loss of cell surface expression for the truncated (MC1R-R306ter) receptor (Figure 6), thus explaining its inability to bind ligand.

DISCUSSION

Two main conclusions can be drawn from our study. First, we have found no evidence in support of a dominant *agouti* allele showing linkage with black coat color in dogs. Our conclusion is supported by several observations. No coding differences were detected

between A^s and the other canine agouti variants. Furthermore, the A^s localization pattern does not resemble the distribution of dominant *agouti* alleles found in other species (i.e. A^Y). Secondly, our study confirms Little and Carver's predictions regarding the existence in dogs of a recessive e allele that causes the inheritance of yellow coat color. In addition, we have provided evidence that e encodes a truncated (MC1R-R306ter), non-functional receptor. This suggestion is supported by the pharmacological characterization (binding and adenylyl cyclase assays) of MC1R-R306ter. Our molecular analysis of the truncated receptor suggests that MC1R-R306ter is non-functional because it fails to reach the plasma membrane. The decreased stability of this receptor further indicates that it is rapidly degraded intracellularly, possibly as a result of incorrect folding in the ER. In summary, these data demonstrate that the genetic interaction between canine *extension* and *agouti* is more analogous to those found in other species than previously predicted. We have found no indication for either a dominant *agouti* or *extension* allele causing eumelanization. Based on this analysis we conclude that black coat color is due to a recessive a allele, as previously shown in rodents, or to an as yet unidentified third locus. In addition, our study demonstrates that the cytoplasmic domain of the MC1-R is required for the functional receptor to achieve its mature conformation and be translocated to the cell surface.

Figure 1. Genomic structure and amino acid sequence of the canine agouti.

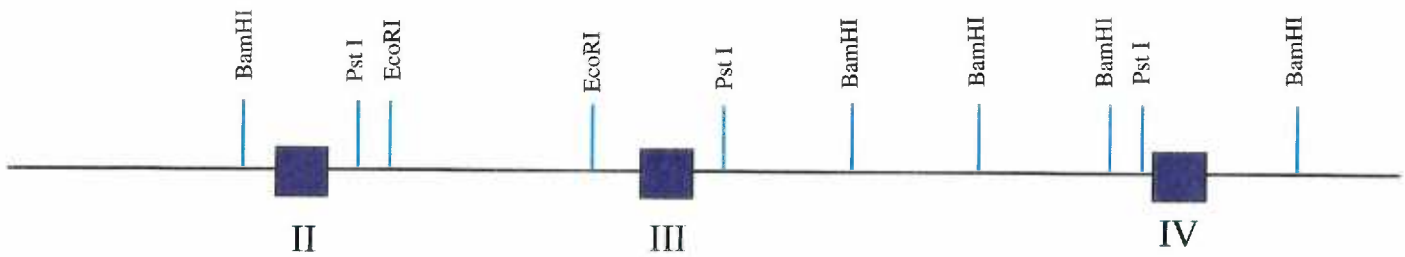
A. Structure of the *agouti* gene.

B. Amino acid sequence alignment of canine and other mammalian agouti proteins.

The alignment includes amino acid sequences of dog, mouse, human, and fox agouti proteins. The three coding exons of agouti are shown in blue, green, and red, respectively.

A.

Dog Agouti Gene



B.

Exon 2

M-agouti	1MDVTRLLLATLVSLCFFTVHSHLALEETLGDDRSLRSNSSMNS
H-agouti	1MDVTRLLLATLLVFLCFFTANSHLPPEEKLRRDDRSLRSNSSVNL
F-agouti	1MNIFRLLLATLLVSLCFLTAYSHLA-EEKPKDDRSLRSNSSVNL
D-agouti	1MNIFRLLLATLLVSLCFLTAYSHLA-EEKPKDDRSLRSNSSVNL

Exon 3

M-agouti	45LDFSSVSIVALNKKSKKISRKEAEKRKRSSKKKASMKKVA--RP
H-agouti	45LDVPSVSIVALNKKSKQIGRKAAEK-KRSSKKEASMKKVV--RP
F-agouti	45LDFPSVSIVALNKKSKKISRKEAEK-KRSSKKKASMKNKARPRP
D-agouti	45LDFPSVSIVALNKKSKKISRKEAEK-KRSSKKKASMKNVARPRP

Exon 4

M-agouti	87PPPS--PCVATRDCKPPAPACCDPCASCQCRFFGSACTCRVLN
H-agouti	87RTPLSAPCVATRNSCKPPAPACCDPCASCQCRFFRSACSCRVLN
F-agouti	87PPPN-PCVATRNSCKSPAPACCDPCASCQCRFFRSACTCR----
D-agouti	87PPPT--PCVATRNSCKSPAPACCDPCASCQCRFFRSACTCRVLN

M-agouti	129PNC
H-agouti	129LNC
F-agouti	129---
D-agouti	129PRC

Figure 2. Expression pattern of the A^s *agouti* allele.

Lane 1: canine kidney (A^s), lane 2: canine spleen (A^s), lane 3: canine liver (A^s), lanes 4-7: canine skin (A^s), lane 15: canine testis (A^s), lanes 8-14: murine tissues (A^Y kidney, liver, spleen, brain, skin).

A. Northern analysis of canine *agouti* mRNA transcripts.

B. 28 S and 18 S mRNA.

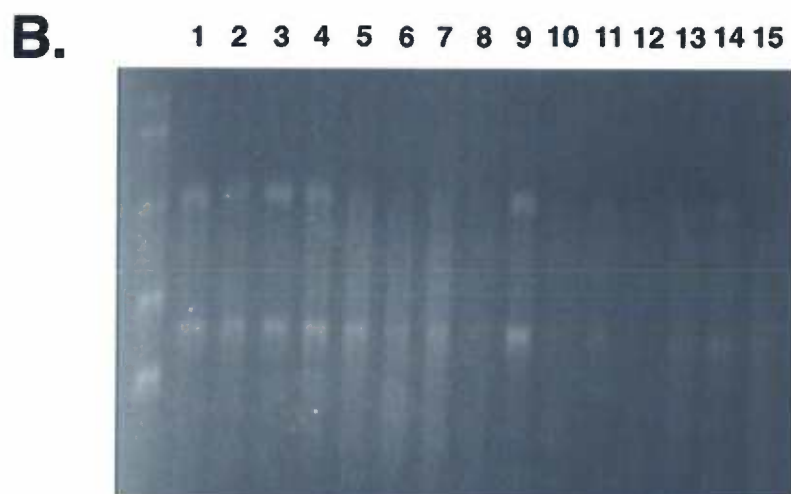


Figure 3. Amino acid sequence of the canine MC1-R.

The alignment includes the amino acid sequences of dog, mouse, human, bovine, panther, fox, and chicken MC1-Rs. Regions of high homology in the transmembrane (TM) and extracellular loops are featured in blue and red, respectively.

```

{-----TM-1-----}
MMC1R 1 MSTQEPQKSLVGSLNS--NATSHLGLATNQSEPWCLYVSIPDGLFLSLGLVSLVENVLVVI
HMC1R 1 MAVQGSQRRLLGSLNSTPTAIPQLGLAANQTGARCLEVSI SDGLFLSLGLVSLVENALVVA
BMC1R 1 MPALGSQRRLLGSLNCTPPATLPFTLAPNRTPGQCLEVSSLDGLFLSLGLVSLVENVLVVA
PMC1R 1 MSVQGP-RXLLGSXNSTSPAAPRLGLAANQTGPRCLEVSVDPGLFLSLGLVSVVENVLVVA
FMC1R 1 MSGQGPQRRLLGSPNATSPTPHFKLAANQTGPRCLEVSI PDGLFLSLGLVSVVENVLVVA
DMC1R 1 MSGQGPQRRLLGSLNGTSPATPHFELAANQTGPRCLEVSI PDGLFLSLGLVSVVENVLVVA
CMC1R 1 MSMLAPLR-LVREFWNASEGNSNATAGAGGAWCQGLD-IPNELFLTGLVSLVENLLVVA

{-----TM-2-----}
MMC1R 60 AITKNRNLHSPMYFICCLALSDLMVSVSIVLETTIILLLEVGILVARVALVQQLDNLIDV
HMC1R 62 TIAKNRNLHSPMYCFICCLALSDLLVSGTNVLETAVILLLEAGALVARAVLQQLDNVIDV
BMC1R 62 AIAKNRNLHSPMYFICCLAVSDDLVSVSNNVLETAVMLLLEAGVLATQA AVVQQLDNVIDV
PMC1R 61 AIAKNRNLHSPMYFICCLAVSDDLVSVSNNVLETAVMLLLEAGTLAGRA AVVQQLDNVIDV
FMC1R 62 AIAKNRNLHSPMYFICCLAVSDDLVSVTNVLETAVMLLLEAGALAAQA AVVQQLDNIIDV
DMC1R 62 AIAKNRNLHSPMYFICCLAVSDDLVSVSNNVLETAVMLLVAACTLAAQA AVVQQLDNIIDV
CMC1R 60 AILKNRNLHSPTYFICCLAVSDNLVSVSNLAKTLFMLLMEHGVLVIRASIVRHMDNVITM

---TM-3-----} {-----TM-4-----}
MMC1R 121 LICGSMVSSSLCFLGIIAIDRYISIFYALRYHSIVTLPRARRAVVGIMVSVSSTLFITYY
HMC1R 123 ITCSSMLSSSLCFLGAIADVDRYISIFYALRYHSIVTLPRAPRAVAIIWVASVVFSTLFIAYY
BMC1R 123 LICGSMVSSSLCFLGAIADVDRYISIFYALRYHSVVTLPRAWRIIAAIWVASILTSLLFITYY
PMC1R 122 LVCGAMVSSSLCFLGAIADVDRYISIFYALRYHSIVTLPRAWRAISAIWVASVLSSTLFIAYY
FMC1R 123 LICGSMVSSSLCFLGAIADVDRYLSIFYALRYHSIVTLPRAWRAISAIWVASVLSSTLFIAYY
DMC1R 123 LICGSMVSSSLCFLGAIADVDRYLSIFYALRYHSIVTLQRAWRAISAIWVANVLSNTLFIAYY
CMC1R 121 LICSSVVSSSLCFLGVIADVDRYITIFYALRYHSIMTLQRAVVIMASVWLASTVSVSTVLITYY

{-----TM-5-----} {--
MMC1R 182 KHTAVLLCLVTFFFLAMLALMAILYAHMFTRACQHVQGIAQLHKRRRSIRQGFSLKGAATLT
HMC1R 184 DHVAVLLCLVTFFFLAMLVLMVAVLYVHMLARACQHAQGIARLHKRQRPVHQGFGLKGAATLT
BMC1R 184 NHKVILLCLVGLFIAMLALMAVLYVHMLARACQHARGIARLQKRQRPVHQGFGLKGAATLT
PMC1R 183 DHTAVLLCLVTFFFVAMLVLMVAVLYVHMLCSTCQHAXGTARLHKRQRPVHQGLGLKGAATLT
FMC1R 184 NHTAVLLCLVSFFVAMLVLMVAVLYVHMLARACQHARGIARLKRQHSHVHQGFGLKGAATLT
DMC1R 184 NHTAVLLCLVSFFVTMLVLMVAVLYVHMLARACQHARGIARLHKRQHFIPQGFGLKGAATLT
CMC1R 182 RNNATILLCLIGFFFLFMLVLMVLYIHMFALACHHVRSISSQK-QPTIYRTSSLKGAATLT

----TM-6-----} {-----TM-7-----}
MMC1R 243 ILLGIFFLCWGPFFFHLILLIVLCFQHPTCSGIFKNFNLFLLIIVLSSVDPLIYAFRSQEL
HMC1R 245 ILLGIFFLCWGPFFFHLTLIVLCFQHPTCGCIFKNFNLFLLIICNAIDPLIYAFHSQEL
BMC1R 245 ILLGVFFLCWGPFFFHLSLIVLCFQHPTCGCIFKNFNLFLLIICNAIVDPLIYAFRSQEL
PMC1R 244 MLLGIFFLCWGPFFFHLSLMVLCFQHPICGCVFKNFNLFLLIICNSIVDPLIYAFRSQEL
FMC1R 245 ILLGIFFLCWGPFFFHLSLMVLCFQHPICGCVFQNFNLFLLIICNSIIDPFIYAFRSQEL
DMC1R 245 ILLGIFFLWGPFFFLHLSLMVLCFQHPICGCVFQNFNLFLLIICNSIIDPFIYAFRSQEL
CMC1R 243 ILLGVFFICWGPFFFHLILIVTCPTNPFCTCFPSYFNLFLLIICNSVVDPLIYAFRSQEL

MMC1R 304 RMTLKEVLLCSW
HMC1R 306 RRTLKEVLTCSW
BMC1R 306 RKTLEQEVLLQCSW
FMC1R 306 RKTLEQEVLLCSW
DMC1R 306 RKTLEQEVLLCSW
CMC1R 304 RRTLREVVLCSW

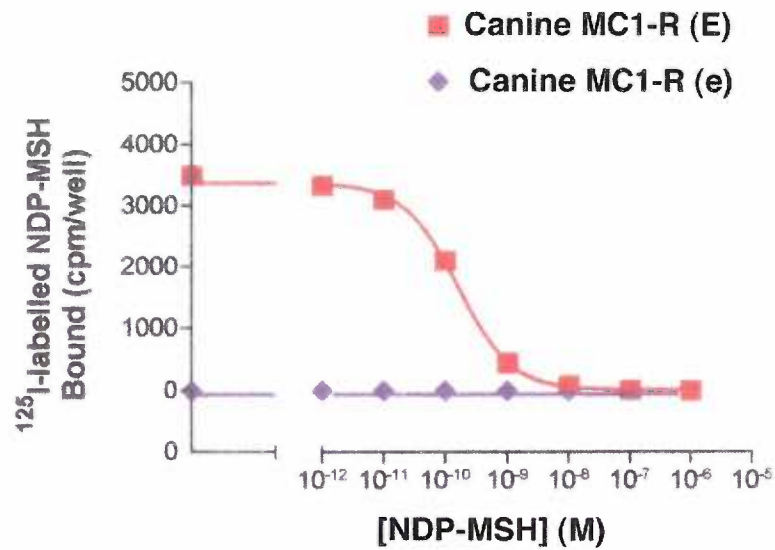
```

Figure 4. The canine *e* allele encodes a non-functional MC1-R.

A. Binding assay.

B. Adenylyl cyclase assay (β -gal).

A.



B.

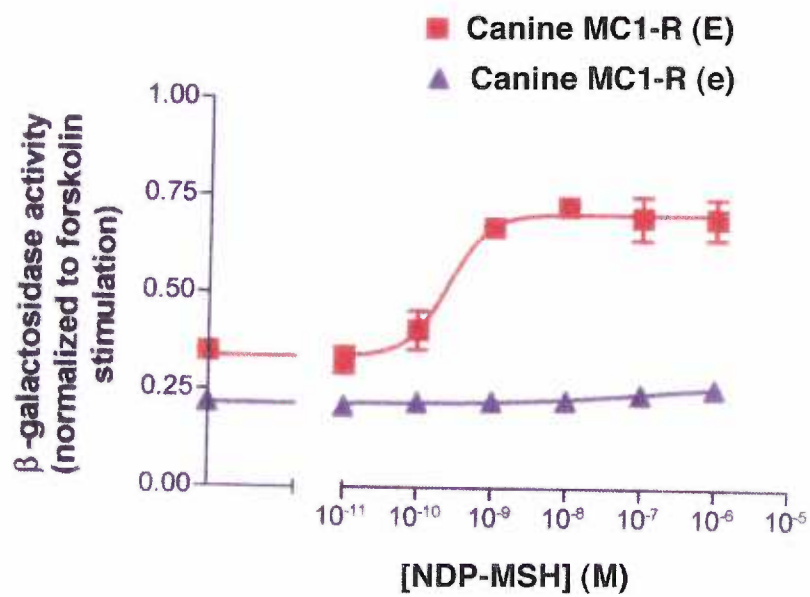


Figure 5. No difference in mRNA levels between full-length (*E*) and truncated MC1R-R306ter (*e*).

A. Northern analysis of HEK 293 cells transiently transfected with either full-length (*E*) or truncated MC1-R (*e*). Ten μ g of total RNA was loaded in each lane. The membrane-bound RNA was probed with a fragment of canine cDNA.

B. 28 S and 18 S mRNA.

A.

MC1-R (E) MC1-R (e)



B.

MC1-R (E) MC1-R (e)

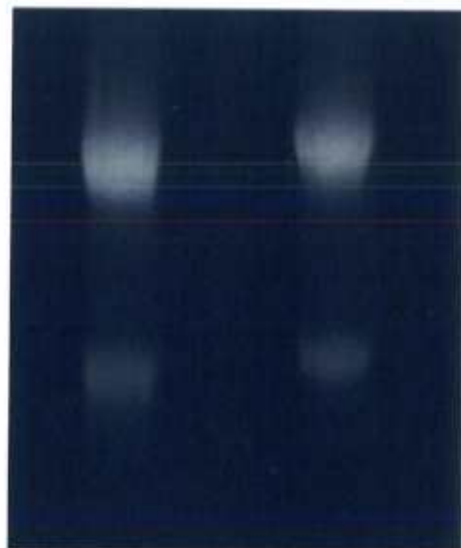


Figure 6. MC1R-R306ter is non-functional because of decreased protein stability and loss of cell surface expression.

Full-length (*E*) and truncated MC1-R (*e*) were tagged at the N-terminus and transiently transfected in HEK 293 cells. Protein levels were determined by Western analysis using the anti-flag M2 antibody.

- A.** Western analysis of whole-cell extracts.
- B.** Western analysis of total membrane preparations.

Untransfected Vector (flag)
only Yellow lab
MSH-r Black lab
MSH-r



← 30-32 kDa

Cell Lysate

Untransfected Vector (flag)
only Yellow lab
MSH-r Black lab
MSH-r



← 30-32 kDa

Membranes

CHAPTER THREE

***MAHOGANY (mg)* STIMULATES FEEDING AND INCREASES BASAL METABOLIC RATE INDEPENDENT OF ITS SUPPRESSION OF AGOUTI**

**Daniela M. Dinulescu^{1,2}, Wei Fan¹, Bruce A. Boston³, Kathleen McCall³, M. Lynn
Lamoreux⁴, Karen J. Moore⁵, Jill Montagno⁵, and Roger D. Cone^{1,2}**

¹Vollum Institute, ²Department of Cell and Developmental Biology, and ³Department of Pediatrics, Oregon Health Sciences University, Portland, OR 97201, ⁴Department of Veterinary Pathobiology, Texas A & M University, College Station, TX 77843, and ⁵Millennium Pharmaceuticals, Inc., 640 Memorial Drive, Cambridge, Massachusetts 02139

Published in *PNAS* **95**, 12707-12712. (1998)

ABSTRACT

The *mahogany* (*mg*) mutation was originally identified as a recessive suppressor of *agouti*, a locus encoding a skin peptide that modifies coat color by antagonizing the melanocyte-stimulating hormone (MSH) receptor or MC1-R. Certain dominant alleles of *agouti* cause an obesity syndrome when ectopic expression of the peptide aberrantly antagonizes the MC4-R, a related MSH receptor expressed in hypothalamic circuitry and involved in the regulation of feeding behavior and metabolism. Recent work has demonstrated that *mg*, when homozygous, blocks not only the ability of *agouti* (A^Y) to induce a yellow coat color when expressed in the skin of the *lethal yellow* mouse, but also the obesity resulting from ectopic expression of *agouti* in the brain. Detailed analysis of *mg/mg* A^Y/a animals, presented here, demonstrates that *mg/mg* blocks the obesity, hyperinsulinemia, and increased linear growth induced by ectopic *agouti* expression. Remarkably, however, the *mg* mutation did not reduce hyperphagia in the A^Y/a mouse. Furthermore, homozygous *mg* induced hyperphagia and an increase in basal metabolic rate in the C57BL/6J mouse in the absence of A^Y . Consequently, although mahogany is broadly required for *agouti* protein action, it also appears to be involved in the control of metabolic rate and feeding behavior independent of its effects on *agouti* signaling.

INTRODUCTION

The 131-amino acid agouti peptide is synthesized in the follicular cells of the dermal papilla and acts in a paracrine fashion on melanocytes where it antagonizes the binding of α -MSH to MC1-R (Lu et al., 1994; Yang et al., 1997). The transcription of the wild-type mouse *agouti* is temporally and spatially regulated, the gene being expressed solely in the skin during part of the hair-growth cycle where it gives rise to a subapical yellow pigment band in the growing hair shaft (Bultman et al., 1992). Several dominant alleles at the mouse *agouti* locus (e.g. *lethal yellow*, A^Y , and *viable yellow*, A^{VY}), however, have an ectopic pattern of expression due to a promoter gene rearrangement (Michaud et al., 1994), and are associated phenotypically with yellow fur, late-onset obesity, hyperphagia, increased linear growth, and non-insulin dependent diabetes (Bultman et al., 1992; Michaud et al., 1994).

Recent studies have provided an explanation for the development of the *lethal yellow* obesity syndrome. *In vitro* experiments using recombinant protein in HEK 293 cell-system have identified agouti not only as a MC1-R antagonist but also as a high affinity, competitive antagonist of a melanocortin receptor subtype, MC4-R (Lu et al., 1994), widely expressed in regions of the hypothalamus known to be involved in the regulation of feeding behavior and metabolism (Gantz et al., 1993b; Mountjoy et al., 1994). Genetic and pharmacological studies have concluded that disruption of MC4-R signaling is the primary cause of the A^Y -induced obesity syndrome (Fan et al., 1997; Huszar et al., 1997). The MC4-R knockout (MC4-R KO) mouse recapitulates all

phenotypic aspects of the *agouti* obesity syndrome (Huszar et al., 1997). Moreover, intracerebroventricular administration of a melanocortin analogue, MTII, a potent agonist of the MC3-R and MC4-R, suppresses feeding behavior in rodents whereas injection of SHU9119, an antagonist of the same receptors, has the opposite effect (Fan et al., 1997). The pharmacological and genetic evidence point out two major conclusions: first, neurons expressing MC4-R exert a tonic inhibition upon feeding behavior and second, development of the *agouti* obesity syndrome is due to chronic antagonism of MC4-R signaling by *agouti*.

The recent discovery in the hypothalamus of another antagonist of MC3-R and MC4-R, the *agouti*-related protein (AGRP) (Ollmann et al., 1997), or *agouti*-related transcript (ART) (Shutter et al., 1997), raises the intriguing possibility that ectopic expression of *agouti* mimics the function of endogenous AGRP in the central control of energy homeostasis. Overexpression of AGRP in the mouse animal model results in an obesity and diabetes phenotype very much like that of A^Y and MC4-R KO mice (Graham et al., 1997; Ollmann et al., 1997), further demonstrating that MC4-R, activated by α -MSH or α -MSH analogues and endogenously antagonized by AGRP, is an important modulator of metabolic state. Future studies will be required to determine if the MC3-R is also involved in the control of energy homeostasis.

The murine *mahogany* (*mg*) and *mahoganoid* (*md*) mutations were identified in the 60 s as recessive suppressors of A^Y -induced pigmentation, which were able to shift melanogenesis from the pheomelanin (red/yellow pigment) pathway towards eumelanin

(black/brown pigment) production (Lane and Green, 1960). Early genetic studies mapped *mahogany* and *mahoganoid* loci to chromosomes 2 and 16, respectively (Green, 1989). The murine *mahogany* locus is characterized by two mutations, *mg*, which originated in the LDJ/Le background, and *mg*^{3J} in the C3HeB/FeJ background (Miller et al., 1997). The *md* coat color mutation originated in the C3H/HeJ genetic background (Miller et al., 1997). Recently, both *mg* and *md* were found to suppress not only the yellow coat color but also the *A*^Y-induced increase in body weight (Miller et al., 1997), suggesting that the normal gene products are required for *agouti* action both in skin and brain. These studies also indicate that *md* and *mg* are partially semidominant, since both mutations show some ability to suppress pheomelanin synthesis as well as obesity in the *A*^Y mouse (*md* only) when heterozygous (Miller et al., 1997). Two possible mechanisms proposed for mahogany action by the recent studies include interference with agouti protein processing or secretion, or disruption of its interaction with melanocortin receptors (Miller et al., 1997).

Although the loss-of-function *mg* mutation has been shown to decrease weight gain in the *A*^Y/- mouse, no detailed analysis of the physiological effects of *mg* in the presence or absence of the *A*^Y gene has been published. Analysis of weight, body composition, linear growth, serum insulin, leptin, glucose, and corticosterone, feeding behavior, circadian rhythms, and basal metabolic rate in *mg/mg A*^Y/*a* and normal *mg/mg a/a* mice is presented here. Data on the effect of the *md* mutation on feeding behavior is also presented.

MATERIALS AND METHODS

Mice. In order to study the action of *mg*, A^Y , and *ob* genes in a uniform genetic background we recovered the *mg* mutation from the LDJ/Le background. All our studies were performed on mice homozygous for the *mg* mutation backcrossed by one of us (MLL) for 6-8 generations to the C57BL/6J background. The A^Y and *ob* alleles were also derived from congenic C57BL/6J mice (Jackson Laboratories, Bar Harbor, ME). Animals homozygous for the *md* mutation and their controls originated in the C3H/HeJ background (Jackson Laboratories, Bar Harbor, ME). Mice were housed as siblings, maintained at $23^{\circ} \pm 1^{\circ}\text{C}$ on a 12h/12h light/dark cycle (7:00-19:00 h), and allowed free access to water and food (Purina, St. Louis, MO). All studies were conducted under guidelines provided by the Animal Care and Use Committee of Oregon Health Sciences University.

Body and Organ Weight. In order to study the effect of *mg/mg* on A^Y -induced weight gain, C57BL/6J mice of four different genotypes ($+/+ a/a$, $+/+ A^Y/a$, *mg/mg a/a*, and *mg/mg A^Y/a*), were regularly weighed as littermates. For organ weight measurements different white fat pads (epididymal, visceral, and dorsal), brown fat, heart, and liver were dissected and weighed. Weight growth curves were also determined for $+/+ a/a$, $+/+ ob/ob$, *mg/mg a/a*, and *mg/mg ob/ob* mice.

Body Length Measurements. Animals were lightly anesthetized with 2% avertin and extended to their maximal length to determine the nose-to-anus distance, a measure of their linear growth.

Food Intake. For measurement of food consumption, animals of four genotypes ($+/+ a/a$, $+/+ A^Y/a$, $mg/mg a/a$, and $mg/mg A^Y/a$) were housed individually for at least two weeks prior to beginning of the experiment. Pre-weighed standard chow pellets (4.5% fat) were provided to mice *ad libitum* in Petri dishes and measurements of the remaining food were taken each 24 h for a 7-day period. In order to minimize food spillage mice were housed in cages with no bedding and they were given only 2-3 food pellets at one time. The effect of md/md on food intake was analyzed by measuring weekly food consumption (9% fat diet) for $md/md A/A$ and $+/+ A/A$ controls. Data from both experiments are presented as g/mouse/day for comparative purposes.

Blood analysis. Animals were sacrificed by cervical dislocation between 16:00 and 18:00 h and trunk blood was collected. Serum insulin and leptin concentrations were determined in duplicate using radioimmunoassay (RIA) kits with rat insulin and recombinant leptin, respectively, as standards (Linco Research, Inc.). For serum corticosterone measurements blood was collected from the tail vein within 1 min of handling and corticosterone levels were measured in the serum using a RIA kit (ICN Biomedicals, Inc., Costa Mesa, CA). Blood glucose concentrations were measured using One-Touch Profile glucose meter (Lifescan, Milpitas, CA).

Motor Activity. Animals were housed individually in metabolic cages equipped with a running wheel (Mini-Mitter Co., Sunriver, OR). The metabolic cages allowed telemetric monitoring of circadian rhythms as assessed via two physiological parameters: temperature and number of wheel turns. The wheel revolutions were quantified by recording the magnetic switch closures of a magnet placed on the revolving wheel. For temperature recordings mice were implanted with a radiotransmitter in the peritoneal cavity and allowed to recover for one week. Temperature was monitored by sampling series of digital pulses from the implanted transmitter.

Basal Metabolic Rate. Oxygen consumption was simultaneously determined for multiple animals by indirect calorimetry using an Oxymax System (Columbus Instruments, Columbus, OH). For this purpose animals were housed in separate chambers maintained at $24^{\circ} \pm 1^{\circ}\text{C}$. Before beginning of the experiment animals were acclimatized to the chambers and then measurements were taken for 4-5 h during the middle of the light cycle (11:00-16:00 h). Samples were recorded every 3 min with the room air reference taken every 30 min and the air flow to chambers 500 ml/min. Basal oxygen consumption was determined for individual curves as the average at the lowest plateau regions that corresponded to resting periods. Total oxygen consumption was the result of all samples recorded corresponding to periods of movement as well as inactivity.

Statistical Analysis. All data are presented as mean \pm SEM. Growth curves were analyzed by ANOVA with multiple measurements. All other statistical comparisons

between different strains were performed by Student's two-tailed t test with $p < 0.05$ considered significant.

RESULTS

mg Suppresses the A^Y -induced Obesity

The main focus of our physiological characterization was to compare and contrast the phenotypes of *mg/mg* A^Y/a and $+/+$ A^Y/a mice, the first step being to determine which of the A^Y -mediated obesity parameters were suppressed by *mg*. We determined growth curves for $+/+$ A^Y/a , *mg/mg* A^Y/a , *mg/mg* a/a , and $+/+$ a/a female mice housed as siblings and maintained on a low-fat rodent chow (Figure 1 A). The weight gain of the animals was monitored regularly between 4 and 24 weeks of age. All weight curves, with the exception of *mg/mg* a/a versus $+/+$ a/a wild-type controls, were significantly different as analyzed by ANOVA with multiple measurements ($p < 0.0001$). As previously reported (Dickerson and Gowen, 1947; Fenton and Chase, 1951), $+/+$ A^Y/a animals are characterized by a progressive increase in their body weight starting at approximately 2 months for female mice as compared to wild-type controls. By 6 months of age there is an approximate 24% increase in the body weights of $+/+$ A^Y/a animals versus *mg/mg* A^Y/a ($p < 0.01$), indicating that *mg* is able to suppress the A^Y -induced weight gain. Similar data on the suppression of A^Y -induced weight increase by *mg/mg* were found in LDJ/Le//C57BL/6J hybrids and in non-littermates in the C57BL/6J background (Miller et al., 1997). In contrast, homozygosity of *mg* was not found to suppress the weight gain in the *ob/ob* mouse during the 20-week period studied (Figure 1 B). The apparent decrease

in body weight of *mg/mg ob/ob* versus *+/+ ob/ob* seen at 16 weeks of age was due to incomplete sampling of weights during this time period ($n = 1-3$), and was not significant, as can be seen by examination of the mean weights at 19 or 20 weeks ($n = 6$). In order to investigate whether the A^Y -induced gain in body weight is due to an increase in body fat mass, various fat pads, heart, and liver from 23-week old animals were dissected and measured. The results presented in Table 1 further show the absence of obesity in *mg/mg A^Y/a* mice. The weights of the different tissues we examined, with the exception of heart, were significantly decreased in *mg/mg A^Y/a* mice, presumably due to less triglyceride accumulation, and were equivalent to those found in wild-type controls (data not shown).

***mg* Suppresses the A^Y -induced Increase in Linear Growth**

Body length (nose-to-anus distance) was determined for 23-week old *+/+ A^Y/a*, *mg/mg A^Y/a*, and *mg/mg a/a* males, respectively. Our results indicate that *+/+ A^Y/a* are approximately 6.1% ($p < 0.001$) longer than *mg/mg A^Y/a* animals and 5.9% ($p < 0.001$) longer than *mg/mg a/a* age-matched controls (Figure 2).

***mg* Blocks the Endocrine Effects of A^Y -induced Obesity: Serum Insulin, Leptin, Glucose, and Corticosterone Measurements**

Blood was collected from 22-week old *+/+ A^Y/a*, *mg/mg A^Y/a*, *mg/mg a/a*, and *+/+ a/a* male animals and assayed for insulin and leptin concentrations. Our analysis indicates that *+/+ A^Y/a* mice exhibit elevated insulin (Figure 3 A) and leptin (Figure 3 B) levels, a 5.6-fold ($p < 0.01$) and a 2.5-fold ($p < 0.01$) increase, respectively, over their *mg/mg A^Y/a*, or *+/+ a/a* counterparts. No significant differences were detected among the other

groups. The high serum leptin and insulin concentrations found in $+/+ A^Y/a$ animals are correlated with their progressive increase in body fat and lipid deposition. The A^Y —induced hyperglycemia was also found to be suppressed by mg as 26-week old $mg/mg A^Y/a$ male animals ($n = 6$) had blood glucose concentrations (114 ± 2.0 mg/dl) significantly lower ($p = 0.0001$) than $+/+ A^Y/a$ (131 ± 3.0 mg/dl, $n = 7$). No differences in basal corticosterone levels were found between genotypes (3-month old males, $n = 5$, data not shown).

***mg/mg A^Y/a* Mice Remain Hyperphagic, and Both *mg* and *md* Independently Induce Hyperphagia**

The progressive weight gain and increase in adipose tissue that characterize $+/+ A^Y/a$ animals result from both increased caloric intake and decreased energy expenditure. We decided therefore to look at both aspects of energy balance. The food consumption of 28-week old females, representing the four genotypes: $mg/mg A^Y/a$, $mg/mg a/a$, $+/+ A^Y/a$, and $+/+ a/a$, was monitored over a 7-day period. In agreement with previous reports (Dickerson and Gowen, 1947), $+/+ A^Y/a$ mice are hyperphagic, their average daily food intake in this assay being significantly higher (5.9 ± 0.1 g/24 h, $p < 0.0001$) than C57BL/6J controls (4.6 ± 0.2 g/24 h). Surprisingly, mg/mg did not appear to reduce A^Y -induced hyperphagia as we found no significant difference between $+/+ A^Y/a$ and $mg/mg A^Y/a$ caloric intake (Figure 4 A), despite a 24% difference in their body weight. Furthermore, mg/mg alone induced hyperphagia, the presence of homozygous mg in the absence of A^Y resulting in an approximate 22% increase in food intake (5.7 ± 0.2 g/24 h versus 4.6 ± 0.2 g/24 h, $p < 0.0001$) over C57BL/6J controls of equal weight. As it was

previously shown that the *mahoganoid* locus encoded a phenocopy of *mahogany* (Lane and Green, 1960; Miller et al., 1997), we examined the effect of *md/md* on food intake as well. Homozygosity for *md* also resulted in hyperphagia (Figure 4 B).

***mg* Increases Motor Activity and Basal Metabolic Rate**

In light of the finding that *mg/mg* mice were hyperphagic, it became essential to determine how these animals remained lean while consuming 22% more calories. Therefore, the two major components of daily energy expenditure, basal metabolic rate (BMR) and energy expenditure due to physical activity, were determined as a function of genotype. Activity on an exercise wheel was measured in *mg/mg A^Y/a* and *+/+ A^Y/a*, as well as in *mg/mg a/a* versus *+/+ a/a* mice. *mg/mg A^Y/a* animals showed increased nighttime activity and a corresponding 0.5°C gain in body temperature correlating with the increased exercise (Figure 5 A, B, representative 48 h traces). During nighttime, *mg/mg A^Y/a* exhibited an approximate 2-fold increase ($p < 0.0001$) in the number of wheel turns over *+/+ A^Y/a* animals (Figure 5 C), whereas *mg/mg a/a* showed a 30% increase in their motor activity ($p < 0.0001$) when compared to wild-type mice (Figure 5 D). We concluded that the absence of mahogany augments physical activity during nighttime. We further analyzed basal metabolic rate in 20- to 28-week old animals. At the time of our experiment *+/+ A^Y/a* mice were significantly heavier than their age-matched *mg/mg A^Y/a* complements (39.7 ± 2.3 g versus 29.1 ± 1.6 g, $p < 0.01$). On a per animal basis, no significant difference in oxygen consumption could be detected when comparing the *+/+ A^Y/a* and *mg/mg A^Y/a* mice (Fig. 5 E). Surprisingly, *mg/mg a/a* animals (27.4 ± 0.9 g) showed an approximate 21% gain ($p < 0.0001$) in their basal metabolic rate over weight-matched

wild-type controls (26.2 ± 0.4 g, Figure 5 F). Our results indicate therefore that *mg/mg* significantly elevates BMR in the normal C57BL/6J animal.

DISCUSSION

Data presented here demonstrate that, with one very important exception (hyperphagia), the *mg* mutation suppresses the phenotypes of the *lethal yellow* obesity syndrome: adult-onset obesity, hyperinsulinemia, hyperleptinemia, hyperglycemia, and increased linear growth. The results show that *mg/mg A^Y/a* mice have a normal body size and adiposity, and their insulin and leptin levels are comparable to wild-type values. The ability of *mg/mg* to suppress the centrally-mediated effects of agouti on feeding and endocrine parameters, as well as the peripherally-mediated inhibition of eumelanin synthesis by agouti in the melanocyte, suggests that mahogany is expressed and functions in both brain and skin. In the *A^Y* mouse, in which the skin agouti peptide is ubiquitously expressed, mahogany is clearly required for agouti function in the hypothalamus. In the C57BL/6J animal, a potential target for mahogany action in the brain, where agouti is not normally expressed, could be the recently discovered hypothalamic agouti-related protein (AGRP). Furthermore, it is noteworthy that according to results presented here the effects of mahogany and mahoganoid are not limited to agouti and/or AGRP since inhibition of the function of either of these proteins (i.e. agouti, AGRP) would not be expected to lead to hyperphagia, but precisely the opposite. Thus, the ability of homozygous *mg* to induce hyperphagia implies the existence of novel pathways for mahogany that are independent of agouti and AGRP signaling. Since hyperphagia in the *mg/mg A^Y/a* mice could be *mg* or

A^Y -driven, it cannot be determined from the data presented here whether *mg* actually suppresses A^Y -induced hyperphagia and concurrently induces hyperphagia via a different pathway. Interestingly, the inability of *mg/mg* to suppress obesity in the *ob/ob* mouse indicates that the effectors dependent upon melanocortins do not include all peptide regulators of energy homeostasis, since if this gene was required for neuropeptide Y (NPY) action (Erickson et al., 1996) it might be expected to ameliorate the obesity resulting from leptin deficiency. Furthermore, immunohistochemistry studies indicate that NPY expression in the hypothalamus (PVH) of *mg* and *mg A^Y* animals is comparable to the wild-type (Figure 6). This finding indicates that the hyperphagia of *mg/mg* animals is not the result of increased hypothalamic NPY expression.

The analysis of the *mg* phenotype demonstrates that in the *a/a* animal homozygous *mg* increases basal metabolic rate (BMR) as well as physical activity. In the A^Y/a mouse, *mg/mg* also elevates physical activity, however an increase in BMR is not detected on a per-animal basis. BMR is the major component of daily energy expenditure, accounting for up to 70% of the caloric utilization. The factors that regulate BMR include hormonal stimuli (i.e. thyroid hormone) and the sympathetic nervous system. These modulators remain to be investigated in the *mg* animal. The phenotype of hyperphagia present in the *mg/mg* mouse could potentially be secondary to elevation of its metabolic rate in an attempt to overcome a negative energy balance and maintain body weight homeostasis. This suggestion is supported by the preliminary observation that *mg* animals lose significantly more body weight than their counterparts following a 24 h fast (*mg/mg a/a*: 4.62 ± 0.29 g versus *+/+ a/a*: 3.38 ± 0.18 g, $p < 0.01$, $n = 4-5$). It is

interesting that mice homozygous for the *md* mutation in the C3H/HeJ background display the same hyperphagia phenotype seen by us in C57BL/6J-*mg/mg* animals, demonstrating that both agouti suppressors can alter feeding behavior independent of background strain.

Based upon the analysis of energy intake and expenditure in *mg/mg* animals we conclude that the pathways in which mahogany functions are largely overlapping with POMC-agouti-AGRP melanocortinergeric neurocircuits, but also appear to include independent pathways regulating metabolic rate and feeding behavior.

We thank Ximena Opitz-Araya and Dee Horne for technical support. This work was funded by grants to RDC (National Institute of Health NIDDK 51730, National Institute of Diabetes and Digestive and Kidney Diseases 51730) and M.L.L. (National Institute of Health EY-10223).

Figure 1.

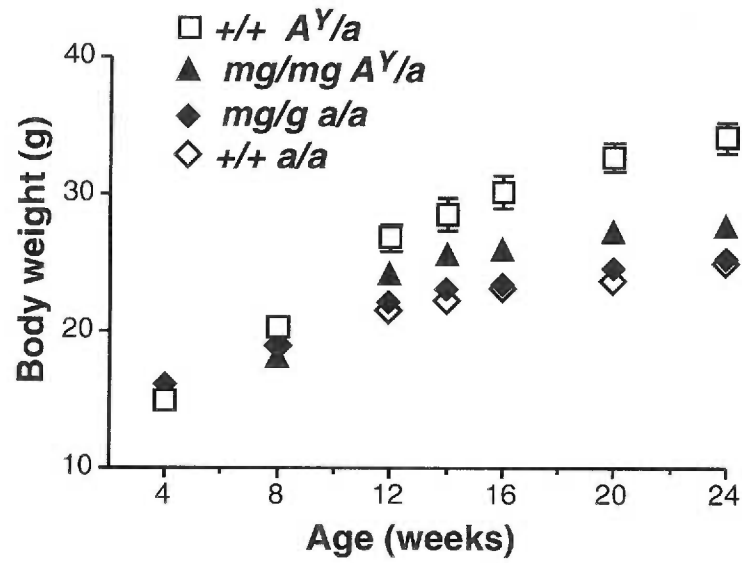
(A). *mg* suppresses the A^Y -induced obesity syndrome.

Data were collected from female animals (n = 4-5 for each genotype).

(B). *mg* has no effect on *ob*-induced weight gain.

Weight growth curves were determined for female *mg/mg ob/ob* (n = 6), *mg/mg a/a* (n = 8), *+/+ ob/ob* (n = 3), and *+/+ a/a* control mice (n = 8). All data are presented as mean \pm SEM.

A.



B.

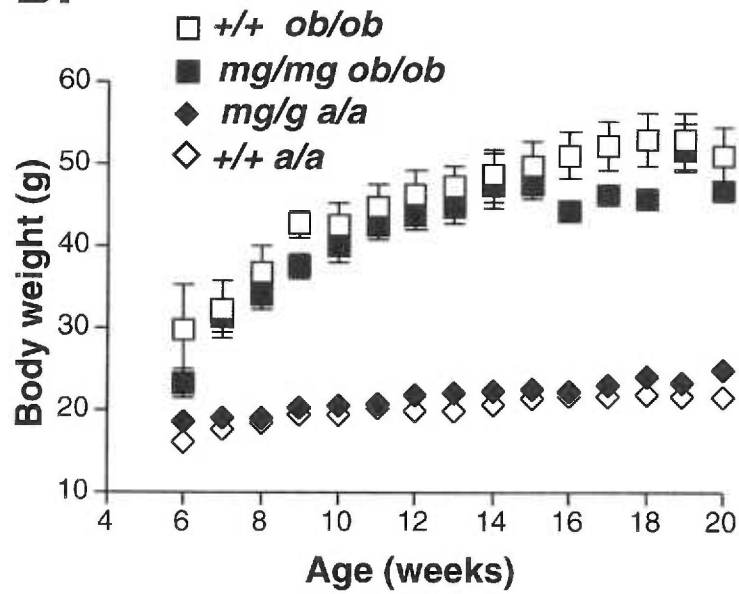


Figure 2. *mg* suppresses the A^Y -induced increase in linear growth.

Body length (naso-anal) measurements were taken from 24- to 28-week old male $+/+ A^Y/a$ ($n = 4$), $mg/mg A^Y/a$ ($n = 3$), and $mg/mg a/a$ animals ($n = 3$). Data are presented as mean \pm SEM. ***, $P < 0.001$.

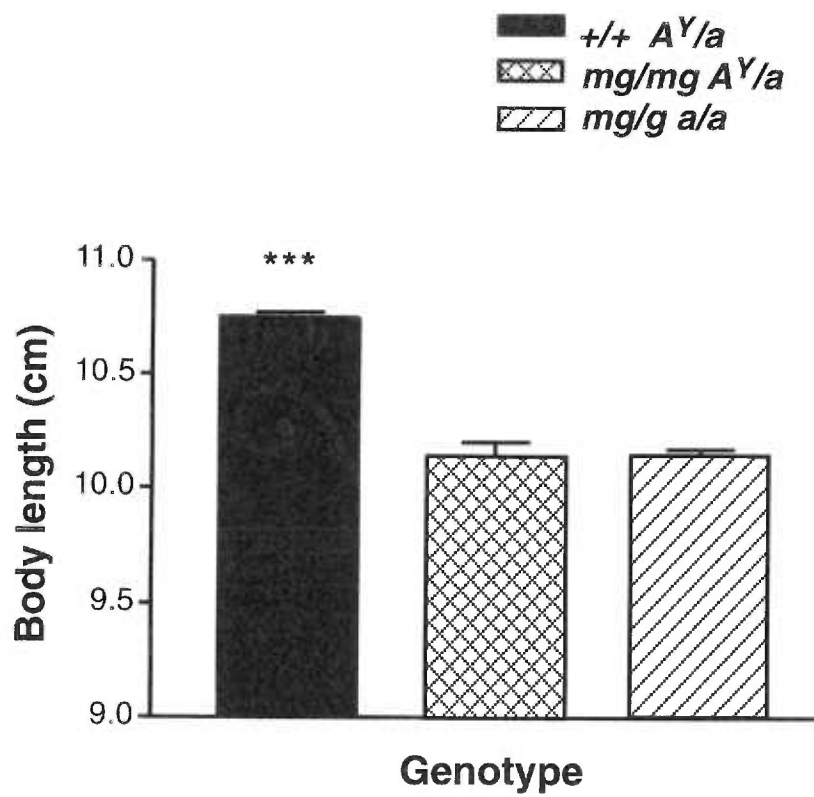


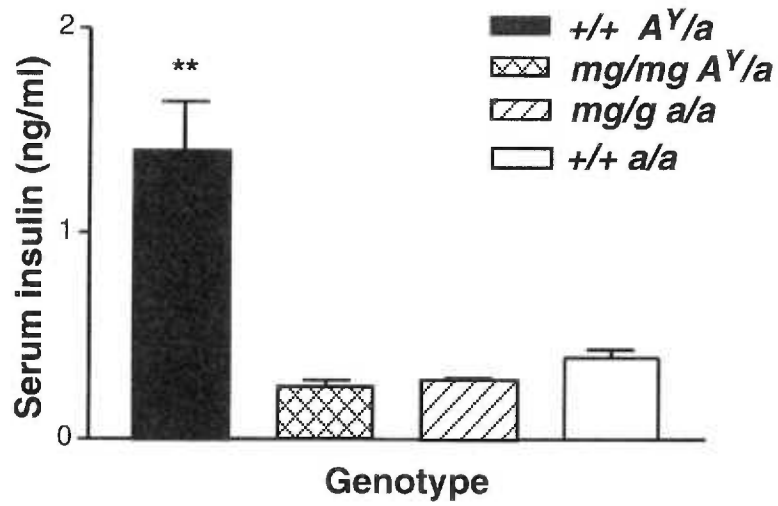
Figure 3. *mg* suppresses the endocrine effects of the *A^Y* obesity syndrome.

(A). Serum insulin.

(B). Serum leptin.

Males (22-week old, n = 5 for each genotype) were used for serum insulin and leptin measurements. All data are presented as mean \pm SEM. **, P < 0.01.

A



B

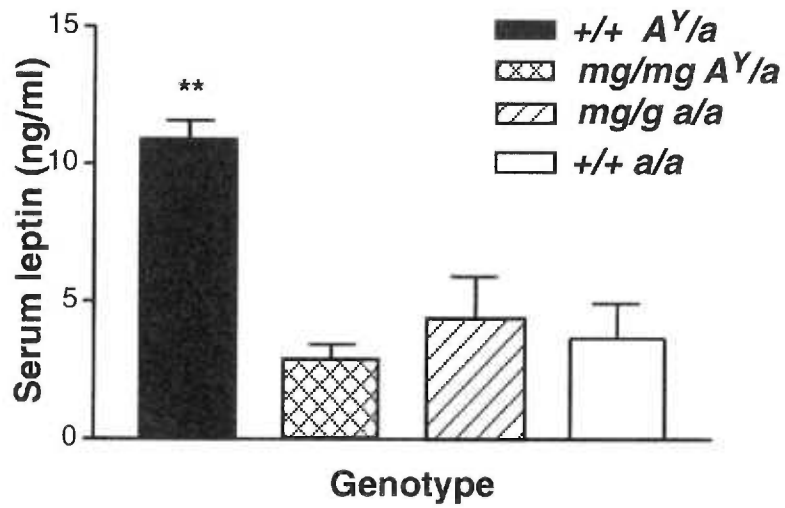


Figure 4. *mg* and *md* independently induce hyperphagia.

(A). Food intake was measured daily over a 7-day period for 28-week old females (n = 4-5 for each group). Data are reported as mean of 7 measurements \pm SEM.

(B). Food consumption of *md/md A/A* males and *+/+ A/A* controls (n = 4 for each genotype) was monitored weekly between 6 and 16 weeks of age. Data are presented as average of 11 measurements \pm SEM. ***, $P \leq 0.0001$.

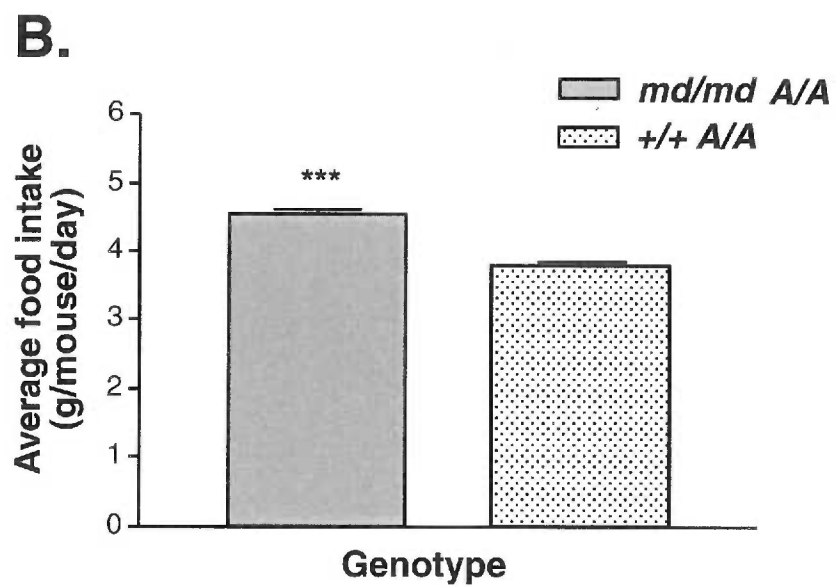
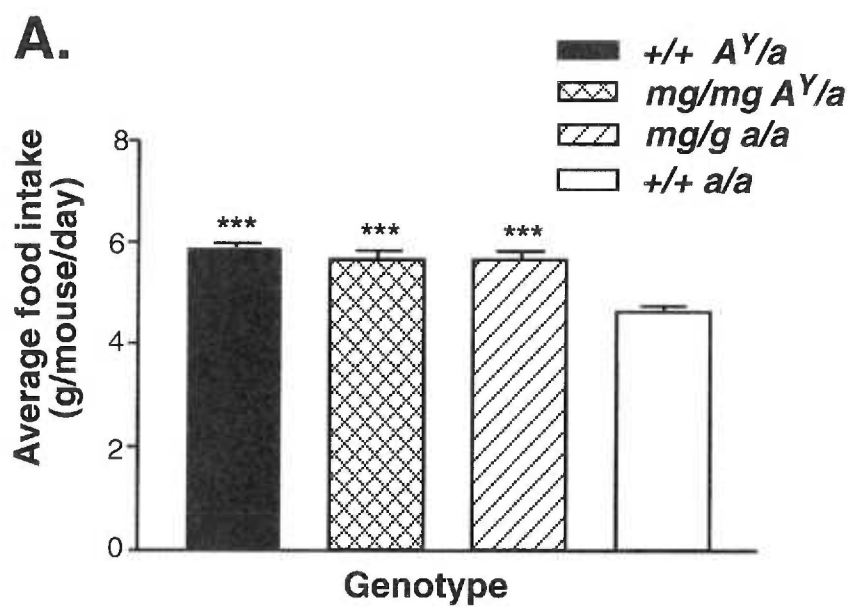


Figure 5. *mg* increases both motor activity and basal metabolic rate.

(A). Circadian rhythm of wheel activity.

(B). Circadian rhythm of body temperature.

Measurements were taken every 1 min during a 48 h time-period for 24- to 28-week old *mg/mg A^y/a* and *+/+ A^y/a* animals (representative traces from 48 h of recording, 2 mice/genotype). The regions of increased activity or temperature correspond to nighttime whereas no or low activity is seen during daytime.

(C) and (D). Quantitative comparison of average physical activity (wheel turns) as measured during nighttime in 20- to 28-week old *mg/mg A^y/a* (n = 7) and *+/+ A^y/a* animals (n = 9) (C), and in 26- to 34-week old *mg/mg a/a* (n = 5) versus *+/+ a/a* wild-type animals (n = 5) (D).

(E). Oxygen consumption of 20- to 28-week old animals *mg/mg A^y/a* and *+/+ A^y/a* mice (n = 8 for each group) as measured by indirect calorimetry.

(F). Oxygen consumption of 20- to 28-week old *mg/mg a/a* versus *+/+ a/a* wild-type animals as determined by indirect calorimetry (n = 11 for each genotype). Both male and female animals were included in Figure 5 measurements. Data in (C), (D), (E), and (F) are reported as mean \pm SEM. ***, P < 0.0001.

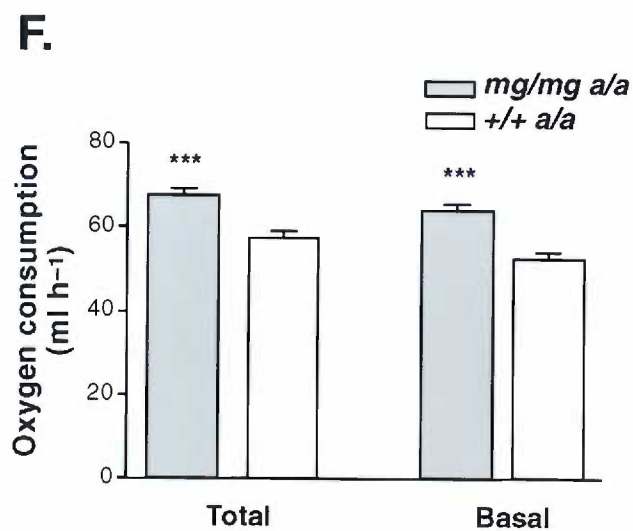
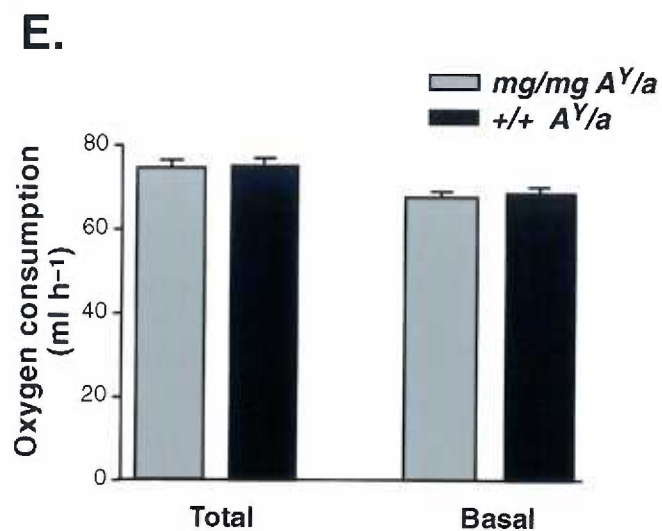
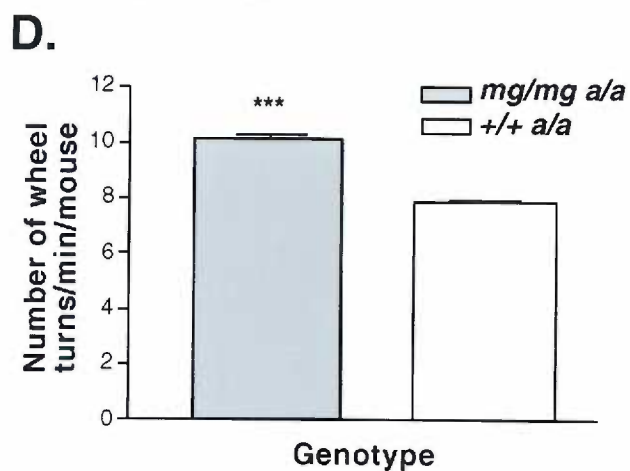
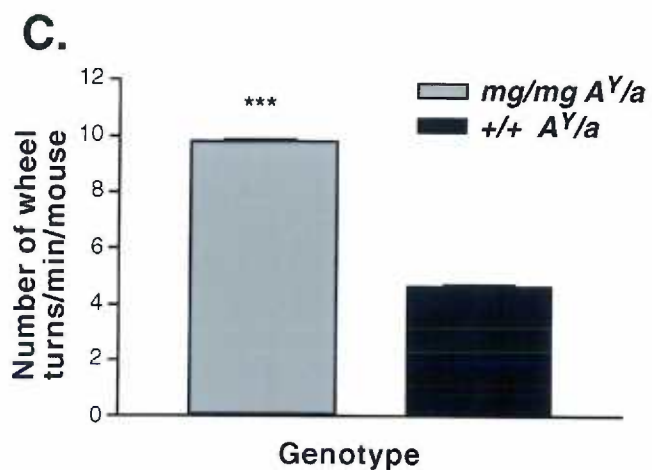
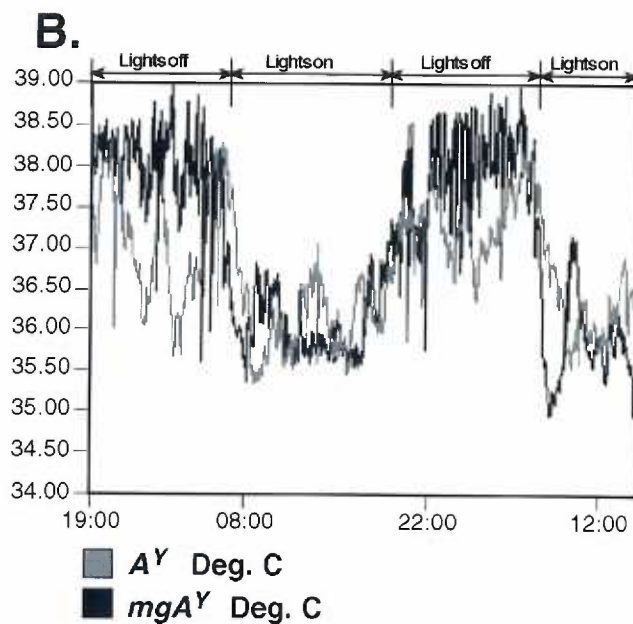
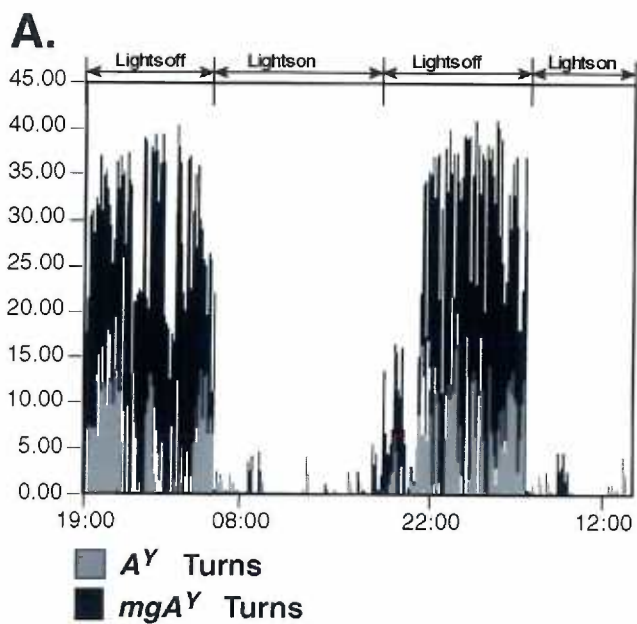


Table 1. *mg* suppresses the A^Y -induced increase in adiposity. White fat pads: epididymal (EPI), visceral = mesenteric + retroperitoneal (VF), dorsal (DF), brown fat (BAT), heart (H), and liver (L) from 23-week old male $+/+$ A^Y/a ($n = 6$) and *mg/mg* A^Y/a animals ($n = 3$) were dissected and weighed. All data are reported as mean \pm SEM.

Table 1. Body and organ weight measurements.

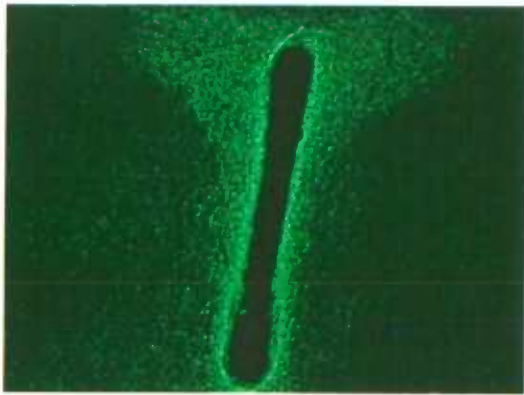
Genotype	Body Weight	VF	EPI	DF
<i>+/+ A^Y/a</i>	35.26 ± 1.72	0.87 ± 0.15	1.49 ± 0.14	0.85 ± 0.09
<i>mg/mg A^Y/a</i>	26.99 ± 0.87	0.33 ± 0.06	0.27 ± 0.03	0.57 ± 0.05
P value	p < 0.05	p < 0.05	p < 0.001	p < 0.05
Genotype	BAT	L	H	
<i>+/+ A^Y/a</i>	0.16 ± 0.02	1.55 ± 0.1	0.18 ± 0.01	
<i>mg/mg A^Y/a</i>	0.08 ± 0.01	1.16 ± 0.1	0.23 ± 0.02	
P value	p < 0.05	p < 0.05	p > 0.05	

Figure 6. Hypothalamic NPY expression is not affected by mahogany.

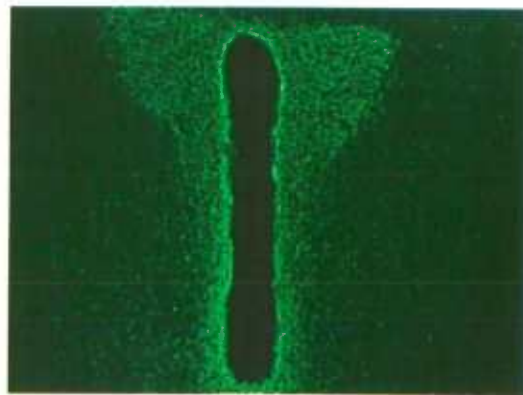
Immunofluorescence studies indicate normal NPY levels in the hypothalamus (PVH) of *mg* and *mg A^Y* animals.

NPY Expression in the PVN

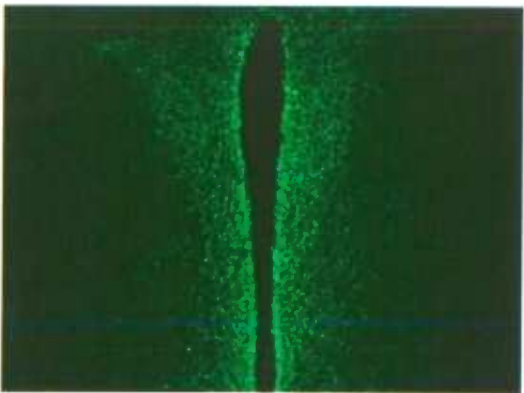
mg/mg a/a



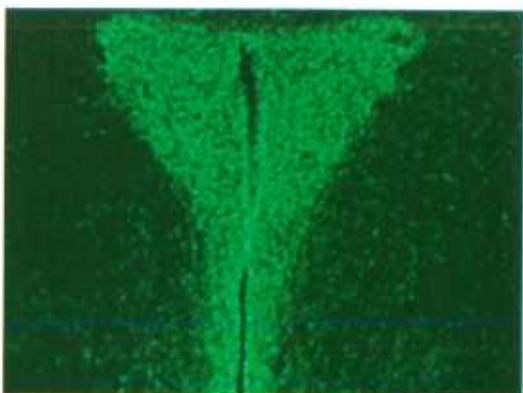
+/+ a/a



mg/mg A^y/a



+/+ A^y/a



CHAPTER FOUR

EFFECTS OF THE CENTRAL MELANOCORTIN SYSTEM ON INSULIN RELEASE AND INSULIN SENSITIVITY

Wei Fan, Daniela M. Dinulescu, Andrew A. Butler, Jeanie Zhou,

Daniel L. Marks and Roger D. Cone

The Vollum Institute, Oregon Health Sciences University, Portland OR 97201

ABSTRACT

The central melanocortin system has been demonstrated to play a pivotal role in energy homeostasis. Genetic disruption of this system causes obesity in both humans and mice. Previous experiments have shown that centrally-administered melanocortin agonists inhibit food intake and stimulate oxygen consumption. Here we report that centrally-administered melanocortin agonists also inhibit basal insulin release, and reduce the rate of glucose disposal. Furthermore, insulin resistance occurs in the young MC4-R knockout (MC4-R KO) mouse prior to the onset of detectable hyperphagia or obesity. These data indicate that the central melanocortin system regulates not only energy intake and expenditure, but also processes related to energy partitioning, as indicated by effects on insulin release and peripheral insulin responsiveness. Previous studies demonstrate a role of excess adipose mass in the development of tissue insulin resistance, leading to type II diabetes. The data presented here show that defects in the central control of glucose homeostasis may be an additional cause of obesity-associated type II diabetes.

INTRODUCTION

Obesity is highly associated with hypersecretion of insulin (hyperinsulinemia) and insulin resistance (reduced insulin sensitivity), and is the most significant risk factor for type 2 diabetes. Despite extensive analysis, the mechanistic relationship between obesity and insulin resistance, hyperinsulinemia, and diabetes is not entirely clear. The central melanocortin system has been demonstrated to play a pivotal role in energy homeostasis. Central pharmacological administration of agonists of the melanocortin-4 receptor (MC4-R) can inhibit energy intake, increase energy expenditure (Cowley et al., 1999; Fan et al., 1997) and reduce body weight (Patterson, 1999; Stair, 1999). Antagonists stimulate feeding (Fan et al., 1997; Kask et al., 1998), decrease oxygen consumption (Cornelius, 1999) and increase body weight (Kask et al., 1999), implying that endogenous melanocortin agonists, released by arcuate nucleus POMC neurons, act to tonically inhibit energy intake and increase energy expenditure. Genetic alterations affecting the central melanocortin system disrupt energy homeostasis and cause obesity in four independent mouse models, mice ectopically expressing agouti, an antagonist of MC4-R (Bultman et al., 1992; Miller et al., 1993), or overexpressing the hypothalamic AGRP (Graham et al., 1997; Ollmann et al., 1997), and mice lacking MC4-R or POMC-derived peptide (Huszar et al., 1997; Yaswen et al., 1999). Furthermore, an obesity syndrome has been characterized in two human families with rare deleterious mutations in POMC gene (Krude et al., 1998), and heterozygous mutations in the MC4-R have also been reported to be associated with pediatric obesity in perhaps as many as 5% of cases (Vaisse et al., 1998; Yeo et al., 1999).

Hyperinsulinemia is one of the common features among all the animal models of obesity and human obesity, and also one of the earliest metabolic alterations observed in melanocortin obesity models. A pancreatic β -cell hyperplasia has been found before any observed obesity in the A^{VY} strain as one of the earliest changes, for example (Warbritton et al., 1994), and a late-onset development of hyperglycemia has also been reported in male A^Y and MC4-R knockout (MC4-R KO) mice which seems to be quite similar to the pathophysiological process of type 2 diabetes (Huszar et al., 1997). These data suggest that the central melanocortin system may be independently involved in the regulation of glucose homeostasis in addition to its regulation of energy intake and energy expenditure (Cowley et al., 1999; Fan et al., 1997). However, existing data do not rigorously address whether the hyperinsulinemia in the agouti obesity syndrome is primary to MC4-R blockade, a developmental consequence of MC4-R blockade, or secondary to the hyperphagia and obesity that develops in this model. To test the potential role of central melanocortin signaling in glucose homeostasis, we have examined the effects of central melanocortin administration on basal serum insulin levels and glucose tolerance, and studied the development of tissue insulin resistance in the MC4-R KO mouse.

MATERIALS AND METHODS

Animals and surgical procedures. C57Bl/6J mice (25-33 g, Jackson Labs), female *ob/ob* mice (60-70 g, Jackson Labs) and their lean controls (+/+ & *ob/+* littermates from *ob/+* crosses, 22-27 g) were housed on a 12:12 light/dark cycle with food (Purina mouse chow) and tap water *ad libitum*. MC4-RKO x SW129 mice (Huszar et al., 1997) were

backcrossed three times into the C57Bl/6J background, and maintained as described above. All studies were conducted according to the NIH Guide for the Care and Use of Laboratory Animal and approved by the Animal Care and Use Committee of the Oregon Health Sciences University.

The animals were anesthetized with halothane and placed in a stereotaxic apparatus (CARTESIAN Research, Inc.). A sterile guide cannula with obturator stylet was stereotaxically implanted into one side of the PVH (0.67-0.77 mm relative to Bregma, 0.38-0.48 mm lateral to midline, and 4.69-4.75 mm below the surface of the skull; for i.c.v. injection in the mouse, the cannula was implanted with the coordinates of 0.5 mm posterior to the bregma, 1-1.6 mm lateral to the midline and 2 mm below the bregma. The cannula was then fixed in place using dental cement. The animals were housed separately after surgery at least one week for recovery before experiments. The positions of the cannulae were verified at the end of experiments by histological analysis; in some animals the position of the cannulae were tested by dye administration prior to sacrifice. Positioning of the cannulae in the more dorsal aspect of the PVH was found to insure the integrity of the third ventricle and prevent dye from entering the cerebrospinal fluid.

RIA assay for serum or plasma insulin. ACSF, MTII (0.1-3 nmol) or leptin (1 μ g) were infused in a total volume of 2 μ l over 30 seconds in lateral ventricle-cannulated mice. In these experiments, the i.c.v. dose-response to MTII or the i.c.v. response to leptin, or i.p. response to phentolamine were completed using the same i.c.v.-cannulated mice. These animals were allowed a washout period of at least one week between treatments

and were rerandomized between experiments. These experiments were carried out at the beginning of the dark cycle (18:00 h) with the food withdrawn and water available *ad libitum*. 0.5-1 h following the i.c.v. injection of the drugs, the blood samples were collected by cutting the tail or by decapitating the animals. Radioimmunoassay of serum insulin was performed as described (Linco Research, Inc.). In animals that received a mixed treatment, the i.c.v. MTII or saline injections were administered immediately after i.p. administration of phentolamine or saline, then the blood samples were collected for insulin RIA at the 0.5-1 h after the i.c.v. injection. For the experiments of MTII effect on insulin in lean animals, the food was withdrawn for 3-4 h before experiment. Blood was drawn 45-60 min after i.c.v. injection from the retro-orbital sinus using a heparinized microcapillary tube. Plasma insulin was measured using a rat sensitive insulin kit (Linco Research, Inc.). Plasma insulin of MC4-RKO and wild type littermates were measured using rat sensitive insulin kit (Linco Research, Inc.) or Mercodia Rat Insulin ELISA, ALPCO from the retro-orbital sinus or tail blood samples.

Blood glucose and glucose tolerance tests. Lean female control mice implanted with cannula in the lateral ventricle or PVH were fasted from 13:00-17:00 h. The blood glucose level was measured with a Blood glucose meter and test strips (Glucometer Elite, Bayer Corporation, Elkhart, IN) from the tail blood of the animals. Glucose (1 mg/g body weight) was administered intraperitoneally at 30 min after i.c.v. or PVH injection of MTII or ACSF, and then the blood glucose level was measured at the time points indicated in the text (15, 30, 45, 60, 90, 120 min) following the i.p. glucose challenge.

Insulin Sensitivity Assay. Insulin sensitivity assay was performed by measuring blood glucose levels following a single subcutaneous injection of human insulin (Humulin, Eli Lilly) with food withdrawn for 3-4 h before experiment.

RESULTS

Melanocortin Administration Lowers Insulin Levels in the *ob/ob* Mouse

Intracerebroventricular (i.c.v.) injection of MTII dose-dependently (0.3, 1, 3 nmol) decreased serum insulin concentration in hyperinsulinemic *Lep^{ob}/Lep^{ob}* mice (Figure 1 a), measured 30-60 min after administration of the compound. 1 nmol MTII reduced serum insulin levels by 72.8% ($n = 10$, $P < 0.001$) compared with the ACSF control group. The effect of i.c.v. administration of leptin (1 μ g) is shown for comparison. In a separate experiment, the blood glucose, at 60 min after 1 nmol of i.c.v. MTII administration, increased to 351.8 ± 44.8 mg/dl from 201.4 ± 18.8 mg/dl ($P < 0.05$, $n = 7$), which paralleled the decreased blood insulin level, indicating that the inhibitory effect of central MTII on insulin release is not secondary to the lowering of the blood glucose (Figure 1 b).

Effect of the Sympathetic System on MTII-induced Lowering of Serum Insulin in the *ob/ob* Mouse

To test the hypothesis that the melanocortin agonist lowers serum insulin by stimulating the sympathetic drive to the pancreas known to inhibit insulin release, the effect of phentolamine, a nonspecific α -adrenoceptor antagonist, on the MTII-mediated reduction of serum insulin was examined. Animals were first injected with phentolamine (0.1-0.5

mg/kg in 0.2 ml saline i.p.) or saline (0.2 ml), then centrally treated with either MTII (1 nmol /2 μ l, i.c.v.), leptin (1 μ g/2 μ l, i.c.v.) or ACSF (2 μ l, i.c.v.). As expected, administration of phentolamine alone (0.1-0.5 mg/kg, i.p.) significantly elevated the basal insulin level from 53.49 ± 4.5 to 83.94 ± 13.6 ng/ml, (Figure 2, $P < 0.01$), due to its ability to block the inhibitory effect of sympathetic tone on insulin release (Kuhn et al., 1987). Preadministration of phentolamine completely blocked the ability of centrally administered MTII to lower serum insulin in leptin-deficient animals (Figure 2, $P < 0.001$ $n = 12$). Phentolamine also blocked the majority of acute insulin-lowering effect by leptin on the *ob/ob* mouse.

Effect of the MTII Agonist on Basal Blood Insulin and Glucose Tolerance in the Lean C57BL/6J Mouse

We next examined the acute effect of centrally administered MTII on serum insulin and glucose tolerance in lean control littermates and C57BL/6J mice. Centrally-administered MTII produced a dose-dependent inhibitory effect on basal plasma insulin levels (Figure 3 a), with 0.37 ± 0.04 ng/ml resulting from 3 nmol MTII treatment versus 0.50 ± 0.04 ng/ml in the ACSF treated group, ($P < 0.05$). Significantly elevated fasting blood glucose levels were seen at 60 min after treatment with 3 nmol MTII (Figure 3 b, $P < 0.05$, $n = 8$). While i.c.v. injection of 1 nmol of MTII did not produce a significant effect on serum insulin, the rate of glucose disposal in response to an intraperitoneal glucose challenge (1 mg/g) was significantly reduced (data not shown) when compared with ACSF-treated control animals. PVH microinjection of MTII (0.45 nmol/0.3 μ l) also resulted in the similar effect on the glucose disposal after glucose challenge (Figure 3 c, $P < 0.01$).

Decreased Peripheral Insulin Sensitivity in the Young Lean MC4-R Knockout Mouse

To explore the pathophysiological role of the melanocortin system in the development of obesity and diabetes, we examined the insulin sensitivity and glucose tolerance in 6-9 week-old MC4-R KO mice and their wild type littermates. At 6-7 weeks of age, there is no difference in the body weights between the MC4-R KO mice and wild type controls (Figure 4 a, $p > 0.05$), however, reduced insulin sensitivity was observed in both female and male MC4-R KO mice compared to the wild types (Figure 4 b, c). A higher fasting insulin level was seen in males tested at 4 weeks in comparison to controls (Figure 4 d, $p < 0.05$). Elevated non-esterified fatty acids (NEFA) induce insulin resistance (Boden, 1997). To determine if the MC4-R KO mouse has a defect in triglyceride metabolism, serum NEFAs were measured, but no difference in blood free fatty acid levels were observed between MC4-R KO mice and their controls tested at the 6-7 weeks (data not shown).

Interestingly, at 8-9 weeks of age, an overt insulin resistance developed in the male MC4-R KO mice (Figure 4 e, $p < 0.01$) with higher blood insulin level than the controls (data not shown). The body weight of male MC4-R KO mice appeared a little heavier than the controls at this time point but is still not significantly so (Figure 4 f). No significant change in glucose tolerance was observed in male or female MC4-R KO mice compared to the controls (Figure 5 a, b).

Glucose homeostasis is the result of the equilibrium between blood glucose appearance and utilization, which is tightly controlled by insulin secretion from the

pancreas, and the peripheral tissue sensitivity to insulin. A role for the melanocortin system in sympathetic outflow in general has already been clearly shown. I.c.v. administration of the MC4-R agonist MTII produced a dose-dependent sympathoexcitation affecting sympathetic nerve activity of brown adipose tissue (BAT) and renal and lumbar beds in rat, while the antagonist SHU9119 completely blocked the sympathoexcitation effects of MTII, as well as renal sympathoexcitation to leptin (Haynes et al., 1999). Central administration of SHU9119 also completely inhibited the leptin-induced increase in UCP-1 mRNA expression in the BAT of rat, which is mediated through the activation of α -adrenoceptor (Satoh et al., 1998); *MC4-R/MC3-R* mRNAs have been found in many structures of the nervous system, which have been implicated in the central control of glucose homeostasis (Frohman and Bernardis, 1971; Goto et al., 1980; Yoshida et al., 1983; Yoshimatsu et al., 1984). For example, in the hypothalamus, *MC4-R* mRNA was found expressed in the lateral hypothalamic area (LHA), ventromedial hypothalamus (VMH), and paraventricular nucleus (PVH) (Mountjoy et al., 1994).

DISCUSSION

Results presented here demonstrate that central administration of MTII, a MC4-R/MC3-R agonist, inhibits insulin release and alters the response to a glucose challenge. Since the inhibitory effect of MTII on insulin release could be completely blocked by phentolamine, a non-specific α -adrenoceptor antagonist, the data support the hypothesis that central melanocortin peptides may act on melanocortin receptors in one or multiple subnuclei in the hypothalamus to increase the sympathetic drive to pancreas (or alter the relative effectiveness of sympathetic versus parasympathetic outflow to favor sympathetic activity) to reduce insulin release. In the young lean MC4-R KO mouse, in which melanocortin signaling is chronically blocked, an increased blood insulin and decreased tissue insulin sensitivity was observed prior to the onset of hyperphagia or obesity in this strain. These data support the hypothesis that the central melanocortin system regulates both insulin release and the tissue sensitivity to insulin. Several controversial proposals exist nowadays about the cause and effect relationship between obesity and diabetes. One is that insulin resistance and hyperinsulinemia are primary causes for the development of obesity and diabetes, and the other is that an increase in body adiposity induces insulin resistance (DeFronzo et al., 1992; Porte et al., 1998). Our results in the MC4-R KO mice model presented here support the notion that insulin resistance is not secondary to the development of obesity in the MC4-R KO, and may even play a causative role in this model. This data raises the possibility of central defects being the primary cause of certain cases of obesity-associated diabetes in humans.

Figure 1. Effect of melanocortin agonist administration on serum insulin in the hyperinsulinemic *ob/ob* mouse.

I.c.v. administration of MTII dose-dependently inhibits serum insulin (**, $P < 0.01$, ***, $P < 0.001$ ACSF vs. drug). The effect of 1 μg of leptin is shown for comparison (a). I.c.v. administration of 1 nmol of MTII elevated blood glucose, ($P < 0.05$) (b).

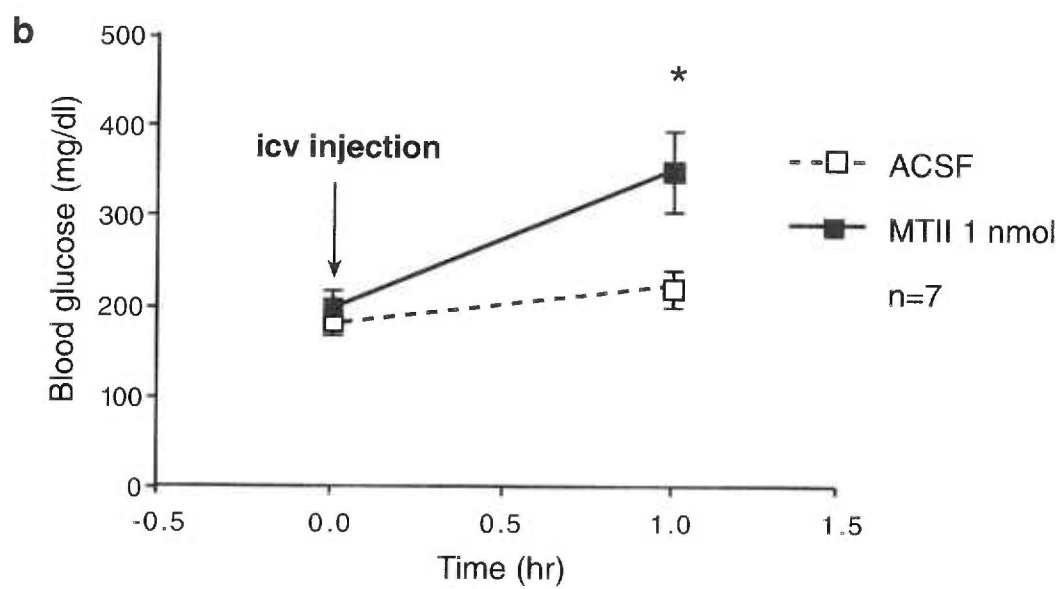
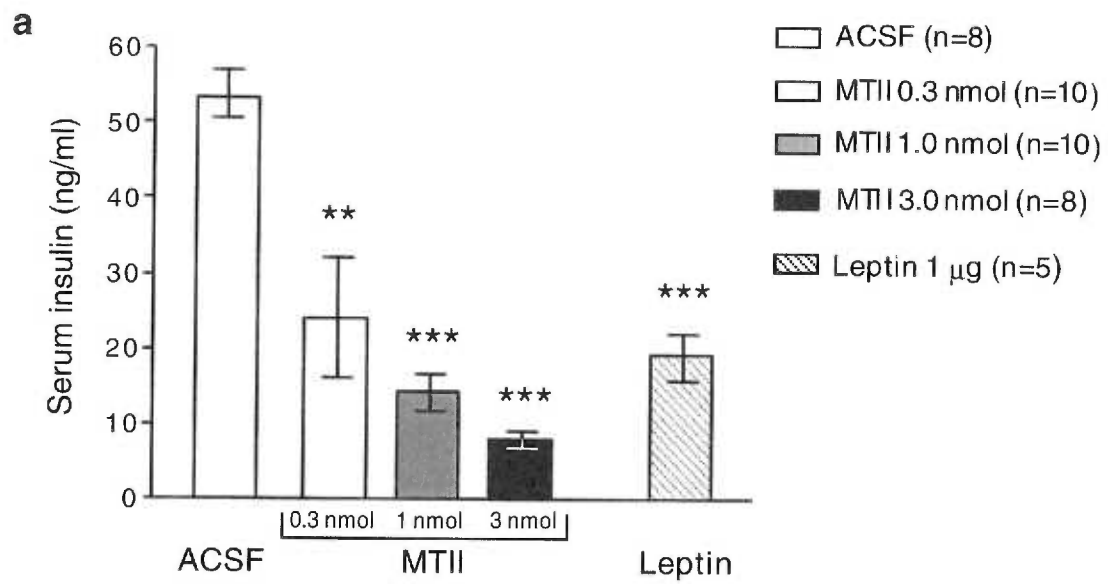


Figure 2. Role of the sympathetic nervous system in the reduction of serum insulin by MTII administration.

I.p. injection of phentolamine (0.1-0.5 mg/kg) elevates fasting serum insulin levels, and blocks the MTII and leptin-induced reduction in serum insulin (**, $P < 0.01$, ***, $P < 0.001$ treatment vs. S-A; ###, $P < 0.001$, P-M vs. S-A; +++, $P < 0.001$, P-L vs. S-L). First letter indicates drug injected i.p., second letter indicates drug by i.c.v. administration. (S = saline, A = ACSF, P = phentolamine, M = MTII, L = leptin).

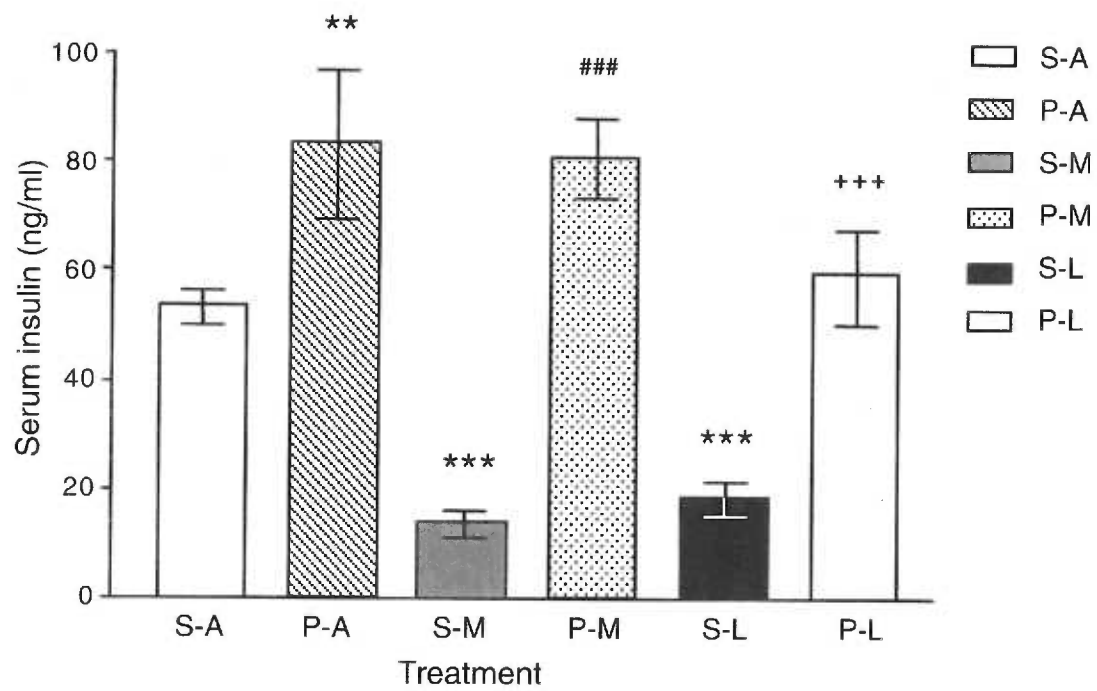


Figure 3. Effect of MTII on insulin release and glucose tolerance in the lean C57Bl/6J mouse.

I.c.v. injection of 3 nmol of MTII decreased blood insulin (a) and elevated blood glucose levels (b). PVH injection of MTII (0.45 nmol/0.3 μ l one side) significantly enhanced the glucose response to an i.p. glucose challenge (1 mg/g wt) compared to that of ACSF controls (c). (*, $P < 0.05$).

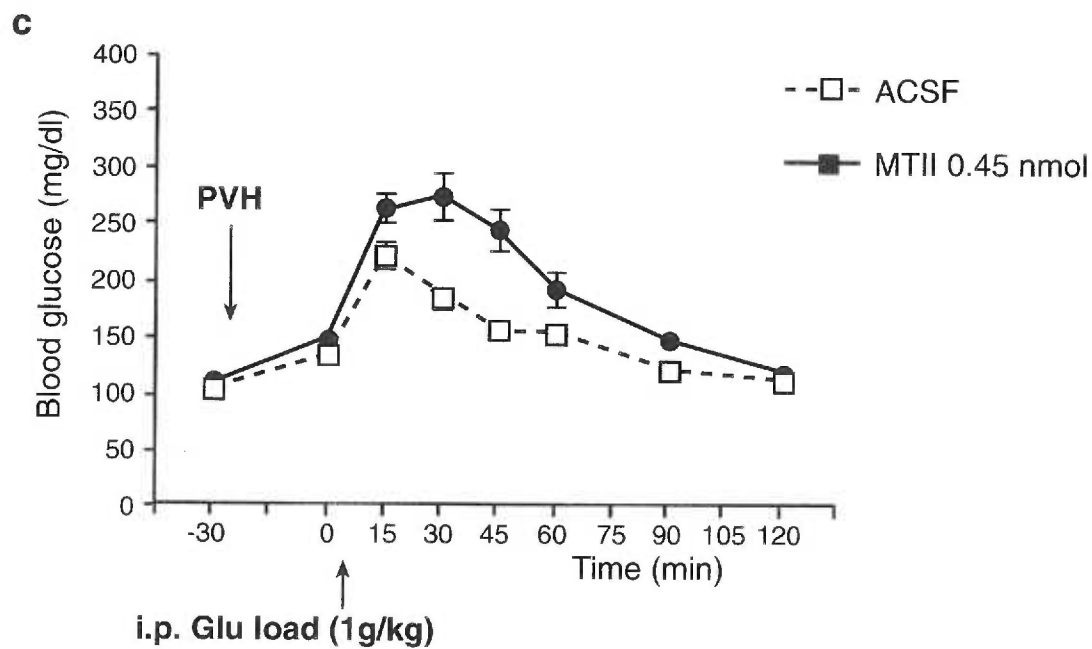
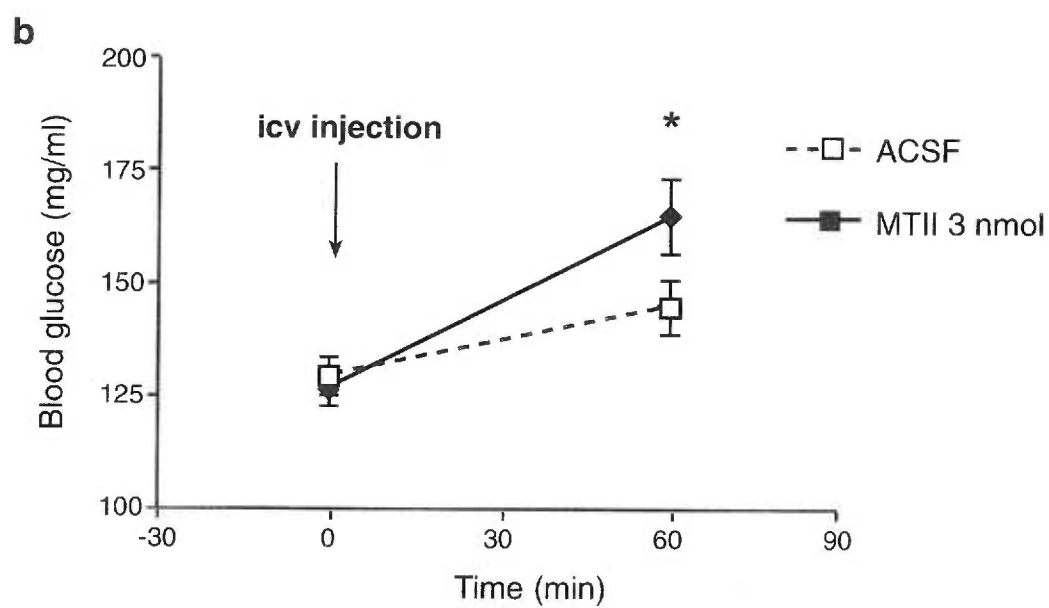
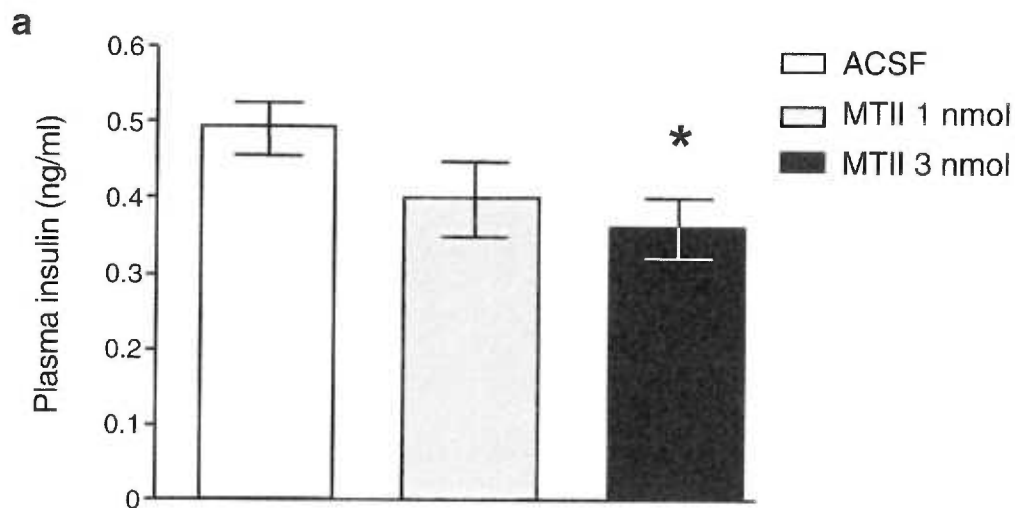


Figure 4. Decreased peripheral insulin sensitivity in the young MC4-R knockout (MC4-R KO) mouse.

There is no difference of the body weights between the MC4-R KO mice and wild type controls at 6-7 weeks of age (a). Reduced insulin sensitivity was observed in both female (b, $P < 0.01$) and male (c, $P < 0.01$) MC4-R KO mice at 6-7 weeks of age. A higher blood insulin level was seen at 4 weeks of male MC4-R KO mouse (d, $P < 0.05$). An overt insulin resistance developed in the male MC4-R KO mice at the 8-9 week of age (e), and the body weight of 8-9 week old MC4-R KO mice appears a little higher than the controls but the difference is not statistically different (f).

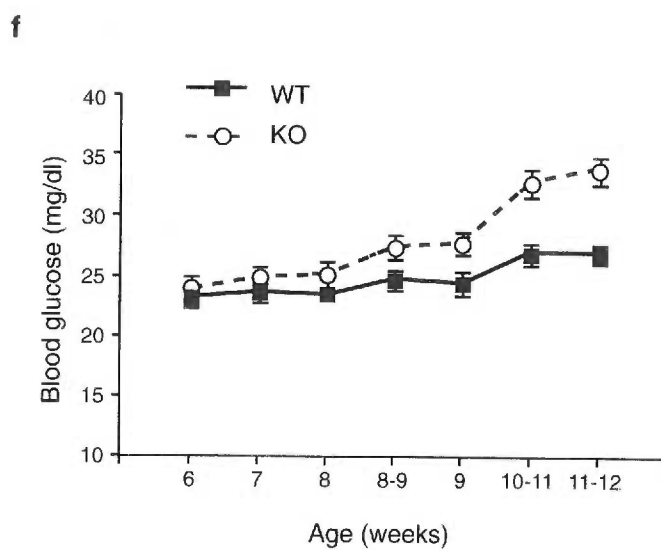
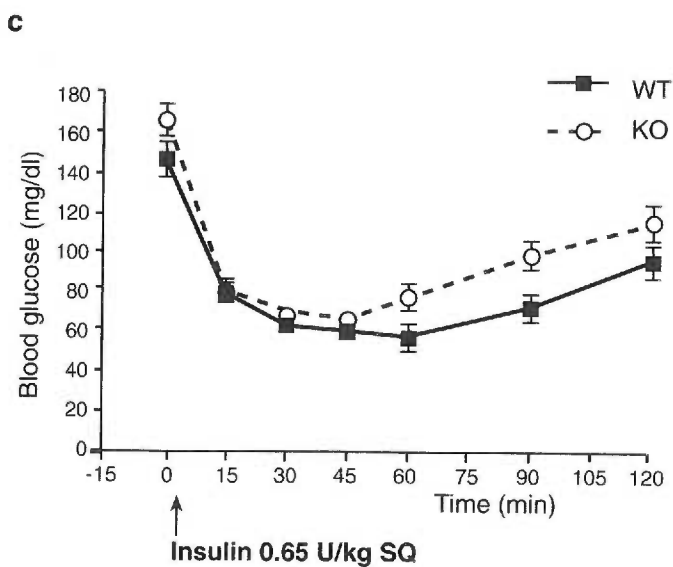
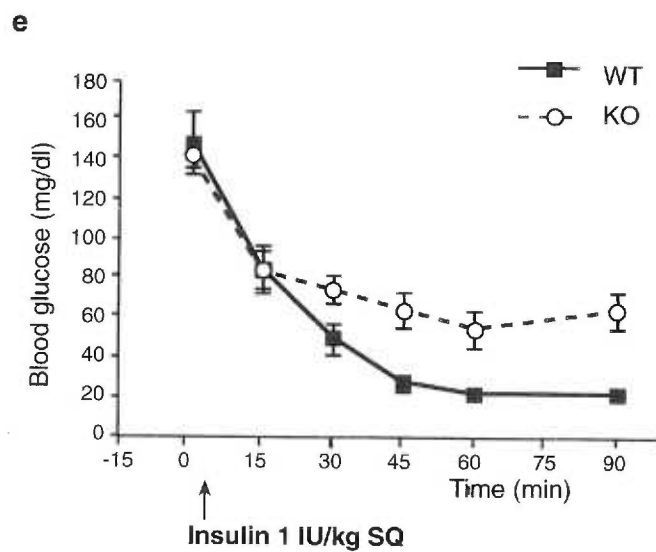
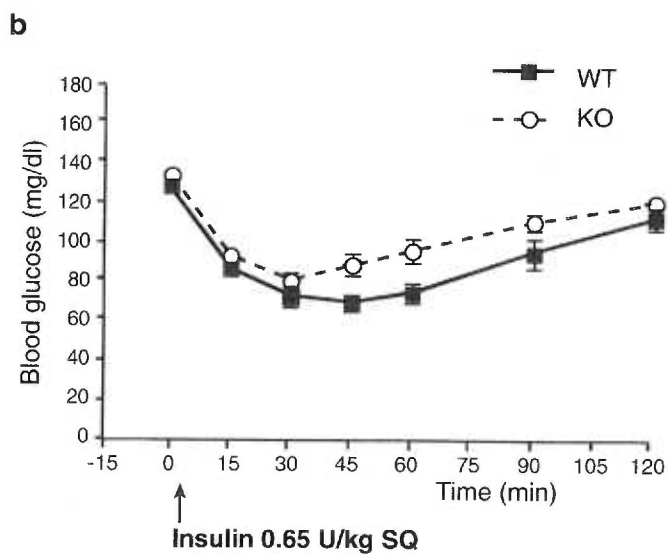
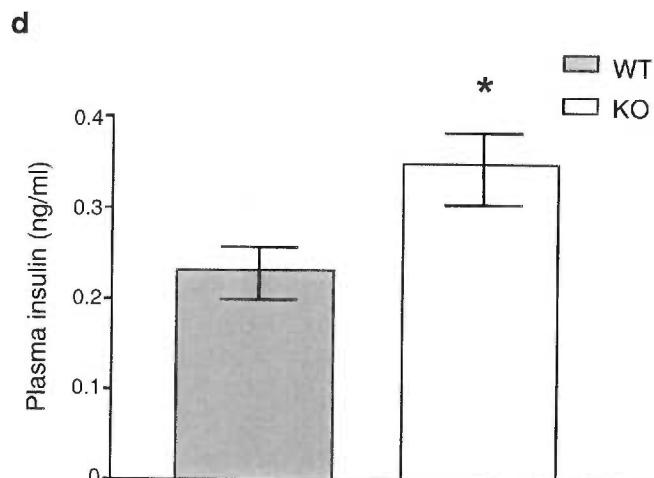
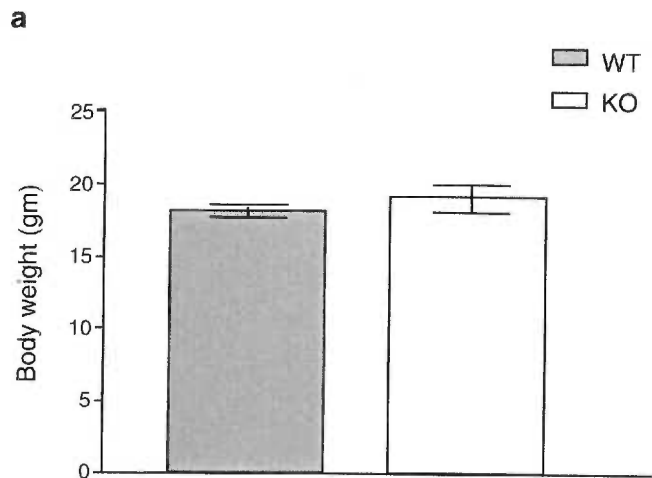
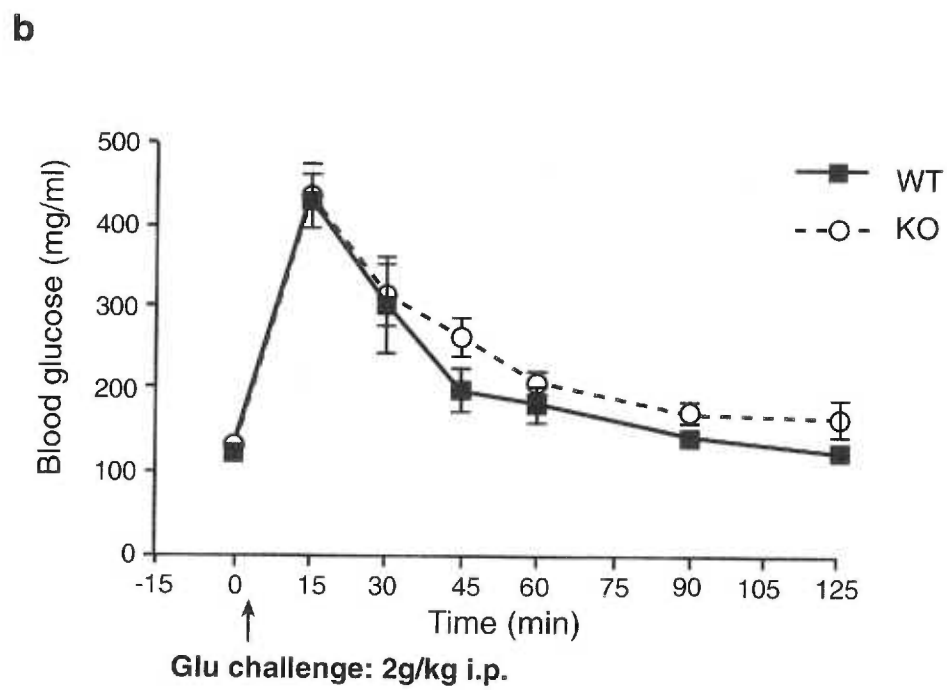
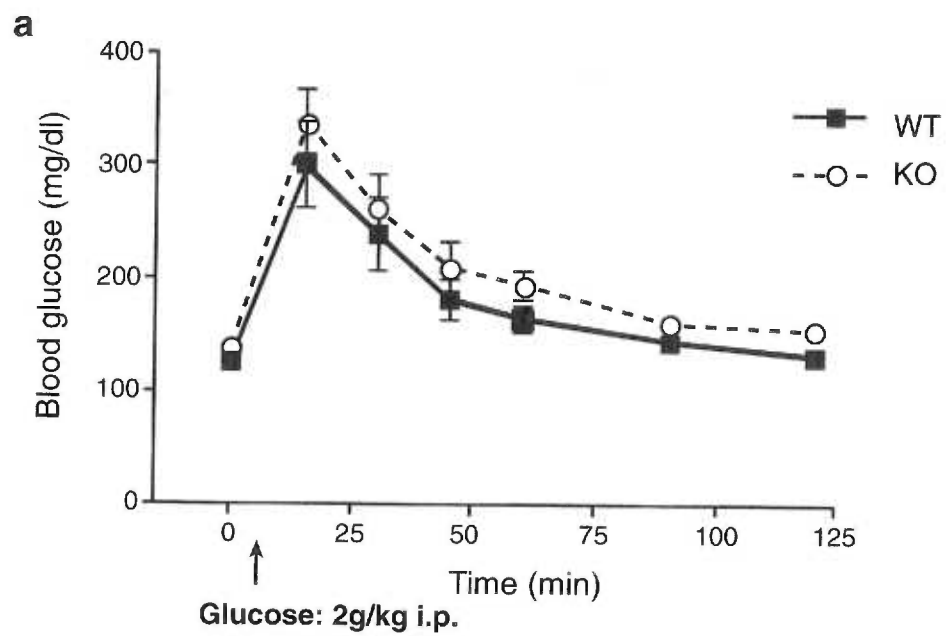


Figure 5. No significant change in glucose tolerance in the 6-7 week-old female (a), or 9-10 week-old male (b) MC4-R KO mice.



CHAPTER FIVE

INCREASED INSULIN SECRETION AND GLUCOSE CLEARANCE RATE IN MICE LACKING MAHOGANY

**Daniela M. Dinulescu^{1,2}, Ruth Thomas^{1,3}, Bruce A. Boston⁴, Kathleen McCall⁴,
and Roger D. Cone^{1,2}**

¹Vollum Institute, ²Department of Cell and Developmental Biology, ³Department of Neuroscience, and ⁴Department of Pediatrics, Oregon Health Sciences University, Portland, OR 97201

ABSTRACT

The present report shows that mahogany plays a critical role in the control of glucose homeostasis. The glucose clearance rate was found to be increased in both lean *mg/mg* and obese *mg/mg ob/ob* mice when compared to control animals. We have determined that this is a direct effect of increased insulin secretion following a glucose challenge. In addition, our report indicates that mahogany does not appear to play a major role in the regulation of peripheral insulin sensitivity. The effects of mahogany on glucose homeostasis appear to be both melanocortin-dependent, MC4-R-mediated, as well as melanocortin-independent. Unlike melanocortins, mahogany is expressed in the pancreas; this suggests a potential direct role for mahogany in the peripheral control of insulin release.

INTRODUCTION

Type II or non-insulin dependent diabetes (NIDDM) is the most common form of diabetes, accounting for more than 90% of the diagnosed cases. It is mostly prevalent in Western countries where it affects approximately 5% of the population (Taylor, 1999). Environmental factors, such as diet and physical activity, as well as genetic causes are responsible for the development of NIDDM. Obesity is now considered to be a high risk factor for developing NIDDM in humans and accounts for the majority of type II diabetic patients. Obesity animal models, such as *ob/ob*, *db/db*, *fa/fa*, and A^Y , also display an overt diabetes phenotype characterized by hyperinsulinemia, hyperglycemia, and insulin resistance.

Recent studies have uncovered new information regarding the pathophysiology of NIDDM. It is now known that NIDDM is a multistep disorder, which progresses from impaired glucose tolerance to the development of overt diabetes. As a result, both humans and animal models of diabetes, such as the insulin receptor (Kulkarni et al., 1999) or glucose transporter 4 (Glut 4) KO mice (Stenbit et al., 1997), develop the disease towards their midlife. Two major causes are known to facilitate the development of NIDDM: a defect in insulin secretion coupled with resistance to insulin-mediated glucose disposal in skeletal, cardiac muscle, and adipose tissue. It has been suggested that the decrease in insulin sensitivity may be the primary event in the development of type II diabetes. This is followed by a gradual dysfunction of pancreatic β -cells, which initially succeed in compensating for the loss of insulin sensitivity by increasing their insulin

secretion, but fail to do so indefinitely. The consequence of the two synergistic effects is the alteration of whole-body glucose homeostasis.

The central melanocortin system has recently been shown to play a key role in the control of glucose homeostasis (Fan et al., 2000). Thus, centrally-administered MC4-R agonists have been found to inhibit basal insulin release and reduce the rate of glucose disposal. In addition, MC4-R KO mice are characterized by a decreased response to insulin administration. In conclusion, acute stimulation of central melanocortin receptors has important effects on both insulin release and peripheral insulin sensitivity. Mahogany has been implicated in the regulation of agouti and AGRP signaling (Dinulescu et al., 1998). The absence of mahogany (i.e. *mg/mg* animals) is presumed to result in a chronic increased melanocortinergetic signaling at both central (MC4-R) and peripheral (MC1-R) melanocortin receptors. Consequently, we decided to investigate whether mahogany had any effects on whole-body glucose homeostasis.

MATERIALS AND METHODS

Animals. The experiments were performed on *mg/mg* animals backcrossed either 6-8 (Figures 2-6) or 12 generations into the C57BL/6J background (Figure 1).

Blood glucose and glucose tolerance tests. Glucose levels were measured with a Blood glucose meter and test strips (Glucometer Elite, Bayer Corporation, Elkhart, IN) from peripheral (tail) blood. Animals were fasted for 3-4 h prior to the experiment. Basal

glucose levels were determined at time 0, followed by intraperitoneal (i.p.) administration of a single dose of glucose (2 mg/g body weight). Blood glucose levels were measured at different time points (15, 30, 45, 60, 90, 120 min) following the glucose challenge.

Insulin sensitivity assay. Blood glucose levels were measured following a single i.p. injection of human insulin (1 mg/g body weight, Humulin, Eli Lilly), with food withdrawn for 3-4 h before experiment.

Insulin release. Glucose was administered i.p. (3 mg/g body weight) to animals fasted overnight; retro-orbital blood was drawn quickly (30 s) at various time points in order to prevent insulin degradation. Glucose-stimulated insulin levels were determined by RIA.

RT-PCR. Total RNA isolated from the pancreas of two *mg/mg* and two control animals was used to amplify by RT-PCR a 600 bp fragment corresponding to the cytoplasmic tail of mahogany.

Statistical analysis. All data are presented as mean \pm SEM. Statistical comparisons between different strains were performed by Student's two-tailed t test (Figure 4) and 2-way ANOVA (Figure 1, 2, 3, and 6) with $p < 0.05$ considered significant.

RESULTS AND DISCUSSION

In order to determine whether mahogany had any effects on whole-body glucose homeostasis we first compared the response of *mg/mg* (12th generation backcrossed into the C57 BL/6J background) and control mice to a glucose tolerance test (2 mg/g body weight administered i.p.). The results of this test indicate that the absence of mahogany results in significantly lower glucose levels at all time points ($P < 0.0001$) (Figure 1). Similar effects were seen in *mg/mg* animals backcrossed 6 to 8 generations into the C57 BL/6J background.

Having established that mahogany plays a role in increasing the glucose clearance rate in lean *mg/mg a/a* animals, we decided to test the importance of this pathway in the most severe genetic model of obesity (*ob/ob*). The *ob/ob* mice are characterized by a progressive development of glucose intolerance and severe insulin resistance, which culminates to overt diabetes by 4-6 months of life. We have thus investigated whether absence of mahogany protects them from developing either insulin resistance and/or diabetes. It is important to mention that no differences were detected in the body weights of *mgob* and *ob* animals. Our analysis indicates a dramatic improvement in the glucose tolerance of *mg/mg ob/ob* mice at all ages (3, 5, and 7 months) (Figure 2 A-C). These results indicate that mahogany has important effects on glucose homeostasis in *ob/ob* animals; *mg/mg ob/ob* males, although, grossly obese (60-80 g) have fairly normal glucose clearance rates. Similar effects were seen in females; the difference between the glucose tolerance of *mg/mg ob/ob* and *ob/ob* female animals was, though, somewhat smaller.

Two mechanisms are potentially responsible for the increased glucose tolerance of *mg/mg* mice: increased pancreatic insulin release or peripheral insulin sensitivity. Both causes were investigated. It does not appear that mahogany has a major influence on peripheral insulin sensitivity in *ob/ob* animals. Thus, insulin tolerance tests reveal a slight improvement, although statistically significant, in the insulin sensitivity of *mg/mg ob/ob* versus *ob/ob* animals (Figure 3 A). The *mg/mg ob/ob* mice remain, however, insulin resistant, suggesting that the absence of mahogany results in a significant but incomplete protection from the insulin resistance associated with the *ob/ob* phenotype. The small differences in peripheral insulin sensitivity detected between *mg/mg ob/ob* and *ob/ob* mice are unlikely to account for the major differences in their glucose clearance rates. This prediction is further confirmed by the results of insulin tolerance tests in *mg/mg* and control animals. Our analysis failed to detect any significant difference between the two groups in response to insulin (Figure 3 B).

We further analyzed the insulin release in *mg/mg* animals following a glucose challenge. Significant increases in glucose-stimulated insulin release in *mg/mg* animals were found at 5, 10, and 30 min (Figure 4). These results suggest that both first-phase (2-5 min) and late-phase insulin secretory responses (15-30 min) to glucose are activated in the absence of mahogany. Thus, the increase in pancreatic insulin secretion detected in *mg/mg* mice is likely to account for the increased glucose clearance rate found in these animals.

Mahogany has a wide area of distribution in the body, being predominantly expressed in brain and adipose tissue. It is possible that mahogany exerts both a central and peripheral control on glucose homeostasis and insulin release. Our analysis indicates that some of mahogany's effects on glucose homeostasis are mediated by MC4-R. Thus, *mg* fails to increase the rate of glucose clearance in MC4-R KO animals (Figure 4). It is conceivable that mahogany has effects on glucose homeostasis that are melanocortin-independent and they may be mediated peripherally. This hypothesis is further supported by the identification by RT-PCR of a specific mahogany transcript in the pancreas (Figure 6). Further experiments are needed to determine whether mahogany is present in pancreatic β -cells and thus directly involved in the peripheral coordination of insulin secretion.

Figure 1. Glucose clearance rate is increased in *mg/mg* animals.

Glucose tolerance test in *mg/mg* and control mice. (males, n = 6). ($P < 0.0001$)

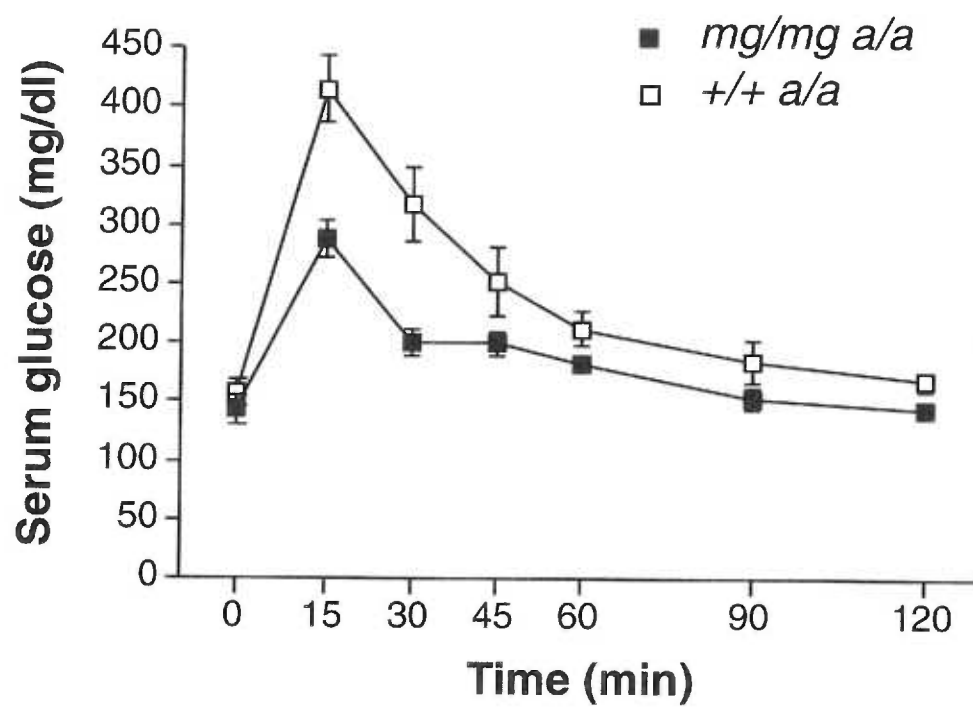
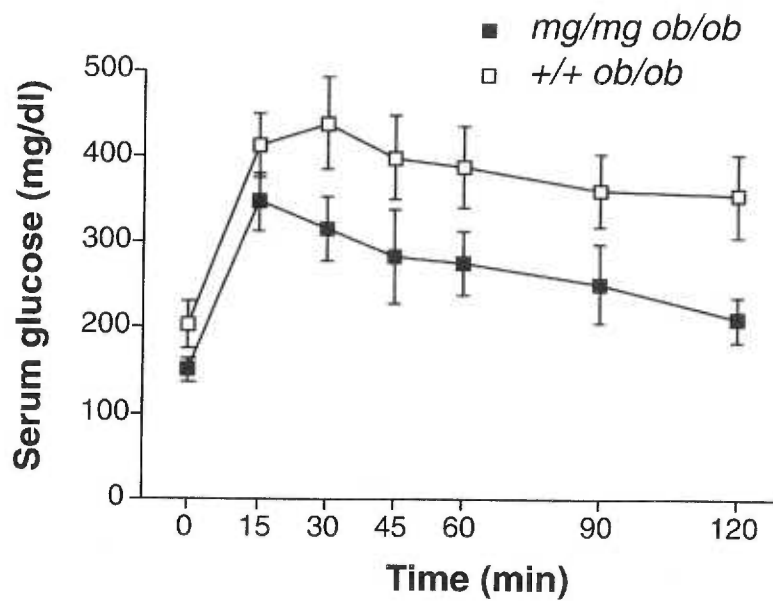


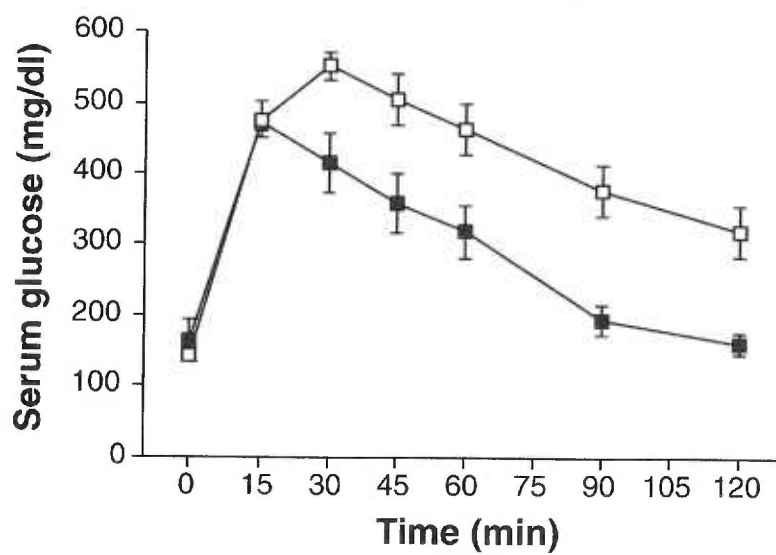
Figure 2. Absence of mahogany protects *ob/ob* animals from developing non-insulin dependent diabetes (NIDDM).

- A. Glucose tolerance test in 3-month old *mg/mg ob/ob* and *+/+ ob/ob* mice. (males, n = 3-7). ($P < 0.0001$)
- B. Glucose tolerance test in 5-month old *mg/mg ob/ob* and *+/+ ob/ob* mice. (males, n = 3-7). ($P < 0.0001$)
- C. Glucose tolerance test in 7-month old *mg/mg ob/ob* and *+/+ ob/ob* mice. (males, n = 3-5). ($P < 0.0001$)

A.



B.



C.

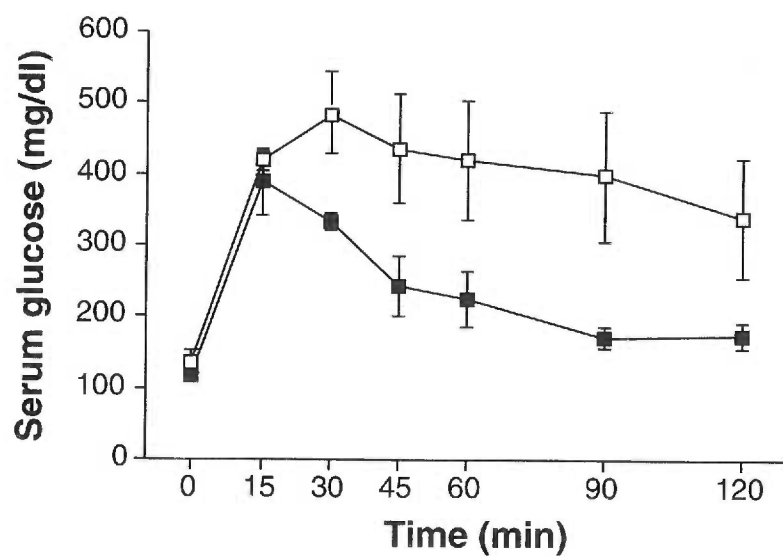


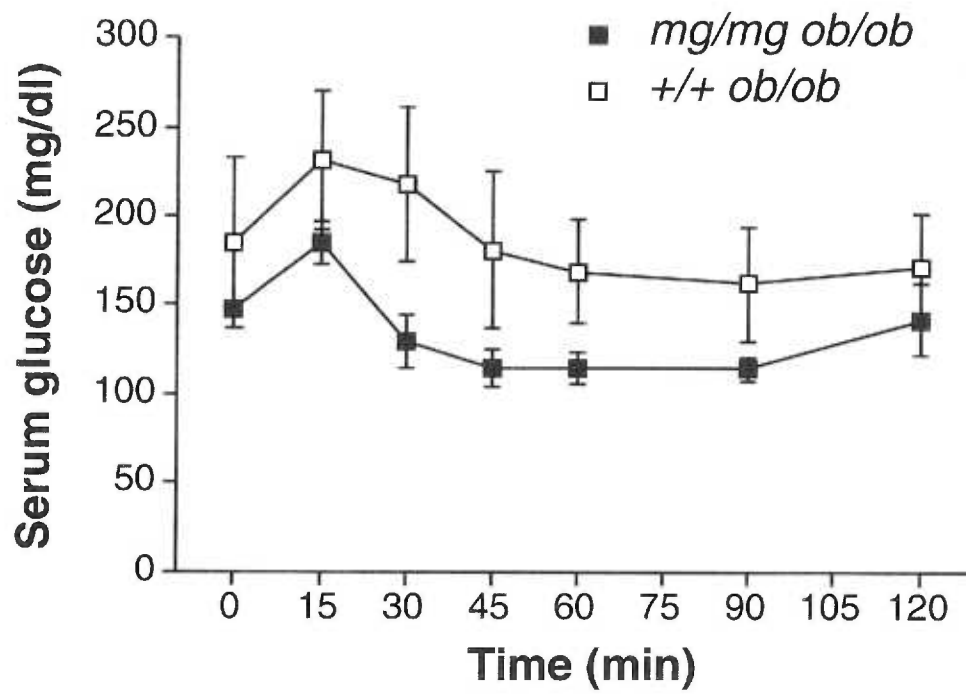
Figure 3. Effect of mahogany on peripheral insulin sensitivity.

A. Insulin tolerance test in 4-month old *mg/mg ob/ob* and *+/+ ob/ob* mice. (males, n = 3-7). ($P < 0.05$)

B. Insulin tolerance test in 5-month old *mg/mg* and control mice. (males, n = 8-10).

There was no statistical difference between the two groups.

A.



B.

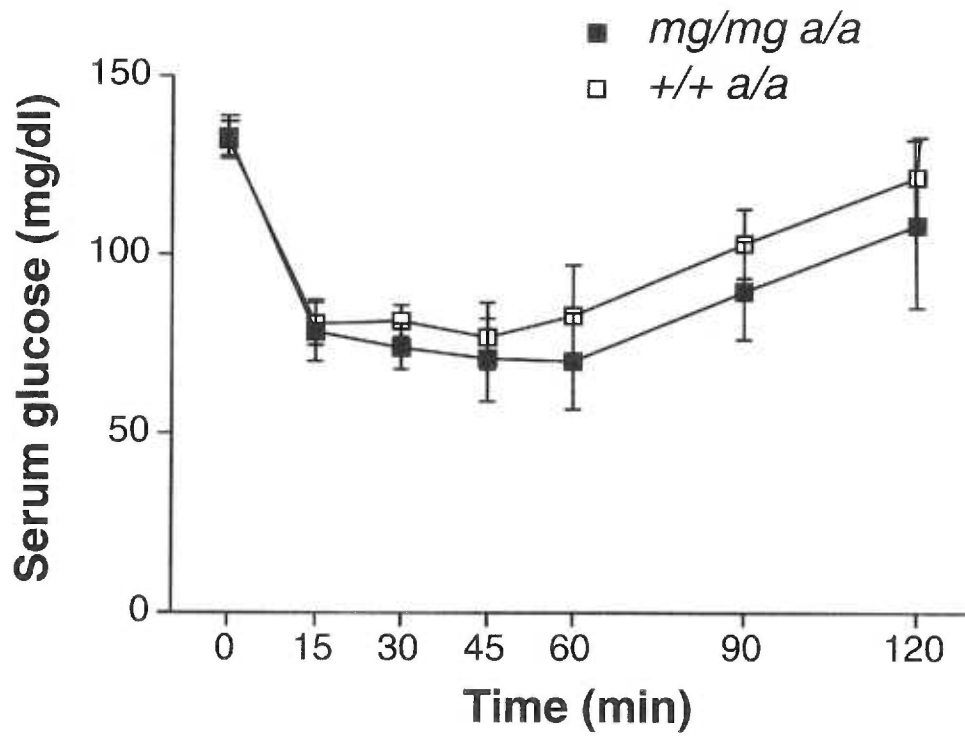


Figure 4. Increased insulin release in response to a glucose challenge in *mg/mg* mice.

Insulin release was measured at various times (0, 5, 15, 30, 45, and 60 min) following a glucose challenge (3 mg/g body weight administered i.p.). A significant increase in the glucose-stimulated insulin release between *mg/mg* and control animals was determined at 5, 10, and 30 min. Values are means \pm SEM.

*** $P < 0.001$, ** $P < 0.01$, $n = 8-10$ (males).

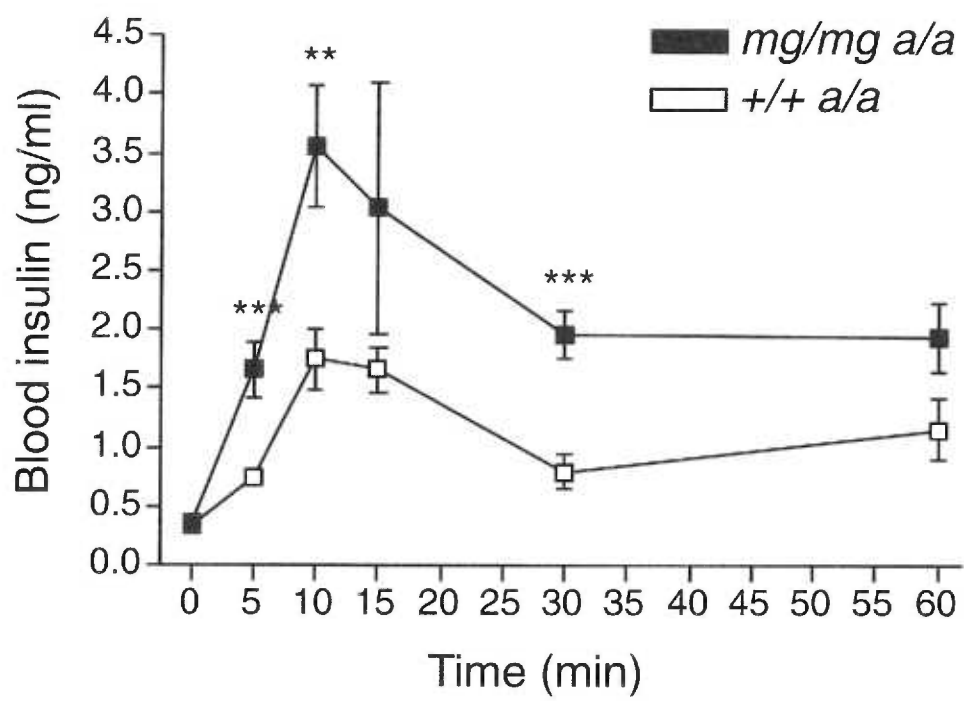


Figure 5. Mahogany has no effects on glucose homeostasis in the absence of a functional MC4-R.

A. Glucose tolerance test in *mg/mg KO/KO* and *mg/mg a/a* mice (males, n = 7). (P > 0.05).

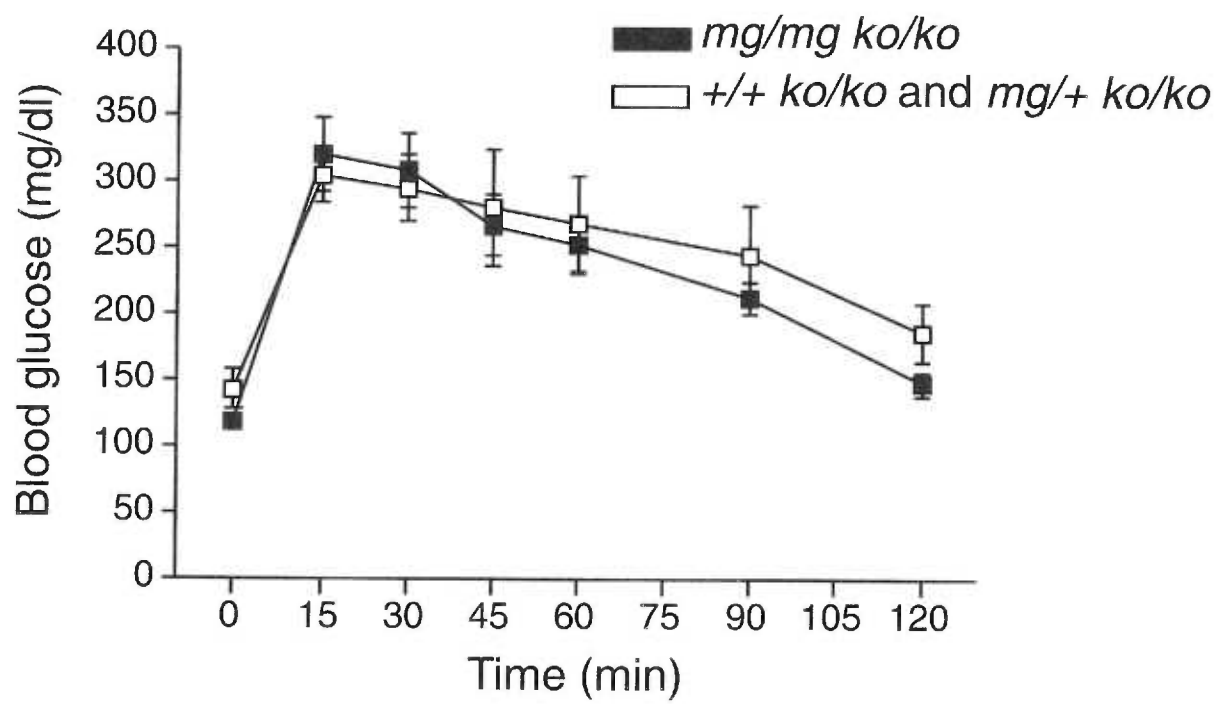
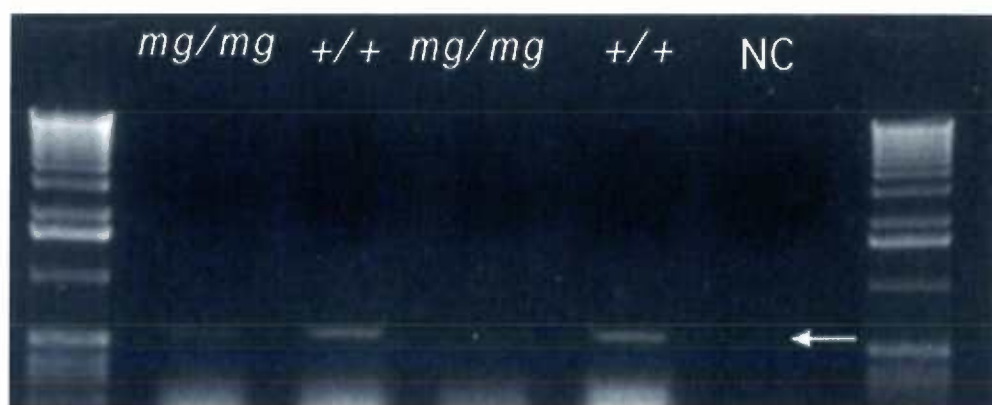


Figure 6. Specific mahogany expression in the pancreas.

Total RNA isolated from the pancreas of two *mg/mg* mice (lanes 1, 3) and two control animals (lanes 2, 4) was used to amplify by RT-PCR a 600 bp fragment corresponding to the cytoplasmic tail of mahogany. Lane 5 is a negative control.



CHAPTER SIX

A ROLE FOR MAHOGANY IN AXONAL GUIDANCE

Daniela M. Dinulescu^{1,2}, Sabrina Diano³, Ruth E. Thomas¹, Jeanie Zhou¹, Wei Fan¹,
Nicholas Ling⁴, Kevin L. Stark⁵, Tamas L. Horvath^{3,6}, and Roger D. Cone^{1,2*}

¹Vollum Institute and ²Department of Cell and Developmental Biology, Oregon Health Sciences University, Portland, OR 97201, ³Department of Obstetrics and Gynecology and ⁶Section of Neurobiology, Yale Medical School, New Haven, CT, ⁴Neurocrine Biosciences Inc., San Diego, CA, ⁵Amgen Inc., Thousand Oaks, CA.

ABSTRACT

Mahogany was recently proposed to be a co-receptor for binding of the agouti proteins to melanocortin receptors (Gunn et al., 1999; Nagle et al., 1999). We report here that agouti-related protein (AGRP) signaling *per se* is not diminished in animals homozygous for a mutation in the *mahogany* gene (*mg/mg*). Thus, *mg/mg* mice do not differ from wild-type mice in their orexigenic response to AGRP administration. Furthermore, *mg/mg* animals develop obesity in response to a constitutively expressed AGRP transgene. However, immunoEM analysis of AGRP and α -melanocyte stimulating hormone (α -MSH) axon terminals in the hypothalamic paraventricular nucleus (PVH) reveals that AGRP axons are quantitatively misrouted and do not make proper contacts with POMC nerve terminals in *mg/mg* mice. We propose that mahogany is a new member of a family of axonal guidance proteins, and is required for the appropriate development of hypothalamic circuitry. The lean phenotype of the *mg/mg* mouse thus results from inadequate contacts between AGRP axons and their melanocortin 4 receptor (MC4-R) target sites.

INTRODUCTION

The central melanocortin system is one of several neurocircuits involved in the central control of energy homeostasis (Cowley et al., 1999; Fan et al., 1997; Kask et al., 1999). The complexity of this system is illustrated by multiple levels of MC4-R regulation, including an agonist (α -MSH), an antagonist (AGRP), and two genes that may be required for antagonist function (*mahogany* and *mahoganoid*). *mg* is a hypomorphic recessive allele at the *mahogany* locus, which was initially identified as a suppressor of dominant *agouti* (A^Y)-induced yellow pigmentation (Lane and Green, 1960). More recently, *mg* homozygosity was also shown to suppress the A^Y -induced obesity syndrome (Dinulescu et al., 1998; Miller et al., 1997). Physiological characterization of *mg/mg* mice further suggests that mahogany protein is also required for hypothalamic AGRP action (Dinulescu et al., 1998). This hypothesis is supported by several observations. First, the *mg/mg* genotype blocks the obesity induced by constitutive *agouti* expression (A^Y), even though *agouti* is not normally present in the central nervous system (CNS). Second, caloric intake and metabolic rate were both altered, in the absence of *agouti*, in *mg/mg a/a* mice (Dinulescu et al., 1998), indicating suppression of some factor necessary for normal maintenance of energy stores in the mouse. Finally, *mahogany* mRNA is expressed in multiple brain regions, including the PVH, where AGRP and α -MSH interaction at the MC4-R contributes to the regulation of energy balance (Cowley et al., 1999; Lu et al., 1999). However, biochemical and/or neuroanatomical evidence proving a direct interaction between mahogany and AGRP have not yet been described.

Mahogany is a member of the developmentally regulated CUB superfamily of cell adhesion and guidance proteins (Gunn et al., 1999; Nagle et al., 1999). They include axonal pathfinding molecules, such as neuropilins, and differentiation proteins of the bone morphogenetic protein 1 (BMP-1) family (Bork and Beckmann, 1993; Giger et al., 1998). Furthermore, human attractin, a previously described cell adhesion molecule that regulates T cell-monocyte interactions (Duke-Cohan et al., 1998), appears to be homologous to the extracellular domain of mahogany (Gunn et al., 1999; Nagle et al., 1999). Based on its structure (i.e. single transmembrane domain protein) and function, mahogany was recently proposed to be a low affinity co-receptor for agouti and AGRP binding to melanocortin receptors (Gunn et al., 1999; Nagle et al., 1999), or possibly a regulator of receptor function.

MATERIALS AND METHODS

Surgical Procedures and Drugs Administration. *mg/mg* and C57Bl/6J control animals were stereotaxically implanted with sterile guide cannulae projecting to the lateral ventricle (coordinates: 0.5 mm posterior to the bregma, 1-1.6 mm lateral to the midline, and 2 mm below the bregma). All *mg/mg* mice used in the experiments, unless otherwise stated, were the 6th to 8th generation backcrossed into the C57Bl/6J background. The animals were allowed at least one week for recovery before experiments. NPY administration (2.5 µg/2 µl) was used as a positive control for the i.c.v. experiments. All compounds were administered in 2 µl of acsf or phosphate-buffered saline. AGRP₈₃₋₁₃₂ and full-length AGRP were provided by Neurocrine Biosciences Inc. and Amgen Inc.,

respectively. AGRP injections were performed on animals fed *ad libitum* (Purina mouse chow, 4.5 % fat) at the beginning of the light phase. All studies were conducted under guidelines provided by the Animal Care and Use Committee of Oregon Health Science University. All data are presented as mean \pm SEM. Dose-response curves were analyzed by 2-way ANOVA. The significance of drug effects at individual time points was determined by two-tailed Student's *t* test.

Body Weight Analysis. *mg/mg* were crossed with AGRP Tg mice (line 44) that were provided by Amgen Inc. (Graham et al., 1997). The body weights of *mg/mg* Tg/+ and *mg/+* Tg/+ animals were recorded weekly for up to 6 months. Data are presented as mean \pm SEM. Weight growth curves were analyzed by ANOVA with repeated measurements.

Light and Electron Microscopic Double Immunohistochemistry. The immunoelectron microscopy studies were conducted on *mg/mg* animals backcrossed for 6 to 8 and 12 generations into the C57Bl/6J background. The α -MSH antibody was generously provided by Dr. Richard Allen (Oregon Health Sciences University). AGRP and mahogany antisera (rabbit polyclonal) were purchased from Phoenix Pharmaceuticals. Perfusion and light and EM experiments were carried out as previously described (24). In order to eliminate bias from the procedure, sections from a control animal were incubated together with sections taken from a *mg/mg* animal. To differentiate between sections, either the control or *mg/mg* tissue block was marked by notching one side of the brain before vibratome sectioning. The analyzer was blinded to the animal type. A dual peroxidase labeling technique [avidin-biotin peroxidase (ABC) and peroxidase anti-peroxidase (PAP) methods]

was employed (20) in which AGRP was visualized by a nickel-ammonium sulfate-intensified diaminobenzidine (DAB) reaction. This gives a very characteristic appearance at both the light and EM levels that is easily distinguishable from that of the α -MSH labeling, which was achieved by a normal DAB reaction. In our experience with double labeling techniques, this method proved to be the most unbiased; all of the reagents for the labeling of the two antigens penetrate the tissue in the same manner. Thus, when switching the approach (from ABC to PAP and vice versa), the results are the same. This is not the case when pre-embedding immunoperoxidase labeling is combined with the pre-embedding immunogold technique because the penetration of the antisera differs. Following visualization of tissue antigens, sections were wet-mounted, and examined under the light microscope. Sections were then embedded for EM analysis as previously described (Horvath et al., 1999). Only those embedded sections containing the same exact part of the PVH were processed. This was determined by the use and comparison of landmarks that included the third ventricle, fornix, optic chiasm, hippocampus, amygdala and the thalamus. Two areas of the parvicellular PVH were focused upon: the periventricular parvicellular PVH that was a 0.1 mm thick layer of cells adjacent to the ependymal layer of the third ventricle, and the medial parvicellular PVH that included a 0.1mm thick layer of cells lateral from the periventricular PVH. The PVH was serially sectioned for EM and examined at a magnification of 10,000 X with the observer blinded to the experimental treatment. A terminal (axon bouton) was identified by the presence of at least ten synaptic vesicles clustered in the area of the pre-synaptic membrane. AGRP and α -MSH axons were easily differentiated. A contact was identified between AGRP and α -MSH boutons if their membranes ran parallel touching each other without interfacing glial

elements. Within a $100\ \mu\text{m}^2$ region, the number of AGRP and α -MSH boutons and their direct contacts were recorded. An F-test analysis of the AGRP and α -MSH counts in the PVH was used to reveal significant non-homogeneity of variances between groups; the Kruskal-Wallis one-way non-parametric analysis of variance was selected for multiple statistical comparisons. The Mann-Whitney U test was used to determine significance of differences between two independent groups. A level of confidence of $p < 0.05$ was adopted for all statistical comparisons.

RESULTS

We investigated whether the co-receptor model can adequately describe the molecular interaction between melanocortin and AGRP by examining the response of *mg/mg* animals to acute AGRP administration and chronic AGRP expression in a transgenic mouse. To examine an alternative model, in which melanocortin is required for the normal development of hypothalamic melanocortin circuitry, we also compared AGRP fiber distribution and interaction with α -MSH projections within the PVH of *mg/mg* and control mice. Previous studies have indicated that *AGRP* mRNA synthesis is confined to neuronal cell bodies localized in the arcuate nucleus of the hypothalamus (Shutter et al., 1997). These neurons are shown to project to many of the same hypothalamic nuclei to which the arcuate nucleus POMC neurons project, including PVH (Broberger et al., 1998). This hypothalamic nucleus integrates AGRP and α -MSH signals (Kalra et al., 1999), which are thought to control energy homeostasis in part by coordinately regulating post-synaptic neurons within the PVH (Cowley et al., 1999).

In initial experiments we utilized the chemically synthesized C-terminal AGRP fragment (AGRP₈₃₋₁₃₂), which exhibited full pharmacological and biological activity, relative to the full-length protein, in stimulating feeding behavior in the rat (Rossi et al., 1998). The response of *mg/mg* and wild-type controls to intracerebroventricular (i.c.v.) administration of AGRP₈₃₋₁₃₂ was compared. Dose-response curves indicated that the lowest AGRP dose able to elicit a significant increase in feeding in both groups was 3 nmol (data not shown). AGRP₈₃₋₁₃₂ peptide was very stable and had long-lasting effects *in vivo*, stimulating the rate of food intake for at least 24 h after the administration of a single dose. No differences in the potency and time course of the response to AGRP₈₃₋₁₃₂ administration (3 nmol) were detected between the two animal groups either in the 1-8 h time period (Figure 1 A, B) or out to 24 h post administration (Figure 1 C, D). We conclude, therefore, that absence of mahogany protein in *mg/mg* animals does not impair the response to exogenous AGRP treatment.

According to the co-receptor hypothesis the N-terminal region of agouti is predicted to interact with mahogany whereas the C-terminal domain attaches itself to the melanocortin receptor (Gunn et al., 1999). It is thus possible that, although *mg/mg* and control animals respond equally well to AGRP₈₃₋₁₃₂, they might display different feeding behaviors when administered full-length AGRP. Consequently, full-length AGRP protein was produced in *E. coli* and administered i.c.v. to both *mg/mg* and wild-type mice (Rosenfeld et al., 1998). 0.3 nmol was found to be the lowest AGRP dose capable of eliciting an increase in food intake in either group. Similar to the results of previous

experiments, we detected no significant differences in the feeding patterns of the two groups following central administration of full-length AGRP (0.3 nmol) (Figure 1 E, F).

We next examined whether the obesity syndrome resulting from chronic expression of AGRP, under the control of a β -actin promoter in transgenic mice (AGRP Tg) (Graham et al., 1997), could be ameliorated by the absence of mahogany. A comparison between the weight curves of *mg/mg* AGRP Tg and *mg/+* AGRP Tg animals reveals no statistical difference in body weights, suggesting that the *mg* mutation is not effective in suppressing the AGRP-induced obesity (Figure 2). Taken together, these results indicate that mahogany is not necessary for AGRP action in an acute administration or a chronic transgenic expression model. Evidently, once AGRP accesses the MC4-R, the absence of mahogany does not prevent it from binding to the receptor and exerting its normal orexigenic activity. This prompted us to investigate whether endogenous AGRP was properly accessing the MC4-R in *mg/mg* animals.

To test whether the endogenous MC4-R agonist response is impaired by the absence of mahogany we administered an α -MSH analogue, MTII, to *mg/mg* and control animals. Centrally administered MTII was previously shown to mimic the effect of the α -MSH agonist and potently inhibit caloric intake in rodents (Fan et al., 1997). Our analysis indicates that *mg/mg* mice are less sensitive to MTII administration (1 nmol) as compared to control animals (Figure 3). No differences were detected between ACSF-treated animals from the two groups during the 8 h post injection. However, the MTII dose-response curves of *mg/mg* and control animals were significantly different ($p < 0.001$) (Figure 3).

The response of wild-type mice to 1 nmol MTII differs from ACSF-treated controls at all time points examined. By contrast, with the exception of the first hour post injection, the response of *mg/mg* mice to MTII administration parallels that of ACSF-treated animals. These data suggest desensitization of the MC4-R in *mg/mg* mice, perhaps resulting from endogenous levels of agonist unimpeded by the normal AGRP antagonist signal at MC4-R target sites in these animals.

Our initial immunohistochemistry experiments looking at AGRP expression in the arcuate nucleus revealed no major differences between *mg/mg* (both *mg/mg a/a* and *mg/mg A^Y/a*) and control animals (Figure 4); the absence of mahogany is thus not likely to influence AGRP synthesis in neuronal cell bodies of the arcuate nucleus. AGRP protein levels in the arcuate nucleus of *db/db* mice, used as positive controls, were significantly elevated, as shown previously (Shutter et al., 1997), and some suppression of AGRP synthesis was seen in *A^Y* mice (Figure 4). We further investigated whether the absence of mahogany had any effect on the structure of AGRP neurons projecting to PVH. AGRP fiber distribution and their interactions with α -MSH projections were analyzed by electron microscopy (EM) in both *mg/mg* and control animals. We focused our attention on two subdivisions (i.e. periventricular and medial) of the parvocellular PVH, which are known to express MC4-R (Cowley et al., 1999) and differ in their efferent projections and physiological roles (Dunn-Meynell et al., 1997; Rho and Swanson, 1989).

Our results indicate major differences between the two animal groups (Figure 5 A-D, Table 1) in both the number of AGRP axon terminals and the percent of direct contacts

established between AGRP and α -MSH boutons in the two PVH areas. In control animals, for instance, there were fewer AGRP boutons in the periventricular PVH ($34.3 \pm 4/100 \mu\text{m}^2$) than medial PVH ($64.2 \pm 8/100 \mu\text{m}^2$, $p < 0.05$); on the contrary, in *mg/mg* mice, the number of AGRP boutons in the periventricular PVH ($46.8 \pm 5/100 \mu\text{m}^2$) did not differ significantly from that of the medial PVH ($45.3 \pm 4/100 \mu\text{m}^2$). No differences were found in the levels of α -MSH boutons between the two animal groups in either the periventricular or medial PVH (Table 1). Furthermore, 19% of AGRP axon terminals, were in direct contact with α -MSH boutons in the periventricular PVH of control mice; this value was significantly higher in *mg/mg* animals (37%, $p < 0.05$) (Figure 5 A, Table 1). By contrast, in the medial PVH, 15% of the AGRP boutons were in direct contact with α -MSH axon terminals in control mice, whereas only 2.5% ($p < 0.05$) of the AGRP boutons contacted α -MSH axon terminals in *mg/mg* animals (Figure 5 A, Table 1). While there were no differences in the total numbers of AGRP and α -MSH boutons in the sum of the two PVH divisions in *mg/mg* mutant and control mice, there seemed to be a shift in the distribution of AGRP boutons in *mg/mg* animals from the medial to the periventricular PVH. In addition, the number of direct contacts between AGRP and α -MSH axon terminals changed significantly in the absence of mahogany, accumulating in the periventricular PVH and significantly decreasing in the medial PVH area.

Interestingly, mahogany immunostaining in the PVH showed predominant labeling of neuronal processes, including axon terminals (Figure 5 I-K). The immunolabeling was frequently associated with the outer membranes of labeled processes (Figure 5 J). Moreover, the immunohistochemistry experiments revealed that *mg* was indeed a loss-of-

function mutation, albeit not complete, at the *mahogany* locus. Thus, some protein expression was detected in the PVH of *mg/mg* animals, although it was very reduced when compared to control mice (Figure 5 E-H). In addition, preliminary evidence revealed predominant mahogany labeling in the periventricular segment of the PVH rather than in more lateral areas corresponding to the medial PVH (Figure 5 F, G).

DISCUSSION

Data presented here show that mahogany is required for the normal development of hypothalamic AGRP circuitry. This report characterizes mahogany as a novel member of the CUB protein family that may modulate changes in energy homeostasis via alterations in the neuronal connectivity of the CNS. Our conclusions raise some doubts about the potential role of mahogany as an obligatory AGRP or agouti co-receptor, as previously proposed (Gunn et al., 1999; Nagle et al., 1999). Thus we show that the post-receptor response to AGRP action is not modified in the absence of mahogany, since *mg/mg* animals have a normal response to either exogenous AGRP administration or constitutive production of AGRP via transgenic expression. In addition, the reduced MTII sensitivity shown by *mg/mg* mice suggests potential desensitization of the MC4-R to α -MSH action, which may reflect an inadequate AGRP signal at MC4-R target sites in these animals. Furthermore, EM analysis indicates that the absence of mahogany does indeed trigger major developmental changes in the distribution of AGRP fibers within the PVH, while no changes are seen for α -MSH projections. In control mice, for instance, a differential distribution of AGRP fibers is detected between periventricular and medial PVH, with the

medial PVH containing significantly more AGRP fibers than the periventricular region. In *mg/mg* mice, however, an equal distribution of AGRP fibers is seen between the two PVH subdivisions, suggesting that in the absence of mahogany the AGRP concentration gradient within the PVH is completely abolished. These findings raise the intriguing possibility that mahogany is an important surface molecule that mediates AGRP axon guidance from the periventricular to medial PVH. This possibility is further supported by the observation that mahogany labeling is seen predominantly on neuronal processes, especially axon terminals. Changes in the neuronal connectivity of the adult CNS are presumed to be contingent upon the relative balance between attractive (growth-inducing) and repulsive (growth-restricting) molecules (Tessier-Lavigne and Goodman, 1996). It is tempting to speculate that mahogany may function as a repellent for AGRP fibers during development, since preliminary immunohistochemistry studies seem to indicate that mahogany and AGRP concentration gradients within the PVH run in opposite directions (lower AGRP, higher mahogany expression in the periventricular PVH, and vice versa in the medial PVH). Interestingly, the CUB domain has previously been shown to be essential for inducing repulsive axon guidance during neurodevelopment by neuropilins (Giger et al., 1998). Furthermore, the *mg* and *md* phenotypes are similar despite their different chromosomal locations (Lane and Green, 1960), suggesting that the mahoganoid protein may be a heterotypic mahogany adhesion partner for axonal pathfinding during neurodevelopment. In addition to differences in routing of AGRP fibers, the immunoEM studies also revealed a striking alteration in the frequency of interaction between AGRP and α -MSH axons in the PVH of *mg/mg* mutant mice. This difference was not due to an overall difference in the amount of AGRP or α -MSH boutons in the PVH; the number of

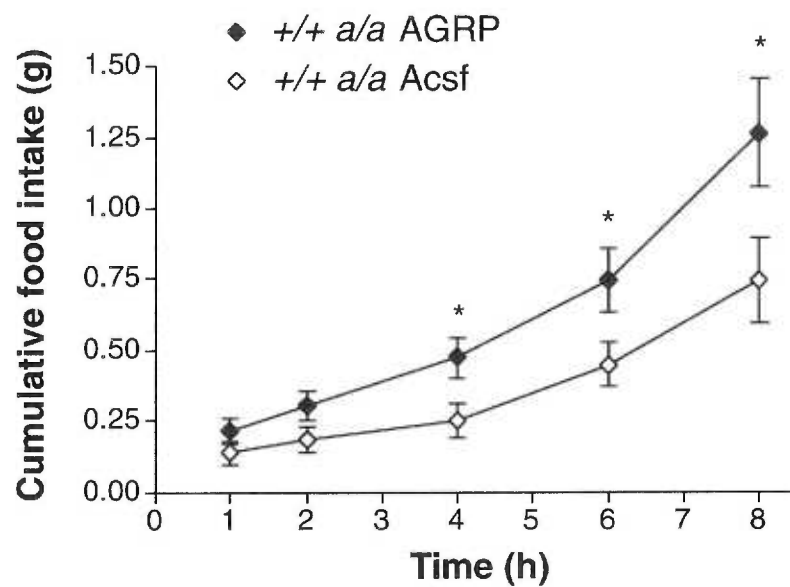
AGRP fibers in the medial PVH decreases 40% in the absence of mahogany, while the number of direct contacts between AGRP and α -MSH boutons is reduced 6-fold. These data suggest that, although some AGRP projections are able to reach the medial PVH in the absence of mahogany, they are misrouted to abnormal target sites and thus fail to contact α -MSH boutons. AGRP appears to be stable and diffuse well across brain tissue (Cowley et al., 1999), thus ectopic expression allows the protein to access the MC4-R and cause obesity, even in the absence of mahogany. In contrast, agouti is highly charged, is known not to diffuse well in skin (Silvers and Russel, 1955), and thus could be expected to be mahogany-dependent for its access to MC4-R sites, even in ectopic expression models.

Due to the fact that various PVH subnuclei participate in different aspects of metabolic regulation (Dunn-Meynell et al., 1997; Rho and Swanson, 1989), the inverse changes we observed in the periventricular and medial PVH may have an etiological role in the increased energy expenditure phenotype of the *mg/mg* mouse. Thus, neurons within the medial parvocellular PVH are known to project to areas of the medulla and spinal cord associated with sympathetic outflow pathways (Dunn-Meynell et al., 1997; Rho and Swanson, 1989). The reduced AGRP signal within the medial parvocellular PVH of *mg/mg* mice is likely to contribute to increased melanocortin signaling at MC4-R and may result in increased energy expenditure via sympathetic nervous system activation. In conclusion, while the mechanism by which mahogany participates in axonal pathfinding remains to be determined, these data identify mahogany as a new axonal guidance protein important for establishing the neuronal connectivity of the mature central nervous system.

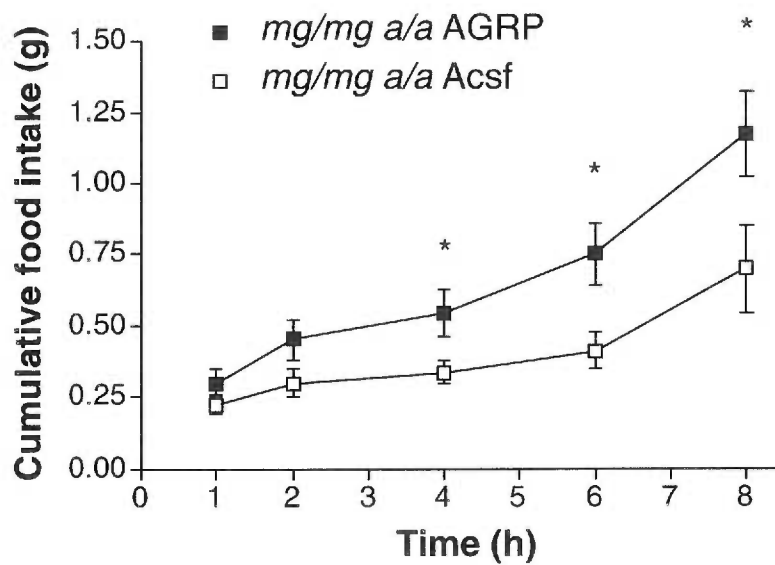
Figure 1. Normal response of *mg/mg* animals to centrally-administered AGRP.

(A-B) Similar responses of C57BL/6J (A) and *mg/mg* animals (B) to centrally administered AGRP₈₃₋₁₃₂ (3 nmol) over an 8 h period (n = 8-10). (C-D) Similar responses of C57BL/6J (C) and *mg/mg* animals (D) to centrally administered AGRP₈₃₋₁₃₂ (3 nmol) over a 24 h period (n = 8-10). (E-F) Similar responses of C57BL/6J (E) and *mg/mg* animals (F) to centrally administered full-length AGRP (0.3 nmol) over a 6 h period (n = 5-10). Values are means \pm SEM. *, $P < 0.05$, **, $p < 0.01$, ***, $p < 0.001$.

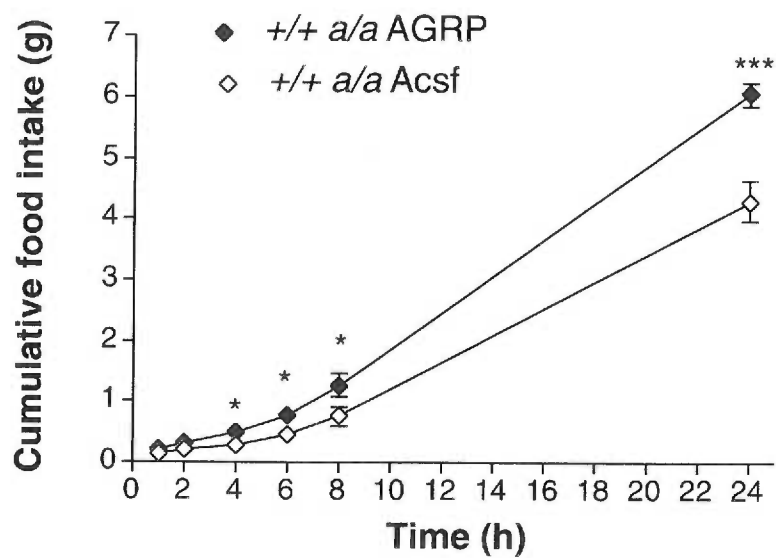
A.



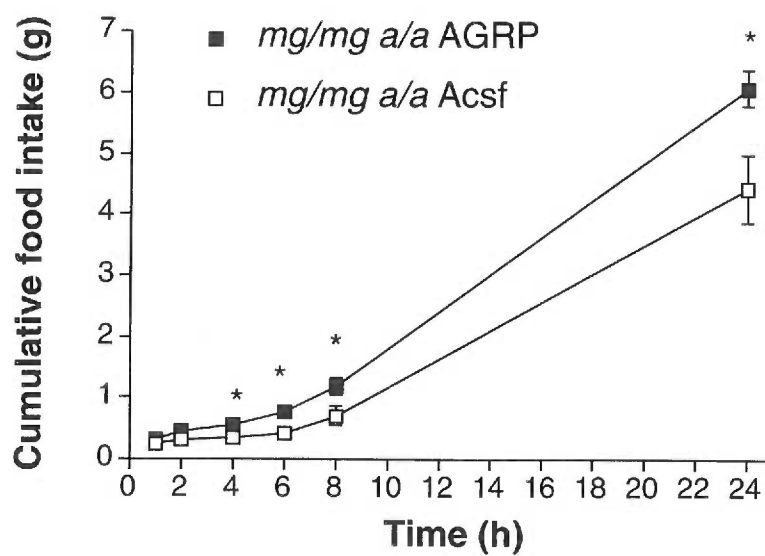
B.



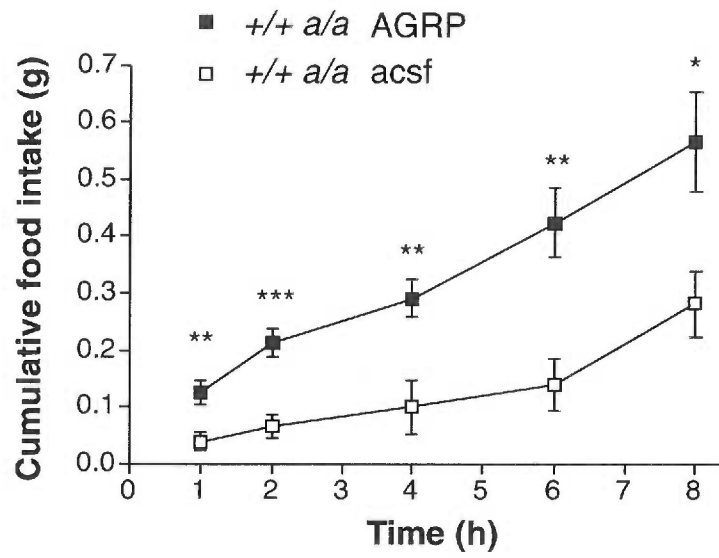
C.



D.



E.



F.

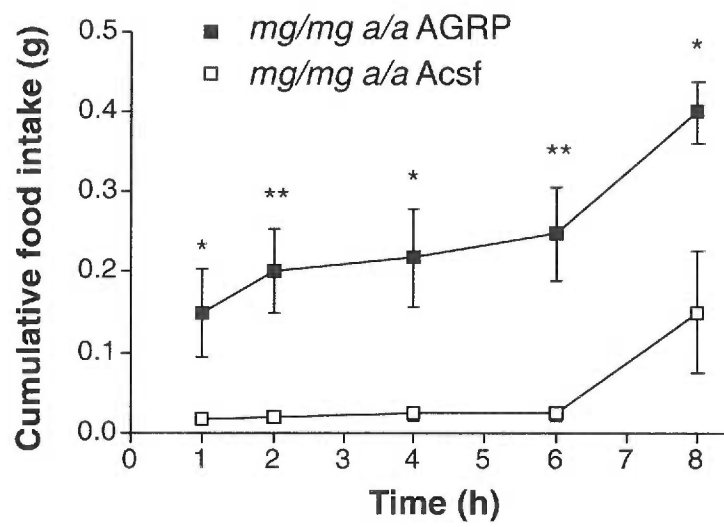


Figure 2. *mg* does not suppress the obesity of AGRP transgenic animals. Weight curves were recorded over a 6-month period for *mg/mg* AGRP Tg, *mg/+* AGRP Tg, *mg/mg* *+/+* animals, and C57 wild-type controls (females, n = 2-13). Values are means \pm SEM. No statistical differences were found between the weight curves of *mg/mg* Tg/*+* and *mg/+* Tg/*+* animals. In addition, the body weights of *mg/mg* Tg/*+* animals were statistically higher than those of *mg/mg* *+/+* animals ($p < 0.001$).

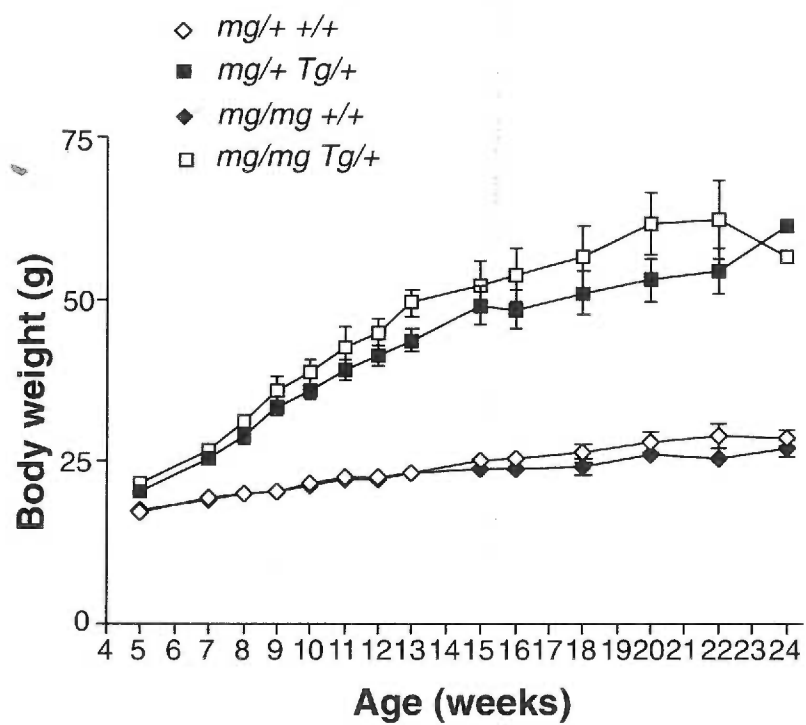


Figure 3. Reduced sensitivity of *mg/mg* animals to centrally administered MTII (1 nmol). Differential responses of *mg/mg* and control (C57BL/6J) animals to centrally administered MTII (1 nmol) recorded over a 8 h period (n = 6-7, p < 0.001 by 2 way ANOVA). Values are means \pm SEM.

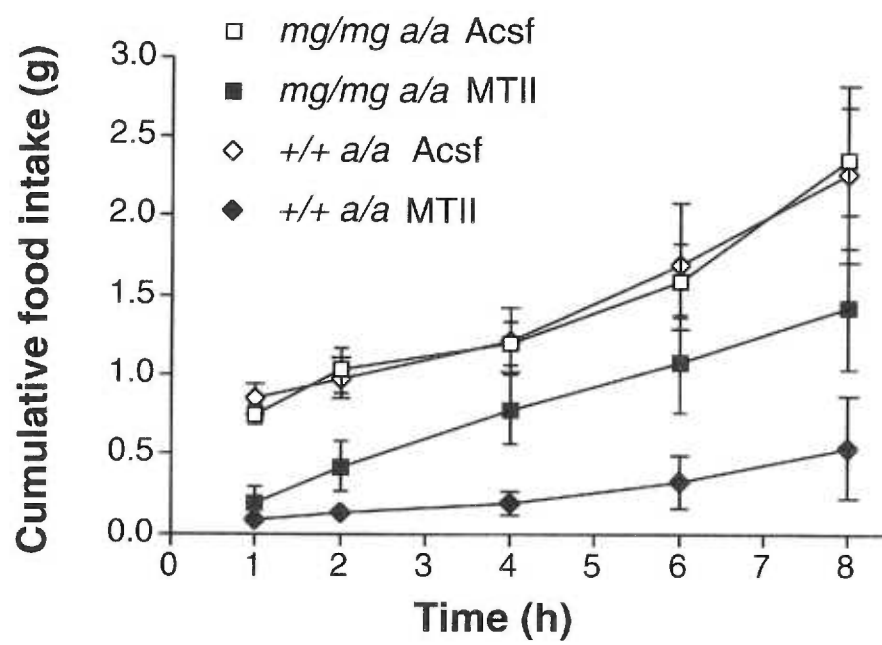
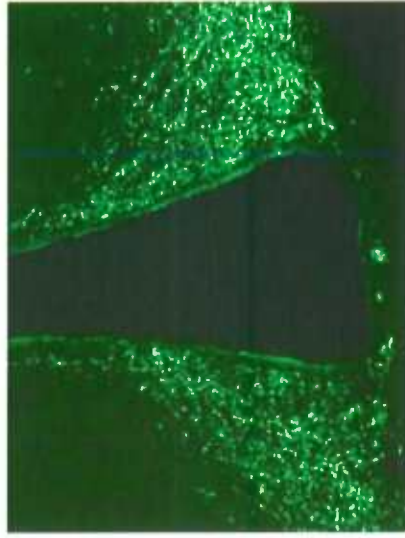
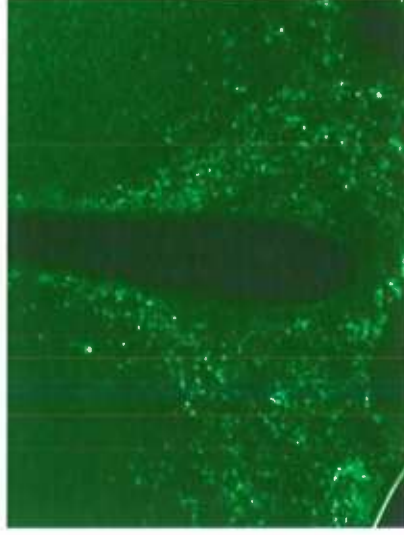


Figure 4. AGRP synthesis is not likely to be affected by mahogany. Comparative analysis of AGRP expression in the arcuate nucleus reveals no difference between *mg/mg a/a*, *mg/mg A^Y/a*, and control animals. The expression pattern of AGRP in *db/db* mice was used as a positive control.

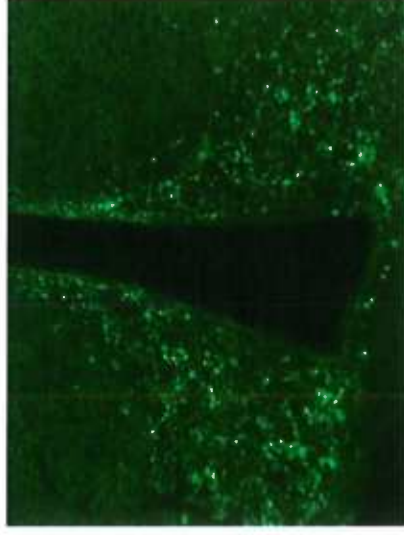
db/db



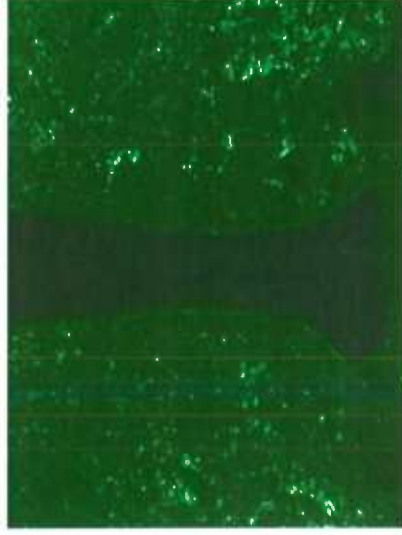
mg/mg a/a



+/+ a/a



mg/mg Ay/a



+/+ Ay/a

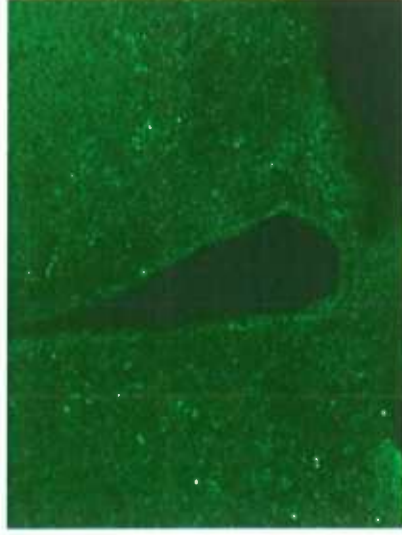


Figure 5. Mahogany controls AGRP axon guidance in the PVH. (A) Electron microscopic analysis of the periventricular and medial parvocellular PVH revealed that the direct axonal interaction between AGRP and α -MSH fibers (see panels B and D) were significantly higher in the periventricular PVH of *mg/mg* compared to control animals (*, $n = 4$, $p < 0.05$). In the medial PVH, the frequency of these interactions was significantly lower in *mg/mg* animals than in control mice (*, $p < 0.05$). In the two subdivision of the parvicellular PVH, the number of AGRP boutons were similar in *mg/mg* mice, while in control animals it was significantly higher in the medial than periventricular PVH ($p < 0.05$). (B-D) Electron micrographs showing direct contacts between AGRP (black immunoprecipitate; white arrowheads) and α -MSH (gray immunoprecipitate; black arrowheads) boutons in the periventricular (A) and medial PVH (D). The number of AGRP and α -MSH boutons in these direct interactions did not represent the majority of either of these axon populations in the PVH. Instead, more frequently AGRP and α -MSH boutons were distant from each other (C). Bar scale represents 1 μ m. (E-H) Light micrographs of the PVH in control (E, F) and *mg/mg* (G, H) animals after immunocytochemical labeling of mahogany protein. The staining intensity of mahogany was higher in the control PVH when compared to the co-incubated sections containing the PVH of *mg/mg* animals (compare panels E and F). Bar scales on panels E and F represent 10 μ m and 100 μ m, respectively. Electron microscopic analysis of mahogany immunostaining in the PVH revealed predominant labeling of neuronal processes (I-K), including axon terminals (I). The immunolabeling was frequently associated with the outer membranes of labeled processes (J). Bar scale represents 1 μ m.

% of AGRP boutons in direct contact with α -MSH axon terminals

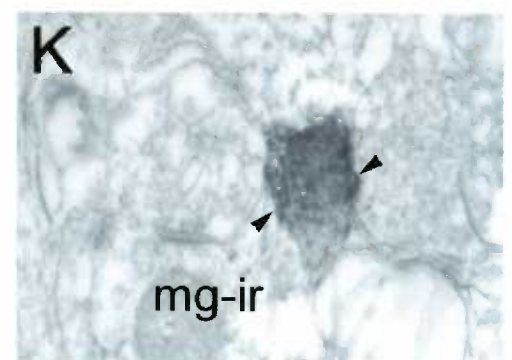
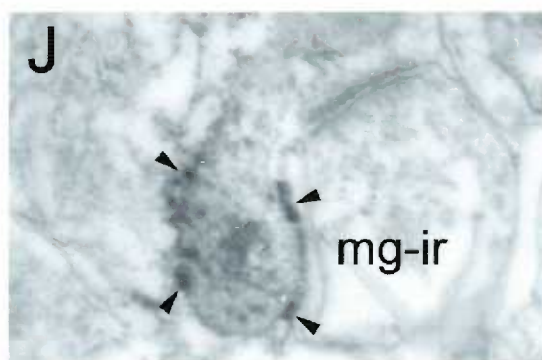
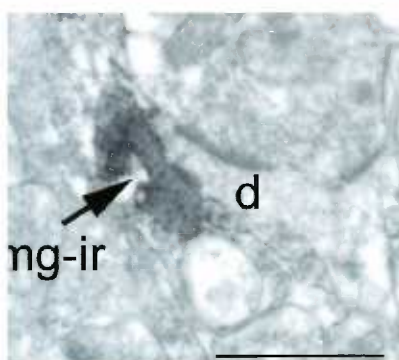
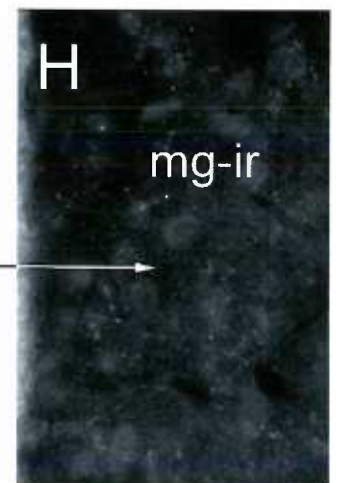
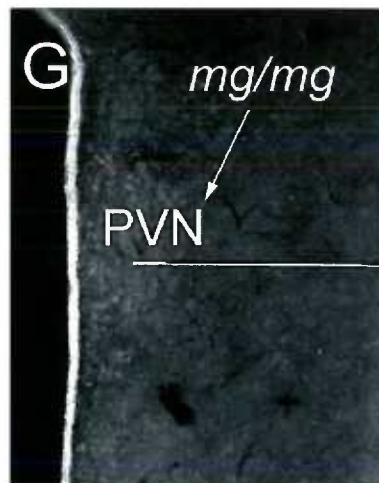
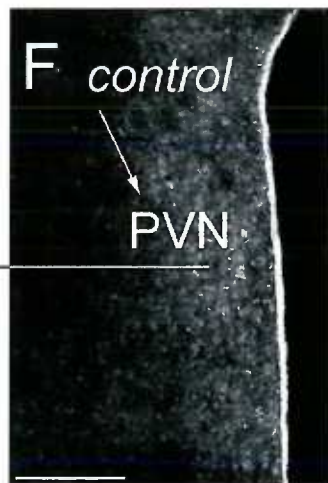
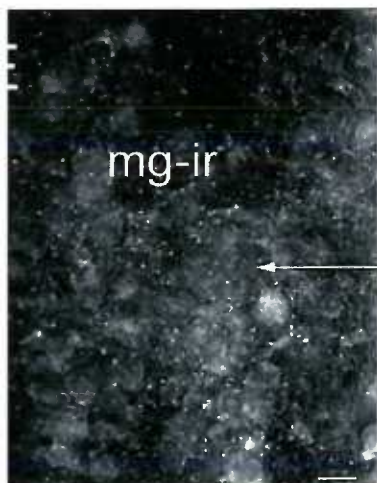
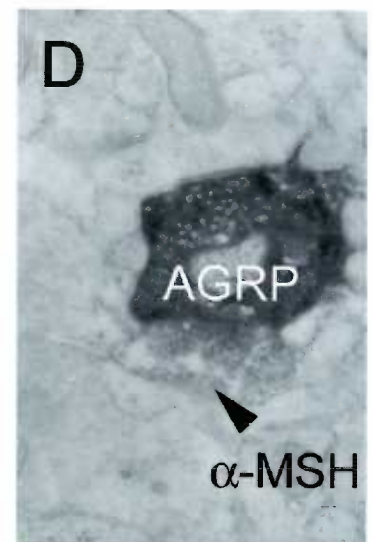
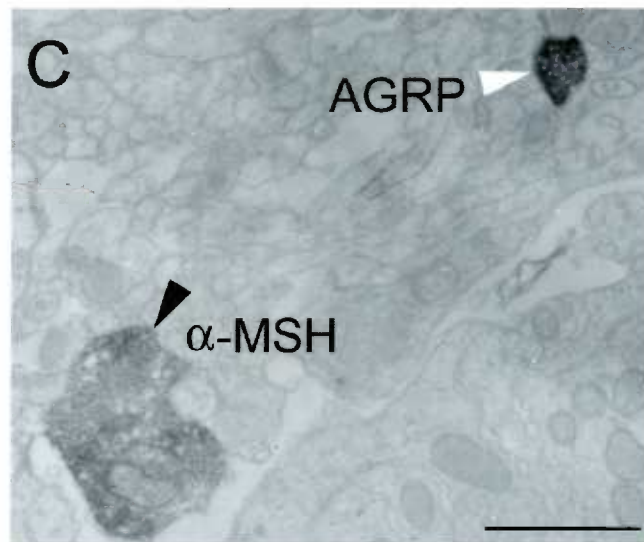
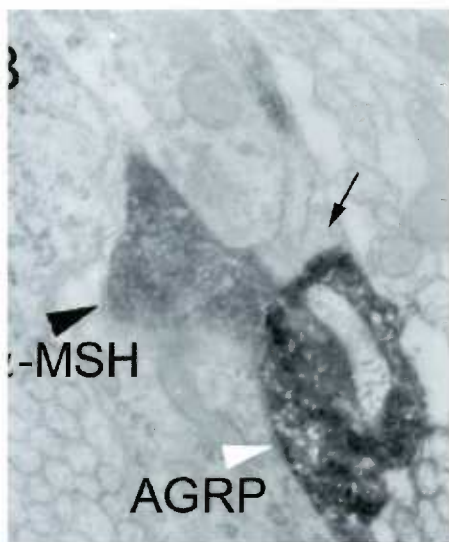
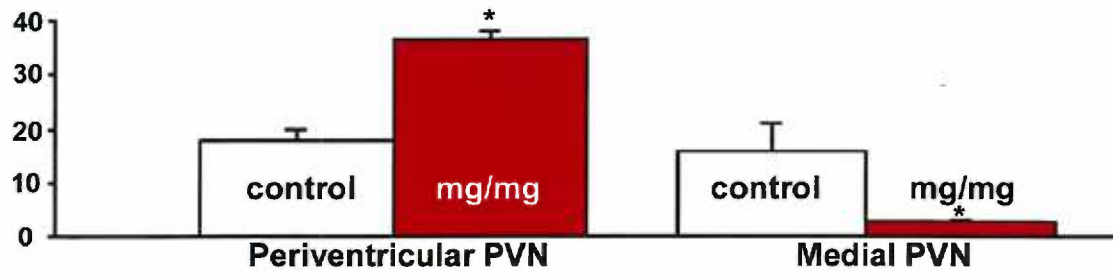


Table 1. Quantitation of α -MSH and AGRP fibers , and their axo-axonal interactions in the periventricular and medial PVH.

STRAIN	AGRP Axon Terminals		α -MSH Axon Terminals		% AGRP in contact with α -MSH	
	Periventricular PVH	Medial PVH	Periventricular PVH	Medial PVH	Periventricular PVH	Medial PVH
<i>mg/mg a/a</i>	46.8 \pm 5	45.3 \pm 4	48.5 \pm 6	22.4 \pm 5	16.1 \pm 1.5 ([#] , p < 0.05)	1.1 \pm 0.2 ([@] , p < 0.05)
<i>+/+ a/a</i>	*34.3 \pm 4	64.2 \pm 8 (* , p < 0.05)	48.4 \pm 6	26.4 \pm 4	[#] 6.8 \pm 0.5	[@] 9.6 \pm 1.2

SUMMARY AND CONCLUSIONS

The genetic analysis of canine *extension* and *agouti* reveals that the relationship between the two loci is analogous to those found in other mammals. We have thus eliminated the claim regarding the existence of a novel dominant *agouti* allele, A^s , that is responsible phenotypically for black coat color in dogs. Our study indicates that canine black pigmentation is most likely due to a recessive *agouti* allele, as is the case with other mammalian species. In addition, we have confirmed that recessive yellow coat color cosegregates with a mutation in MC1R, which abolishes the cytoplasmic domain of the receptor. As a result, the truncated MC1R-R306ter is unable to either bind the ligand or transduce the hormonal signal downstream to adenylyl cyclase. No differences in mRNA levels were found between wild-type and the mutant receptor; the protein level of the truncated receptor was, however, greatly reduced compared to the wild-type, suggesting a decrease in protein stability. In addition, we have demonstrated a loss of cell surface expression for the mutant receptor. Our data thus suggest that MC1R-R306ter fails to reach the plasma membrane and is rapidly degraded intracellularly, possibly because of protein misfolding in the ER. This hypothesis remains to be further investigated.

The main focus of my thesis has been the physiological and molecular characterization of mahogany. We have thus determined that mahogany plays a major role in the central control of energy homeostasis, aside from its effects on *agouti* signaling. Both metabolic rate and motor activity were found to be increased in *mg/mg* mice, presumably via activation of the sympathetic nervous system (SNS). This hypothesis is

supported by several observations. First, plasma thyroid hormone levels in *mg/mg* animals are normal (Dinulescu, unpublished results); thus, the thyroid axis is not likely to play a major role in the stimulation of their metabolism. Secondly, administration of MC4-R agonists, is associated with increased metabolism, via SNS activation [(Cowley et al., 1999), Fan unpublished results]. Likewise, the *mg/mg* mouse, a chronic model of increased melanocortinergic signaling, is likely to be characterized by increased sympathetic activation. Finally, mahogany is expressed in regions of the spinal cord (i.e. the intermediolateral nucleus) that are responsible for the sympathetic innervation of peripheral organs, such as brown adipose tissue (BAT) and heart (Lu et al., 1999). Further studies are needed to establish whether mahogany can indeed increase sympathetic nerve traffic to thermogenic BAT and other tissues.

Mahogany was also shown to play a critical role in the control of glucose homeostasis. Glucose tolerance in both normal *mg/mg* and obese *mg/mg ob/ob* mice was improved compared to control animals. This turned out to be a direct effect of increased insulin secretion following a glucose challenge. The effects of mahogany on glucose homeostasis appear to be both MC4-R mediated as well as melanocortin-independent. This conclusion stems from several observations. In the absence of a functional MC4-R (i.e. MC4-R KO) *mg* fails to increase the rate of glucose clearance. However, acute stimulation of the central melanocortin system (MC4-R) appears to have opposite effects on glucose homeostasis, it reduces the rate of glucose disposal and inhibits insulin secretion. In addition, we have demonstrated that the melanocortin system is involved in the control of peripheral insulin sensitivity. By contrast, mahogany does not appear to

play a major role in the regulation of peripheral insulin sensitivity. It is possible that these differences are the result of acute versus chronic (i.e. *mg/mg*) increased melanocortinergic signaling. Conversely, some of mahogany's effects on glucose homeostasis are not mediated by melanocortin pathways. Furthermore, we have now determined that, unlike melanocortins, mahogany is expressed in the pancreas; this suggests a potential role for mahogany in the peripheral control of insulin release. Further investigations will determine whether mahogany is present in β -cells and thus directly involved in coordinating the process of insulin secretion.

Finally, our analysis has provided insight into the molecular mechanism of mahogany action in the central nervous system. We have compared and contrasted the pattern of AGRP fiber distribution and their interaction with α -MSH projections in the hypothalamus of *mg/mg* and control animals. Our study has focused on two subdivisions (i.e. periventricular and medial) of the parvocellular PVH that are known to have different efferent projections and physiological roles. New evidence is provided that supports the role of mahogany in mediating AGRP axonal guidance during neurodevelopment, most likely via a repulsion mechanism. Further biochemical experiments are required to provide a direct proof for this hypothesis.

REFERENCES

1. Adan, R.A., A.W. Szklarczyk, J. Oosterom, J.H. Brakkee, W.A. Nijenhuis, W.M. Schaaper, R.H. Melloen, and W.H. Gispen. 1999. Characterization of melanocortin receptor ligands on cloned brain melanocortin receptors and on grooming behavior in the rat. *Eur J Pharmacol* 378: 249-258.
2. Al-Noaemi, M.C., J.A. Biggins, J.A. Edwardson, J.R. McDermott, and A.I. Smith. 1982. Corticotrophin-related peptides in the intermediate lobe of the rodent pituitary gland: characterization by high performance liquid chromatography and radioimmunoassay. *Regul Pept* 3: 351-359.
3. Al-Obeidi, F., V.J. Hruby, A.M. Castrucci, and M.E. Hadley. 1989. Design of potent linear alpha-melanotropin 4-10 analogues modified in positions 5 and 10. *J Med Chem* 32: 174-179.
4. Alvaro, J.D., J.B. Tatro, and R.S. Duman. 1997. Melanocortins and opiate addiction. *Life Sci* 61: 1-9.
5. Alvaro, J.D., J.B. Tatro, J.M. Quillan, M. Fogliano, M. Eisenhard, M.R. Lerner, E.J. Nestler, and R.S. Duman. 1996. Morphine down-regulates melanocortin-4 receptor expression in brain regions that mediate opiate addiction. *Mol Pharmacol* 50: 583-591.
6. Barnea, A. and G. Cho. 1983. Acetylation of adrenocorticotropin and beta-endorphin by hypothalamic and pituitary acetyltransferases. *Neuroendocrinology* 37: 434-439.
7. Baskin, D.G., M.W. Schwartz, R.J. Seeley, S.C. Woods, D. Porte, Jr., J.F. Breininger, Z. Jonak, J. Schaefer, M. Krouse, C. Burghardt, L.A. Campfield, P. Burn, and

- J.P. Kochan. 1999. Leptin receptor long-form splice-variant protein expression in neuron cell bodies of the brain and co-localization with neuropeptide Y mRNA in the arcuate nucleus. *J Histochem Cytochem* 47: 353-362.
8. Benjannet, S., N. Rondeau, R. Day, M. Chretien, and N.G. Seidah. 1991. PC1 and PC2 are proprotein convertases capable of cleaving proopiomelanocortin at distinct pairs of basic residues. *Proc Natl Acad Sci U S A* 88: 3564-3568.
9. Bennett, H.P. 1984. Isolation and characterization of the 1 to 49 amino-terminal sequence of pro-opiomelanocortin from bovine posterior pituitaries. *Biochem Biophys Res Commun* 125: 229-236.
10. Bennett, H.P., C.A. Browne, and S. Solomon. 1982. Characterization of eight forms of corticotropin-like intermediary lobe peptide from the rat intermediary pituitary. *J Biol Chem* 257: 10096-10102.
11. Bennett, H.P., P.L. Brubaker, M.A. Seger, and S. Solomon. 1983. Human phosphoserine 31 corticotropin1-39. Isolation and characterization. *J Biol Chem* 258: 8108-8112.
12. Blanchard, S.G., C.O. Harris, O.R. Ittoop, J.S. Nichols, D.J. Parks, A.T. Truesdale, and W.O. Wilkison. 1995. Agouti antagonism of melanocortin binding and action in the B16F10 murine melanoma cell line. *Biochemistry* 34: 10406-10411.
13. Boden, G. 1997. Role of fatty acids in the pathogenesis of insulin resistance and NIDDM [published erratum appears in Diabetes 1997 Mar;46(3):536]. *Diabetes* 46: 3-10.
14. Bohlen, P., F. Esch, T. Shibasaki, A. Baird, N. Ling, and R. Guillemin. 1981. Isolation and characterization of a gamma 1-melanotropin-like peptide from bovine neurointermediate pituitary. *FEBS Lett* 128: 67-70.

15. Bork, P. and G. Beckmann. 1993. The CUB domain. A widespread module in developmentally regulated proteins. *J Mol Biol* 231: 539-545.
16. Bork, P. and R.F. Doolittle. 1994. Drosophila kelch motif is derived from a common enzyme fold. *J Mol Biol* 236: 1277-1282.
17. Bourbonnais, Y. and P. Crine. 1985. Post-translational incorporation of [35S]sulfate into oligosaccharide side chains of pro-opiomelanocortin in rat intermediate lobe cells. *J Biol Chem* 260: 5832-5837.
18. Box, N.F., J.R. Wyeth, L.E. O'Gorman, N.G. Martin, and R.A. Sturm. 1997. Characterization of melanocyte stimulating hormone receptor variant alleles in twins with red hair. *Hum Mol Genet* 6: 1891-1897.
19. Broberger, C., J. Johansen, C. Johansson, M. Schalling, and T. Hokfelt. 1998. The neuropeptide Y/agouti gene-related protein (AGRP) brain circuitry in normal, anorectic, and monosodium glutamate-treated mice. *Proc Natl Acad Sci U S A* 95: 15043-15048.
20. Browne, C.A., H.P. Bennett, and S. Solomon. 1981. The isolation of characterization of gamma 3-melanotropin from the neurointermediary lobe of the rat pituitary. *Biochem Biophys Res Commun* 100: 336-343.
21. Bultman, S.J., M.L. Klebig, E.J. Michaud, H.O. Sweet, M.T. Davisson, and R.P. Woychik. 1994. Molecular analysis of reverse mutations from nonagouti (a) to black-and-tan (a(t)) and white-bellied agouti (Aw) reveals alternative forms of agouti transcripts. *Genes Dev* 8: 481-490.
22. Bultman, S.J., E.J. Michaud, and R.P. Woychik. 1992. Molecular characterization of the mouse agouti locus. *Cell* 71: 1195-1204.

23. Bultman, S.J., L.B. Russell, G.A. Gutierrez-Espeleta, and R.P. Woychik. 1991. Molecular characterization of a region of DNA associated with mutations at the agouti locus in the mouse. *Proc Natl Acad Sci U S A* 88: 8062-8066.
24. Burbach, J.P. and V.M. Wiegant. 1984. Isolation and characterization of alpha-endorphin and gamma-endorphin from single human pituitary glands. *FEBS Lett* 166: 267-272.
25. Bures, E.J., J.O. Hui, Y. Young, D.T. Chow, V. Katta, M.F. Rohde, L. Zeni, R.D. Rosenfeld, K.L. Stark, and M. Haniu. 1998. Determination of disulfide structure in agouti-related protein (AGRP) by stepwise reduction and alkylation. *Biochemistry* 37: 12172-12177.
26. Campfield, L.A., F.J. Smith, Y. Guisez, R. Devos, and P. Burn. 1995. Recombinant mouse OB protein: evidence for a peripheral signal linking adiposity and central neural networks [see comments]. *Science* 269: 546-549.
27. Carver, E.A. 1984. Coat color genetics of the German shepherd dog. *J. Hered.* 75: 247-252.
28. Castrucci, A.M., M.E. Hadley, T.K. Sawyer, B.C. Wilkes, F. al-Obeidi, D.J. Staples, A.E. de Vaux, O. Dym, M.F. Hintz, J.P. Riehm, and et al. 1989. Alpha-melanotropin: the minimal active sequence in the lizard skin bioassay. *Gen Comp Endocrinol* 73: 157-163.
29. Ceriani, G., J. Diaz, S. Murphree, A. Catania, and J.M. Lipton. 1994a. The neuropeptide alpha-melanocyte-stimulating hormone inhibits experimental arthritis in rats. *Neuroimmunomodulation* 1: 28-32.

30. Ceriani, G., A. Macaluso, A. Catania, and J.M. Lipton. 1994b. Central neurogenic antiinflammatory action of alpha-MSH: modulation of peripheral inflammation induced by cytokines and other mediators of inflammation. *Neuroendocrinology* 59: 138-143.
31. Chehab, F.F., M.E. Lim, and R. Lu. 1996. Correction of the sterility defect in homozygous obese female mice by treatment with the human recombinant leptin. *Nat Genet* 12: 318-320.
32. Chen, H., O. Charlat, L.A. Tartaglia, E.A. Woolf, X. Weng, S.J. Ellis, N.D. Lakey, J. Culpepper, K.J. Moore, R.E. Breitbart, G.M. Duyk, R.I. Tepper, and J.P. Morgenstern. 1996. Evidence that the diabetes gene encodes the leptin receptor: identification of a mutation in the leptin receptor gene in db/db mice. *Cell* 84: 491-495.
33. Chen, W., T.S. Shields, P.J. Stork, and R.D. Cone. 1995. A colorimetric assay for measuring activation of Gs- and Gq-coupled signaling pathways. *Anal Biochem* 226: 349-354.
34. Cheng, M.C., A.I. Smith, J.A. Clements, and J.W. Funder. 1987. N-acetylated endorphins in ovine anterior pituitary and neuro- intermediate lobe. *Peptides* 8: 1045-1050.
35. Cheung, C.C., D.K. Clifton, and R.A. Steiner. 1997. Proopiomelanocortin neurons are direct targets for leptin in the hypothalamus. *Endocrinology* 138: 4489-4492.
36. Chhajlani, V., R. Muceniece, and J.E. Wikberg. 1993. Molecular cloning of a novel human melanocortin receptor [published erratum appears in *Biochem Biophys Res Commun* 1996 Jan 17;218(2):638]. *Biochem Biophys Res Commun* 195: 866-873.
37. Chretien, M., N.G. Seidah, and M. Dennis. 1984. Processing of precursor polyproteins in rat brain: regional differences in the acetylation of POMC peptides. *In:*

Muller, E.E., Genazzani, A.R. (eds) *Central and Peripheral Endorphins: Basic and Clinical Aspects*, Raven Press, New York: 27.

38. Clement, K., C. Vaisse, N. Lahlou, S. Cabrol, V. Pelloux, D. Cassuto, M. Gormelen, C. Dina, J. Chambaz, J.M. Lacorte, A. Basdevant, P. Bougneres, Y. Lebouc, P. Froguel, and B. Guy-Grand. 1998. A mutation in the human leptin receptor gene causes obesity and pituitary dysfunction [see comments]. *Nature* 392: 398-401.
39. Cody, J.D., X.T. Reveles, D.E. Hale, D. Lehman, H. Coon, and R.J. Leach. 1999. Haplosufficiency of the melanocortin-4 receptor gene in individuals with deletions of 18q. *Hum Genet* 105: 424-427.
40. Cone, R.D. 2000. Melanocortin receptors. *Humana Press, Totowa, New Jersey*.
41. Cone, R.D., K.G. Mountjoy, L.S. Robbins, J.H. Nadeau, K.R. Johnson, L. Roselli-Reh fuss, and M.T. Mortrud. 1993. Cloning and functional characterization of a family of receptors for the melanotropic peptides. *Ann N Y Acad Sci* 680: 342-363.
42. Considine, R.V., E.L. Considine, C.J. Williams, M.R. Nyce, P. Zhang, I. Opentanova, J.P. Ohannesian, J.W. Kolaczynski, T.L. Bauer, J.H. Moore, and J.F. Caro. 1996. Mutation screening and identification of a sequence variation in the human ob gene coding region. *Biochem Biophys Res Commun* 220: 735-739.
43. Cornelius, P. 1999. The role of central melanocortin receptors in the regulation of metabolic rate. *The Endocrine Society's 81st Annual Meeting* (OR3-4): 66.
44. Cowley, M.A., N. Pronschuk, W. Fan, D.M. Dinulescu, W.F. Colmers, and R.D. Cone. 1999. Integration of NPY, AGRP, and melanocortin signals in the hypothalamic paraventricular nucleus: evidence of a cellular basis for the adipostat. *Neuron* 24: 155-163.

45. Cox, N.J., M. Frigge, D.L. Nicolae, P. Concannon, C.L. Hanis, G.I. Bell, and A. Kong. 1999. Loci on chromosomes 2 (NIDDM1) and 15 interact to increase susceptibility to diabetes in Mexican Americans. *Nat Genet* 21: 213-215.
46. Crine, P., C. Gianoulakis, N.G. Seidah, F. Gossard, P.D. Pezalla, M. Lis, and M. Chretien. 1978. Biosynthesis of beta-endorphin from beta-lipotropin and a larger molecular weight precursor in rat pars intermedia. *Proc Natl Acad Sci U S A* 75: 4719-4723.
47. Crine, P., F. Gossard, N.G. Seidah, L. Blanchette, M. Lis, and M. Chretien. 1979. Concomitant synthesis of beta-endorphin and alpha-melanotropin from two forms of pro-opiomelanocortin in the rat pars intermedia. *Proc Natl Acad Sci U S A* 76: 5085-5089.
48. Danforth, C.H. 1927. *J. Hered.* 18: 153-162.
49. DeFronzo, R.A., R.C. Bonadonna, and E. Ferrannini. 1992. Pathogenesis of NIDDM. A balanced overview. *Diabetes Care* 15: 318-368.
50. Dickerson, G.E. and J.W. Gowen. 1947. Hereditary obesity and efficient food utilization in mice. *Science* 105: 496-498.
51. Dinulescu, D.M., W. Fan, B.A. Boston, K. McCall, M.L. Lamoreux, K.J. Moore, J. Montagno, and R.D. Cone. 1998. *Mahogany (mg)* stimulates feeding and increases basal metabolic rate independent of its suppression of agouti. *Proc Natl Acad Sci U S A* 95: 12707-12712.
52. Drickamer, K. 1995. Multiplicity of lectin-carbohydrate interactions [news; comment]. *Nat Struct Biol* 2: 437-439.
53. Duke-Cohan, J.S., J. Gu, D.F. McLaughlin, Y. Xu, G.J. Freeman, and S.F. Schlossman. 1998. Attractin (DPPT-L), a member of the CUB family of cell adhesion and

guidance proteins, is secreted by activated human T lymphocytes and modulates immune cell interactions. *Proc Natl Acad Sci U S A* 95: 11336-11341.

54. Dunn-Meynell, A.A., E. Govek, and B.E. Levin. 1997. Intracarotid glucose selectively increases Fos-like immunoreactivity in paraventricular, ventromedial and dorsomedial nuclei neurons. *Brain Res* 748: 100-106.

55. Ebihara, K., Y. Ogawa, G. Katsuura, Y. Numata, H. Masuzaki, N. Satoh, M. Tamaki, T. Yoshioka, M. Hayase, N. Matsuoka, M. Aizawa-Abe, Y. Yoshimasa, and K. Nakao. 1999. Involvement of agouti-related protein, an endogenous antagonist of hypothalamic melanocortin receptor, in leptin action. *Diabetes* 48: 2028-2033.

56. Echwald, S.M., S.B. Rasmussen, T.I. Sorensen, T. Andersen, A. Tybjaerg-Hansen, J.O. Clausen, L. Hansen, T. Hansen, and O. Pedersen. 1997. Identification of two novel missense mutations in the human OB gene. *Int J Obes Relat Metab Disord* 21: 321-326.

57. Echwald, S.M., T.I. Sorensen, T. Andersen, A. Tybjaerg-Hansen, J.O. Clausen, and O. Pedersen. 1999. Mutational analysis of the proopiomelanocortin gene in Caucasians with early onset obesity. *Int J Obes Relat Metab Disord* 23: 293-298.

58. Eipper, B.A. and R.E. Mains. 1980. Structure and biosynthesis of pro-adrenocorticotropin/endorphin and related peptides. *Endocr Rev* 1: 1-27.

59. Eipper, B.A. and R.E. Mains. 1981. Further analysis of post-translational processing of beta-endorphin in rat intermediate pituitary. *J Biol Chem* 256: 5689-5695.

60. Eipper, B.A., L. Park, H.T. Keutmann, and R.E. Mains. 1986. Amidation of joining peptide, a major pro-ACTH/endorphin-derived product peptide. *J Biol Chem* 261: 8686-8694.

61. Erickson, J.C., G. Hollopeter, and R.D. Palmiter. 1996. Attenuation of the obesity syndrome of ob/ob mice by the loss of neuropeptide Y [see comments]. *Science* 274: 1704-1707.
62. Fan, W., B.A. Boston, R.A. Kesterson, V.J. Hruby, and R.D. Cone. 1997. Role of melanocortinergic neurons in feeding and the agouti obesity syndrome [see comments]. *Nature* 385: 165-168.
63. Fan, W., D.M. Dinulescu, A.A. Butler, J. Zhou, D.L. Marks, and R.D. Cone. 2000. Effects of the central melanocortin system on insulin release and insulin sensitivity. *Endocrinology (in press)*.
64. Farooqi, I.S., S.A. Jebb, G. Langmack, E. Lawrence, C.H. Cheetham, A.M. Prentice, I.A. Hughes, M.A. McCamish, and S. O'Rahilly. 1999. Effects of recombinant leptin therapy in a child with congenital leptin deficiency [see comments]. *N Engl J Med* 341: 879-884.
65. Fenton, P.F. and H.B. Chase. 1951. Effect of diet on obesity of yellow mice in inbred lines. *Proc. Soc. Exp. Biol.* 77: 420-422.
66. Florijn, W.J., A.H. Mulder, D.H. Versteeg, and W.H. Gispen. 1993. Adrenocorticotropin/alpha-melanocyte-stimulating hormone (ACTH/MSH)- like peptides modulate adenylate cyclase activity in rat brain slices: evidence for an ACTH/MSH receptor-coupled mechanism. *J Neurochem* 60: 2204-2211.
67. Fong, T.M., C. Mao, T. MacNeil, R. Kalyani, T. Smith, D. Weinberg, M.R. Tota, and L.H. Van der Ploeg. 1997. ART (protein product of agouti-related transcript) as an antagonist of MC-3 and MC-4 receptors. *Biochem Biophys Res Commun* 237: 629-631.

68. Frohman, L.A. and L.L. Bernardis. 1971. Effect of hypothalamic stimulation on plasma glucose, insulin, and glucagon levels. *Am J Physiol* 221: 1596-1603.
69. Gantz, I., Y. Konda, T. Tashiro, Y. Shimoto, H. Miwa, G. Munzert, S.J. Watson, J. DelValle, and T. Yamada. 1993a. Molecular cloning of a novel melanocortin receptor. *J Biol Chem* 268: 8246-8250.
70. Gantz, I., H. Miwa, Y. Konda, Y. Shimoto, T. Tashiro, S.J. Watson, J. DelValle, and T. Yamada. 1993b. Molecular cloning, expression, and gene localization of a fourth melanocortin receptor. *J Biol Chem* 268: 15174-15179.
71. Gantz, I., Y. Shimoto, Y. Konda, H. Miwa, C.J. Dickinson, and T. Yamada. 1994. Molecular cloning, expression, and characterization of a fifth melanocortin receptor. *Biochem Biophys Res Commun* 200: 1214-1220.
72. Gee, C.E. and J.L. Roberts. 1983. In situ hybridization histochemistry: a technique for the study of gene expression in single cells. *DNA* 2: 157-163.
73. Geschwind, H., R.A. Huseby, and R. Nishioka. 1972. The effect of melanocyte-stimulating hormone on coat color in the mouse. *Recent Prog Horm Res* 28: 91-130.
74. Ghilardi, N., S. Ziegler, A. Wiestner, R. Stoffel, M.H. Heim, and R.C. Skoda. 1996. Defective STAT signaling by the leptin receptor in diabetic mice. *Proc Natl Acad Sci U S A* 93: 6231-6235.
75. Giger, R.J., E.R. Urquhart, S.K. Gillespie, D.V. Levengood, D.D. Ginty, and A.L. Kolodkin. 1998. Neuropilin-2 is a receptor for semaphorin IV: insight into the structural basis of receptor function and specificity [see comments]. *Neuron* 21: 1079-1092.

76. Glembofski, C.C. 1982. Characterization of the peptide acetyltransferase activity in bovine and rat intermediate pituitaries responsible for the acetylation of beta-endorphin and alpha-melanotropin. *J Biol Chem* 257: 10501-10509.
77. Glyn-Ballinger, J.R., G.L. Bernardini, and J.M. Lipton. 1983. alpha-MSH injected into the septal region reduces fever in rabbits. *Peptides* 4: 199-203.
78. Goto, Y., R.G. Carpenter, M. Berelowitz, and L.A. Frohman. 1980. Effect of ventromedial hypothalamic lesions on the secretion of somatostatin, insulin, and glucagon by the perfused rat pancreas. *Metabolism* 29: 986-990.
79. Gotoda, T., B.S. Manning, A.P. Goldstone, H. Imrie, A.L. Evans, A.D. Strosberg, P.M. McKeigue, J. Scott, and T.J. Aitman. 1997a. Leptin receptor gene variation and obesity: lack of association in a white British male population. *Hum Mol Genet* 6: 869-876.
80. Gotoda, T., J. Scott, and T.J. Aitman. 1997b. Molecular screening of the human melanocortin-4 receptor gene: identification of a missense variant showing no association with obesity, plasma glucose, or insulin. *Diabetologia* 40: 976-979.
81. Graham, M., J.R. Shutter, U. Sarmiento, I. Sarosi, and K.L. Stark. 1997. Overexpression of Agrt leads to obesity in transgenic mice [letter]. *Nat Genet* 17: 273-274.
82. Green, M.C. 1989. Genetic Variants and Strains of the Laboratory Mouse. eds. Lyon, M.F. & Searle, A.G. (Oxford Univ. Press, Oxford): 12-403.
83. Gu, W., Z. Tu, P.W. Kley, A. Kissebah, L. Duprat, J. Lee, W. Chin, S. Maruti, N. Deng, S.L. Fisher, L.S. Franco, P. Burn, K.A. Yagaloff, J. Nathan, S. Heymsfield, J. Albu, F.X. Pi-Sunyer, and D.B. Allison. 1999. Identification and functional analysis of novel human melanocortin-4 receptor variants. *Diabetes* 48: 635-639.

84. Gunn, T.M., K.A. Miller, L. He, R.W. Hyman, R.W. Davis, A. Azarani, S.F. Schlossman, J.S. Duke-Cohan, and G.S. Barsh. 1999. The mouse mahogany locus encodes a transmembrane form of human attractin. *Nature* 398: 152-156.
85. Guttman, S. 1961. Influence of the structure of the N-terminal extremity of alpha-MSH on the melanophore stimulating activity of this hormone. *Experientia* 17: 265-267.
86. Hager, J., C. Dina, S. Francke, S. Dubois, M. Houari, V. Vatin, E. Vaillant, N. Lorentz, A. Basdevant, K. Clement, B. Guy-Grand, and P. Froguel. 1998. A genome-wide scan for human obesity genes reveals a major susceptibility locus on chromosome 10. *Nat Genet* 20: 304-308.
87. Hakansson, M.L., A.L. Hulting, and B. Meister. 1996. Expression of leptin receptor mRNA in the hypothalamic arcuate nucleus-- relationship with NPY neurones. *Neuroreport* 7: 3087-3092.
88. Halaas, J.L., K.S. Gajiwala, M. Maffei, S.L. Cohen, B.T. Chait, D. Rabinowitz, R.L. Lallone, S.K. Burley, and J.M. Friedman. 1995. Weight-reducing effects of the plasma protein encoded by the obese gene [see comments]. *Science* 269: 543-546.
89. Hanis, C.L., E. Boerwinkle, R. Chakraborty, D.L. Ellsworth, P. Concannon, B. Stirling, V.A. Morrison, B. Wapelhorst, R.S. Spielman, K.J. Gogolin-Ewens, J.M. Shepard, S.R. Williams, N. Risch, D. Hinds, N. Iwasaki, M. Ogata, Y. Omori, C. Petzold, H. Rietzch, H.E. Schroder, J. Schulze, N.J. Cox, S. Menzel, V.V. Boriraj, X. Chen, and et al. 1996. A genome-wide search for human non-insulin-dependent (type 2) diabetes genes reveals a major susceptibility locus on chromosome 2 [see comments]. *Nat Genet* 13: 161-166.

90. Harrold, J.A., G. Williams, and P.S. Widdowson. 1999. Changes in hypothalamic agouti-related protein (AGRP), but not alpha-MSH or pro-opiomelanocortin concentrations in dietary-obese and food-restricted rats. *Biochem Biophys Res Commun* 258: 574-577.
91. Haskell-Luevano, C., P. Chen, C. Li, K. Chang, M.S. Smith, J.L. Cameron, and R.D. Cone. 1999. Characterization of the neuroanatomical distribution of agouti-related protein immunoreactivity in the rhesus monkey and the rat. *Endocrinology* 140: 1408-1415.
92. Haynes, W.G., D.A. Morgan, A. Djalali, W.I. Sivitz, and A.L. Mark. 1999. Interactions between the melanocortin system and leptin in control of sympathetic nerve traffic. *Hypertension* 33: 542-547.
93. Hinney, A., I. Becker, O. Heibult, K. Nottebom, A. Schmidt, A. Ziegler, H. Mayer, W. Siegfried, W.F. Blum, H. Remschmidt, and J. Hebebrand. 1998a. Systematic mutation screening of the pro-opiomelanocortin gene: identification of several genetic variants including three different insertions, one nonsense and two missense point mutations in probands of different weight extremes. *J Clin Endocrinol Metab* 83: 3737-3741.
94. Hinney, A., A. Bornscheuer, M. Depenbusch, B. Mierke, A. Tolle, H. Mayer, W. Siegfried, H. Remschmidt, and J. Hebebrand. 1997. Absence of leptin deficiency mutation in extremely obese German children and adolescents [letter]. *Int J Obes Relat Metab Disord* 21: 1190.
95. Hinney, A., A. Bornscheuer, M. Depenbusch, B. Mierke, A. Tolle, K. Middeke, A. Ziegler, H. Roth, G. Gerber, K. Zamzow, A. Ballauff, A. Hamann, H. Mayer, W. Siegfried, G. Lehmkuhl, F. Poustka, M.H. Schmidt, H. Hermann, B.M. Herpertz-

- Dahlmann, M. Fichter, H. Remschmidt, and J. Hebebrand. 1998b. No evidence for involvement of the leptin gene in anorexia nervosa, bulimia nervosa, underweight or early onset extreme obesity: identification of two novel mutations in the coding sequence and a novel polymorphism in the leptin gene linked upstream region [see comments]. *Mol Psychiatry* 3: 539-543.
96. Hinney, A., A. Schmidt, K. Nottebom, O. Heibult, I. Becker, A. Ziegler, G. Gerber, M. Sina, T. Gorg, H. Mayer, W. Siegfried, M. Fichter, H. Remschmidt, and J. Hebebrand. 1999. Several mutations in the melanocortin-4 receptor gene including a nonsense and a frameshift mutation associated with dominantly inherited obesity in humans. *J Clin Endocrinol Metab* 84: 1483-1486.
97. Hixson, J.E., L. Almasy, S. Cole, S. Birnbaum, B.D. Mitchell, M.C. Mahaney, M.P. Stern, J.W. MacCluer, J. Blangero, and A.G. Comuzzie. 1999. Normal variation in leptin levels in associated with polymorphisms in the proopiomelanocortin gene, POMC. *J Clin Endocrinol Metab* 84: 3187-3191.
98. Hogben, L.T. and F.R. Winton. 1922. Studies on the pituitary. The melanophore stimulant in posterior lobe extracts. *Biochem. J.* 16: 619-630.
99. Horvath, T.L., S. Diano, and A.N. van den Pol. 1999. Synaptic interaction between hypocretin (orexin) and neuropeptide Y cells in the rodent and primate hypothalamus: a novel circuit implicated in metabolic and endocrine regulations. *J Neurosci* 19: 1072-1087.
100. Hoshina, H., G. Hortin, and I. Boime. 1982. Rat pro-opiomelanocortin contains sulfate. *Science* 217: 63-64.
101. Hruby, V.J., D. Lu, S.D. Sharma, A.L. Castrucci, R.A. Kesterson, F.A. al-Obeidi, M.E. Hadley, and R.D. Cone. 1995. Cyclic lactam alpha-melanotropin analogues of Ac-

- Nle4-cyclo[Asp5, D- Phe7,Lys10] alpha-melanocyte-stimulating hormone-(4-10)-NH₂ with bulky aromatic amino acids at position 7 show high antagonist potency and selectivity at specific melanocortin receptors. *J Med Chem* 38: 3454-3461.
102. Hruby, V.J., B.C. Wilkes, M.E. Hadley, F. Al-Obeidi, T.K. Sawyer, D.J. Staples, A.E. de Vaux, O. Dym, A.M. Castrucci, M.F. Hintz, and et al. 1987. alpha-Melanotropin: the minimal active sequence in the frog skin bioassay. *J Med Chem* 30: 2126-2130.
103. Huang, Q.H., M.L. Entwistle, J.D. Alvaro, R.S. Duman, V.J. Hruby, and J.B. Tatro. 1997. Antipyretic role of endogenous melanocortins mediated by central melanocortin receptors during endotoxin-induced fever. *J Neurosci* 17: 3343-3351.
104. Huang, Q.H., V.J. Hruby, and J.B. Tatro. 1998. Systemic alpha-MSH suppresses LPS fever via central melanocortin receptors independently of its suppression of corticosterone and IL-6 release. *Am J Physiol* 275: R524-530.
105. Huang, Q.H., V.J. Hruby, and J.B. Tatro. 1999. Role of central melanocortins in endotoxin-induced anorexia. *Am J Physiol* 276: R864-871.
106. Huang, X.F., I. Koutcherov, S. Lin, H.Q. Wang, and L. Storlien. 1996. Localization of leptin receptor mRNA expression in mouse brain. *Neuroreport* 7: 2635-2638.
107. Hunt, G. and A.J. Thody. 1995. Agouti protein can act independently of melanocyte-stimulating hormone to inhibit melanogenesis. *J Endocrinol* 147: R1-4.
108. Hunt, G., C. Todd, and A.J. Thody. 1996. Unresponsiveness of human epidermal melanocytes to melanocyte- stimulating hormone and its association with red hair. *Mol Cell Endocrinol* 116: 131-136.
109. Huszar, D., C.A. Lynch, V. Fairchild-Huntress, J.H. Dunmore, Q. Fang, L.R. Berkemeier, W. Gu, R.A. Kesterson, B.A. Boston, R.D. Cone, F.J. Smith, L.A. Campfield,

- P. Burn, and F. Lee. 1997. Targeted disruption of the melanocortin-4 receptor results in obesity in mice. *Cell* 88: 131-141.
110. Jackson, I.J. 1993. Molecular genetics. Colour-coded switches [news] [see comments]. *Nature* 362: 587-588.
111. Jackson, I.J. 1999. The mahogany mouse mutation: further links between pigmentation, obesity and the immune system. *Trends Genet* 15: 429-431.
112. Jackson, R.S., J.W. Creemers, S. Ohagi, M.L. Raffin-Sanson, L. Sanders, C.T. Montague, J.C. Hutton, and S. O'Rahilly. 1997. Obesity and impaired prohormone processing associated with mutations in the human prohormone convertase 1 gene [see comments]. *Nat Genet* 16: 303-306.
113. Kalra, S.P., M.G. Dube, S. Pu, B. Xu, T.L. Horvath, and P.S. Kalra. 1999. Interacting appetite-regulating pathways in the hypothalamic regulation of body weight. *Endocr Rev* 20: 68-100.
114. Kask, A., R. Pakkila, A. Irs, L. Rago, J.E. Wikberg, and H.B. Schioth. 1999. Long-term administration of MC4 receptor antagonist HS014 causes hyperphagia and obesity in rats. *Neuroreport* 10: 707-711.
115. Kask, A., L. Rago, F. Mutulis, R. Pakkila, J.E. Wikberg, and H.B. Schioth. 1998. Selective antagonist for the melanocortin 4 receptor (HS014) increases food intake in free-feeding rats. *Biochem Biophys Res Commun* 245: 90-93.
116. Kennedy, G.C. 1953. The role of depot fat in the hypothalamic control of food intake in the rat. *Proc. R. Soc. Lond. B. Biol. Sci.* 140: 579-592.

117. Khong, C.K., D.M. Dinulescu, N. Ling, and R.D.C. Cone, R.D. 1999. Development of an ^{125}I -AGRP crosslinking method for identification and biochemical characterization of the melanocortin-4 receptor. *Endocrine Soc. Abstracts*: 226.
118. Kiefer, L.L., J.M. Veal, K.G. Mountjoy, and W.O. Wilkison. 1998. Melanocortin receptor binding determinants in the agouti protein. *Biochemistry* 37: 991-997.
119. Klebig, M.L., J.E. Wilkinson, J.G. Geisler, and R.P. Woychik. 1995. Ectopic expression of the agouti gene in transgenic mice causes obesity, features of type II diabetes, and yellow fur [see comments]. *Proc Natl Acad Sci U S A* 92: 4728-4732.
120. Klemcke, H.G. and W.G. Pond. 1991. Porcine adrenal adrenocorticotrophic hormone receptors: characterization, changes during neonatal development, and response to a stressor. *Endocrinology* 128: 2476-2488.
121. Klungland, H., D.I. Vage, L. Gomez-Raya, S. Adalsteinsson, and S. Lien. 1995. The role of melanocyte-stimulating hormone (MSH) receptor in bovine coat color determination. *Mamm Genome* 6: 636-639.
122. Krude, H., H. Biebermann, W. Luck, R. Horn, G. Brabant, and A. Gruters. 1998. Severe early-onset obesity, adrenal insufficiency and red hair pigmentation caused by POMC mutations in humans. *Nat Genet* 19: 155-157.
123. Kuhn, C.M., C. Cochrane, M.N. Feinglos, and R.S. Surwit. 1987. Exaggerated peripheral responses to catecholamines contributes to stress-induced hyperglycemia in the ob/ob mouse. *Pharmacol Biochem Behav* 26: 491-495.
124. Kulkarni, R.N., J.C. Bruning, J.N. Winnay, C. Postic, M.A. Magnuson, and C.R. Kahn. 1999. Tissue-specific knockout of the insulin receptor in pancreatic beta cells creates an insulin secretory defect similar to that in type 2 diabetes. *Cell* 96: 329-339.

125. Kwon, H.Y., S.J. Bultman, C. Loffler, W.J. Chen, P.J. Furdon, J.G. Powell, A.L. Usala, W. Wilkison, I. Hansmann, and R.P. Woychik. 1994. Molecular structure and chromosomal mapping of the human homolog of the agouti gene. *Proc Natl Acad Sci U S A* 91: 9760-9764.
126. Labbe, O., F. Desarnaud, D. Eggerickx, G. Vassart, and M. Parmentier. 1994. Molecular cloning of a mouse melanocortin 5 receptor gene widely expressed in peripheral tissues. *Biochemistry* 33: 4543-4549.
127. Lane, P.W. and M.C. Green. 1960. Mahogany, a recessive color mutation in linkage group V of the mouse. *J. Hered.* 51: 228-230.
128. Lefkowitz, R.J., S. Cotecchia, P. Samama, and T. Costa. 1993. Constitutive activity of receptors coupled to guanine nucleotide regulatory proteins. *Trends Pharmacol Sci* 14: 303-307.
128. Li, S.J., K. Varga, P. Archer, V.J. Hruby, S.D. Sharma, R.A. Kesterson, R.D. Cone, and G. Kunos. 1996. Melanocortin antagonists define two distinct pathways of cardiovascular control by alpha- and gamma-melanocyte-stimulating hormones. *J Neurosci* 16: 5182-5188.
129. Little, C.C. 1957. The inheritance of coat color in dogs. Howell Book House, Macmillan Publishing Co., New York.
130. Lu, D., D. Willard, I.R. Patel, S. Kadwell, L. Overton, T. Kost, M. Luther, W. Chen, R.P. Woychik, W.O. Wilkison, and et al. 1994. Agouti protein is an antagonist of the melanocyte-stimulating-hormone receptor. *Nature* 371: 799-802.

131. Lu, X., T.M. Gunn, K. Shieh, G.S. Barsh, H. Akil, and S.J. Watson. 1999. Distribution of Mahogany/Attractin mRNA in the rat central nervous system. *FEBS Lett* 462: 101-107.
132. Mac Neil, S., S.K. Johnson, S.S. Bleehen, B.L. Brown, and S. Tomlinson. 1981. Stimulation of the adenylate cyclase of A B16 melanoma cell line by pro- opiocortin-related peptides--a structure-activity study. *Regul Pept* 2: 193-200.
133. Mackie, C., M.C. Richardson, and D. Schulster. 1972. Studies on an isolated adrenal cell suspension: adenosine 3',5'-cyclic monophosphate production and effects of adrenocorticotrophin and adenosine 3',5'-cyclic monophosphate. *J Endocrinol* 52: 23-24.
134. Maestrini, E., L. Tamagnone, P. Longati, O. Cremona, M. Gulisano, S. Bione, F. Tamanini, B.G. Neel, D. Toniolo, and P.M. Comoglio. 1996. A family of transmembrane proteins with homology to the MET-hepatocyte growth factor receptor. *Proc Natl Acad Sci U S A* 93: 674-678.
135. Maffei, M., H. Fei, G.H. Lee, C. Dani, P. Leroy, Y. Zhang, R. Proenca, R. Negrel, G. Ailhaud, and J.M. Friedman. 1995. Increased expression in adipocytes of ob RNA in mice with lesions of the hypothalamus and with mutations at the db locus. *Proc Natl Acad Sci U S A* 92: 6957-6960.
136. Maffei, M., M. Stoffel, M. Barone, B. Moon, M. Dammerman, E. Ravussin, C. Bogardus, D.S. Ludwig, J.S. Flier, M. Talley, and et al. 1996. Absence of mutations in the human OB gene in obese/diabetic subjects. *Diabetes* 45: 679-682.
137. Mains, R.E. and B.A. Eipper. 1979. Synthesis and secretion of corticotropins, melanotropins, and endorphins by rat intermediate pituitary cells. *J Biol Chem* 254: 7885-7894.

138. Matsuoka, N., Y. Ogawa, K. Hosoda, J. Matsuda, H. Masuzaki, T. Miyawaki, N. Azuma, K. Natsui, H. Nishimura, Y. Yoshimasa, S. Nishi, D.B. Thompson, and K. Nakao. 1997. Human leptin receptor gene in obese Japanese subjects: evidence against either obesity-causing mutations or association of sequence variants with obesity. *Diabetologia* 40: 1204-1210.
139. Mercer, J.G., N. Hoggard, L.M. Williams, C.B. Lawrence, L.T. Hannah, P.J. Morgan, and P. Trayhurn. 1996a. Coexpression of leptin receptor and preproneuropeptide Y mRNA in arcuate nucleus of mouse hypothalamus. *J Neuroendocrinol* 8: 733-735.
140. Mercer, J.G., N. Hoggard, L.M. Williams, C.B. Lawrence, L.T. Hannah, and P. Trayhurn. 1996b. Localization of leptin receptor mRNA and the long form splice variant (Ob-Rb) in mouse hypothalamus and adjacent brain regions by in situ hybridization. *FEBS Lett* 387: 113-116.
141. Michaud, E.J., S.J. Bultman, M.L. Klebig, M.J. van Vugt, L.J. Stubbs, L.B. Russell, and R.P. Woychik. 1994. A molecular model for the genetic and phenotypic characteristics of the mouse lethal yellow (Ay) mutation. *Proc Natl Acad Sci U S A* 91: 2562-2566.
142. Miller, K.A., T.M. Gunn, M.M. Carrasquillo, M.L. Lamoreux, D.B. Galbraith, and G.S. Barsh. 1997. Genetic studies of the mouse mutations mahogany and mahoganoid. *Genetics* 146: 1407-1415.
143. Miller, M.W., D.M. Duhl, H. Vrieling, S.P. Cordes, M.M. Ollmann, B.M. Winkes, and G.S. Barsh. 1993. Cloning of the mouse agouti gene predicts a secreted protein ubiquitously expressed in mice carrying the lethal yellow mutation. *Genes Dev* 7: 454-467.

144. Miltenberger, R.J., R.L. Mynatt, B.D. Bruce, W.O. Wilkison, R.P. Woychik, and E.J. Michaud. 1999. An agouti mutation lacking the basic domain induces yellow pigmentation but not obesity in transgenic mice. *Proc Natl Acad Sci U S A* 96: 8579-8584.
145. Mizuno, T.M., S.P. Kleopoulos, H.T. Bergen, J.L. Roberts, C.A. Priest, and C.V. Mobbs. 1998. Hypothalamic pro-opiomelanocortin mRNA is reduced by fasting and [corrected] in ob/ob and db/db mice, but is stimulated by leptin [published erratum appears in Diabetes 1998 Apr;47(4):696]. *Diabetes* 47: 294-297.
146. Mizuno, T.M., H. Makimura, J. Silverstein, J.L. Roberts, T. Lopingco, and C.V. Mobbs. 1999. Fasting regulates hypothalamic neuropeptide Y, agouti-related peptide, and proopiomelanocortin in diabetic mice independent of changes in leptin or insulin. *Endocrinology* 140: 4551-4557.
147. Mizuno, T.M. and C.V. Mobbs. 1999. Hypothalamic agouti-related protein messenger ribonucleic acid is inhibited by leptin and stimulated by fasting. *Endocrinology* 140: 814-817.
148. Montague, C.T., I.S. Farooqi, J.P. Whitehead, M.A. Soos, H. Rau, N.J. Wareham, C.P. Sewter, J.E. Digby, S.N. Mohammed, J.A. Hurst, C.H. Cheetham, A.R. Earley, A.H. Barnett, J.B. Prins, and S. O'Rahilly. 1997. Congenital leptin deficiency is associated with severe early-onset obesity in humans. *Nature* 387: 903-908.
149. Mountjoy, K.G. 1994. The human melanocyte stimulating hormone receptor has evolved to become "super-sensitive" to melanocortin peptides. *Mol Cell Endocrinol* 102: R7-11.

150. Mountjoy, K.G., M.T. Mortrud, M.J. Low, R.B. Simerly, and R.D. Cone. 1994. Localization of the melanocortin-4 receptor (MC4-R) in neuroendocrine and autonomic control circuits in the brain. *Mol Endocrinol* 8: 1298-1308.
151. Mountjoy, K.G., L.S. Robbins, M.T. Mortrud, and R.D. Cone. 1992. The cloning of a family of genes that encode the melanocortin receptors. *Science* 257: 1248-1251.
- Mountjoy, K.G. and J.M. Wild. 1998. Melanocortin-4 receptor mRNA expression in the developing autonomic and central nervous systems. *Brain Res Dev Brain Res* 107: 309-314.
152. Murthy, A.S., R.E. Mains, and B.A. Eipper. 1986. Purification and characterization of peptidylglycine alpha-amidating monooxygenase from bovine neurointermediate pituitary. *J Biol Chem* 261: 1815-1822.
153. Naggert, J.K., L.D. Fricker, O. Varlamov, P.M. Nishina, Y. Rouille, D.F. Steiner, R.J. Carroll, B.J. Paigen, and E.H. Leiter. 1995. Hyperproinsulinaemia in obese fat/fat mice associated with a carboxypeptidase E mutation which reduces enzyme activity. *Nat Genet* 10: 135-142.
154. Nagle, D.L., S.H. McGrail, J. Vitale, E.A. Woolf, B.J. Dussault, Jr., L. DiRocco, L. Holmgren, J. Montagno, P. Bork, D. Huszar, V. Fairchild-Huntress, P. Ge, J. Keilty, C. Ebeling, L. Baldini, J. Gilchrist, P. Burn, G.A. Carlson, and K.J. Moore. 1999. The mahogany protein is a receptor involved in suppression of obesity. *Nature* 398: 148-152.
155. Nakayama, M., D. Nakajima, T. Nagase, N. Nomura, N. Seki, and O. Ohara. 1998. Identification of high-molecular-weight proteins with multiple EGF-like motifs by motif-trap screening. *Genomics* 51: 27-34.

156. Newton, J.M., A.L. Wilkie, L. He, S.A. Jordan, D.L. Metallinos, N.G. Holmes, I.J. Jackson, and G.S. Barsh. 2000. Melanocortin 1 receptor variation in the domestic dog [In Process Citation]. *Mamm Genome* 11: 24-30.
157. O'Donohue, T.L. 1983. Identification of endorphin acetyltransferase in rat brain and pituitary gland. *J Biol Chem* 258: 2163-2167.
158. Olivera, B.M., J. Rivier, J.K. Scott, D.R. Hillyard, and L.J. Cruz. 1991. Conotoxins. *J Biol Chem* 266: 22067-22070.
159. Ollmann, M.M. and G.S. Barsh. 1999. Down-regulation of melanocortin receptor signaling mediated by the amino terminus of Agouti protein in *Xenopus melanophores*. *J Biol Chem* 274: 15837-15846.
160. Ollmann, M.M., M.L. Lamoreux, B.D. Wilson, and G.S. Barsh. 1998. Interaction of Agouti protein with the melanocortin 1 receptor in vitro and in vivo. *Genes Dev* 12: 316-330.
161. Ollmann, M.M., B.D. Wilson, Y.K. Yang, J.A. Kerns, Y. Chen, I. Gantz, and G.S. Barsh. 1997. Antagonism of central melanocortin receptors in vitro and in vivo by agouti-related protein [published erratum appears in *Science* 1998 Sep 11;281(5383):1615]. *Science* 278: 135-138.
162. Orwoll, E., J.W. Kendall, L. Lamorena, and R. McGilvra. 1979. Adrenocorticotropin and melanocyte-stimulating hormone in the brain. *Endocrinology* 104: 1845-1852.
163. Ozata, M., I.C. Ozdemir, and J. Licinio. 1999. Human leptin deficiency caused by a missense mutation: multiple endocrine defects, decreased sympathetic tone, and immune system dysfunction indicate new targets for leptin action, greater central than peripheral

- resistance to the effects of leptin, and spontaneous correction of leptin-mediated defects. *J Clin Endocrinol Metab* 84: 3686-3695.
164. Palkovits, M., E. Mezey, and R.L. Eskay. 1987. Pro-opiomelanocortin-derived peptides (ACTH/beta-endorphin/alpha-MSH) in brainstem baroreceptor areas of the rat. *Brain Res* 436: 323-338.
165. Pankov, Y.A. 1999. Adipose tissue as an endocrine organ regulating growth, puberty, and other physiological functions. *Biochemistry (Mosc)* 64: 601-609.
166. Patterson, T. 1999. Chronic infusion of a melanocortin receptor agonist causes weight loss due to decreased food intake and increased metabolic rate. *Abstracts Society for Neuroscience, 29th Annual Meeting* 25(1: 248.3): 618.
167. Pelleymounter, M.A., M.J. Cullen, M.B. Baker, R. Hecht, D. Winters, T. Boone, and F. Collins. 1995. Effects of the obese gene product on body weight regulation in ob/ob mice [see comments]. *Science* 269: 540-543.
168. Perry, W.L., T. Nakamura, D.A. Swing, L. Secrest, B. Eagleson, C.M. Hustad, N.G. Copeland, and N.A. Jenkins. 1996. Coupled site-directed mutagenesis/transgenesis identifies important functional domains of the mouse agouti protein. *Genetics* 144: 255-264.
169. Porte, D., Jr., R.J. Seeley, S.C. Woods, D.G. Baskin, D.P. Figlewicz, and M.W. Schwartz. 1998. Obesity, diabetes and the central nervous system. *Diabetologia* 41: 863-881.
170. Rau, H., B.J. Reaves, S. O'Rahilly, and J.P. Whitehead. 1999. Truncated human leptin (delta133) associated with extreme obesity undergoes proteasomal degradation after defective intracellular transport. *Endocrinology* 140: 1718-1723.

171. Rho, J.H. and L.W. Swanson. 1989. A morphometric analysis of functionally defined subpopulations of neurons in the paraventricular nucleus of the rat with observations on the effects of colchicine. *J Neurosci* 9: 1375-1388.
172. Robbins, L.S., J.H. Nadeau, K.R. Johnson, M.A. Kelly, L. Roselli-Rehfuss, E. Baack, K.G. Mountjoy, and R.D. Cone. 1993. Pigmentation phenotypes of variant extension locus alleles result from point mutations that alter MSH receptor function. *Cell* 72: 827-834.
173. Rolland, V., K. Clement, I. Dugail, B. Guy-Grand, A. Basdevant, P. Froguel, and M. Lavau. 1998. Leptin receptor gene in a large cohort of massively obese subjects: no indication of the fa/fa rat mutation. Detection of an intronic variant with no association with obesity. *Obes Res* 6: 122-127.
174. Roselli-Rehfuss, L., K.G. Mountjoy, L.S. Robbins, M.T. Mortrud, M.J. Low, J.B. Tatro, M.L. Entwistle, R.B. Simerly, and R.D. Cone. 1993. Identification of a receptor for gamma melanotropin and other proopiomelanocortin peptides in the hypothalamus and limbic system. *Proceedings of the National Academy of Sciences of the United States of America* 90: 8856-8860.
175. Rosenfeld, R.D., L. Zeni, A.A. Welcher, L.O. Narhi, C. Hale, J. Marasco, J. Delaney, T. Gleason, J.S. Philo, V. Katta, J. Hui, J. Baumgartner, M. Graham, K.L. Stark, and W. Karbon. 1998. Biochemical, biophysical, and pharmacological characterization of bacterially expressed human agouti-related protein. *Biochemistry* 37: 16041-16052.
176. Rossi, M., M.S. Kim, D.G. Morgan, C.J. Small, C.M. Edwards, D. Sunter, S. Abusnana, A.P. Goldstone, S.H. Russell, S.A. Stanley, D.M. Smith, K. Yagaloff, M.A. Ghatei, and S.R. Bloom. 1998. A C-terminal fragment of Agouti-related protein increases

- feeding and antagonizes the effect of alpha-melanocyte stimulating hormone in vivo. *Endocrinology* 139: 4428-4431.
177. Rotimi, C.N., A.G. Comuzzie, W.L. Lowe, A. Luke, J. Blangero, and R.S. Cooper. 1999. The quantitative trait locus on chromosome 2 for serum leptin levels is confirmed in African-Americans. *Diabetes* 48: 643-644.
178. Samama, P., G. Pei, T. Costa, S. Cotecchia, and R.J. Lefkowitz. 1994. Negative antagonists promote an inactive conformation of the beta 2- adrenergic receptor. *Mol Pharmacol* 45: 390-394.
180. Satoh, N., Y. Ogawa, G. Katsuura, Y. Numata, H. Masuzaki, Y. Yoshimasa, and K. Nakao. 1998. Satiety effect and sympathetic activation of leptin are mediated by hypothalamic melanocortin system. *Neurosci Lett* 249: 107-110.
181. Sawyer, T.K., V.J. Hruby, P.S. Darman, and M.E. Hadley. 1982. [half-Cys4, half-Cys10]-alpha-Melanocyte-stimulating hormone: a cyclic alpha-melanotropin exhibiting superagonist biological activity. *Proc Natl Acad Sci U S A* 79: 1751-1755.
182. Sawyer, T.K., P.J. Sanfilippo, V.J. Hruby, M.H. Engel, C.B. Heward, J.B. Burnett, and M.E. Hadley. 1980. 4-Norleucine, 7-D-phenylalanine-alpha-melanocyte-stimulating hormone: a highly potent alpha-melanotropin with ultralong biological activity. *Proc Natl Acad Sci U S A* 77: 5754-5758.
183. Schauer, E., F. Trautinger, A. Kock, A. Schwarz, R. Bhardwaj, M. Simon, J.C. Ansel, T. Schwarz, and T.A. Luger. 1994. Proopiomelanocortin-derived peptides are synthesized and released by human keratinocytes. *J Clin Invest* 93: 2258-2262.

184. Schioth, H.B., S.R. Phillips, R. Rudzish, M.A. Birch-Machin, J.E. Wikberg, and J.L. Rees. 1999. Loss of function mutations of the human melanocortin 1 receptor are common and are associated with red hair. *Biochem Biophys Res Commun* 260: 488-491.
185. Schwartz, M.W., R.J. Seeley, S.C. Woods, D.S. Weigle, L.A. Campfield, P. Burn, and D.G. Baskin. 1997. Leptin increases hypothalamic pro-opiomelanocortin mRNA expression in the rostral arcuate nucleus. *Diabetes* 46: 2119-2123.
186. Seidah, N.G. and M. Chretien. 1981. Complete amino acid sequence of a human pituitary glycopeptide: an important maturation product of pro-opiomelanocortin. *Proc Natl Acad Sci U S A* 78: 4236-4240.
187. Seidah, N.G., J. Rochemont, J. Hamelin, S. Benjannet, and M. Chretien. 1981. The missing fragment of the pro-sequence of human pro-opiomelanocortin: sequence and evidence for C-terminal amidation. *Biochem Biophys Res Commun* 102: 710-716.
188. Shutter, J.R., M. Graham, A.C. Kinsey, S. Scully, R. Luthy, and K.L. Stark. 1997. Hypothalamic expression of ART, a novel gene related to agouti, is up-regulated in obese and diabetic mutant mice. *Genes Dev* 11: 593-602.
189. Silvers, W.K. 1958. An experimental approach to action of genes at the agouti locus in the mouse. *J. Exp. Zool.* 137:181-196.
190. Silvers, W.K. 1961. Genes and the pigment cells of mammals. *Science* 134: 368-373.
191. Silvers, W.K. 1979. The coat colors of mice: a model for mammalian gene action and interaction. *Springer-Verlag, New York*: 6-44.
192. Silvers, W.K. and E.S. Russel. 1955. An experimental approach to action of genes at the agouti locus in the mouse. *J.Exp.Zool.* 130: 199-220.

193. Sina, M., A. Hinney, A. Ziegler, T. Neupert, H. Mayer, W. Siegfried, W.F. Blum, H. Remschmidt, and J. Hebebrand. 1999. Phenotypes in three pedigrees with autosomal dominant obesity caused by haploinsufficiency mutations in the melanocortin-4 receptor gene. *Am J Hum Genet* 65: 1501-1507.
194. Smith, A.I. and J.W. Funder. 1988. Proopiomelanocortin processing in the pituitary, central nervous system, and peripheral tissues. *Endocr Rev* 9: 159-179.
195. Smith, A.I., A.B. Keith, J.A. Edwardson, J.A. Biggins, and J.R. McDermott. 1982. Characterization of corticotropin-like immunoreactive peptides in rat brain using high performance liquid chromatography. *Neurosci Lett* 30: 133-138.
196. Smyth, D.G., D.E. Massey, S. Zakarian, and M.D. Finnle. 1979. Endorphins are stored in biologically active and inactive forms: isolation of alpha-N-acetyl peptides. *Nature* 279: 252-254.
197. Stair, J. 1999. Feeding behavior in rats chronically treated with melanocortin agonist , MTII. *Abstracts Society for Neuroscience, 29th Annual Meeting, 1999* 25(1:248.5): 619.
198. Stanley, S.A., C.J. Small, M.S. Kim, M.M. Heath, L.J. Seal, S.H. Russell, M.A. Ghatei, and S.R. Bloom. 1999. Agouti related peptide (Agrp) stimulates the hypothalamo pituitary gonadal axis in vivo & in vitro in male rats. *Endocrinology* 140: 5459-5462.
199. Stenbit, A.E., T.S. Tsao, J. Li, R. Burcelin, D.L. Geenen, S.M. Factor, K. Houseknecht, E.B. Katz, and M.J. Charron. 1997. GLUT4 heterozygous knockout mice develop muscle insulin resistance and diabetes [see comments]. *Nat Med* 3: 1096-1101.

200. Strobel, A., T. Issad, L. Camoin, M. Ozata, and A.D. Strosberg. 1998. A leptin missense mutation associated with hypogonadism and morbid obesity [news]. *Nat Genet* 18: 213-215.
201. Takeuchi, T., T. Kobunai, and H. Yamamoto. 1989. Genetic control of signal transduction in mouse melanocytes. *J Invest Dermatol* 92: 239S-242S.
202. Tartaglia, L.A., M. Dembski, X. Weng, N. Deng, J. Culpepper, R. Devos, G.J. Richards, L.A. Campfield, F.T. Clark, J. Deeds, and et al. 1995. Identification and expression cloning of a leptin receptor, OB-R. *Cell* 83: 1263-1271.
203. Tatro, J.B. 1990. Melanotropin receptors in the brain are differentially distributed and recognize both corticotropin and alpha-melanocyte stimulating hormone. *Brain Res* 536: 124-132.
204. Tatro, J.B. 1993. Brain receptors for central and peripheral melanotropins. *Ann N Y Acad Sci* 680: 621-625.
205. Tatro, J.B. and M.L. Entwistle. 1994a. Distribution of melanocortin receptors in the lower brainstem of the rat. *Ann N Y Acad Sci* 739: 311-314.
206. Tatro, J.B. and M.L. Entwistle. 1994b. Heterogeneity of brain melanocortin receptors suggested by differential ligand binding in situ. *Brain Res* 635: 148-158.
207. Tatro, J.B. and S. Reichlin. 1987. Specific receptors for alpha-melanocyte-stimulating hormone are widely distributed in tissues of rodents. *Endocrinology* 121: 1900-1907.
208. Taylor, S.I. 1999. Deconstructing type 2 diabetes. *Cell* 97: 9-12.
209. Tessier-Lavigne, M. and C.S. Goodman. 1996. The molecular biology of axon guidance. *Science* 274: 1123-1133.

210. Thomas, L., R. Leduc, B.A. Thorne, S.P. Smeekens, D.F. Steiner, and G. Thomas. 1991. Kex2-like endoproteases PC2 and PC3 accurately cleave a model prohormone in mammalian cells: evidence for a common core of neuroendocrine processing enzymes. *Proc Natl Acad Sci U S A* 88: 5297-5301.
211. Thorne, B.A., O.H. Viveros, and G. Thomas. 1991. Expression and processing of mouse proopiomelanocortin in bovine adrenal chromaffin cells. A model system to study tissue-specific prohormone processing. *J Biol Chem* 266: 13607-13615.
212. Thornton, J.E., C.C. Cheung, D.K. Clifton, and R.A. Steiner. 1997. Regulation of hypothalamic proopiomelanocortin mRNA by leptin in ob/ob mice. *Endocrinology* 138: 5063-5066.
213. Tota, M.R., T.S. Smith, C. Mao, T. MacNeil, R.T. Mosley, L.H. Van der Ploeg, and T.M. Fong. 1999. Molecular interaction of Agouti protein and Agouti-related protein with human melanocortin receptors. *Biochemistry* 38: 897-904.
214. Vage, D.I., D. Lu, H. Klungland, S. Lien, S. Adalsteinsson, and R.D. Cone. 1997. A non-epistatic interaction of agouti and extension in the fox, *Vulpes vulpes*. *Nat Genet* 15: 311-315.
215. Vaisse, C., K. Clement, B. Guy-Grand, and P. Froguel. 1998. A frameshift mutation in human MC4R is associated with a dominant form of obesity [letter]. *Nat Genet* 20: 113-114.
216. Vrieling, H., D.M. Duhl, S.E. Millar, K.A. Miller, and G.S. Barsh. 1994. Differences in dorsal and ventral pigmentation result from regional expression of the mouse agouti gene. *Proc Natl Acad Sci U S A* 91: 5667-5671.

217. Warbritton, A., A.M. Gill, T.T. Yen, T. Bucci, and G.L. Wolff. 1994. Pancreatic islet cells in preobese yellow Avy/- mice: relation to adult hyperinsulinemia and obesity. *Proc Soc Exp Biol Med* 206: 145-151.
218. Weis, W.I. and K. Drickamer. 1996. Structural basis of lectin-carbohydrate recognition. *Annu Rev Biochem* 65: 441-473.
219. Willard, D.H., W. Bodnar, C. Harris, L. Kiefer, J.S. Nichols, S. Blanchard, C. Hoffman, M. Moyer, W. Burkhardt, J. Weiel, and et al. 1995. Agouti structure and function: characterization of a potent alpha- melanocyte stimulating hormone receptor antagonist. *Biochemistry* 34: 12341-12346.
220. Wilson, B.D., D. Bagnol, C.B. Kaelin, M.M. Ollmann, I. Gantz, S.J. Watson, and G.S. Barsh. 1999. Physiological and anatomical circuitry between Agouti-related protein and leptin signaling. *Endocrinology* 140: 2387-2397.
221. Wilson, B.D., M.M. Ollmann, L. Kang, M. Stoffel, G.I. Bell, and G.S. Barsh. 1995. Structure and function of ASP, the human homolog of the mouse agouti gene. *Hum Mol Genet* 4: 223-230.
222. Wintzen, M. and B.A. Gilchrist. 1996. Proopiomelanocortin, its derived peptides, and the skin [published erratum appears in J Invest Dermatol 1996 Sep;107(3):444]. *J Invest Dermatol* 106: 3-10.
223. Yang, Y.K., C.J. Dickinson, Q. Zeng, J.Y. Li, D.A. Thompson, and I. Gantz. 1999a. Contribution of melanocortin receptor exoloops to Agouti-related protein binding. *J Biol Chem* 274: 14100-14106.

- Yang, Y.K., M.M. Ollmann, B.D. Wilson, C. Dickinson, T. Yamada, G.S. Barsh, and I. Gantz. 1997. Effects of recombinant agouti-signaling protein on melanocortin action. *Mol Endocrinol* 11: 274-280.
- Yang, Y.K., D.A. Thompson, C.J. Dickinson, J. Wilken, G.S. Barsh, S.B. Kent, and I. Gantz. 1999b. Characterization of Agouti-related protein binding to melanocortin receptors. *Mol Endocrinol* 13: 148-155.
- Yaswen, L., N. Diehl, M.B. Brennan, and U. Hochgeschwender. 1999. Obesity in the mouse model of pro-opiomelanocortin deficiency responds to peripheral melanocortin [see comments]. *Nat Med* 5: 1066-1070.
- Yen, T.T., A.M. Gill, L.G. Frigeri, G.S. Barsh, and G.L. Wolff. 1994. Obesity, diabetes, and neoplasia in yellow A(vy)/- mice: ectopic expression of the agouti gene. *Faseb J* 8: 479-488.
- Yeo, G.S., I.S. Farooqi, S. Aminian, D.J. Halsall, R.G. Stanhope, G. Butler, and S. O'Rahilly. 1999. Mutations in the melanocortin-4 receptor gene are associated with severe human obesity. *Proc. 81th Ann. Meeting Endocrine Soc.* The Endocrine Society Press, Bethesda, MD, USA: 66.
- Yeo, G.S., I.S. Farooqi, S. Aminian, D.J. Halsall, R.G. Stanhope, and S. O'Rahilly. 1998. A frameshift mutation in MC4R associated with dominantly inherited human obesity [letter]. *Nat Genet* 20: 111-112.
- Yoshida, T., J.W. Kemnitz, and G.A. Bray. 1983. Lateral hypothalamic lesions and norepinephrine turnover in rats. *J Clin Invest* 72: 919-927.

Yoshimatsu, H., A. Nijima, Y. Oomura, K. Yamabe, and T. Katafuchi. 1984. Effects of hypothalamic lesion on pancreatic autonomic nerve activity in the rat. *Brain Res* 303: 147-152.

Zakarian, S. and D.G. Smyth. 1982. Distribution of beta-endorphin-related peptides in rat pituitary and brain. *Biochem J* 202: 561-571.

Zemel, M.B. 1998. Nutritional and endocrine modulation of intracellular calcium: implications in obesity, insulin resistance and hypertension. *Mol Cell Biochem* 188: 129-136.

Zhang, Y., R. Proenca, M. Maffei, M. Barone, L. Leopold, and J.M. Friedman. 1994. Positional cloning of the mouse obese gene and its human homologue [published erratum appears in *Nature* 1995 Mar 30;374(6521):479] [see comments]. *Nature* 372: 425-432.